doi : 10.17596/0002620

MR19-02
(2019 5/24-6/14)
Preliminary Cruise Report

2019
JAMSTEC

Note

This cruise report is a preliminary documentation as of the end of cruise. This report is not necessarily corrected even if there is any inaccurate description. This report is subject to be revised without notice. Some data on this report may be raw or unprocessed. If you are going to use or refer the data on this report, it is recommended to ask the Chief Scientist for latest status. Users of information on this report are requested to submit Publication Report to JAMSTEC.

Acknowledgments

We are grateful to the captain and crew of the R/V MIRAI for their support during the cruise.

Chief Scientist of MR19-02

Tetsuichi Fujiki
JAMSTEC

Contents of MR19-02 Preliminary Cruise Report

1. Outline of MR19-02

1.1 Cruise information

Cruise ID: MR19-02

Research vessel: MIRAI

Cruise title: The observational study to construct and to extend the western Pacific super site network

Cruise period (port call):

24 May (Shimizu, Shizuoka, Japan) – 14 June 2019 (Sekine, Aomori, Japan)

Research area: The western North Pacific

Ship Captain: Haruhiko Inoue (Nippon Marine Enterprises, Ltd.)

Chief Scientist:

Tetsuichi Fujiki (Research Institute for Global Change, JAMSTEC)

Deputy Chief Scientist:

Katsunori Kimoto (Research Institute for Global Change, JAMSTEC)

Representative of the Science Party:

Akira Nagano (Research Institute for Global Change, JAMSTEC)

1.2 Cruise participants

Scientists

Tetsuichi Fujiki	JAMSTEC
Katsunori Kimoto	JAMSTEC
Minoru Kitamura	JAMSTEC
Koji Sugie	JAMSTEC
Makio Honda	JAMSTEC
Kazuhiko Matsumoto	JAMSTEC
Hiroshi Uchida	JAMSTEC
Masahide Wakita	JAMSTEC
Yoshihisa Mino	Nagoya University
Osamu Abe	Nagoya University
Noriaki Natori	Soka University
Gu Qianyi	Soka University
Arisa Takashima	Tohoku University

Research Engineers

Jun Matsuoka	Marine Works Japan, Ltd.
Katsunori Sagishima	Marine Works Japan, Ltd.

Hideki Yamamoto	Marine Works Japan, Ltd.
Yasuhiro Arii	Marine Works Japan, Ltd.
Shinichiro Yokogawa	Marine Works Japan, Ltd.
Keitaro Matsumoto	Marine Works Japan, Ltd.
Hiroshi Hoshino	Marine Works Japan, Ltd.
Masahiro Orui	Marine Works Japan, Ltd.
Atsushi Ono	Marine Works Japan, Ltd.
Yuko Miyoshi	Marine Works Japan, Ltd.
Shinsuke Toyoda	Marine Works Japan, Ltd.
Hiroki Ushiromura	Marine Works Japan, Ltd.
Shungo Oshitani	Marine Works Japan, Ltd.
Hironori Sato	Marine Works Japan, Ltd.
Yasushi Hashimoto	Marine Works Japan, Ltd.
Takayuki Sunagawa	Marine Works Japan, Ltd.
Shintaro Amikura	Marine Works Japan, Ltd.
Wataru Tokunaga	Nippon Marine Enterprises, Ltd.
Satomi Ogawa	Nippon Marine Enterprises, Ltd.

1.3 Research brief

1.3(a) Study of "Nutrient Missing Source" in the oligotrophic region

Based on the comparison study of biogeochemistry in the northwestern North Pacific eutrophic subarctic region and oligotrophic subtropical region (K2S1 project), it was clarified that biological activity in the subtropical region is comparable to or slightly larger than that in the subarctic region. In order to verify the support mechanism of biological activity, that is the mechanism of nutrient supply, time-series sediment trap experiment was initiated in 2014 at about 4900 m of the station KEO. This station is the time-series station maintained by National Ocean and Atmosphere Administration (NOAA) Pacific Marine Environmental Laboratory (PMEL). Surface buoy with meteorological sensors and physical oceanographic sensors have been deployed at station KEO since 2004. Therefore, these time-series data of meteorology and physical oceanography can be utilized to interpret time-series variability in sediment trap data. Owing to simultaneous analysis of time-series data obtained by NOAA surface buoy and JAMSTEC sediment trap between 2014 and 2016, it was verified that mesoscale cyclonic eddy potentially plays a role in nutrient supplier (Honda et al. PEPS 2018). In order to evaluate other potential mechanisms such as typhoon and aeolian dust input, sediment trap experiment and another time-series observation has been continued at station KEO.

During this cruise, at station KEO, we observed vertical profiles in biogeochemical components such as nutrients, carbon chemistry, phytoplankton pigments and primary productivity late May. In addition, in order to study marine particulate organic carbon (POC) optically, backscatter meters with fluorometer were deployed at station KEO and other stations. By analyzing backscatter meters' data and chlorophyll and POC measured onboard (and on land laboratory later), empirical equations for estimating POC and chlorophyll with backscatter meter will be proposed in near future and temporal variability in POC and its vertical attenuation will be discussed.

(b) Time-series observations for marine ecosystem dynamics research in the subarctic western North Pacific

The subarctic western North Pacific is a cyclonic upwelling gyre (western subarctic gyre; WSG) that extends from the northeast of Japan to near the international dateline. To investigate the spatial and temporal variability of biogeochemical processes in the WSG, time-series observations have been carried out since 1997 at stations KNOT (44ºN, 155ºE) and /or K2 (47ºN, 160ºE) in the WSG, indicating that ocean acidification was rapidly progressing in this gyre. However, the effect of ocean acidification on lower trophic levels in this region is not well understood. To better understand the response of lower trophic level ecosystem to multiple environmental stressors (e.g., warming, acidification and deoxygenation), we conducted the following observations and operations during this cruise

(1) Recovery and deployment of hybrid profiling buoy system
(2) CTD cast and water sampling/biochemical analysis
(3) Assessment of phytoplankton productivity by fast repetition rate fluorometry
(4) Observation of zooplankton biomass by acoustic zooplankton fish profiler
(5) Zooplankton sampling by using the VMPS, ORI and NORPAC nets
(6) Particle collection by using in situ filtration system
(7) On-deck incubation experiments
(8) Measurements of shortwave and longwave radiation
(9) Upper ocean current measurements by shipboard ADCP
(10) Sea surface water sampling
(11) Deployment of biogeochemical Argo floats
(12) Rain sampling
(13) Meteorological observations
(14) Satellite image acquisition

1.4 Cruise track and log

Cruise track:

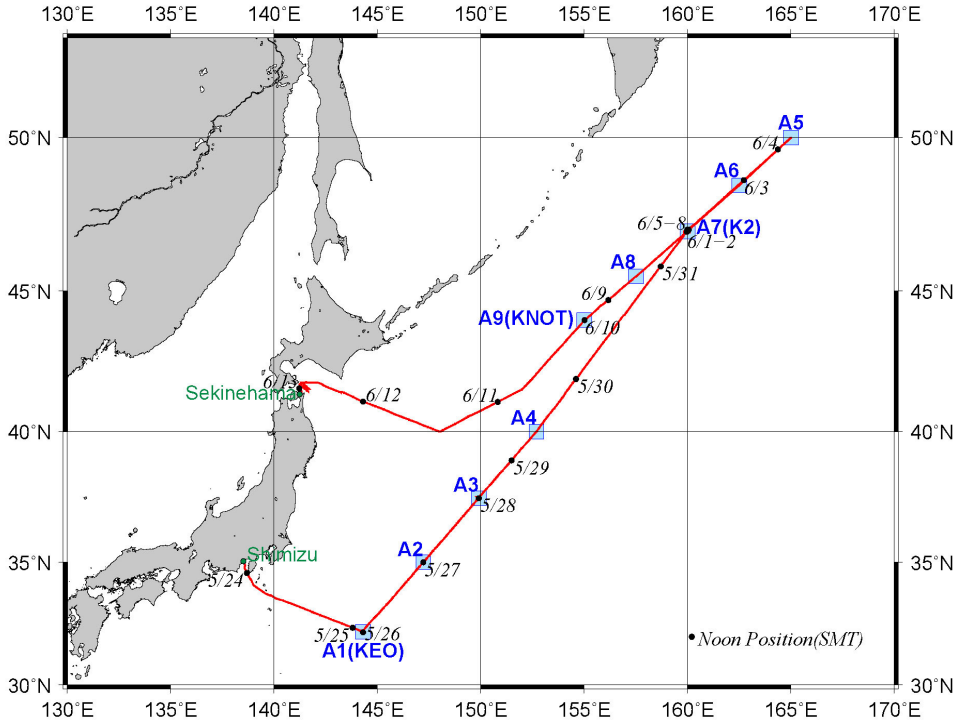

Cruise log:

U.T.C.		S.M.T.		Position		Event logs
Date	Time	Date	Time	Lat.	Lon.	
5.24	0:00	5.24	9:00	35-02.30N	138-30.60E	Departure from Shimizu
	5:11		14:11	34-09.81N	138-57.71E	Sea water pump start
	7:00		16:00	33-52.81N	139-21.26E	EPCS observation start
	7:34		16:34	33-48.30N	139-29.04E	MBES observation start
5.25	5:12	5.25	14:12	32-12.45N	144-16.70E	Arrival at A1 (KEO)
	5:18		14:18	32-12.36N	144-17.12E	ARGO float (BGC) deployment #01
	5:36		14:36	32-12.15N	144-18.03E	CTD cast #01 suspended due to sensor trouble
	6:51		15:51	32-12.95N	144-17.85E	CTD cast #02 (5975 m)
	8:30		17:30	32-12.95N	144-17.85E	Surface water sampling by bucket
	11:42		20:42	32-14.15N	144-17.54E	NORPAC net #01-01 (300 m)
	12:05		21:05	32-14.40N	144-17.53E	NORPAC net #01-02 (300 m)
	12:29		21:29	32-14.68N	144-17.55E	NORPAC net #01-03 (300 m)
	12:50		21:50	32-14.92N	144-17.58E	NORPAC net #01-04 (300 m)
	13:17		22:17	32-15.24N	144-17.61E	Twin NORPAC net #01 (150 m)
	13:34		22:34	32-15.40N	144-17.53E	AZFP #01 (150 m)
	14:28		23:28	32-16.00N	144-18.00E	Calibration for magnetometer #01
	17:07	5.26	2:07	32-12.21N	144-18.10E	CTD cast #03 (300 m)
	17:23		2:23	32-12.21N	144-18.10E	Surface water sampling by bucket
	18:21		3:21	32-12.93N	144-18.46E	FRRF #01 (150 m)
	19:56		4:56	32-11.92N	144-18.00E	In situ filtration system #01 (3000 m)
5.26	2:57		11:57	32-11.09N	144-17.87E	CTD cast #04 (150 m)
	3:05		12:05	32-11.09N	144-17.87E	Surface water sampling by bucket
	3:28		12:28	32-11.55N	144-17.97E	FRRF #02 (150 m)
	4:02		13:02	32-11.93N	144-18.10E	AZFP #02 (150 m)
	4:30		13:30	32-12.35N	144-18.31E	Twin NORPAC net #02 (150 m)
	5:00		14:00	32-12.47N	144-18.40E	VMPS net #01-01 (500 m)
	5:38		14:38	32-12.53N	144-18.38E	VMPS net #01-02 (150 m)
	6:07		15:07	32-12.89N	144-18.43E	AZFP #03 (150 m)
	6:39		15:39	32-13.70N	144-18.73E	Twin NORPAC net #03 (150 m)
	6:53		15:53	32-14.00N	144-18.94E	FRRF #03 (150 m)
	7:29		16:29	32-14.54N	144-19.17E	NORPAC net #02-01 (200 m)
	7:48		16:48	32-14.54N	144-19.17E	NORPAC net #02-02 (200 m)
	8:05		17:05	32-14.54N	144-19.17E	NORPAC net #02-03 (200 m)
	8:30		17:30	32-16.04N	144-19.88E	Departure from A1 (KEO)
5.27	2:55	5.27	11:55	34-59.88N	147-12.90E	Arrival at A2
	2:58		11:58	34-59.55N	147-12.45E	CTD cast #05 (5793 m)
	4:31		13:31	34-59.55N	147-12.46E	Surface water sampling by bucket
	7:14		16:14	34-58.79N	147-11.91E	AZFP #04 (150 m)
	7:44		16:44	34-58.00N	147-11.40E	Twin NORPAC net #04 (150 m)
	8:08		17:08	34-57.77N	147-11.31E	VMPS net #02-01 (500 m)
	8:44		17:44	34-57.39N	147-11.23E	VMPS net #02-02 (150 m)
	9:09		18:09	34-57.16N	147-11.10E	NORPAC net #03-01 (200 m)
	9:30		18:30	34-57.16N	147-11.10E	NORPAC net #03-02 (200 m)
	9:48		18:48	34-57.16N	147-11.10E	NORPAC net #03-03 (200 m)
	10:12		19:12	34-55.70N	147-10.51E	Departure from A2
5.28	3:01	5.28	12:01	37-30.01N	149-53.92E	Arrival at A3

	3:01		12:01	37-30.02N	149-53.77E	CTD cast #06 (150 m)
	3:10		12:10	37-30.01N	149-53.81E	Surface water sampling by bucket
	3:34		12:34	37-29.78N	149-53.48E	FRRF #04 (150 m)
	4:20		13:20	37-29.90N	149-53.36E	VMPS net #03-01 (500 m)
	4:59		13:59	37-29.90N	149-53.36E	VMPS net #03-02 (150 m)
	5:31		14:31	37-30.41N	149-52.20E	CTD cast #07 (5985 m)
	7:05		16:05	37-30.42N	149-52.21E	Surface water sampling by bucket
	9:47		18:47	37-31.31N	149-51.01E	NORPAC net #04-01 (150 m)
	10:01		19:01	37-31.31N	149-51.01E	NORPAC net #04-02 (150 m)
	10:18		19:18	37-31.31N	149-51.01E	NORPAC net #04-03 (150 m)
	10:36		19:36	37-31.56N	149-50.55E	NORPAC net #05-01 (300 m)
	11:02		20:02	37-31.56N	149-50.55E	NORPAC net #05-02 (300 m)
	11:30		20:30	37-31.56N	149-50.55E	NORPAC net #05-03 (300 m)
	11:55		20:55	37-31.56N	149-50.55E	NORPAC net #05-04 (300 m)
	12:22		21:22	37-32.05N	149-49.42E	AZFP #05 (150 m)
	13:02		22:02	37-32.29N	149-48.86E	Twin NORPAC net #05 (150 m)
	16:26	5.29	1:26	37-29.79N	149-54.15E	FRRF #05 (150 m)
	17:05		2:05	37-30.06N	149-53.83E	CTD cast #08 (300 m)
	17:20		2:20	37-30.06N	149-53.83E	Surface water sampling by bucket
	18:12		3:12	37-30.66N	149-53.93E	Departure from A3
5.29	9:30		18:30	39-59.60N	152-40.22E	Arrival at A4
	9:40		18:40	39-59.94N	152-41.12E	CTD cast #09 (5658 m)
	11:14		20:14	39-59.93N	152-41.20E	Surface water sampling by bucket
	13:47		22:47	39-59.90N	152-41.05E	VMPS net #04-01 (500 m)
	14:24		23:24	39-59.90N	152-41.05E	VMPS net #04-02 (150 m)
	14:57		23:57	40-00.01N	152-41.05E	NORPAC net #06-01 (150 m)
	15:12	5.30	0:12	40-00.01N	152-41.05E	NORPAC net #06-02 (150 m)
	15:26		0:26	40-00.01N	152-41.05E	NORPAC net #06-03 (150 m)
	16:00		1:00	40-01.15N	152-42.49E	Departure from A4
5.30	13:00		22:00	-	-	Time adjustment +1 hour (SMT=UTC+10h)
5.31	8:34	5.31	18:34	46-58.00N	159-56.00E	Calibration for magnetometer #02
	9:12		19:12	46-58.86N	159-55.23E	Arrival at A7 (K2)
	12:00		22:00	-	-	Time adjustment +1 hour (SMT=UTC+11h)
	21:18	6.1	8:18	47-00.46N	159-56.34E	VMPS net #05-01 (500 m)
	22:02		9:02	47-00.46N	159-56.34E	VMPS net #05-02 (150 m)
	22:37		9:37	47-00.44N	159-56.37E	NORPAC net #07-01 (150 m)
	22:52		9:52	47-00.44N	159-56.37E	NORPAC net #07-02 (150 m)
	23:06		10:06	47-00.44N	159-56.37E	NORPAC net #07-03 (150 m)
	23:28		10:28	47-00.93N	159-56.52E	CTD cast #10 (300 m)
	23:41		10:41	47-01.00N	159-56.60E	Surface water sampling by bucket
6.1	0:38		11:38	47-00.82N	159-58.34E	Mooring system recovery
	15:01	6.2	2:01	47-00.50N	159-58.38E	FRRF #06 (100 m)
	15:27		2:27	47-00.43N	159-58.43E	CTD cast #11 (300 m)
	15:42		2:42	47-00.43N	159-58.43E	Surface water sampling by bucket
	17:57		4:57	47-00.59N	159-58.57E	AZFP #06 (150 m)
	18:30		5:30	47-00.30N	159-58.95E	Twin NORPAC net #06 (150 m)
	19:00		6:00	47-00.43N	159-58.87E	In situ filtration system #02 (700 m)
6.2	0:04		11:04	47-03.28N	159-58.90E	CTD cast #12 (200 m) suspended due to sensor trouble
	0:51		11:51	47-03.65N	159-59.01E	FRRF #07 (100 m)
	1:12		12:12	47-03.77N	159-59.27E	AZFP #07 (150 m)
	1:43		12:43	47-04.02N	159-59.58E	Twin NORPAC net #07 (150 m)
	2:16		13:16	47-04.12N	159-59.68E	CTD cast #13 (3000 m)
	3:09		14:09	47-04.34N	159-59.98E	Surface water sampling by bucket

	4:24		15:24	47-04.38N	160-00.33E	ARGO float (BGC) deployment #02
	4:26		15:26	47-04.32N	160-00.31E	ARGO float (BGC) deployment #03
	5:22		16:22	47-00.33N	159-57.98E	CTD cast #14 (5200 m)
	6:46		17:46	47-00.33N	159-57.98E	Surface water sampling by bucket
	9:28		20:28	47-00.34N	159-56.24E	MBES mapping survey (above K2)
	10:58		21:58	47-00.75N	159-58.38E	AZFP #08 (150 m)
	11:29		22:29	47-00.44N	159-58.16E	Twin NORPAC net #08 (150 m)
	11:43		22:43	47-00.49N	159-57.98E	NORPAC net #08-01 (300 m)
	12:05		23:05	47-00.49N	159-57.98E	NORPAC net #08-02 (300 m)
	12:33		23:33	47-00.49N	159-57.98E	NORPAC net #08-03 (300 m)
	13:12	6.3	0:12	47-02.08N	160-00.01E	Departure from A7 (K2)
6.3	2:58		13:58	48-55.00N	163-08.83E	CTD cast #15 (150 m)
	10:48		21:48	49-59.15N	164-58.58E	Arrival at A5
	10:51		21:51	50-00.00N	165-00.00E	Calibration for magnetometer #03
	14:27	6.4	1:27	49-59.98N	164-59.94E	FRRF #08 (100 m)
	14:57		1:57	50-00.01N	164-59.95E	CTD cast #16 (300 m)
	15:10		2:10	50-00.01N	164-59.95E	Surface water sampling by bucket
	15:56		2:56	50-00.01N	164-59.99E	NORPAC net #09-01 (150 m)
	16:10		3:10	50-00.01N	164-59.99E	NORPAC net #09-02 (150 m)
	16:23		3:23	50-00.01N	164-59.99E	NORPAC net #09-03 (150 m)
	16:53		3:53	50-00.03N	165-00.06E	CTD cast #17 (5493 m)
	18:20		5:20	50-00.03N	165-00.06E	Surface water sampling by bucket
	20:50		7:50	49-59.83N	164-59.97E	VMPS net #06-01 (500 m)
	21:29		8:29	49-59.83N	164-59.97E	VMPS net #06-02 (150 m)
	21:55		8:55	49-59.96N	164-59.64E	FRRF #09 (100 m)
	22:30		9:30	49-59.07N	164-58.38E	Departure from A5
6.4	8:42		19:42	48-30.74N	162-31.33E	Arrival at A6
	8:55		19:55	48-29.97N	162-29.91E	CTD cast #18 (5725 m)
	10:28		21:28	48-29.97N	162-29.91E	Surface water sampling by bucket
	12:59		23:59	48-30.12N	162-29.92E	VMPS net #07-01 (500 m)
	13:40	6.5	0:40	48-30.12N	162-29.92E	VMPS net #07-02 (200 m)
	14:09		1:09	48-30.00N	162-29.92E	NORPAC net #10-01 (150 m)
	14:22		1:22	48-30.00N	162-29.92E	NORPAC net #10-02 (150 m)
	14:35		1:35	48-30.00N	162-29.92E	NORPAC net #10-03 (150 m)
	15:00		2:00	48-29.12N	162-28.51E	Departure from A6
6.5	1:30		12:30	47-00.27N	159-58.16E	Arrival at A7 (K2)
	2:01		13:01	47-00.38N	159-58.42E	CTD cast #19 (200 m)
	2:11		13:11	47-00.38N	159-58.42E	Surface water sampling by bucket
	20:58	6.6	7:58	47-01.90N	160-04.69E	Mooring system deployment
6.6	1:15		12:15	46-59.87N	159-58.52E	Mooring calibration (sinker fixed position)
	3:50		14:50	46-58.00N	160-06.12E	MBES mapping survey (around K2)
	9:58		20:58	47-01.37N	160-00.53E	NORPAC net #11-01 (300 m)
	10:20		21:20	47-01.37N	160-00.53E	NORPAC net #11-02 (300 m)
	18:05	6.7	5:05	46-59.37N	160-00.83E	CTD cast #20 (500 m)
	18:21		5:21	46-59.37N	160-00.83E	Surface water sampling by bucket
	19:11		6:11	46-59.20N	160-00.50E	VMPS net #08-01 (500 m)
	19:45		6:45	46-59.20N	160-00.50E	VMPS net #08-02 (150 m)
	20:08		7:08	46-58.90N	16-00.10E	AZFP #09 (150 m)
	20:36		7:36	46-58.70N	160-00.20E	Twin NORPAC net #09 (150 m)
	21:00		8:00	46-58.75N	160-00.31E	In situ filtration system #03 (3000 m)
6.7	3:56		14:56	47-01.90N	160-00.40E	AZFP #10 (150 m)

	4:28		15:28	47-01.74N	160-00.26E	Twin NORPAC net #10 (150 m)
	5:02		16:02	47-01.56N	160-00.14E	CTD cast #21 (500 m)
	5:19		16:19	47-01.56N	160-00.14E	Surface water sampling by bucket
	14:55	6.8	1:55	47-01.57N	159-57.21E	FRRF #10 (100 m)
	15:27		2:27	47-01.46N	159-57.16E	CTD cast #22 (300 m)
	15:40		2:40	47-01.46N	159-57.17E	Surface water sampling by bucket
	16:33		3:33	47-01.46N	159-57.17E	NORPAC net #12-01 (150 m)
	16:47		3:47	47-01.46N	159-57.17E	NORPAC net #12-02 (150 m)
	17:00		4:00	47-01.46N	159-57.17E	NORPAC net #12-03 (150 m)
	17:53		4:53	47-01.00N	159-57.00E	CTD cast #23 (5190 m)
	20:18		7:18	47-01.02N	159-56.98E	Surface water sampling by bucket
6.8	0:49		11:49	46-59.14N	159-57.60E	FRRF #11 (100 m)
	1:18		12:18	46-58.77N	159-57.36E	Departure from A7 (K2)
	11:42		22:42	45-30.23N	157-31.47E	Arrival at A8
	13:59	6.9	0:59	45-30.02N	157-29.97E	CTD cast #24 (4940 m)
	15:17		2:17	45-30.02N	157-29.97E	Surface water sampling by bucket
	17:41		4:41	45-30.00N	157-29.90E	VMPS net #09-01 (500 m)
	18:18		5:18	45-30.00N	157-29.90E	VMPS net #09-01 (150 m)
	18:42		5:42	45-30.18N	157-30.18E	NORPAC net #13-01 (150 m)
	18:56		5:56	45-30.18N	157-30.18E	NORPAC net #13-02 (150 m)
	19:24		6:24	45-28.88N	157-27.79E	Departure from A8
6.9	2:57		13:57	44-27.42N	155-44.27E	CTD cast #25 (150 m)
	6:36		17:36	44-01.07N	155-02.60E	Arrival at A9 (KNOT)
	6:44		17:44	44-00.00N	155-01.00E	Calibration for magnetometer #04
	9:58		20:58	44-00.02N	154-59.96E	NORPAC net #14-01 (300 m)
	10:27		21:27	44-00.02N	154-59.96E	NORPAC net #14-02 (300 m)
	10:55		21:55	44-00.02N	154-59.96E	NORPAC net #14-03 (300 m)
	14:56	6.10	1:56	44-00.02N	155-00.50E	FRRF #12 (100 m)
	15:23		2:23	44-00.10N	155-00.13E	CTD cast #26 (300 m)
	15:41		2:41	44-00.11N	155-00.14E	Surface water sampling by bucket
	16:35		3:35	44-00.20N	155-00.51E	VMPS net #10-01 (500 m)
	17:18		4:18	44-00.20N	155-00.51E	VMPS net #10-02 (150 m)
	19:01		6:01	44-00.24N	155-00.34E	CTD cast #27 (5300 m)
	20:28		7:28	44-00.24N	155-00.34E	Surface water sampling by bucket
	23:06		10:06	44-00.27N	155-00.48E	AZFP #11 (150 m)
	23:33		10:33	44-00.25N	155-00.52E	Twin NORPAC net #11 (150 m)
	23:52		10:52	44-00.25N	155-00.52E	NORPAC net #15-01 (150 m)
	0:05		11:05	44-00.25N	155-00.52E	NORPAC net #15-02 (150 m)
	0:18		11:18	44-00.25N	155-00.52E	NORPAC net #15-03 (150 m)
6.10	0:35		11:35	43-59.94N	155-00.84E	FRRF #13 (100 m)
	1:58		12:58	43-59.94N	155-00.06E	CTD cast #28 (1000 m)
	2:22		13:22	43-59.95N	155-00.06E	Surface water sampling by bucket
	2:53		13:53	43-59.81N	155-00.03E	Twin NORPAC net #12 (150 m)
	3:09		14:09	43-59.62N	154-59.99E	AZFP #12 (150 m)
	3:54		14:54	43-59.14N	154-59.73E	CTD cast #29 (1000 m)
	4:48		15:48	43-58.58N	154-59.15E	Departure from A9 (KNOT)
6.11	11:00	6.11	22:00	-	-	Time adjustment -1 hour (SMT=UTC+10h)
6.12	4:00	6.12	14:00	41-16.89N	143-47.72E	EPCS observation finish
	4:03		14:03	41-17.17N	143-46.96E	Sea water pump finish
	12:00		22:00	-	-	Time adjustment -1 hour (SMT=UTC+09h)

	17:00	6.13	2:00	41-48.00N	142-00.13E	ADCP survey off Sekinehama
6.13	8:41		17:41	41-37.17N	141-18.92E	MBES observation finish
	8:44		17:44	41-36.60N	141-18.70E	SSV pump finish
6.14	0:00	6.14	9:00	-	-	Arrival at Sekinehama

2. Ship observations and measurements

2.1 Meteorological observations

2.1 (a) Surface meteorological observations

Tetsuichi FUJIKI (JAMSTEC RIGC)
Wataru TOKUNAGA (NME)
Satomi OGAWA (NME)
Yoichi INOUE (MIRAI crew)

(1) Objectives

Surface meteorological parameters are observed as a basic dataset of the meteorology. These parameters provide the temporal variation of the meteorological condition surrounding the ship.

(2) Methods

Surface meteorological parameters were observed during this cruise. In this cruise, we used two systems for the observation.

i) MIRAI Surface Meteorological observation (SMet) system

Instruments of SMet system are listed in Table2.1(a).1 and measured parameters are listed in Table2.1(a).2 Data were collected and processed by KOAC-7800 weather data processor made by Koshin-Denki, Japan. The data set consists of 6 seconds averaged data.

ii) Shipboard Oceanographic and Atmospheric Radiation (SOAR) measurement system

SOAR system designed by BNL (Brookhaven National Laboratory, USA) consists of major five parts.

a) Portable Radiation Package (PRP) designed by BNL - short and long wave downward radiation.
b) Analog meteorological data sampling with CR1000 logger manufactured by Campbell Inc. Canada - wind, pressure, and rainfall (by a capacitive rain gauge) measurement.
c) Digital meteorological data sampling from individual sensors - air temperature, relative humidity and rainfall (by optical rain gauge) measurement.
d) Photosynthetically Available Radiation (PAR) sensor manufactured by Biospherical Instruments Inc. (USA) - PAR measurement.
e) Scientific Computer System (SCS) developed by NOAA (National Oceanic and Atmospheric Administration, USA) - centralized data acquisition and logging of all data sets.

SCS recorded PRP data every 6 seconds, CR1000 data every second, air temperature and relative humidity data every 2 seconds, ORG data every 6 seconds and PAR data every 6 seconds. SCS composed “Event data (JamMet_PARUV)” from these data and ship’s navigation data. Instruments and their locations are listed in Table2.1(a).3 and measured parameters are listed in Table2.1(a).4.

For the quality control as post processing, we checked the following sensors, before and after the cruise.

i) Young rain gauge (SMet and SOAR)

Inspect of the linearity of output value from the rain gauge sensor to change input value by adding fixed quantity of test water.

ii) Barometer (SMet and SOAR)

Comparison with the portable barometer value, PTB220, VAISALA

iii) Thermometer (air temperature and relative humidity) (SMet and SOAR)

Comparison with the portable thermometer value, HMP75, VAISALA

(3) Preliminary results

Fig.2.1(a).1 shows the time series of the following parameters;

Wind (SOAR)
Air temperature (SMet)
Relative humidity (SMet)
Precipitation (SOAR, ORG)
Short/long wave radiation (SOAR)
Barometric Pressure (SMet)
Sea surface temperature (SMet)
Significant wave height (SMet)

(4) Data archives

All data obtained during this cruise will be submitted to the Data Management Group (DMG) in JAMSTEC, and will be archived there.

(5) Remarks (Times in UTC)

i) The following period, sea surface temperature of SMet data was available.
05:15 24 May 2019 - 04:03 12 June 2019

ii) FRSR data was not acquired through this cruise due to sensor failure.

iii) The following periods, anemometer of SMet data was error due to mechanical trouble.
08:45 31 May 2019 - 09:29 31 May 2019
11:38 31 May 2019 - 11:50 31 May 2019

iv) The following period, anemometer of SMet used foremast sensor
00:00 24 May 2019 - 11:50 31 May 2019

v) The following period, anemometer of SMet used aftermast sensor
11:50 31 May 2019 - 00:00 14 June 2019

vi) The following period, PAR data was not effective due to the sensor connection error.
00:00 24 May 2019 - 09:07 24 May 2019

vii) The following periods, significant wave height(bow) data were invalid due to mechanical trouble.
03:55 28 May 2019 to 10:55 29 May 2019
22:55 12 June 2019 to 10:55 13 June 2019
21:55 13 June 2019 to 22:55 13 June 2019

viii) The following time, increasing of SMet capacitive rain gauge data were invalid due to transmitting for MF/HF or VHF radio.
05:21 26 May 2019
02:00 08 June 2019
02:18 12 June 2019

ix) The following days, short wave radiation were increased at night time.
30 May 2019
11 June 2019
12 June 2019
13 June 2019

Table2.1(a).1. Instruments and installation locations of MIRAI Surface Meteorological observation system

Sensors	Type	Manufacturer	Location (altitude from surface)
Anemometer	KS-5900	Koshin Denki, Japan	foremast (25 m) aftermast (37m)
Tair/RH with aspirated radiation shield	HMP155 43408 Gill	Vaisala, Finland R.M. Young, USA	compass deck (20 m) starboard side and port side
Thermometer: SST	RFN2-0	Koshin Denki, Japan	4th deck (-1m, inlet -5m)
Barometer	Model-370	Setra System, USA	captain deck (13 m) weather observation room
Rain gauge	50202	R. M. Young, USA	compass deck (19 m)
Optical rain gauge	ORG-815DR	Osi, USA	compass deck (18 m)
Radiometer (short wave)	MS-802	Eko Seiki, Japan	radar mast (28 m)
Radiometer (long wave)	MS-202	Eko Seiki, Japan	radar mast (28 m)
Wave height meter	WM-2	Tsurumi-seiki, Japan	bow (10 m), aft (8 m)

Table2.1(a).2. Parameters of MIRAI Surface Meteorological observation system

Parameter	Units	Remarks
1 Latitude	degree	
2 Longitude	degree	
3 Ship's speed	knot	Mirai log
4 Ship's heading	degree	Mirai gyro
5 Relative wind speed	m/s	6sec./10min. averaged
6 Relative wind direction	degree	6sec./10min. averaged
7 True wind speed	m/s	6sec./10min. averaged
8 True wind direction	degree	6sec./10min. averaged
9 Barometric pressure	hPa	adjusted to sea surface level 6sec. averaged
10 Air temperature (starboard side)	degC	6sec. averaged
11 Air temperature (port side)	degC	6sec. averaged
12 Dewpoint temperature (starboard side)	degC	6sec. averaged
13 Dewpoint temperature (port side)	degC	6sec. averaged
14 Relative humidity (starboard side)	%	6sec. averaged
15 Relative humidity (port side)	%	6sec. averaged
16 Sea surface temperature	degC	6sec. averaged
17 Rain rate (optical rain gauge)	mm/hr	hourly accumulation
18 Rain rate (capacitive rain gauge)	mm/hr	hourly accumulation
19 Down welling shortwave radiation	W/m^2	6sec. averaged
20 Down welling infra-red radiation	W/m^2	6sec. averaged
21 Significant wave height (bow)	m	hourly
22 Significant wave height (aft)	m	hourly
23 Significant wave period (bow)	second	hourly
24 Significant wave period (aft)	second	hourly

Table2.1(a).3. Instruments and installation locations of SOAR system

Sensors (Meteorological)	Type	Manufacturer	Location (altitude from surface)
Anemometer	05106	R.M. Young, USA	foremast (26 m)
Barometer	PTB210	Vaisala, Finland	foremast (23 m)
with pressure port	61002 Gill	R.M. Young, USA	
Rain gauge	50202	R.M. Young, USA	foremast (25 m)
Tair/RH	HMP155	Vaisala, Finland	foremast (23 m)
with aspirated radiation shield	43408 Gill	R.M. Young, USA	
Optical rain gauge	ORG-815DR	Osi, USA	foremast (25 m)

Sensors (PRP)	Type	Manufacturer	Location (altitude from surface)
Radiometer (short wave)	PSP	Epply Labs, USA	foremast (25 m)
Radiometer (long wave)	PIR	Epply Labs, USA	foremast (25 m)
Fast rotating shadowband radiometer		Yankee, USA	foremast (25 m)

Sensor (PAR&UV)	Type	Manufacturer	Location (altitude from surface)
PAR&UV sensor	PUV-510	Biospherical Instruments Inc., USA	Navigation deck (18m)

Table2.1(a).4. Parameters of SOAR system (JamMet)

Parameter		Units	Remarks
1	Latitude	degree	
2	Longitude	degree	
3	SOG	knot	
4	COG	degree	
5	Relative wind speed	m/s	
6	Relative wind direction	degree	
7	Barometric pressure	hPa	
8	Air temperature	degC	
9	Relative humidity	%	
10	Rain rate (optical rain gauge)	mm/hr	
11	Precipitation (capacitive rain gauge)	mm/hr	reset at 50 mm
12	Down welling shortwave radiation	W/m^2	
13	Down welling infra-red radiation	W/m^2	
14	Defuse irradiance	W/m^2	
15	PAR	$microE/cm^2/sec$	
16	UV 305 nm	$microW/cm^2/nm$	
17	UV 320 nm	$microW/cm^2/nm$	
18	UV 340 nm	$microW/cm^2/nm$	
19	UV 380 nm	$microW/cm^2/nm$	

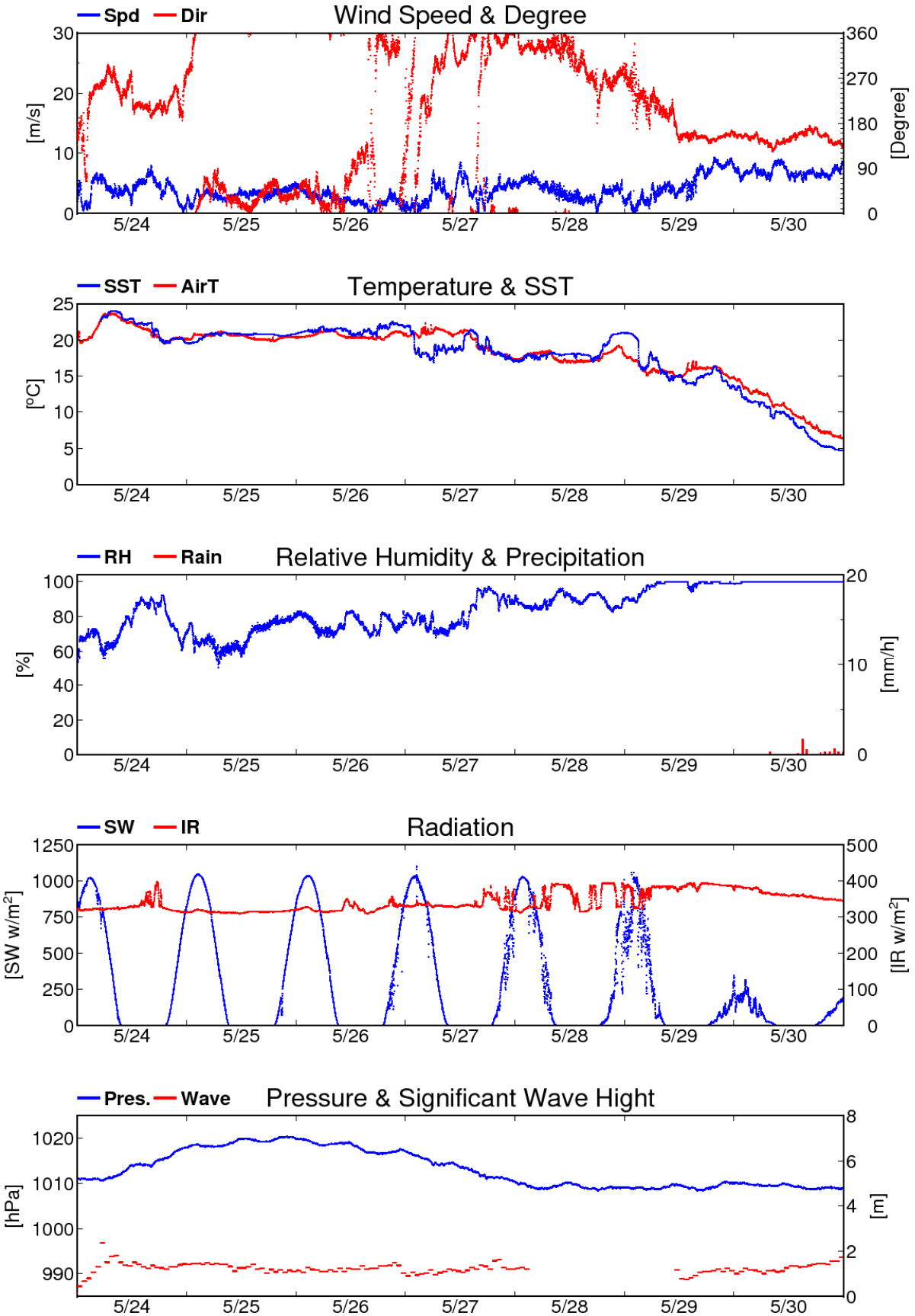

Fig. 2.1(a).1 Time series of surface meteorological parameters during the cruise

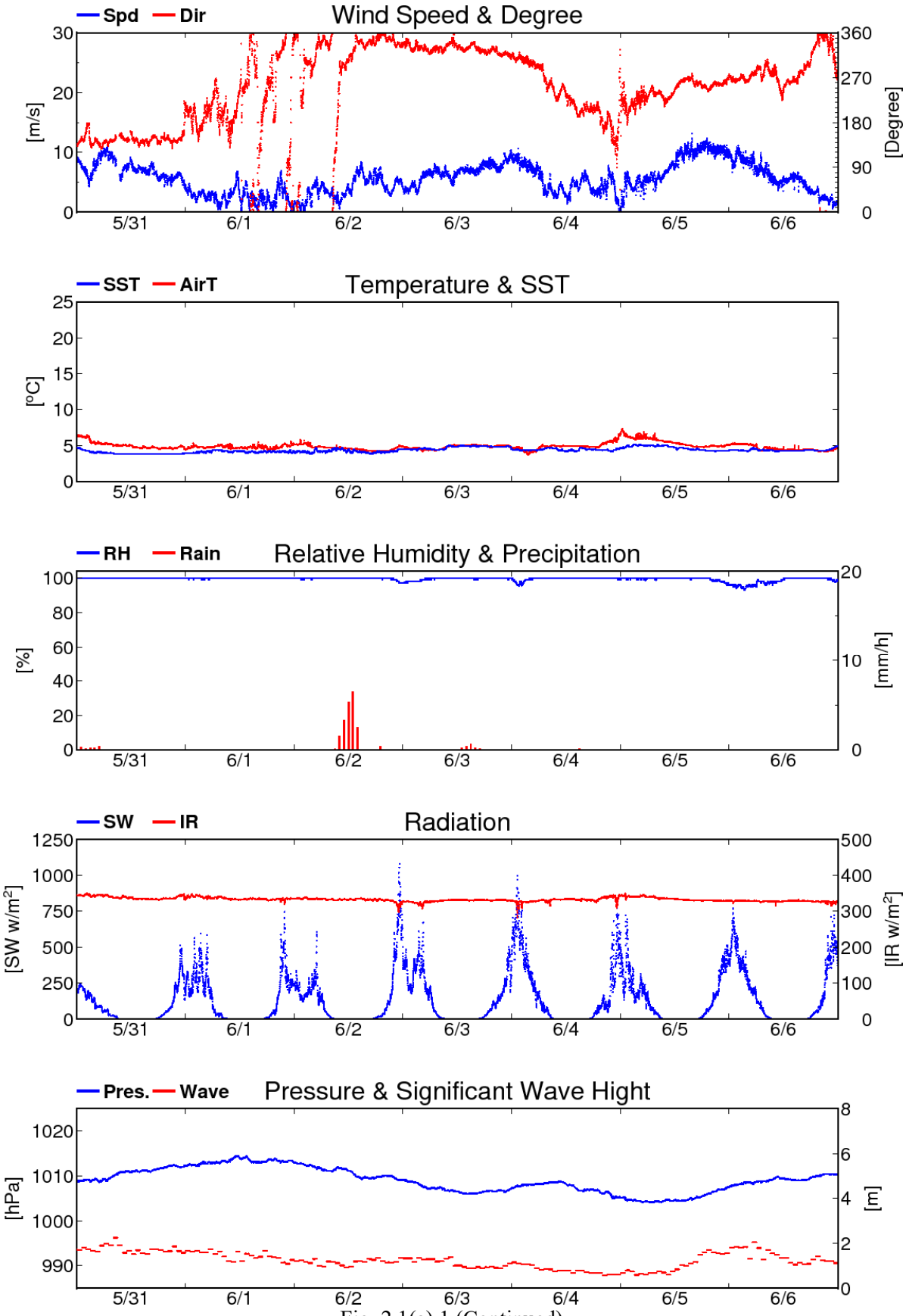

Fig. 2.1(a).1 (Continued)

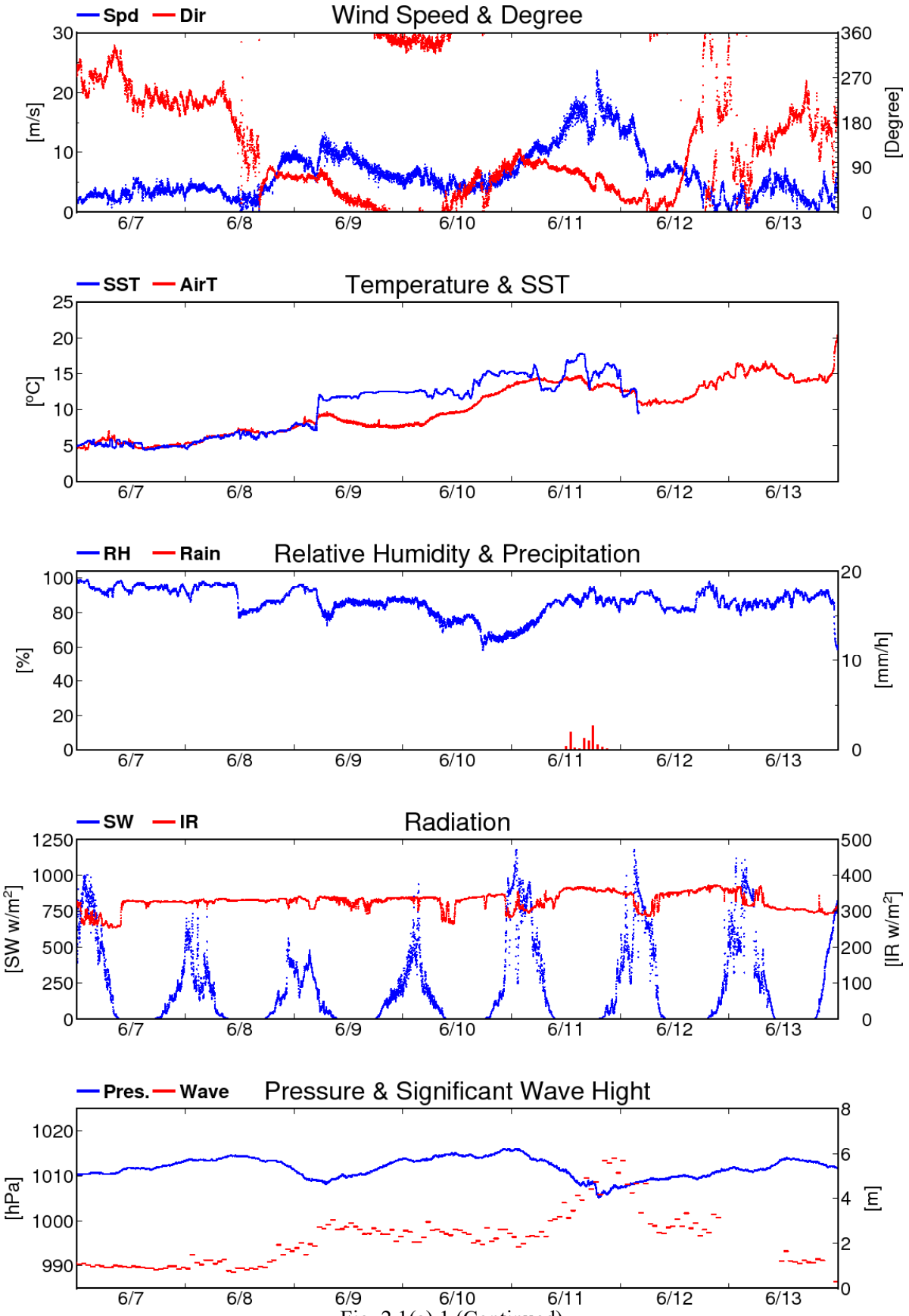

Fig. 2.1(a).1 (Continued)

2.1 (b) Ceilometer observation

Tetsuichi FUJIKI (JAMSTEC RIGC)
Wataru TOKUNAGA (NME)
Satomi OGAWA (NME)
Yoishi INOUE (MIRAI crew)

(1) Objectives

The information of cloud base height and the liquid water amount around cloud base is important to understand the process on formation of the cloud. As one of the methods to measure them, the ceilometer observation was carried out.

(2) Parameters

i) Cloud base height [m].
ii) Backscatter profile, sensitivity and range normalized at 10 m resolution.
iii) Estimated cloud amount [oktas] and height [m]; Sky Condition Algorithm.

(3) Methods

We measured cloud base height and backscatter profile using ceilometer (CL51, VAISALA, Finland). Major parameters for the measurement configuration are shown in Table2.1(b).1.

Table2.1(b).1. Major parameters

Laser source:	Indium Gallium Arsenide (InGaAs) Diode
Transmitting center wavelength:	910±10 nm at 25 degC
Transmitting average power:	19.5 mW
Repetition rate:	6.5 kHz
Detector:	Silicon avalanche photodiode (APD)
Responsibility at 905 nm:	65 A/W
Cloud detection range:	0 ~ 13 km
Measurement range:	0 ~ 15 km
Resolution:	10 meter in full range
Sampling rate:	36 sec
Sky Condition:	Cloudiness in octas (0 ~ 9) (0:Sky Clear, 1:Few, 3:Scattered, 5-7:Broken, 8:Overcast, 9:Vertical Visibility)

(4) Preliminary results

Fig.2.1(b).1 shows the time series plot of the lowest, second and third cloud base height during the cruise.

(5) Data archives

All data obtained during this cruise will be submitted to the Data Management Group (DMG) in JAMSTEC, and will be archived there.

(6) Remarks (Times in UTC)

i) Window Cleaning
01:40 23 June 2019

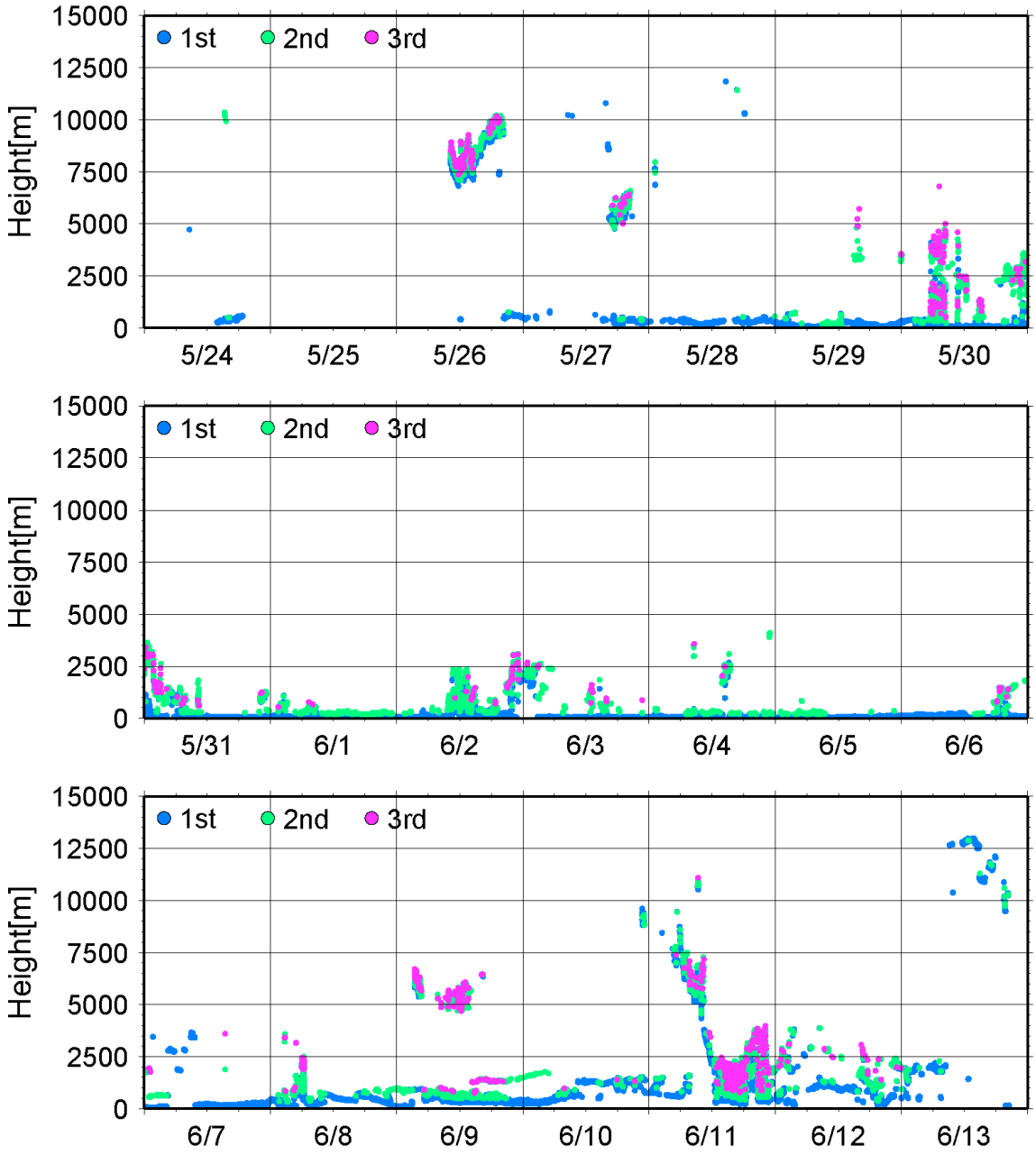

Fig.2.1(b).1 First (Blue), 2nd (Green) and 3rd (Red) lowest cloud base height during the cruise.

2.1 (c) Rain sampling at the marine Atmosphere

Fumikazu TAKETANI (JAMSTEC RIGC)
Kazuhiko MATSUMOTO (JAMSTEC RIGC)
Makio HONDA (JAMSTEC RIGC)
Yugo KANAYA (JAMSTEC RIGC)

(1) Objectives

To investigate contribution of the rain as a nutrients to the marine ecosystem.

(2) Instruments and methods

Rain sample was corrected using an auto-changing rain sampler. The interval of sampling time was 3-h. These sampling logs are listed in Table 2.1.1. To investigate the nutrients such as nitrate, phosphate, and iron, etc. in the rain, these samples are going to be analyzed in laboratory.

Table 2.1.1. Observation log for rain sampling.

On board ID	Date Collected					Latitude			Longitude		
	YYYY	MM	DD	hh:mm:ss	UTC/JST	Deg.	Min.	N/S	Deg.	Min.	E/W
MR1902-R001	2019	05	30	1:00	UTC	41	39.65	N	154	19.72	E
MR1902-R002	2019	05	30	4:00	UTC	42	9.70	N	154	51.41	E
MR1902-R003	2019	05	30	7:00	UTC	42	41.37	N	155	22.91	E
MR1902-R004	2019	05	30	10:00	UTC	43	11.70	N	155	53.92	E
MR1902-R006	2019	05	30	16:00	UTC	44	13.85	N	156	59.70	E
MR1902-R007	2019	05	30	19:00	UTC	44	44.76	N	157	31.82	E
MR1902-R008	2019	05	30	22:00	UTC	45	15.32	N	158	3.87	E
MR1902-R009	2019	05	31	1:00	UTC	45	45.47	N	158	36.30	E
MR1902-R010	2019	05	31	4:00	UTC	46	16.06	N	159	9.59	E
MR1902-R011	2019	05	31	7:00	UTC	46	47.12	N	159	43.89	E
MR1902-R021	2019	06	02	7:00	UTC	47	0.24	N	159	57.87	E
MR1902-R022	2019	06	02	10:00	UTC	47	0.33	N	159	58.30	E
MR1902-R023	2019	06	02	13:00	UTC	47	4.65	N	160	4.18	E
MR1902-R024	2019	06	02	16:00	UTC	47	29.44	N	160	45.72	E
MR1902-R026	2019	06	03	7:00	UTC	49	30.90	N	164	10.02	E
MR1902-R027	2019	06	03	10:00	UTC	49	56.48	N	164	54.14	E
MR1902-R028	2019	06	03	13:00	UTC	49	59.82	N	164	59.56	E
MR1902-R029	2019	06	03	16:00	UTC	50	0.01	N	164	59.94	E
MR1902-R030	2019	06	03	19:00	UTC	49	59.96	N	165	0.08	E
MR1902-R035	2019	06	04	19:00	UTC	47	50.63	N	161	23.42	E

2.1 (d) Lidar Observation

Masaki KATSUMATA (JAMSTEC RIGC)
Kyoko TANIGUCHI (JAMSTEC RIGC)
Wataru TOKUNAGA (NME)
Satomi OGAWA (NME)

(1) Objective

The objective of this observation is to capture the vertical distribution of clouds, aerosols, and water vapor in high spatio-temporal resolution.

(2) Instrumentations and Methods

The Mirai Lidar system transmits a 10-Hz pulse laser in three wavelengths: 1064nm, 532nm, 355nm. For cloud and aerosol observation, the system detects Mie scattering at these wavelengths. The separate detections of parallel and perpendicular components at 532 nm and 355 nm obtain additional characteristics of the targets. The system also detects Raman water vapor signals at 660 nm and 408nm, Raman nitrogen signals at 607 nm and 387nm at nighttime. Based on the signal ratio of Raman water vapor to Raman nitrogen, the system offers water vapor mixing ratio profiles.

(3) Preliminary Results

The lidar system observed the lower atmosphere throughout the cruise, except on EEZs and territorial waters without permission. All data will be reviewed after the cruise to maintain data quality.

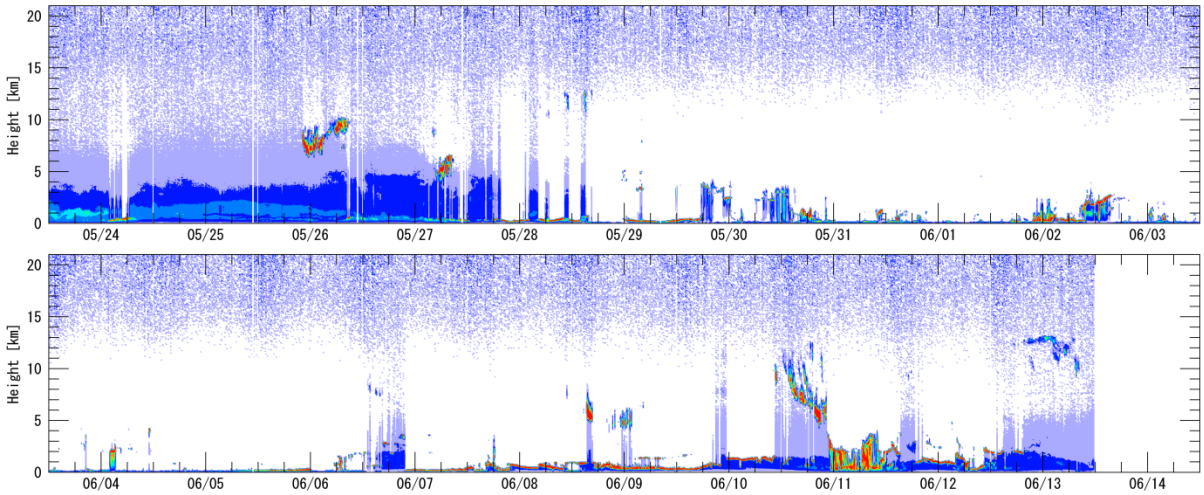

Figure 2.1.d.1 Preliminary result of 532 nm attenuated backscattering intensity obtained during the cruise.

(4)Data Archive

All data obtained during this cruise will be submitted to the JAMSTEC Data Management Group (DMG).

2.2 Geophysical observation

2.2 (a) Swath bathymetric survey

Tetsuichi FUJIKI (JAMSTEC RIGC)
Wataru TOKUNAGA (NME)
Satomi OGAWA (NME)
Yoichi INOUE (MIRAI crew)

(1) Introduction

The objective of Multi-Beam Echo Sounding system (MBES) is collecting continuous bathymetric data along ship's track to make a contribution to geological and geophysical investigations and global data sets. In addition, we need to estimate the depth at the location A7(K2) of deployment of mooring buoy in order to design these mooring systems.

(2) Data Acquisition

The "SEABEAM 3012" on R/V MIRAI was used for bathymetry mapping during this cruise.

To get accurate sound velocity of water column for ray-path correction of acoustic multibeam, we used Surface Sound Velocimeter (SSV) data to get the sea surface (6.62m) sound velocity, and the deeper depth sound velocity profiles were calculated by temperature and salinity profiles from CTD and Argo float data by the equation in Del Grosso (1974) during the cruise.

(3) Preliminary Results

The results will be published after primary processing.

(4) Data Archives

All data obtained during this cruise will be submitted to the Data Management Group (DMG) in JAMSTEC, and will be archived there.

2.2 (b) Sea surface gravity

Tetsuichi FUJIKI (JAMSTEC RIGC)
Wataru TOKUNAGA (NME)
Satomi OGAWA (NME)
Yoichi INOUE (MIRAI crew)

(1) Introduction

The local gravity is an important parameter in geophysics and geodesy. We collected gravity data at the sea surface.

(2) Parameters

Relative Gravity [CU: Counter Unit]
[mGal] = (coef1: 0.9946) * [CU]

(3) Data Acquisition

We measured relative gravity using LaCoste and Romberg air-sea gravity meter S-116 (Micro-G LaCoste, LLC) during this cruise.

To convert the relative gravity to absolute gravity at Shimizu and Sekinehama as the reference points.

(4) Preliminary Results

Absolute gravity table is shown in Table 2.2(b).1.

Table 2.2(b).1. Absolute gravity table of this cruise

No.	Date m/d	UTC	Port	Absolute Gravity [mGal]	Sea Level [cm]	Ship Draft [cm]	Gravity at Sensor *1 [mGal]	S-116 Gravity [mGal]
#1	5/23	09:05	Shimizu	979729.49	211	648	979730.40	12010.17
#2	6/14	06:00	Sekinehama	980371.87	247	630	980372.85	12651.73

*1: Gravity at Sensor = Absolute Gravity + Sea Level*0.3086/100 + (Draft-530)/100*0.2222

(5) Data Archive

All data obtained during this cruise will be submitted to the Data Management Group (DMG) in JAMSTEC, and will be archived there.

2.2 (c) Sea surface magnetic field

Tetsuichi FUJIKI (JAMSTEC RIGC)
Wataru TOKUNAGA (NME)
Satomi OGAWA (NME)
Yoichi INOUE (MIRAI crew)

(1) Introduction

Measurement of magnetic force on the sea is required for the geophysical investigations of marine magnetic anomaly caused by magnetization in upper crustal structure. We measured geomagnetic field using a three-component magnetometer during this cruise.

(2) Instruments

A shipboard three-component magnetometer system (Tierra Tecnica SFG2018) is equipped on-board R/V MIRAI. Three-axes flux-gate sensors with ring-cored coils are fixed on the fore mast. Outputs from the sensors are digitized by a 20-bit A/D converter (1 nT/LSB), and sampled at 8 times per second. Ship's heading, pitch, and roll are measured by the Inertial Navigation System (INS) for controlling attitude of a Doppler radar. Ship's position and speed data are taken from LAN every second.

(3) Principle of ship-board geomagnetic vector measurement

The relation between a magnetic-field vector observed on-board, *Hob*, (in the ship's fixed coordinate system) and the geomagnetic field vector, *F*, (in the Earth's fixed coordinate system) is expressed as:

$$Hob = A * R * P * Y * F + Hp \quad \text{(a)}$$

where, *R*, *P* and *Y* are the matrices of rotation due to roll, pitch and heading of a ship, respectively. *A* is a 3 x 3 matrix which represents magnetic susceptibility of the ship, and *Hp* is a magnetic field vector produced by a permanent magnetic moment of the ship's body. Rearrangement of Eq. (a) makes

$$R * Hob + Hbp = R * P * Y * F \quad \text{(b)}$$

where $R = A^{-1}$, and $Hbp = -R * Hp$. The magnetic field, *F*, can be obtained by measuring *R*, *P*, *Y* and *Hob*, if *R* and *Hbp* are known. Twelve constants in *R* and *Hbp* can be determined by measuring variation of *Hob* with *R*, *P* and *Y* at a place where the geomagnetic field, *F*, is known.

(4) Preliminary results

The results will be published after primary processing.

(5) Data Archive

All data obtained during this cruise will be submitted to the Data Management Group

(DMG) in JAMSTEC, and will be archived there

(6) Remarks (Times in UTC)

The following periods, we made a “figure-eight” turn (a pair of clockwise and anti-clockwise rotation) for calibration of the ship’s magnetic effect.

14:28 - 14:57 25 May 2019 around 32-16N, 144-18E
08:34 - 09:04 31 May 2019 around 46-58N, 159-56E
10:51 - 11:19 03 June 2019 around 50-00N, 165-00E
06:44 - 07:14 09 June 2019 around 44-00N, 155-01E

2.3 (a) Shipboard ADCP

Tetsuichi FUJIKI (JAMSTEC RIGC)
Ken'ichi SASAKI (JAMSTEC MIO)
Wataru TOKUNAGA (NME)
Satomi OGAWA (NME)
Yoichi INOUE (MIRAI crew)

(1) Objectives

To obtain continuous measurement data of the current profile along the ship's track.

(2) Instruments and methods

Upper ocean current measurements were made in this cruise, using the hull-mounted Acoustic Doppler Current Profiler (ADCP) system. For most of its operation, the instrument was configured for water-tracking mode. Bottom-tracking mode, interleaved bottom-ping with water-ping, was made to get the calibration data for evaluating transducer misalignment angle in the shallow water. The system consists of following components;

1. R/V MIRAI has installed the Ocean Surveyor for vessel-mount ADCP (frequency 76.8 kHz; Teledyne RD Instruments, USA). It has a phased-array transducer with single ceramic assembly and creates 4 acoustic beams electronically. We mounted the transducer head rotated to a ship-relative angle of 45 degrees azimuth from the keel.
2. For heading source, we use ship's gyro compass (Tokyo Keiki, Japan), continuously providing heading to the ADCP system directory. Additionally, we have Inertial Navigation System (Phins, IXBLUE SAS, France) which provide high-precision heading, attitude information, pitch and roll. They are stored in ".N2R" data files with a time stamp.
3. Differential GNSS system (StarPack-D, Fugro, Netherlands) providing precise ship's position.
4. We used VmDas software version 1.49(TRDI) for data acquisition.
5. To synchronize time stamp of ping with Computer time, the clock of the logging computer is adjusted to GPS time server continuously by the application software.
6. Fresh water is charged in the sea chest to prevent bio fouling at transducer face.
7. The sound speed at the transducer does affect the vertical bin mapping and vertical velocity measurement, and that is calculated from temperature, salinity (constant value; 35.0 PSU) and depth (6.5 m; transducer depth) by equation in Medwin (1975).

Data was configured for "8 m" layer intervals starting about 23m below sea surface, and recorded every ping as raw ensemble data (.ENR). Additionally, 15 seconds averaged data were recorded as short-term average (.STA). 300 seconds averaged data were long-term average (.LTA), respectively.

(3) Parameters

Major parameters for the measurement, Direct Command, are shown in Table 2.3.1.

Table 2.3.1. Major parameters

Bottom-Track Commands

BP = 001 Pings per Ensemble (almost less than 1,300m depth)

Environmental Sensor Commands

EA = 04500 Heading Alignment (1/100 deg)

ED = 00065 Transducer Depth (0 - 65535 dm)

EF = +001 Pitch/Roll Divisor/Multiplier (pos/neg) [1/99 - 99]

EH = 00000 Heading (1/100 deg)

ES = 35 Salinity (0-40 pp thousand)

EX = 00000 Coordinate Transform (Xform:Type; Tilts; 3Bm; Map)

EZ = 10200010 Sensor Source (C; D; H; P; R; S; T; U)

C (1): Sound velocity calculates using ED, ES, ET (temp.)

D (0): Manual ED

H (2): External synchro

P (0), R (0): Manual EP, ER (0 degree)

S (0): Manual ES

T (1): Internal transducer sensor

U (0): Manual EU

EV = 0 Heading Bias(1/100 deg)

Water-Track Commands

WA = 255 False Target Threshold (Max) (0-255 count)

WC = 120 Low Correlation Threshold (0-255)

WD = 111 100 000 Data Out (V; C; A; PG; St; Vsum; Vsum^2; #G; P0)

WE = 1000 Error Velocity Threshold (0-5000 mm/s)

WF = 0800 Blank After Transmit (cm)

WN = 100 Number of depth cells (1-128)

WP = 00001 Pings per Ensemble (0-16384)

WS = 800 Depth Cell Size (cm)

WV = 0390 Mode 1 Ambiguity Velocity (cm/s radial)

(4) Preliminary results

Horizontal velocity along the ship's track is presented in fig.2.3.1. In vertical direction, the data are averaged from 35 to 60m.

(5) Data Archives

All data obtained during this cruise will be submitted to the Data Management Group (DMG) in JAMSTEC, and will be archived there.

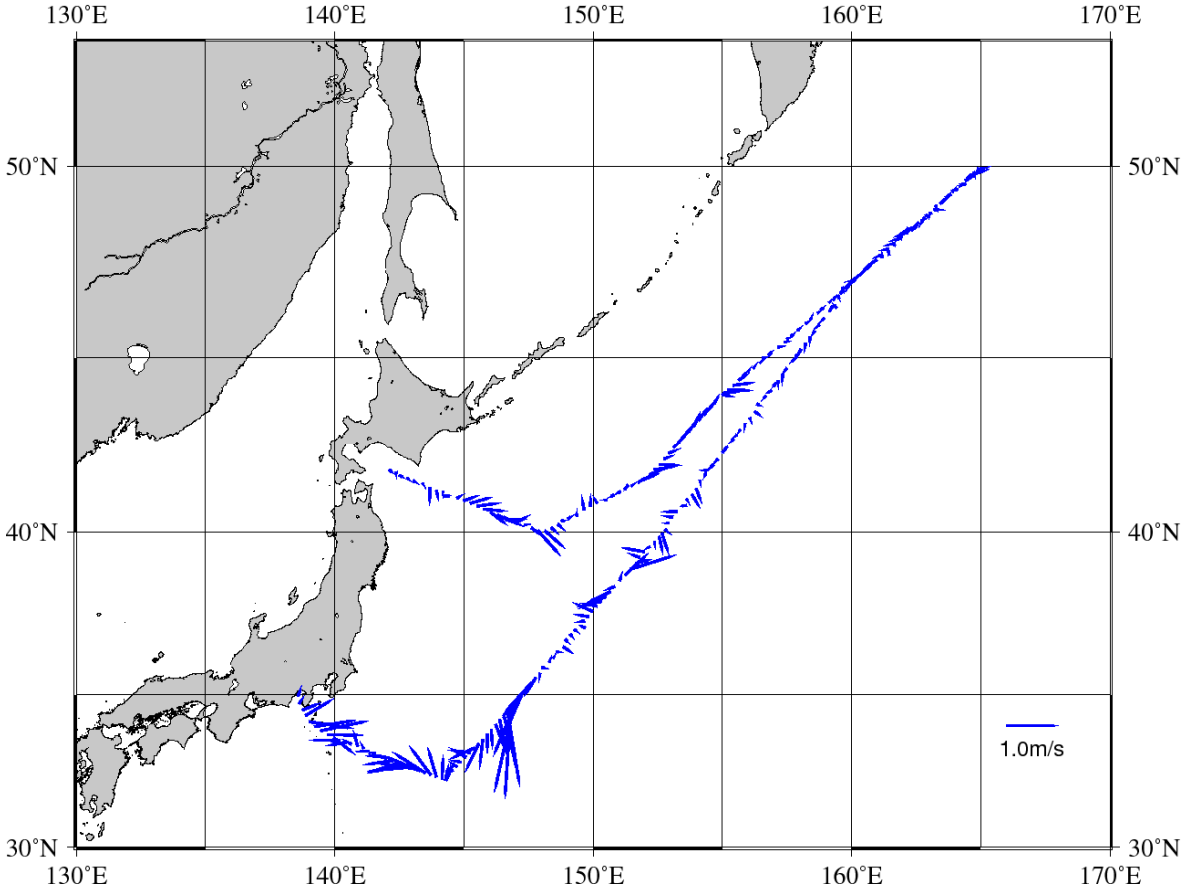

Fig.2.3.1. Horizontal Velocity along the ship's track
(60 min. Average / Layer:35-60m)

2.3 (b) Specific studies of ADCP in the east Tsugaru Strait

Tetsuichi FUJIKI (JAMSTEC RIGC)
Ken'ichi SASAKI (JAMSTEC MIO)

(1) Objectives

The Tsugaru Strait is a major strait connecting the Sea of Japan and the North Pacific. In the eastern part of this strait, surface current is constantly monitored by ocean radar. The current profile was acquired for the purpose of comparing with the radar data.

(2) Preliminary results

Horizontal velocity along the ship's track is presented in Fig.2.3.2. In vertical direction, the data are averaged from 35 to 60m. An example of radar data is also shown in Fig. 2.3.3 for reference.

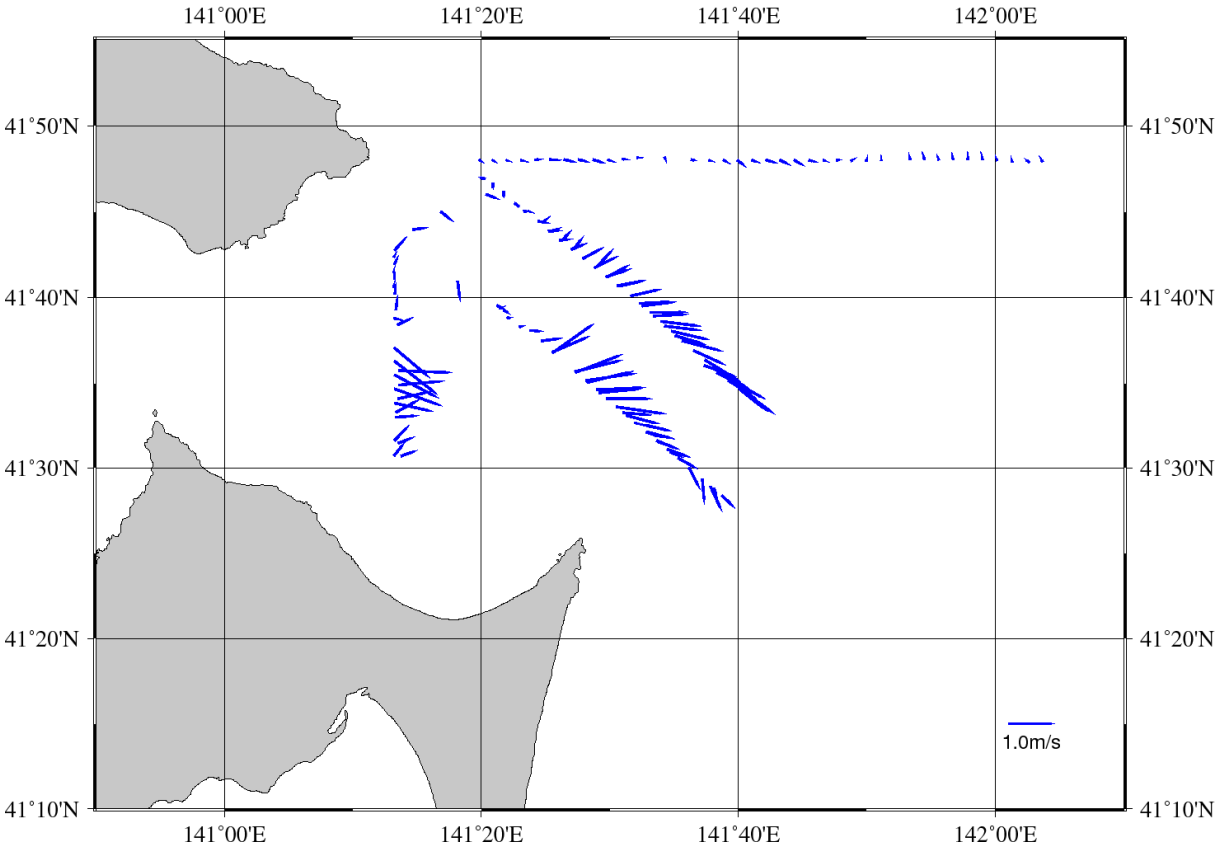

Fig.2.3.2. Horizontal Velocity around the east Tsugaru Strait
(5 min. Average / Layer:35-60m)

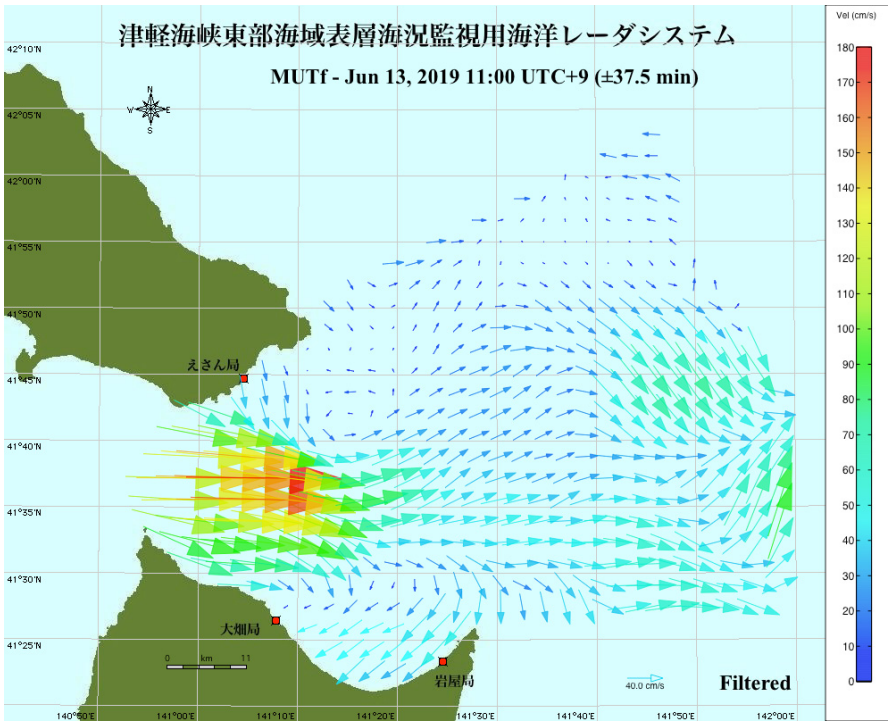

Fig.2.3.3. Example of surface current map of the east Tsugaru Strait observed by ocean radar

2.4 CTD cast and water sampling

Hiroshi UCHIDA (JAMSTEC RIGC)
Masahide WAKITA (JAMSTEC MIO)
Shinsuke TOYODA (MWJ)
Yasushi HASHIMOTO (MWJ)
Hironori SATO (MWJ)
Shintaro AMIKURA (MWJ)
Jun MATSUOKA (MWJ)

(1) Winch arrangements

The CTD package was deployed from starboard side by using 4.5 Ton Traction Winch System (Dynacon, Inc., Bryan, Texas, USA), which was renewed on the R/V Mirai in April 2014 (e.g. Fukasawa et al., 2004). Primary system components include a complete CTD Traction Winch System with a 9.53 mm armored cable (Rochester Wire & Cable, LLC, Culpeper, Virginia, USA).

(2) Overview of the equipment

The CTD system was SBE 911plus system (Sea-Bird Electronics, Inc., Bellevue, Washington, USA). The SBE 911plus system controls 12-, 24-, or 36-position SBE 32 Carousel Water Sampler. The Carousel accepts 12-litre Niskin-X water sample bottles (OTE model 110, Ocean Test Equipment, Fort Lauderdale, Florida, USA, or model 1010X, General Oceanics, Inc., Miami, Florida, USA). The SBE 9plus was mounted horizontally in a 36-position or 12-position carousel frame. SBE's temperature (SBE 3) and conductivity (SBE 4) sensor modules were used with the SBE 9plus underwater unit. The pressure sensor is mounted in the main housing of the underwater unit and is ported to outside through the oil-filled plastic capillary tube. A modular unit of underwater housing pump (SBE 5T) flushes water through sensor tubing at a constant rate independent of the CTD's motion, and pumping rate (3000 rpm) remain nearly constant over the entire input voltage range of 12-18 volts DC. Flow speed of pumped water in standard TC duct is about 2.4 m/s. One set or two sets of temperature and conductivity modules were used. An SBE's dissolved oxygen sensor (SBE 43) was placed between the primary conductivity sensor and the pump module. Auxiliary sensors, a Deep Ocean Standards Thermometer (SBE 35), an altimeter (PSA-916T; Teledyne Benthos, Inc., North Falmous, Massachusetts, USA), an oxygen optodes (RINKO-III; JFE Advantech Co., Ltd, Nishinomiya, Hyogo, Japan), a fluorometers (Seapoint sensors, Inc., Kingston, New Hampshire, USA), a transmissometer (C-Star Transmissometer; WET Labs, Inc., Philomath, Oregon, USA), a turbidity meter (Seapoint Sensors, Inc., Exeter, New Hampshire, USA), a Photosynthetically Active Radiation (PAR) sensor (Satlantic, LP, Halifax, Nova Scotia, Canada), a colored dissolved organic matter (Seapoint Sensors, Inc.), and a refractive index density sensor were also used with the SBE 9plus underwater unit.

To minimize rotation of the CTD package, a heavy stainless frame (total weight of the CTD package without sea water in the bottles is about 900 kg) was used with an aluminum plate (54 × 90 cm) and a compact underwater slip ring swivel (Hanayuu Co., Ltd., Shizuoka, Japan) (Uchida et al., 2018).

Summary of the system used in this cruise

36-position Carousel system

Deck unit:

SBE 11plus, S/N 11P54451-0872

Under water unit:

SBE 9plus, S/N 09P54451-1027 (117457)

Temperature sensor:

SBE 3, S/N 031524

Conductivity sensor:

SBE 4, S/N 041203

Oxygen sensor:

SBE 43, S/N 432471

JFE Advantech RINKO-III, S/N 0037 (foil batch no. 182822 with pressure aging)

Pump:

SBE 5T, S/N 054598

Altimeter:

PSA-916T, S/N 1157

Deep Ocean Standards Thermometer:

SBE 35, S/N 0045

Fluorometer:

Seapoint Sensors, Inc., S/N 3618 (measurement range: 0-15 g/L) (Gain: 10X)

Turbidity meter:

Seapoint Sensors, Inc., S/N 14953 (measurement range: 0-25 FTU) (Gain: 100X)

Transmissometer:

C-Star, S/N CST-1726DR

PAR:

Satlantic LP, S/N 1025

CDOM:

Seapoint Sensors, Inc., S/N 6223 (measurement range: 0-50 QSU) (Gain: 30X)

Carousel Water Sampler:

SBE 32, S/N 3227443-0391

Water sample bottle:

12-litre OTE model 110 (Ocean Test Equipment, Inc.)

(#1, #3-36: non Teflon coating or Teflon coating for clean sampling)

12-litter model 1010X (General Oceanics, Inc.)

(#2: non Teflon coating)

Refractive index density sensor:

JAMSTEC (see section 2.18)

12-position Carousel system

Deck unit:

SBE 11plus, S/N 11P54451-0872

Under water unit:

SBE 9plus, S/N 09P21746-0575 (79492)

Temperature sensor:

SBE 3, S/N 03P4421 (primary)

SBE 3, S/N 03P4418 (secondary)

Conductivity sensor:

SBE 4, S/N 043063 (primary)

SBE 4, S/N 043064 (secondary)

Pump:

SBE 5T, S/N 053293 (primary)

SBE 5T, S/N 053118 (secondary)

Carousel Water Sampler:

SBE 32, S/N 3222295-0171 (for station A07S003)

SBE 32, S/N 3221875-0240 (for stations A07S006 and A07S007)

Water sample bottle:

12-litre OTE model 110 (Ocean Test Equipment, Inc.)

(#1-12: Teflon coating)

(3) Pre-cruise calibration

i. Pressure

The Paroscientific series 4000 Digiquartz high pressure transducer (Model 415K: Paroscientific, Inc., Redmond, Washington, USA) uses a quartz crystal resonator whose frequency of oscillation varies with pressure induced stress with 0.01 per million of resolution over the absolute pressure range of 0 to 15000 psia (0 to 10332 dbar). Also, a quartz crystal temperature signal is used to compensate for a wide range of temperature changes at the time of an observation. The pressure sensor has a nominal accuracy of 0.015 % FS (1.5 dbar), typical stability of 0.0015 % FS/month (0.15 dbar/month), and resolution of 0.001 % FS (0.1 dbar). Since the pressure sensor measures the absolute value, it inherently includes atmospheric pressure (about 14.7 psi). SEASOFT subtracts 14.7 psi from computed pressure automatically.

Pre-cruise sensor calibrations for linearization were performed at SBE, Inc. The time drift of the pressure sensor is adjusted by periodic recertification corrections against electronic dead-weight testers (Model E-DWT-H, Fluke Co., Phoenix, Arizona, USA) calibrated by Ohte Giken, Inc., Tsukuba, Ibaraki, Japan.

A70 Me-L, S/N 181, 15 January 2019

A200Me-L, S/N 1305, 15 January 2019

The corrections are performed at JAMSTEC, Yokosuka, Kanagawa, Japan by Marine Works Japan Ltd. (MWJ), Yokohama, Kanagawa, Japan, usually once in a year in order to monitor sensor time drift and linearity.

S/N 1027, 19 April 2019

slope = 0.99987502

offset = −1.46467

S/N 0575, 18 April 2019

slope = 0.99978013

offset = 2.71561

ii. Temperature (SBE 3)

The temperature sensing element is a glass-coated thermistor bead in a stainless-steel tube, providing a pressure-free measurement at depths up to 10500 (6800) m by titanium (aluminum) housing. The SBE 3 thermometer has a nominal accuracy of 1 mK, typical stability of 0.2 mK/month, and resolution of 0.2 mK at 24 samples per second. The premium temperature sensor, SBE 3plus, is a more rigorously tested and calibrated version of standard temperature sensor (SBE 3).

Pre-cruise sensor calibrations were performed at SBE, Inc.

S/N 031525, 27 February 2019
S/N 03P4421, 25 October 2018
S/N 03P4418, 25 October 2018

iii. Conductivity (SBE 4)

The flow-through conductivity sensing element is a glass tube (cell) with three platinum electrodes to provide in-situ measurements at depths up to 10500 (6800) m by titanium (aluminum) housing. The SBE 4 has a nominal accuracy of 0.0003 S/m, typical stability of 0.0003 S/m/month, and resolution of 0.00004 S/m at 24 samples per second. The conductivity cells have been replaced to newer style cells for deep ocean measurements.

Pre-cruise sensor calibrations were performed at SBE, Inc.

S/N 041203, 21 February 2019
S/N 043063, 17 October 2018
S/N 043064, 17 October 2018

The value of conductivity at salinity of 35, temperature of 15 °C (IPTS-68) and pressure of 0 dbar is 4.2914 S/m.

iv. Oxygen (SBE 43)

The SBE 43 oxygen sensor uses a Clark polarographic element to provide in-situ measurements at depths up to 7000 m. The range for dissolved oxygen is 120 % of surface saturation in all natural waters, nominal accuracy is 2 % of saturation, and typical stability is 2 % per 1000 hours.

Pre-cruise sensor calibration was performed at SBE, Inc.

S/N 432471, 05 March 2019

v. Deep Ocean Standards Thermometer

Deep Ocean Standards Thermometer (SBE 35) is an accurate, ocean-range temperature sensor that can be standardized against Triple Point of Water and Gallium Melt Point cells and is also capable of measuring temperature in the ocean to depths of 6800 m. The SBE 35 was used to calibrate the SBE 3 temperature sensors in situ (Uchida et al., 2015).

Pre-cruise sensor linearization was performed at SBE, Inc.

S/N 0045, 27 October 2002

Then the SBE 35 is certified by measurements in thermodynamic fixed-point cells of the TPW (0.01 °C) and GaMP (29.7646 °C). The slow time drift of the SBE 35 is adjusted by periodic recertification corrections. Pre-cruise sensor calibration was performed at RIGC/JAMSTEC by using fixed-point cells traceable to NMIJ temperature standards.

S/N 0045, 1 April 2019 (slope and offset correction)

Slope = 1.000025

Offset = −0.001039

The time required per sample = 1.1 × NCYCLES + 2.7 seconds. The 1.1 seconds is total time per an acquisition cycle. NCYCLES is the number of acquisition cycles per sample and was set to 4. The 2.7 seconds is required for converting the measured values to temperature and storing average in EEPROM.

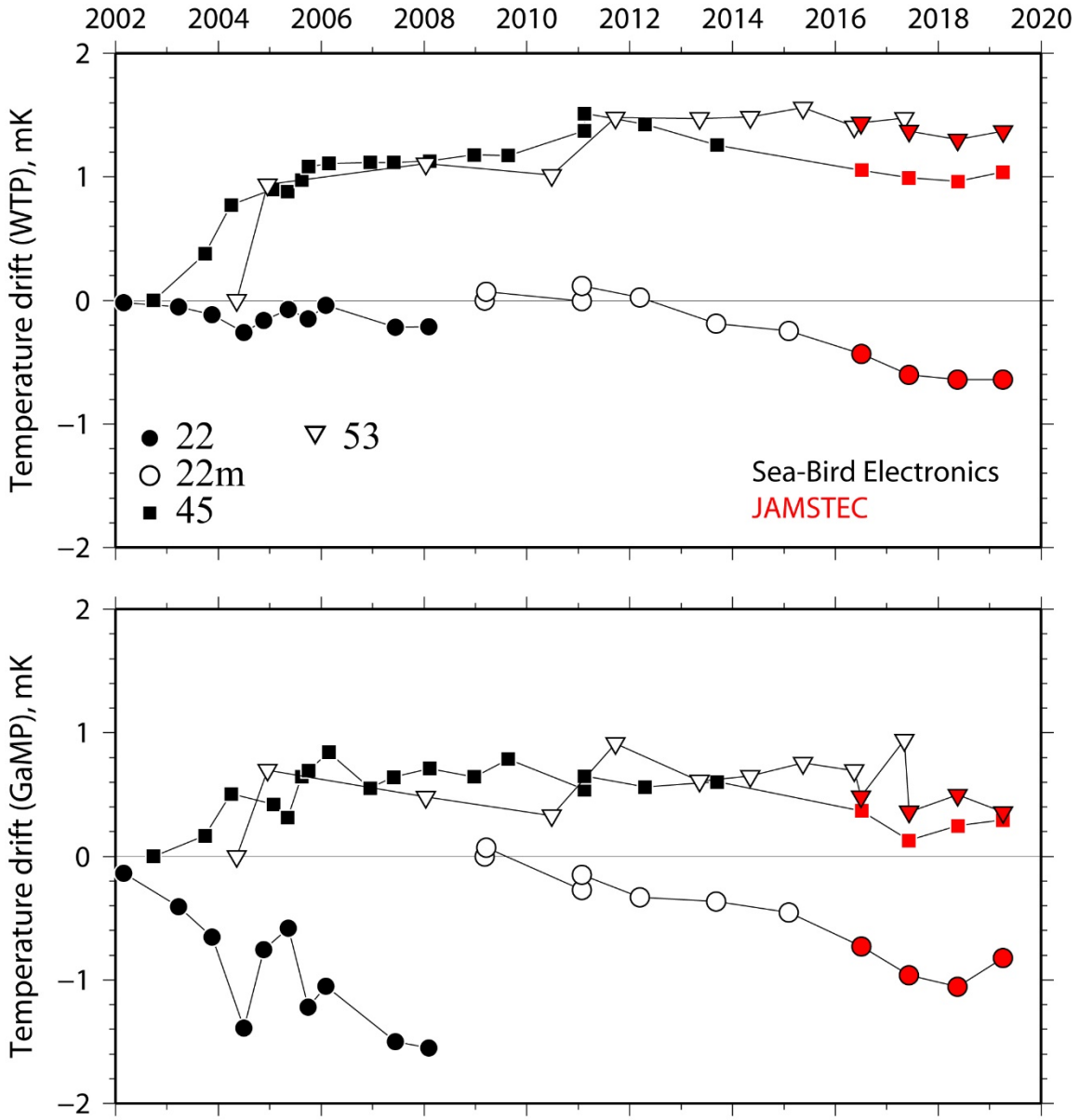

Figure 2.4.1. Time drifts (temperature offsets relative to the first calibration) of six reference thermometers (SBE 35) based on laboratory calibrations in fixed-point cells. Results performed at JAMSTEC are shown in red marks.

vi. Altimeter

Benthos PSA-916T Sonar Altimeter (Teledyne Benthos, Inc.) determines the distance of the target from the unit by generating a narrow beam acoustic pulse and measuring the travel time for the pulse to bounce back from the target surface. It is rated for operation in water depths up to 10000 m. The PSA-916T uses the nominal speed of sound of 1500 m/s.

vii. Oxygen optode (RINKO)

RINKO (JFE Advantech Co., Ltd.) is based on the ability of selected substances to act as dynamic fluorescence quenchers. RINKO model III is designed to use with a CTD system which accept an auxiliary analog sensor, and is designed to operate down to 7000 m.

Data from the RINKO can be corrected for the time-dependent, pressure-induced effect by means of the same method as that developed for the SBE 43 (Edwards et al., 2010). The calibration coefficients, H1 (amplitude of hysteresis correction), H2 (curvature function for hysteresis), and H3 (time constant for hysteresis) were determined empirically as follows.

H1 = 0.0065
H2 = 5000 dbar
H3 = 2000 seconds

Outputs from RINKO are the raw phase shift data. The RINKO can be calibrated by the modified Stern-Volmer equation slightly modified from a method by Uchida et al. (2010):

$$O_2\ (\mu mol/l) = [(V_0 / V)^E - 1] / K_{sv}$$

where V is voltage, V_0 is voltage in the absence of oxygen, K_{sv} is Stern-Volmer constant. The coefficient E corrects nonlinearity of the Stern-Volmer equation. The V_0 and the K_{sv} are assumed to be functions of temperature as follows.

$$K_{sv} = C_0 + C_1 \times T + C_2 \times T^2$$
$$V_0 = 1 + C_3 \times T$$
$$V = C_4 + C_5 \times V_b$$

where T is CTD temperature (°C) and V_b is raw output (volts). V_0 and V are normalized by the output in the absence of oxygen at 0°C. The oxygen concentration is calculated using accurate temperature data from the CTD temperature sensor instead of temperature data from the RINKO. The pressure-compensated oxygen concentration O_{2c} can be calculated as follows.

$$O_{2c} = O_2\ (1 + C_p p / 1000)$$

where p is CTD pressure (dbar) and C_p is the compensation coefficient. Since the sensing foil of the optode is permeable only to gas and not to water, the optode oxygen must be corrected for salinity. The salinity-compensated oxygen can be calculated by multiplying the factor of the effect of salt on the oxygen solubility (Garcia and Gordon, 1992).

Pre-cruise sensor calibrations were not performed.

viii. Fluorometer

The Seapoint Chlorophyll Fluorometer (Seapoint Sensors, Inc., Kingston, New Hampshire, USA) provides in-situ measurements of chlorophyll-a at depths up to 6000 m. The instrument uses modulated blue LED lamps and a blue excitation filter to excite chlorophyll-a. The fluorescent light emitted by the chlorophyll-a passes through a red emission filter and is detected by a silicon photodiode. The low level signal is then processed using synchronous demodulation circuitry, which generates an output voltage proportional to chlorophyll-a concentration.

ix. Transmissometer

The C-Star Transmissometer (WET Labs, Inc., Philomath, Oregon, USA) measures light transmittance at a single wavelength (650 nm) over a know path (25 cm). In general, losses of light propagating through water can be attributed to two primary causes: scattering and absorption. By projecting a collimated beam of light through the water and placing a focused receiver at a known distance away, one can quantify these losses. The ratio of light gathered by the receiver to the amount originating at the source is known as the beam transmittance. Suspended particles, phytoplankton, bacteria and dissolved organic matter contribute to the losses sensed by the instrument. Thus, the instrument provides information both for an indication of the total concentrations of matter in the water as well as for a value of the water clarity.

Light transmission T_r (in %) and beam attenuation coefficient c_p are calculated from the sensor output (V in volt) as follows.

$$T_r = (c_0 + c_1 V) \times 100$$

$$c_p = -(1 / 0.25) \ln(T_r / 100)$$

x. Turbidity meter

The Seapoint turbidity meter (Seapoint Sensors, Inc., Kingston, New Hampshire, USA) detects light scattered by particles suspended in water at depths up to 6000 m. The sensor generates an output voltage proportional to turbidity or suspended solids. The unique optical design confines the sensing volume to within 5 cm of the sensor.

xi. PAR

Photosynthetically Active Radiation (PAR) sensors (Satlantic, LP, Halifax, Nova Scotia, Canada) provide highly accurate measurements of PAR (400 – 700 nm) for a wide range of aquatic and terrestrial applications. The ideal spectral response for a PAR sensor is one that gives equal emphasis to all photons between 400 – 700 nm. Satlantic PAR sensors use a high quality filtered silicon photodiode to provide a near equal spectral response across the entire wavelength range of the measurement.

Pre-cruise sensor calibration was performed at Satlantic, LP.

S/N 1025, 6 July 2015

xii. CDOM

The Seapoint Ultraviolet Fluorometer (SUVF) is a high-performance, low power instrument for in situ measurement of chromophoric dissolved organic matter (CDOM) at depths up to 6000 m. The SUVF uses modulated ultraviolet LED lamps and optical filter for excitation. The fluorescent light signal passes through a blue emission filter and is detected by a silicon photodiode. The SUFV is operated without a pump and the sensing volume is left open to the surrounding water.

(4) Data collection and processing

i. Data collection

CTD system was powered on at least 20 minutes in advance of the data acquisition to stabilize the pressure sensor and was powered off at least two minutes after the operation in order to acquire pressure data on the ship's deck.

The package was lowered into the water from the starboard side and held 10 m beneath the

surface in order to activate the pump. After the pump was activated, the package was lifted to the surface and lowered at a rate of 1.0 m/s to 200 m (or 300 m when significant wave height was high) then the package was stopped to operate the heave compensator of the crane. The package was lowered again at a rate of 1.2 m/s to the bottom. For the up cast, the package was lifted at a rate of 1.1 m/s except for bottle firing stops. As a rule, the bottle was fired after waiting from the stop for more than 30 seconds and the package was stayed at least 5 seconds for measurement of the SBE 35 at each bottle firing stops. For depths where vertical gradient of water properties was expected to be large (from surface to thermocline), the bottle was exceptionally fired after waiting from the stop for 60 seconds to enhance exchanging the water between inside and outside of the bottle. At 200 m (or 300 m) from the surface, the package was stopped to stop the heave compensator of the crane.

Water samples were collected using a SBE 32 Carousel Water Sampler with 12-litre Niskin-X bottles.

Data acquisition software

SEASAVE-Win32, version 7.23.2

iii. Data processing

SEASOFT consists of modular menu driven routines for acquisition, display, processing, and archiving of oceanographic data acquired with SBE equipment. Raw data are acquired from instruments and are stored as unmodified data. The conversion module DATCNV uses instrument configuration and calibration coefficients to create a converted engineering unit data file that is operated on by all SEASOFT post processing modules. The following are the SEASOFT and original software data processing module sequence and specifications used in the reduction of CTD data in this cruise.

Data processing software

SBEDataProcessing-Win32, version 7.26.7.114

DATCNV converted the raw data to engineering unit data. DATCNV also extracted bottle information where scans were marked with the bottle confirm bit during acquisition. The duration was set to 4.4 seconds, and the offset was set to 0.0 second. The hysteresis correction for the SBE 43 data (voltage) was applied for both profile and bottle information data.

TCORP (original module, version 1.1) corrected the pressure sensitivity of the SBE 3 for both profile and bottle information file.

RINKOCOR (original module, version 1.0) corrected the time-dependent, pressure-induced effect (hysteresis) of the RINKO for both profile data.

RINKOCORROS (original module, version 1.0) corrected the time-dependent, pressure-induced effect (hysteresis) of the RINKO for bottle information data by using the hysteresis-corrected profile data.

BOTTLESUM created a summary of the bottle data. The data were averaged over 4.4 seconds.

ALIGNCTD converted the time-sequence of sensor outputs into the pressure sequence to ensure that all calculations were made using measurements from the same parcel of water. For an SBE 9plus CTD with the ducted temperature and conductivity sensors and a 3000-rpm pump, the typical net advance of the conductivity relative to the temperature is 0.073 seconds. So, the SBE 11plus deck unit was set to advance the primary and the secondary conductivity for 1.73 scans (1.75/24 = 0.073 seconds). However, since many spikes were observed in salinity/density data, the conductivity data was compensated by 0.020 seconds returning sensor output relative to the temperature data. Oxygen data are also systematically delayed with respect to depth mainly because of the long time constant of the oxygen

sensor and of an additional delay from the transit time of water in the pumped plumbing line. This delay was compensated by 5 seconds advancing the SBE 43 oxygen sensor output (voltage) relative to the temperature data. Delay of the RINKO data was also compensated by 1 second advancing sensor output (voltage) relative to the temperature data. Delay of the transmissometer data was also compensated by 2 seconds advancing sensor output (voltage) relative to the temperature data. Delay of the transmissometer data was also compensated by 2 seconds advancing sensor output (voltage) relative to the temperature data.

WILDEDIT marked extreme outliers in the data files. The first pass of WILDEDIT obtained an accurate estimate of the true standard deviation of the data. The data were read in blocks of 1000 scans. Data greater than 10 standard deviations were flagged. The second pass computed a standard deviation over the same 1000 scans excluding the flagged values. Values greater than 20 standard deviations were marked bad. This process was applied to pressure, temperature, conductivity, and SBE 43 output.

CELLTM used a recursive filter to remove conductivity cell thermal mass effects from the measured conductivity. Typical values used were thermal anomaly amplitude alpha = 0.03 and the time constant 1/beta = 7.0.

FILTER performed a low pass filter on pressure with a time constant of 0.15 seconds. In order to produce zero phase lag (no time shift) the filter runs forward first then backwards.

WFILTER performed as a median filter to remove spikes in fluorometer, turbidity meter, transmissometer, and CDOM data. A median value was determined by 49 scans of the window. For CDOM data, an additional box-car filter with a window of 361 scans was applied to remove noise.

SECTIONU (original module, version 1.1) selected a time span of data based on scan number in order to reduce a file size. The minimum number was set to be the start time when the CTD package was beneath the sea-surface after activation of the pump. The maximum number was set to be the end time when the depth of the package was 1 dbar below the surface. The minimum and maximum numbers were automatically calculated in the module.

LOOPEDIT marked scans where the CTD was moving less than the minimum velocity of 0.0 m/s (traveling backwards due to ship roll).

DESPIKE (original module, version 1.0) removed spikes of the data. A median and mean absolute deviation was calculated in 1-dbar pressure bins for both down- and up-cast, excluding the flagged values. Values greater than 4 mean absolute deviations from the median were marked bad for each bin. This process was performed 2 times for temperature, conductivity, SBE 43, and RINKO output.

DERIVE was used to compute oxygen (SBE 43).

BINAVG averaged the data into 1-dbar pressure bins. The center value of the first bin was set equal to the bin size. The bin minimum and maximum values are the center value plus and minus half the bin size. Scans with pressures greater than the minimum and less than or equal to the maximum were averaged. Scans were interpolated so that a data record exist every dbar.

BOTTOMCUT (original module, version 0.1) deleted the deepest pressure bin when the averaged scan number of the deepest bin was smaller than the average scan number of the bin just above.

DERIVE was re-used to compute salinity, potential temperature, and density.

SPLIT was used to split data into the down cast and the up cast.

Remaining spikes in the CTD data were manually eliminated from the 1-dbar-averaged data. The data gaps resulting from the elimination were linearly interpolated with a quality flag of 6.

(5) Post-cruise calibration

Post-cruise calibration was performed only for the 36-position Carousel CTD system, data necessary for in-situ calibration was not taken from the 12-position Carousel CTD system.

i. Pressure

The CTD pressure sensor offset in the period of the cruise was estimated from the pressure readings on the ship deck. For best results the Paroscientific sensor was powered on for at least 20 minutes before the operation. In order to get the calibration data for the pre- and post-cast pressure sensor drift, the CTD deck pressure was averaged over first and last one minute, respectively. Then the atmospheric pressure deviation from a standard atmospheric pressure (14.7 psi) was subtracted from the CTD deck pressure to check the pressure sensor time drift. The atmospheric pressure was measured at the captain deck (20 m high from the base line) and sub-sampled one-minute interval as a meteorological data.

The pre- and the post-casts deck pressure data showed temperature dependency for the pressure sensor (Fig. 2.4.2). The post-cruise correction of the pressure data is not deemed necessary for the pressure sensor.

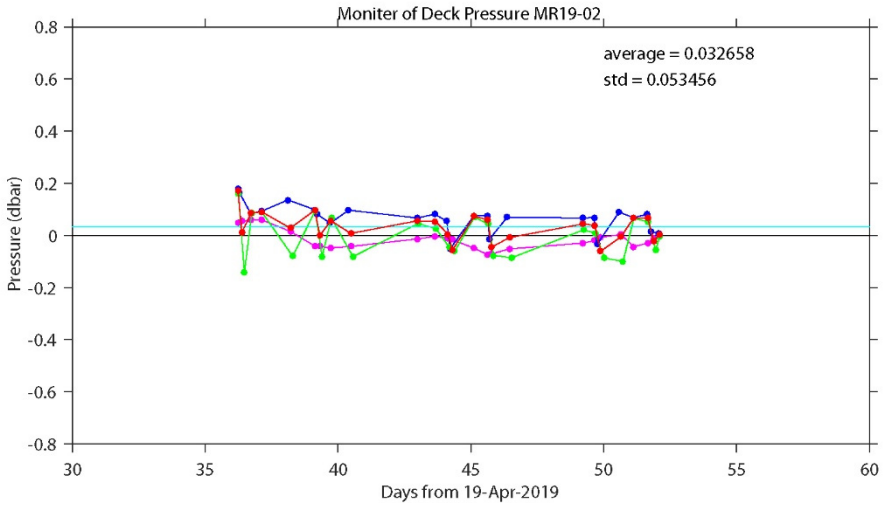

Figure 2.4.2. Time series of the CTD deck pressure. Atmospheric pressure deviation (magenta dots) from a standard atmospheric pressure was subtracted from the CTD deck pressure. Blue and green dots indicate pre- and post-cast deck pressures, respectively. Red dots indicate averages of the pre- and the post-cast deck pressures.

ii. Temperature

The CTD temperature sensors (SBE 3) were calibrated with the SBE 35 according to a method by Uchida et al. (2015). Post-cruise sensor calibration for the SBE 35 will be performed at JAMSTEC in April 2020. The CTD temperature was calibrated as

Calibrated temperature = $T - (c_0 \times P + c_1)$

c_0 = 7.93713835e-09

c_1 = 2.6414e-04

where T is CTD temperature in °C, P is pressure in dbar, and c_0 and c_1 are calibration coefficients. The

coefficients were determined using the data for the depths deeper than 1950 dbar. The primary temperature data were used for the post-cruise calibration. The result of the post-cruise calibration is shown in Figs. 2.4.3.

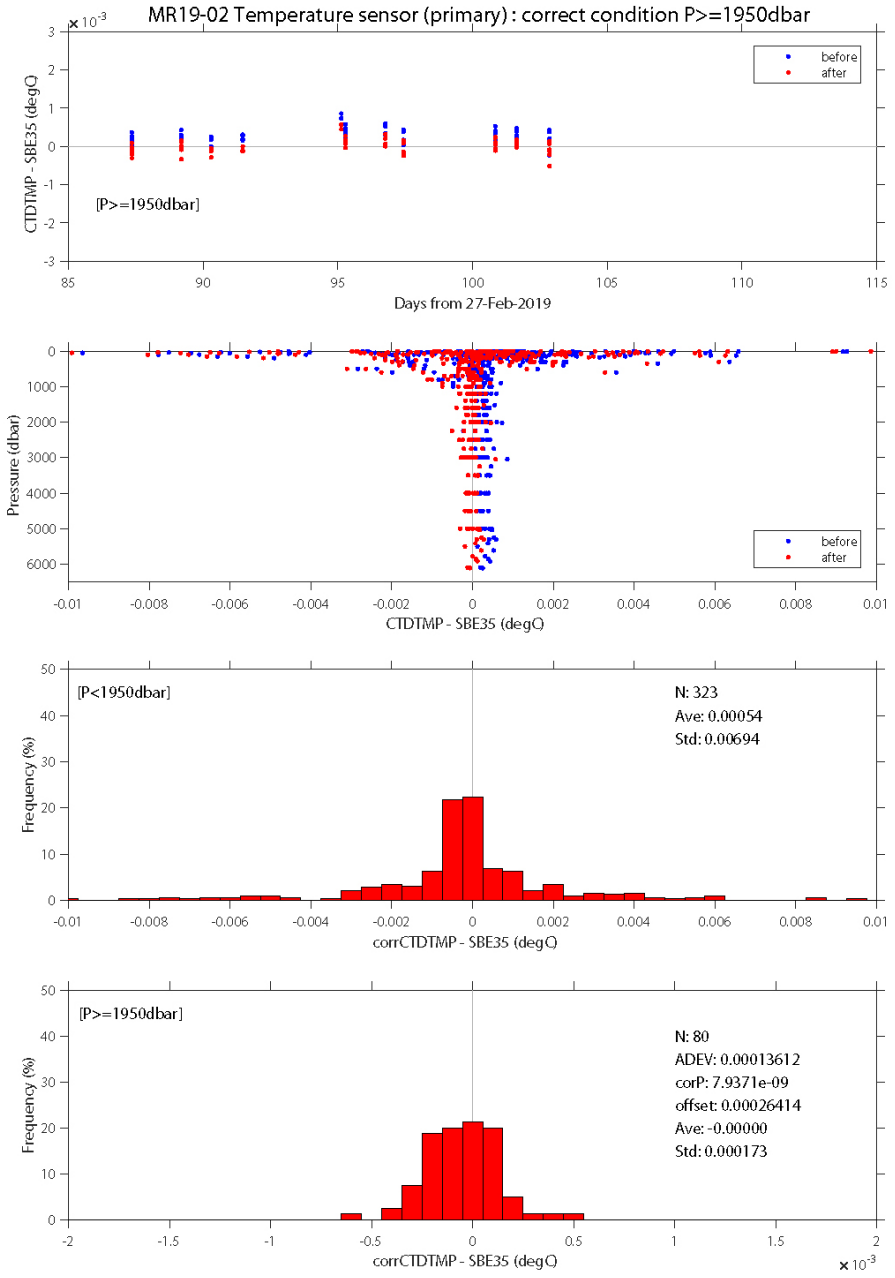

Figure 2.4.3. Difference between the CTD temperature and the SBE 35. Blue and red dots indicate before and after the post-cruise calibration using the SBE 35 data, respectively. Lower two panels show histogram of the difference after the calibration.

iii. Salinity

The discrepancy between the CTD conductivity and the conductivity calculated from the bottle salinity data with the CTD temperature and pressure data is considered to be a function of conductivity and pressure. The CTD conductivity was calibrated as

Calibrated conductivity =

$C - (c_0 \times C + c_1 \times P + c_2 \times C \times P + c_3 \times P^2 + c_4 \times C \times P^2 + c_5 \times C^2 \times P^2 + c_6 \times t + c_7)$

c_0 = 8.0106544413e-05

c_1 = -1.6747631815e-06

c_2 = 6.4774156818e-07

c_3 = 2.3979363885e-10

c_4 = -3.2639816208e-10

c_5 = 7.2277345111e-11

c_6 = 4.7014622630e-06

c_7 = -5.3783717140e-04

where C is CTD conductivity in S/m, P is pressure in dbar, t is time in days, and c_0, c_1, c_2, c_3, c_4, c_5, c_6 and c_7 are calibration coefficients. The best fit sets of coefficients were determined by a least square technique to minimize the deviation from the conductivity calculated from the bottle salinity data. The primary conductivity data created by the software module ROSSUM were used after the post-cruise calibration for the temperature data. Data obtained in leg 1 were only used to determine the coefficients. The results of the post-cruise calibration for the CTD salinity is shown in Fig. 2.4.4.

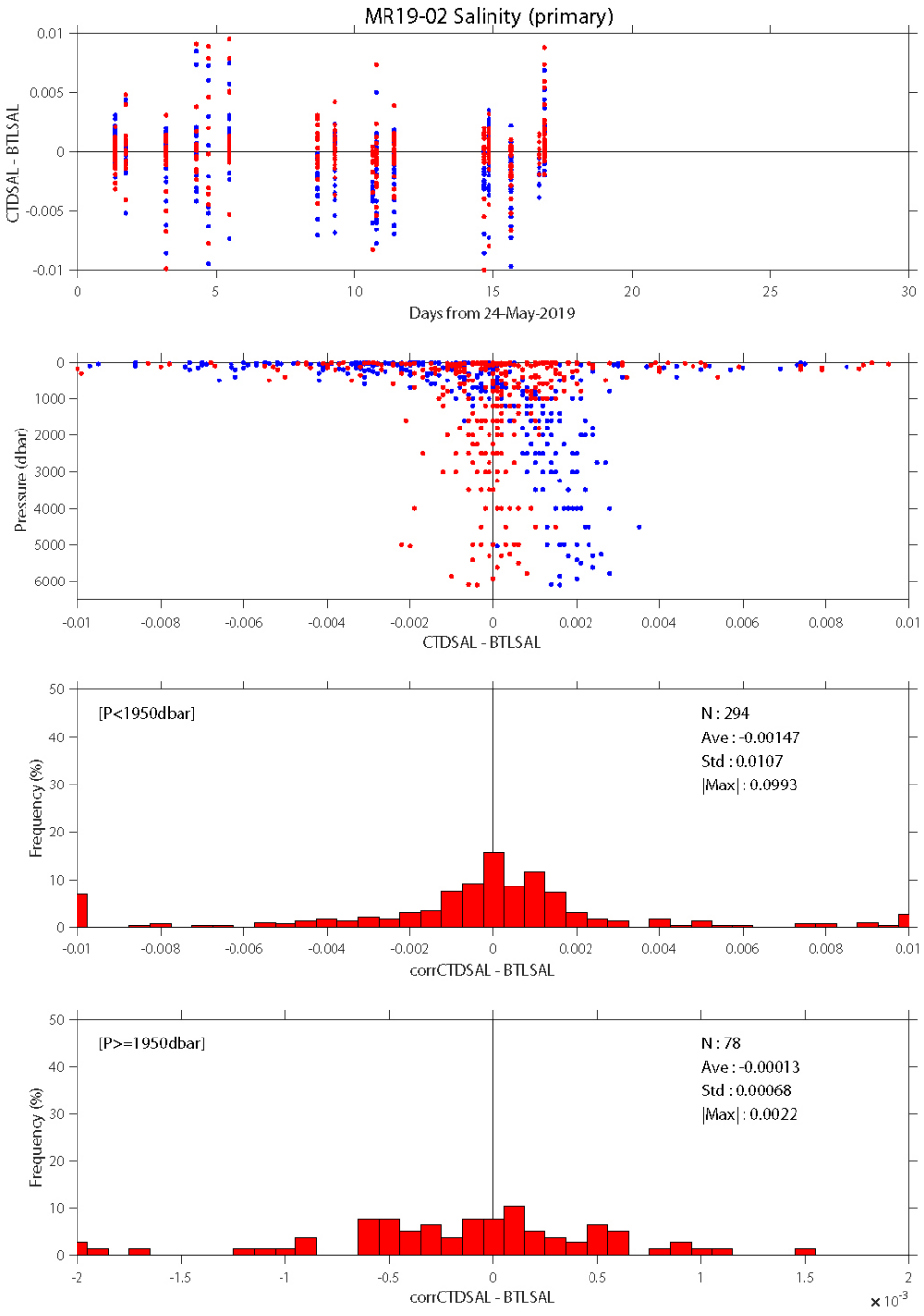

Figure 2.4.4. Difference between the CTD salinity (primary) and the bottle salinity. Blue and red dots indicate before and after the post-cruise calibration, respectively. Lower two panels show histogram of the difference after the calibration.

iv. Dissolved oxygen

The RINKO oxygen sensor was calibrated and used as the CTD oxygen data, since the RINKO has a fast time response. The pressure-hysteresis corrected RINKO data was calibrated by the modified Stern-Volmer equation, basically according to a method by Uchida et al. (2010) with slight modification:

$$[O_2]\ (\mu mol/l) = [(V_0 / V)^{1.2} - 1] / K_{sv} \times (1 + C_p \times P / 1000)$$

and

$$K_{sv} = C_0 + C_1 \times T + C_2 \times T^2$$
$$V_0 = 1 + C_3 \times T$$
$$V = C_4 + C_5 \times V_b + C_6 \times t + C_7 \times t \times V_b$$
$$C_0 = 4.493515397185548e\text{-}03$$
$$C_1 = 1.686060883288776e\text{-}04$$
$$C_2 = 2.990764054512574e\text{-}06$$
$$C_3 = -1.926000872481562e\text{-}03$$
$$C_4 = -7.966711319581195e\text{-}02$$
$$C_5 = 0.2993992466127368$$
$$C_6 = -1.460100704573292e\text{-}03$$
$$C_7 = 1.028318760264891e\text{-}03$$
$$C_p = 0.024$$

where V_b is the RINKO output (voltage), V_0 is voltage in the absence of oxygen, T is temperature in °C, P is pressure in dbar, t is exciting time (days) integrated from the first CTD cast, and C0, C1, C2, C3, C4, C5, C6, C7, and Cp are calibration coefficients. The calibration coefficients were determined by minimizing the sum of absolute deviation with a weight from the bottle oxygen data. The revised quasi-Newton method (DMINF1) was used to determine the sets. The post-cruise calibrated temperature and salinity data were used for the calibration. Data obtained in legs 1 and 2 were used to determine the coefficients. The results of the post-cruise calibration for the RINKO oxygen is shown in Fig. 2.4.5.

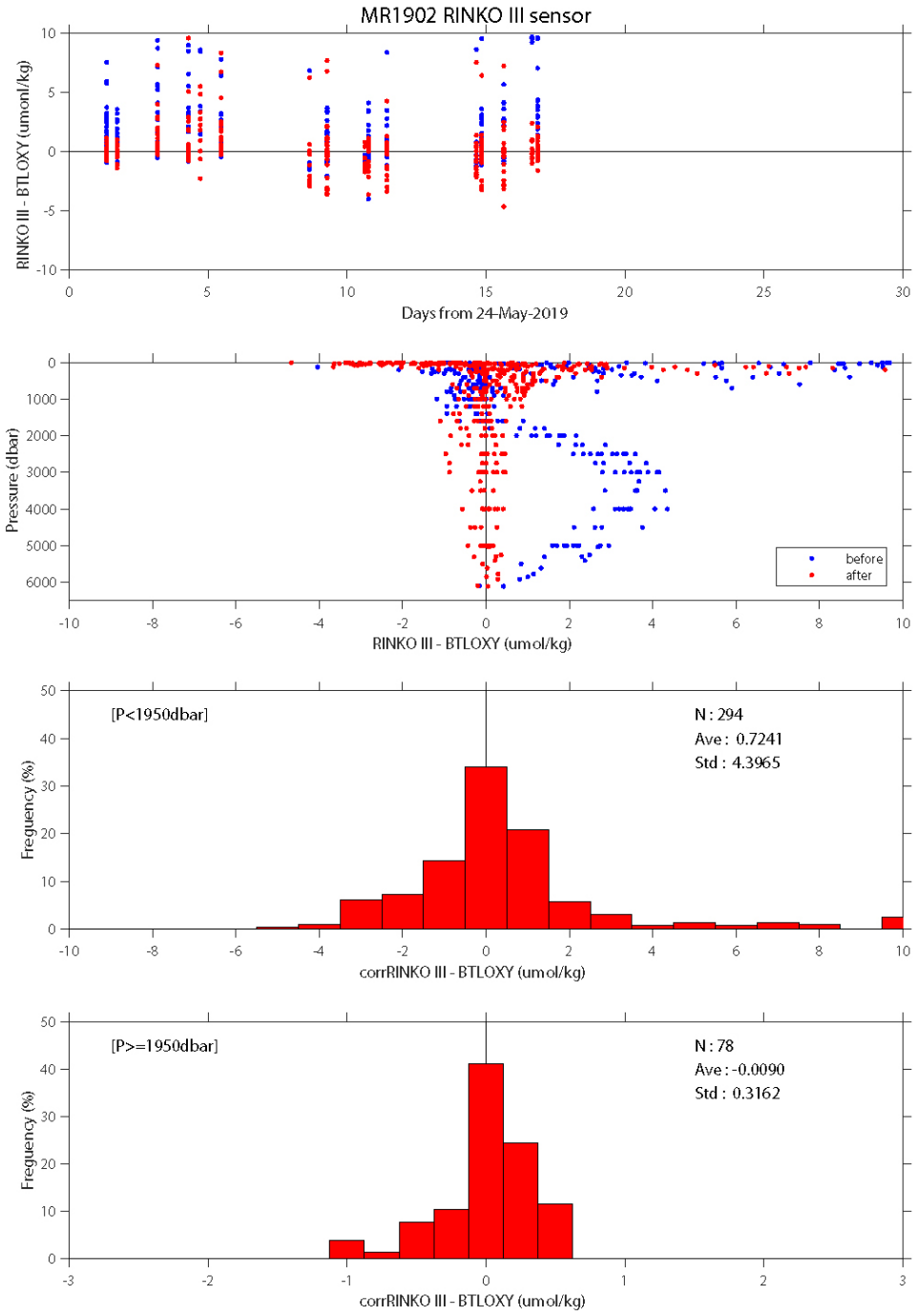

Figure 2.4.5. Difference between the CTD oxygen and the bottle oxygen. Blue and red dots indicate before and after the post-cruise calibration, respectively. Lower two panels show histogram of the difference after the calibration.

v. Fluorescence

The CTD fluorometer (FLUOR in µg/L) was calibrated by comparing with the bottle sampled chlorophyll-a as

$FLUORc = c_0 + c_1 \times FLUOR$

For A01, A05, A06, A07, A09, A10, A11

$c_0 = -0.0235275025536116$, $c_1 = 0.784250085120388$ (for FLUOR < 0.5)

$c_0 = 0.100582179379197$, $c_1 = 0.536030721254772$ (for FLUOR >= 0.5)

For A02, A03, A04

$c_0 = -0.0191574316656626$, $c_1 = 0.638581055522087$ (for FLUOR < 0.5)

$c_0 = 0.197764848604389$, $c_1 = 0.204736494981984$ (for FLUOR >= 0.5)

For A08

$c_0 = -0.0554800612739042$, $c_1 = 1.84933537579681$ (for FLUOR < 0.3)

$c_0 = 0.291864623797961$, $c_1 = 0.691519758890591$ (for FLUOR >= 0.3)

where c_0 and c_1 are calibration coefficients. The bottle sampled data obtained at dark condition [PAR (Photosynthetically Available Radiation) < 50 µE/(m^2 sec)] were used for the calibration, since sensitivity of the fluorometer to chlorophyll *a* is different at nighttime and daytime. The results of the post-cruise calibration for the fluorometer is shown in Fig. 2.4.6.

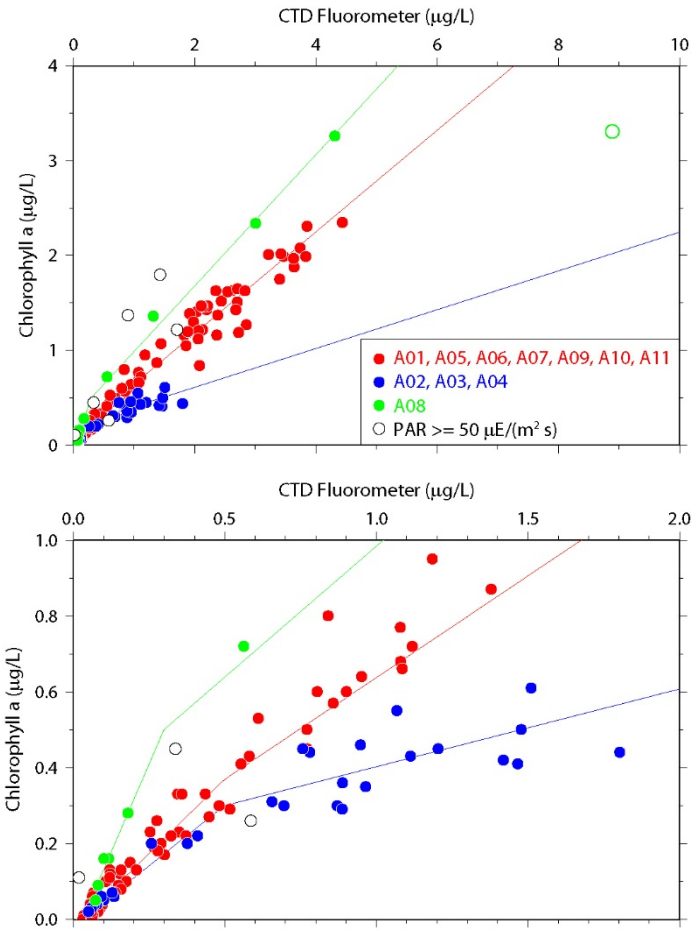

Figure 2.4.6. Comparison of the CTD fluorometer and the bottle sampled chlorophyll-a. The regression lines are also shown.

vi. Transmission

The transmissometer (T_r in %) is calibrated as

$T_r = (V–V_d) / (V_r–V_d) \times 100$

wehre V is the measured signal (voltage), V_d is the dark offset for the instrument, and V_r is the signal for clear water. V_d can be obtained by blocking the light path. V_d and V_{air}, which is the signal for air, were measured on deck before each cast after wiping the optical windows with ethanol. V_d was constant (0.0012) during the cruise. Vr is estimated from the measured maximum signal in the deep ocean at each cast. Since the transmissometer drifted in time, Vr is expressed as

$V_r = c_0 \times \exp(c_1 \times t) + c_2 \times t + c_3$

$c_0 = 4.960194543272681e-02$

$c_1 = -0.3587755284514953$

$c_2 = 6.546883624954382e-03$

$c_3 = 4.633426048332384$

where t is working time (in days) of the transmissometer from the first cast, and c_0, c_1, c_2 and c_3 are calibration coefficients. Maximum signal was extracted for each cast. Data whose depth of the maximum signal was shallower than 1300 dbar were not used to estimate V_r.

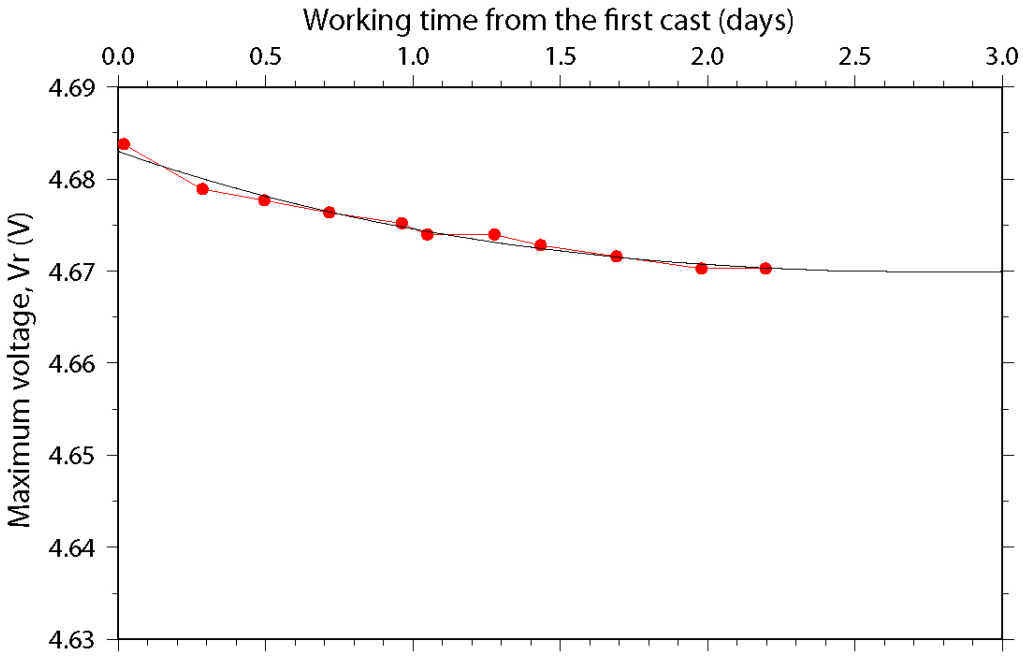

Figure 2.4.7. Time series of the maximum signal (Vr). The fitting curve is also shown.

vii. Colored dissolved organic material

It is known that output from the CDOM sensor is affected by the temperature change (Yamashita et al., 2015). The temperature effect on the CDOM sensor was evaluated in the laboratory before and after the cruise. The effect of temperature is standardized as:

$CDOM_r = CDOM / [1 + \rho \times (T - T_r)]$

$T_r = 20.0$

$\rho = -0.0062$

where CDOM is the output from the CDOM sensor, T is temperature in °C, Tr is reference temperature, and ρ is the temperature coefficient ($°C^{-1}$). Since output from the CDOM sensor was largely shifted in leg 1, the temperature coefficient evaluated after the cruise is used. In addition, Pressure hysteresis (difference between down- and up-cast profiles) was seen in the output. Therefore, the down-cast profile was corrected to much with up-cast profile as:

$CDOM_c = CDOM_r \times (1 - c_0 \times [P_{max} - P])$

For A01

$c_0 = 3.5e\text{-}6$

$P_{max} = P_{max}$

For A02, A03

$c_0 = 3.5e\text{-}6$

$P_{max} = 4000$ dbar

For A04

$c_0 = 3.5e\text{-}6$

$P_{max} = 3000$ dbar

For A06, A07, A08, A09, A10, A11

$c_0 = 0.0$

where P is pressure in dbar, P_{max} is maximum pressure in dbar at the cast, and c_0 is the correction coefficient.

viii. Photosynthetically active radiation

The PAR sensor was calibrated with an offset correction. The offset was estimated from the data measured in the deep ocean during the cruise. The corrected data (PARc) is calculated from the raw data (PAR) as follows:

$PARc\ [\mu E\ m^{-2}\ s^{-1}] = PAR - 0.104.$

(6) References

Edwards, B., D. Murphy, C. Janzen and N. Larson (2010): Calibration, response, and hysteresis in deep-sea dissolved oxygen measurements, J. Atmos. Oceanic Technol., 27, 920–931.

Fukasawa, M., T. Kawano and H. Uchida (2004): Blue Earth Global Expedition collects CTD data aboard Mirai, BEAGLE 2003 conducted using a Dynacon CTD traction winch and motion-compensated crane, Sea Technology, 45, 14–18.

García, H. E. and L. I. Gordon (1992): Oxygen solubility in seawater: Better fitting equations. Limnol. Oceanogr., 37 (6), 1307–1312.

Uchida, H., G. C. Johnson, and K. E. McTaggart (2010): CTD oxygen sensor calibration procedures,

The GO-SHIP Repeat Hydrography Manual: A collection of expert reports and guidelines, IOCCP Rep., No. 14, ICPO Pub. Ser. No. 134. Yamashita, Y., C.-J. Liu, H. Ogawa, J. Nishioka, H. Obata, and H. Saito (2015): Application of an in situ fluorometer to determine the distribution of fluorescent organic matter in the open ocean, *Marine Chemistry*, 177, 298–305.

Uchida, H., T. Nakano, J. Tamba, J.V. Widiatmo, K. Yamazawa, S. Ozawa, and T. Kawano (2015): Deep ocean temperature measurement with an uncertainty of 0.7 mK, *J. Atmos. Oceanic Technol.*, 32, 2199–2210, doi:10.1175/JTECH-D-15-0013.1.

Uchida, H., Y. Maeda, and S. Kawamata (2018): Compact underwater slip ring swivel, Minimizing effect of CTD package rotation on data quality, *Sea Technology*, 30–32, November.

(7) Data archive

These data obtained in this cruise will be submitted to the Data Management Group of JAMSTEC, and will be opened to the public via "Data Research System for Whole Cruise Information in JAMSTEC (DARWIN)" in JAMSTEC web site.
<http://www.godac.jamstec.go.jp/darwin/e>

2.5 Salinity measurement

Masahide WAKITA (JAMSTEC MIO)
Shungo OSHITANI (MWJ)

(1) Objective

To measure bottle salinity obtained by CTD casts, bucket sampling, RAS, and the continuous sea surface water monitoring system (TSG).

(2) Methods

a. Salinity Sample Collection

Seawater samples were collected with 12 liter water sampling bottles, bucket, RAS, and TSG. The salinity sample bottles of the 250ml brown glass bottles with screw caps were used for collecting the sample water. Each bottle was rinsed three times with the sample water, and filled with sample water to the bottle shoulder. The salinity sample bottles for TSG were sealed with a plastic cone and screw cap because we took into consideration the possibility of storage for about one month. These caps were rinsed three times with the sample water before use. The bottles were stored for more than 24 hours in the laboratory before the salinity measurement.

The Kind and number of samples taken as shown as follows;

Table 2.5-1 Kind and number of samples

Kind of Samples	Number of samples
Samples for CTD and Bucket	408
Samples for RAS	58
Samples for TSG	18
Total	484

b. Instruments and Method

The salinity measurement on R/V MIRAI was carried out during the cruise of MR19-02 using the salinometer (Model 8400B “AUTOSAL”; Guildline Instruments Ltd.: S/N 72874) with an additional peristaltic-type intake pump (Ocean Scientific International, Ltd.). Three precision digital thermometers (1502A; FLUKE: S/N B78466 and B81549) were used for monitoring the ambient temperature and the bath temperature of the salinometers.

The specifications of AUTOSAL salinometer and thermometer are shown as follows;

Salinometer (Model 8400B “AUTOSAL”; Guildline Instruments Ltd.)

Measurement Range	: 0.005 to 42 (PSU)
Accuracy	: Better than ±0.002 (PSU) over 24 hours without re-standardization
Maximum Resolution	: Better than ±0.0002 (PSU) at 35 (PSU)

Thermometer (1502A: FLUKE)

Measurement Range	: 16 to 30 deg C (Full accuracy)
Resolution	: 0.001 deg C
Accuracy	: 0.006 deg C (@ 0 deg C)

The measurement system was almost the same as Aoyama *et al.* (2002). The salinometer was operated in the air-conditioned ship's laboratory at a bath temperature of 24 deg C. The ambient temperature varied from approximately 21 deg C to 23 deg C, while the bath temperature was very stable and varied within +/- 0.002 deg C on rare occasion. The measurement for each sample was carried out with the double conductivity ratio and defined as the median of 31 readings of the salinometer. Data collection was started 5 seconds after filling the cell with the sample and it took about 10 seconds to collect 31 readings by the personal computer. Data were taken for the sixth and seventh filling of the cell after rinsing five times. In the case of the difference between the double conductivity ratio of these two fillings being smaller than 0.00002, the average value of the double conductivity ratio was used to calculate the bottle salinity with the algorithm for practical salinity scale, 1978 (UNESCO, 1981). If the difference was greater than or equal to 0.00003, an eighth filling of the cell was done. In the case of the difference between the double conductivity ratio of these two fillings being smaller than 0.00002, the average value of the double conductivity ratio was used to calculate the bottle salinity. In the case of the double conductivity ratio of eighth filling did not satisfy the criteria above, we measured a ninth filling of the cell and calculated the bottle salinity. The measurement was conducted in about 8 hours per day and the cell was cleaned with neutral detergent after the measurement of the day.

(3) Results

a. Standard Seawater

Standardization control of the salinometer was set to 559 and all measurements were carried out at this setting. The value of STANDBY was 24+6005～6010 and that of ZERO was 0.0-0000～0004. The conductivity ratio of IAPSO Standard Seawater batch P162 was 0.99983 (the double conductivity ratio was 1.99966) and was used as the standard for salinity. 25 bottles of P162 were

measured.

Fig.2.5-1 shows the time series of the double conductivity ratio for the Standard Seawater batch P162 before correction. The average of the double conductivity ratio was 1.99959 and the standard deviation was 0.00003, which is equivalent to 0.0006 in salinity.

Fig.2.5-2 shows the time series of the double conductivity ratio for the Standard Seawater batch P162 after correction. The average of the double conductivity ratio after correction was 1.99966 and the standard deviation was 0.00002, which is equivalent to 0.0003 in salinity

The specifications of SSW used in this cruise are shown as follows ;

Batch	:	P162
Conductivity ratio	:	0.99983
Salinity	:	34.993
Use by	:	16th April 2021

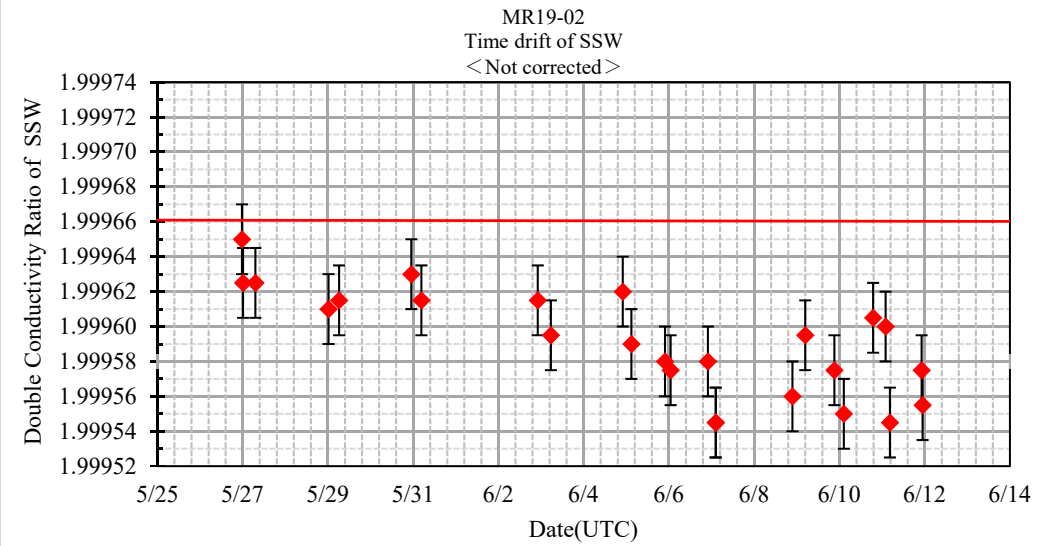

Fig. 2.5-1 Time series of the double conductivity ratio for the Standard Seawater batch P162 (Before correction)

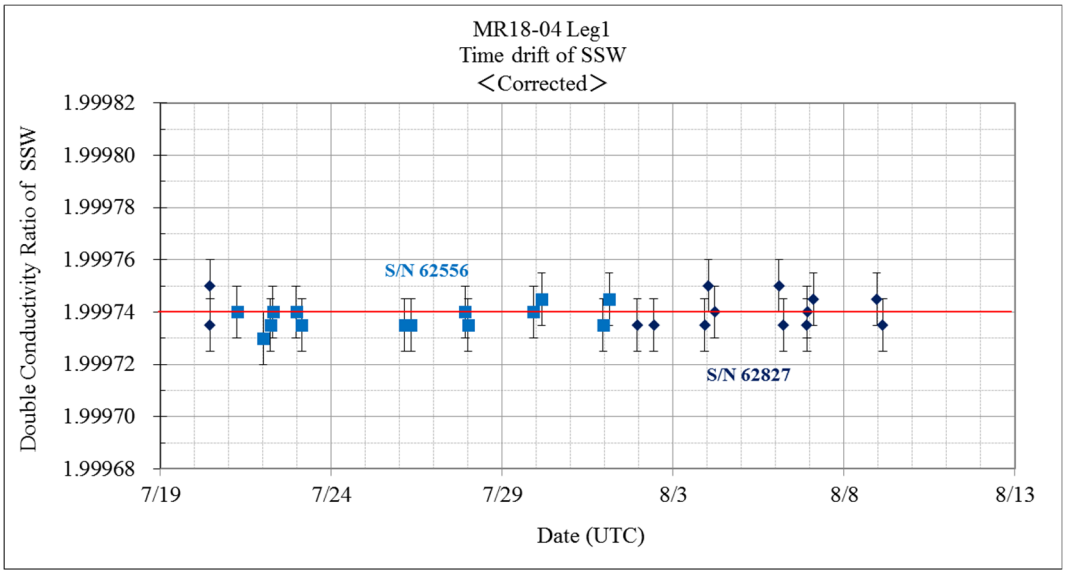

Fig. 2.5-2 Time series of the double conductivity ratio for the Standard Seawater batch P162 (After correction)

b. Sub-Standard Seawater

Sub-standard seawater was made from sea water filtered by a pore size of 0.2 micrometer and stored in a 20-liter container made of polyethylene and stirred for at least 24 hours before start measuring. It was measured about every 6 samples in order to check for the possible sudden drifts of the salinometer.

c. Replicate Samples

We estimated the precision of this method using 24 pairs of replicate samples taken from the same water sampling bottle. Fig.2.5-3 shows the histogram of the absolute difference between each pair of the replicate samples. The average and the standard deviation of absolute difference among 24 pairs of replicate samples were 0.0004 and 0.0004 in salinity, respectively.

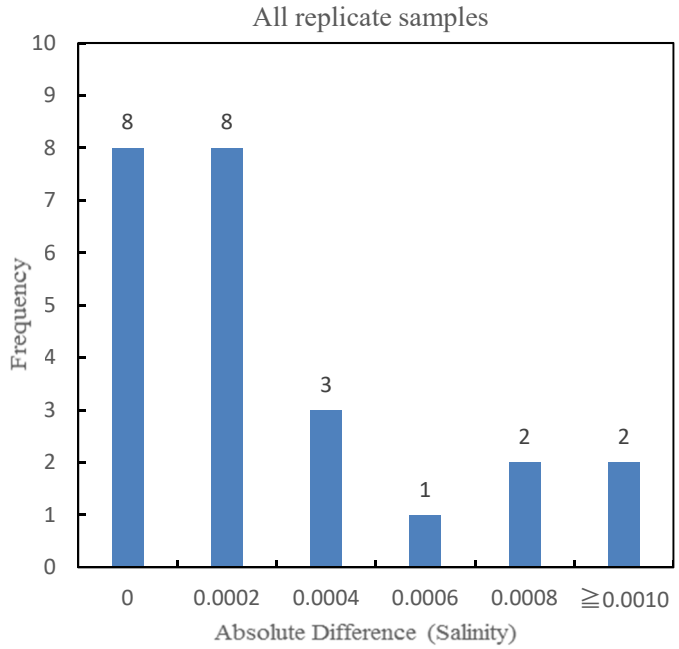

Fig. 2.5-3 The histogram of the double conductivity ratio for the absolute difference of replicate samples

(4) Data archive

These raw datasets will be submitted to JAMSTEC Data Management Group (DMG).

(5) Reference

・Aoyama, M. , T. Joyce, T. Kawano and Y. Takatsuki: Standard seawater comparison up to P129. Deep-Sea Research, I, Vol. 49, 1103～1114, 2002

・UNESCO : Tenth report of the Joint Panel on Oceanographic Tables and Standards. UNESCO Tech. Papers in Mar. Sci., 36, 25 pp., 1981

2.6 Dissolved Oxygen

Masahide WAIKTA (JAMSTEC MIO)
Katsunori SAGISHIMA (MWJ)
Hideki YAMAMOTO (MWJ)
Takayuki SUNAGAWA (MWJ)

(1) Objective

Determination of dissolved oxygen in seawater by Winkler titration.

(2) Parameters

Dissolved Oxygen

(3) Instruments and Methods

Following procedure is based on winkler method (Dickson, 1996; Culberson, 1991).

a. Instruments

Burette for sodium thiosulfate and potassium iodate;
Automatic piston burette (APB-610 / APB-620) manufactured by Kyoto Electronics Manufacturing Co., Ltd. / 10 cm^3 of titration vessel

Detector;
Automatic photometric titrator (DOT-15X) manufactured by Kimoto Electric Co., Ltd.

Software;

DOT_Terminal Ver. 1.2.0

b. Reagents

Pickling Reagent I: Manganese(II) chloride solution (3 mol dm^{-3})
Pickling Reagent II:
Sodium hydroxide (8 mol dm^{-3}) / Sodium iodide solution (4 mol dm^{-3})
Sulfuric acid solution (5 mol dm^{-3})
Sodium thiosulfate (0.025 mol dm^{-3})
Potassium iodate (0.001667 mol dm^{-3})

c. Sampling

Seawater samples were collected with Niskin bottle attached to the CTD/Carousel Water Sampling System (CTD system). Seawater for oxygen measurement was transferred from the bottle to a volume calibrated flask (ca. 100 cm^3), and three times volume of the flask was overflowed. Temperature was simulteneously measured by digital thermometer during the overflowing. After transfering the sample, two reagent solutions (Reagent I and II) of 1 cm^3 each were added immediately and the stopper was inserted carefully into the flask. The sample flask was then shaken vigorously to mix the contents and to disperse the precipitate finely throughout. After the precipitate has settled at least halfway down the flask, the flask was shaken again vigorously to disperse the precipitate. The sample flasks containing pickled samples were stored in a laboratory until they were titrated.

d. Sample measurement

For over two hours after the re-shaking, the pickled samples were measured on board. Sulfuric acid solution with its volume of 1 cm^3 and a magnetic stirrer bar were put into the sample flask and the sample was stirred. The samples were titrated by sodium thiosulfate solution whose morality was determined by potassium iodate solution. Temperature of sodium thiosulfate during titration was recorded by a digital thermometer. Dissolved oxygen concentration (μmol kg^{-1}) was calculated by sample temperature during seawater sampling, salinity of the sensor on CTD system, flask volume, and titrated volume of sodium thiosulfate solution without the blank. During this cruise, 2 sets of the titration apparatus were used.

e. Standardization and determination of the blank

Concentration of sodium thiosulfate titrant was determined by potassium iodate solution. Pure potassium iodate was dried in an oven at 130 ºC, and 1.7835 g of it was dissolved in deionized water and diluted to final weight of 5 kg in a flask. After 10 cm^3 of the standard potassium iodate solution was added to an another flask using a volume-calibrated dispenser, 90 cm^3 of deionized water, 1 cm^3 of sulfuric acid solution, and 1 cm^3 of pickling reagent solution II and I were added in order. Amount of titrated volume of sodium thiosulfate for this diluted standard potassium iodate solution (usually 5 times measurements average) gave the morality of sodium thiosulfate titrant.

The oxygen in the pickling reagents I (1 cm^3) and II (1 cm^3) was assumed to be 7.6×10^{-8} mol (Murray et al., 1968). The blank due to other than oxygen was determined as follows. First, 1 and 2 cm^3 of the standard potassium iodate solution were added to each flask using a calibrated dispenser. Then 100 cm^3 of deionized water, 1 cm^3 of sulfuric acid solution, 1 cm^3 of pickling II reagent solution, and same volume of pickling I reagent solution were added into the flask in order. The blank was determined by difference between the first (1 cm^3 of potassium iodate) titrated volume of the sodium thiosulfate and the second (2 cm^3 of potassium iodate) one. The titrations were conducted for 3 times

and their average was used as the blank value.

(4) Observation log

a. Standardization and determination of the blank

Table 2.6-1 shows results of the standardization and the blank determination during this cruise.

Table 2.6-1 Results of the standardization and the blank determinations during cruise

Date (yyyy/mm/dd)	Potassium iodate ID	Sodium thiosulfate ID	DOT-15X (No.9)		DOT-15X (No.10)		Stations
			E.P. (cm^3)	Blank (cm^3)	E.P. (cm^3)	Blank (cm^3)	
2019/5/26	K1805F03	T-19B	3.956	-0.007	3.957	0.000	A01M002, A01M003, A02M001, A03M002, A03M003, A04M001
2019/5/31	K1805F04	T-19B	3.953	-0.006	3.954	0.003	A07M005, A06M001,
2019/5/31	K1805F04	T-19B	3.953	-0.006	3.953	0.005	A07M002, A05M001, A05M002
2019/6/7	K1805F05	T-19B	3.955	-0.005	3.956	0.007	A07M010, A09M002
2019/6/7	K1805F05	T-19B	3.955	-0.005	3.956	0.006	A07M009, A08M001, A09M001
2019/6/11	K1805F06	T-19B	3.957	-0.007	3.960	0.008	

b. Repeatability of sample measurement

Replicate samples were taken at every CTD casts. The standard deviation of the replicate measurement (Dickson et al., 2007) was 0.13 μmol kg^{-1} (n=36).

(5) Data archives

These data obtained in this cruise will be submitted to the Data Management Group (DMG) of JAMSTEC, and will opened to the public via “Data Research System for Whole Cruise Information in JAMSTEC (DARWIN)” in JAMSTEC web site.
<http://www.godac.jamstec.go.jp/darwin/e>

(6) References

Culberson, C. H. (1991). *Dissolved Oxygen.* WHPO Publication 91-1.

Dickson, A. G. (1996). Determination of dissolved oxygen in sea water by Winkler titration. In *WOCE Operations Manual*, Part 3.1.3 Operations & Methods, WHP Office Report WHPO 91-1.

Dickson, A. G., Sabine, C. L., & Christian, J. R.(Eds.), (2007). *Guide to best practices for ocean CO_2 measurements, PICES Special Publication 3*: North Pacific Marine Science Organization.

Murray, C. N., Riley, J. P., & Wilson, T. R. S. (1968). The solubility of oxygen in Winklerreagents used for the determination of dissolved oxygen. *Deep Sea Res.*, 15, 237-238.

2.7 Nutrients

Masahide WAKITA (JAMSTEC MIO)
Shinichiro YOKOGAWA (MWJ)
Yuko MIYOSHI (MWJ)

(1) Objectives

The objectives of nutrients analyses during the R/V Mirai MR19-02 cruise in the Western Pacific Ocean, of which EXPOCODE is 49NZ20190524, is as follows:

- Describe the present status of nutrients concentration with excellent comparability using certified reference material of nutrient in seawater.

(2) Parameters

The determinants are nitrate, nitrite, silicate, phosphate and ammonia in the Western Pacific Ocean

(3) Instruments and methods

(3.1) Analytical detail using QuAAtro 2-HR systems (BL TEC K.K.)

Nitrate + nitrite and nitrite are analyzed following a modification of the method of Grasshoff (1976). The sample nitrate is reduced to nitrite in a cadmium tube the inside of which is coated with metallic copper. The sample stream after reduction is treated with an acidic, sulfanilamide reagent to produce a diazonium ion. N-1-Naphthylethylenediamine Dihydrochloride added to the sample stream to produce a red azo dye. With reduction of the nitrate to nitrite, both nitrate and nitrite react and are measured; without reduction, only nitrite reacts. Thus, for the nitrite analysis, no reduction is performed and the alkaline buffer is not necessary. Nitrate is computed by difference.

The silicate method is analogous to that described for phosphate. The method used is essentially that of Grasshoff et al. (1999). Silicomolybdic acid is first formed from the silicate in the sample and molybdic acid. The silicomolybdic acid is reduced to silicomolybdous acid, or "molybdenum blue," using ascorbic acid.

The phosphate analysis is a modification of the procedure of Murphy and Riley (1962). Molybdic acid is added to the seawater sample to form phosphomolybdic acid which is in turn reduced to phosphomolybdous acid using L-ascorbic acid as the reductant.

The ammonia in seawater is mixed with an alkaline containing EDTA, ammonia as gas state is formed from seawater. The ammonia (gas) is absorbed in sulfuric acid by way of 0.5 μm pore size membrane filter (ADVANTEC PTFE) at the dialyzer attached to analytical system. The ammonia absorbed in sulfuric acid is determined by coupling with phenol and hypochlorite to form indophenols blue. Wavelength using ammonia analysis is 630 nm, which is absorbance of indophenols blue.

The details of modification of analytical methods for four parameters, Nitrate, Nitrite, Silicate and Phosphate, used in this cruise are also compatible with the methods described in nutrients section in GO-SHIP repeat hydrography manual (Hydes et al., 2010), while an analytical method of ammonium is compatible with Determination of ammonia in seawater using a vaporization membrane permeability

method (Kimura, 2000). The flow diagrams and reagents for each parameter are shown in Figures 2.7.1 to 2.7.5.

(3.2) Nitrate + Nitrite Reagents

50 % Triton solution

50 mL Triton™ X-100 provided by Sigma-Ardrich Japan G. K. (CAS No. 9002-93-1), were mixed with 50 mL Ethanol (99.5 %).

Imidazole (buffer), 0.06 M (0.4 % w/v)

Dissolve 4 g Imidazole (CAS No. 288-32-4), in 1000 mL Ultra-pure water, add 2 mL Hydrogen chloride (CAS No. 7647-01-0). After mixing, 1 mL 50 % Triton solution is added.

Sulfanilamide, 0.06 M (1 % w/v) in 1.2 M HCl

Dissolve 10 g 4-Aminobenzenesulfonamide (CAS No. 63-74-1), in 900 mL of Ultra-pure water, add 100 mL Hydrogen chloride (CAS No. 7647-01-0). After mixing, 2 mL 50 % Triton solution is added.

NED, 0.004 M (0.1 % w/v)

Dissolve 1 g N-(1-Naphthalenyl)-1,2-ethanediamine, dihydrochloride (CAS No. 1465-25-4), in 1000 mL of Ultra-pure water and add 10 mL Hydrogen chloride (CAS No. 7647-01-0). After mixing, 1 mL 50 % Triton solution is added. This reagent was stored in a dark bottle.

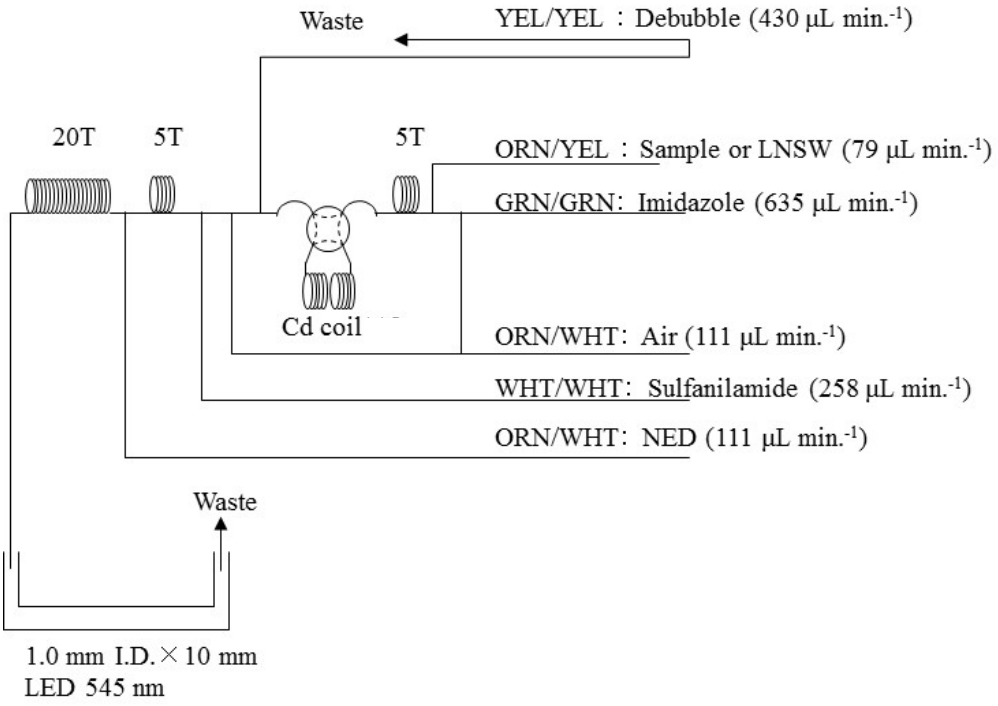

Figure 2.7.1 NO_3+NO_2 (1ch.) Flow diagram.

(3.3) Nitrite Reagents

50 % Triton solution

50 mL Triton™ X-100 provided by Sigma-Ardrich Japan G. K. (CAS No. 9002-93-1), were mixed

with 50 mL Ethanol (99.5 %).

Sulfanilamide, 0.06 M (1 % w/v) in 1.2 M HCl

Dissolve 10 g 4-Aminobenzenesulfonamide (CAS No. 63-74-1), in 900 mL of Ultra-pure water, add 100 mL Hydrogen chloride (CAS No. 7647-01-0). After mixing, 2 mL 50 % Triton solution is added.

NED, 0.004 M (0.1 % w/v)

Dissolve 1 g N-(1-Naphthalenyl)-1,2-ethanediamine, dihydrochloride (CAS No. 1465-25-4), in 1000 mL of Ultra-pure water and add 10 mL Hydrogen chloride (CAS No. 7647-01-0). After mixing, 1 mL 50 % Triton solution is added. This reagent was stored in a dark bottle.

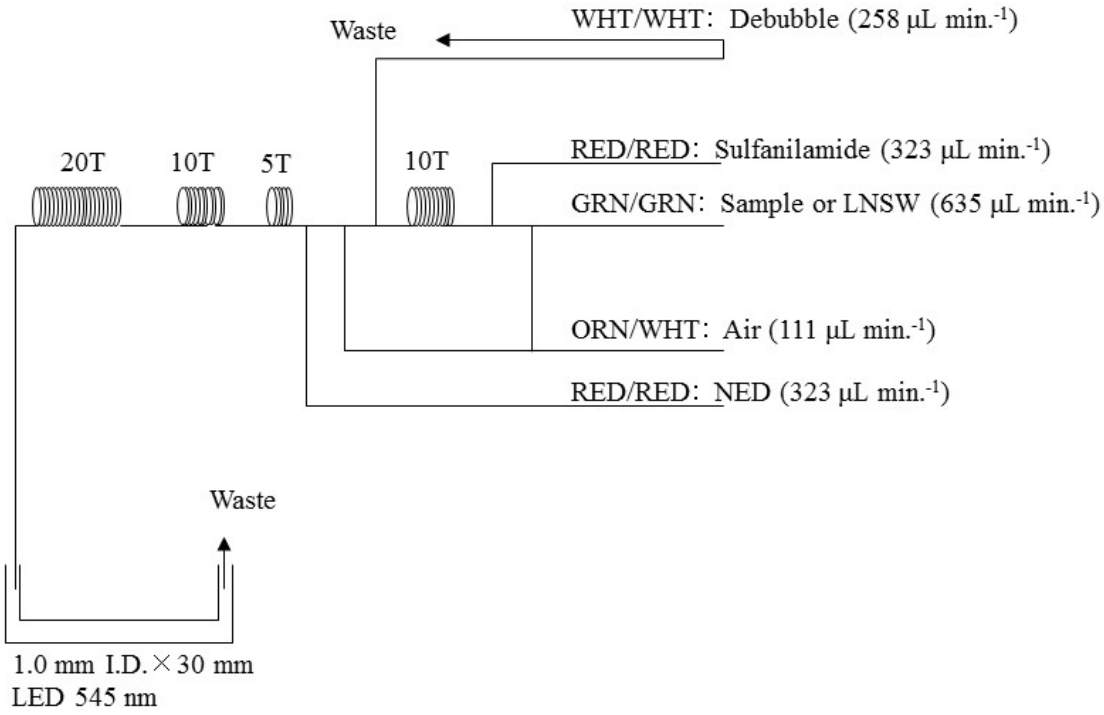

Figure 2.7.2 NO_2 (2ch.) Flow diagram.

(3.4) Silicate Reagents

15 % Sodium dodecyl sulfate solution

75 g Sodium dodecyl sulfate (CAS No. 151-21-3) were mixed with 425 mL Ultra-pure water.

Molybdic acid, 0.06 M (2 % w/v)

Dissolve 15 g Sodium molybdate dihydrate (CAS No. 10102-40-6), in 980 mL Ultra-pure water, add 8 mL Sulfuric acid (CAS No. 7664-93-9). After mixing, 20 mL 15 % Sodium dodecyl sulfate solution is added.

Oxalic acid, 0.6 M (5 % w/v)

Dissolve 50 g Oxalic acid (CAS No. 144-62-7), in 950 mL of Ultra-pure water.

Ascorbic acid, 0.01 M (3 % w/v)

Dissolve 2.5 g L-Ascorbic acid (CAS No. 50-81-7), in 100 mL of Ultra-pure water. This reagent was freshly prepared at every day.

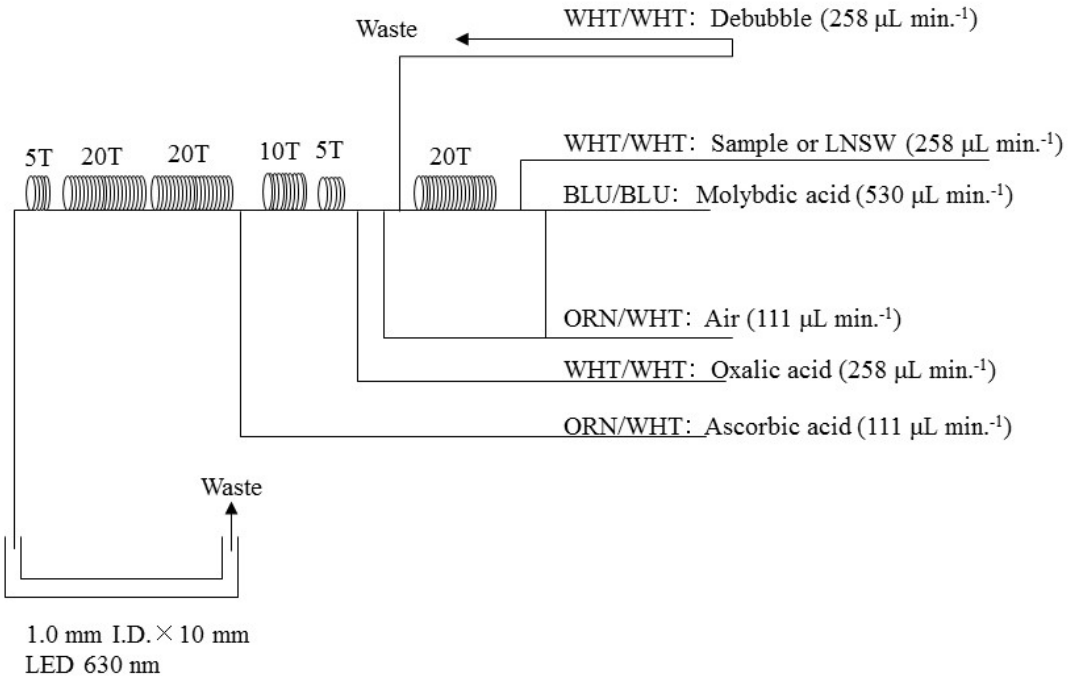

Figure 2.7.3 SiO_2 (3ch.) Flow diagram.

(3.5) Phosphate Reagents

15 % Sodium dodecyl sulfate solution

75 g Sodium dodecyl sulfate (CAS No. 151-21-3) were mixed with 425 mL Ultra-pure water.

Stock molybdate solution, 0.03 M (0.8 % w/v)

Dissolve 8 g Sodium molybdate dihydrate (CAS No. 10102-40-6), and 0.17 g Antimony potassium tartrate trihydrate (CAS No. 28300-74-5), in 950 mL of Ultra-pure water and added 50 mL Sulfuric acid (CAS No. 7664-93-9).

PO_4 color reagent

Dissolve 1.2 g L-Ascorbic acid (CAS No. 50-81-7), in 150 mL of stock molybdate solution. After mixing, 3 mL 15 % Sodium dodecyl sulfate solution is added. This reagent was freshly prepared before every measurement.

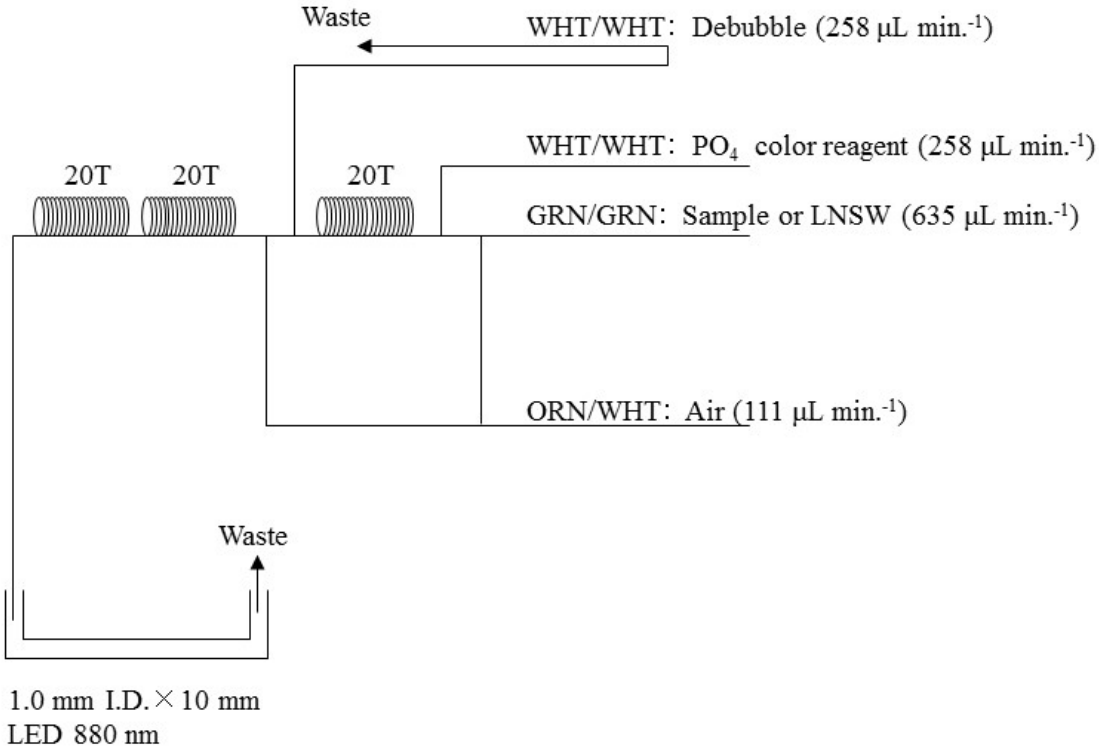

Figure 2.7.4 PO_4 (4ch.) Flow diagram.

(3.6) Ammonia Reagents

30 % Triton solution

30 mL Triton™ X-100 provided by Sigma-Ardrich Japan G. K. (CAS No. 9002-93-1), were mixed with 70 mL Ultra-pure water.

EDTA

Dissolve 41 g tetrasodium;2-[2-[bis(carboxylatomethyl)amino]ethyl-(carboxylatemethyl)amino]acetate;tetrahydrate (CAS No. 13235-36-4), and 2 g Boric acid (CAS No. 10043-35-3), in 200 mL of Ultra-pure water. After mixing, 1 mL 30 % Triton solution is added. This reagent is prepared at a week about.

NaOH liquid

Dissolve 5 g Sodium hydroxide (CAS No. 1310-73-2), and 16 g tetrasodium;2-[2-[bis(carboxylatomethyl)amino]ethyl-(carboxylatomethyl)amino]acetate;tetrahydrate (CAS No. 13235-36-4) in 100 mL of Ultra-pure water. This reagent is prepared at a week about.

Stock nitroprusside

Dissolve 0.25 g Sodium nitroferricyanide dihydrate (CAS No. 13755-38-9) in 100 mL of Ultra-pure water and add 0.2 mL 1M Sulfuric acid. Stored in a dark bottle and prepared at a month about.

Nitroprusside solution

Mix 4 mL stock nitroprusside and 5 mL 1M Sulfuric acid in 500 mL of Ultra-pure water. After mixing, 2 mL 30 % Triton solution is added. This reagent is stored in a dark bottle and prepared at every

2 or 3 days.

Alkaline phenol

Dissolve 10 g Phenol (CAS No. 108-95-2), 5 g Sodium hydroxide (CAS No. 1310-73-2) and 2 g Sodium citrate dihydrate (CAS No. 6132-04-3), in 200 mL Ultra-pure water. Stored in a dark bottle and prepared at a week about.

NaClO solution

Mix 5 mL Sodium hypochlorite (CAS No. 7681-52-9) in 45 mL Ultra-pure water. Stored in a dark bottle and fleshly prepared before every measurement. This reagent is prepared 0.3 % available chlorine.

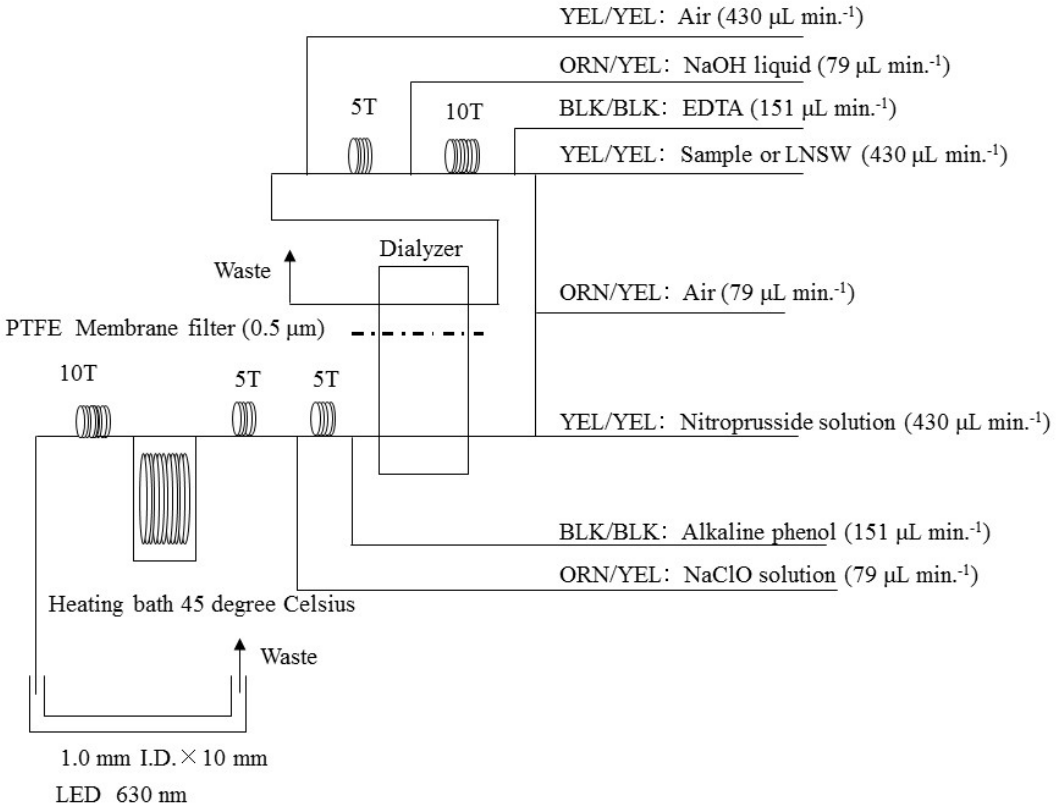

Figure 2.7.5 NH_4 (5ch.) Flow diagram.

(3.7) Sampling procedures

Sampling of nutrients followed that oxygen, salinity and trace gases. Samples were drawn into a virgin 10 mL polyacrylates vials without sample drawing tubes. These were rinsed three times before filling and vials were capped immediately after the drawing. The vials are put into water bath adjusted to ambient temperature, 23.6 ± 1.3 degree Celsius, in about 30 minutes before use to stabilize the temperature of samples.

No transfer was made and the vials were set an auto sampler tray directly. Samples were analyzed after collection within 24 hours.

(3.8) Data processing

Raw data from QuAAtro 2-HR were treated as follows:

- Check baseline shift.
- Check the shape of each peak and positions of peak values taken, and then change the positions of peak values taken if necessary.
- Carry-over correction and baseline drift correction were applied to peak heights of each samples followed by sensitivity correction.
- Baseline correction and sensitivity correction were done basically using liner regression.
- Load pressure and salinity from uncalibrate CTD data to calculate density of seawater tentatively. To calculate the final nutrients concentration we used bottle salinity from AUTOSAL, while in case of P.E. cast we used CTD data.
- Calibration curves to get nutrients concentration were assumed second order equations.

(3.9) Summary of nutrients analysis

We made 11 QuAAtro runs for the water columns sample collected by 19 casts at 9 stations during this cruise. The total amount of layers of the seawater sample reached to 751. We made basically duplicate measurement.

(4) Station list

The sampling station list for nutrients is shown in Table 2.7.1.

Table 2.7.1 List of stations.

Station	Cast	Date (UTC)	Position*		Depth (m)
		(mmddyy)	Latitude	Longitude	
A01	2	052519	32-21.59N	144-29.75E	5987
A01	3	052519	32-20.35N	144-30.17E	5983
A01	4	052619	32-18.48N	144-29.78E	5866
A02	1	052719	34-99.25N	147-20.76E	5817
A03	1	052819	37-50.02N	149-89.69E	5981
A03	2	052819	37-50.70N	149-87.01E	5997
A03	3	052819	37-50.10N	149-89.72E	5978
A04	1	052919	39-99.89N	152-68.67E	5672
A07	1	053119	47-01.67N	159-94.33E	5203
A07	2	060119	47-00.72N	159-97.38E	5216
A07	5	060219	47-00.54N	159-96.65E	5215
A05	1	060319	50-00.02N	164-99.91E	5513
A05	2	060319	50-00.05N	165-00.10E	5517
A06	1	060419	48-49.95N	162-49.85E	5740
A07	9	060719	47-02.43N	159-95.28E	5206
A07	10	060719	47-01.70N	159-94.97E	5206
A08	1	060819	45-50.03N	157-49.95E	4952
A09	1	060919	44-00.18N	155-00.24E	5306
A09	2	060919	44-00.40N	155-00.57E	5310

*: Position indicates latitude and longitude where CTD reached maximum depth at the cast.

(5) Certified Reference Material of nutrients in seawater

KANSO CRMs (Lot: CK, CD, CJ, CB, BZ) were used to ensure the comparability and traceability of nutrient measurements during this cruise. The details of CRMs are shown below.

Production

KANSO CRMs are certified reference material (CRM) for inorganic nutrients in seawater. These were produced by KANSO Co.,Ltd. This certified reference material has been produced using autoclaved natural seawater on the basis of quality control system under ISO Guide 34 (JIS Q 0034).

KANSO Co.,Ltd. has been accredited under the Accreditation System of National Institute of Technology and Evaluation (ASNITE) as a CRM producer since 2011. (Accreditation No.: ASNITE 0052 R)

Property value assignment

The certified values are arithmetic means of the results of 30 bottles from each batch (measured in duplicates) analysed by KANSO Co.,Ltd. and Japan Agency for Marine-Earth Science and Technology (JAMSTEC) using the colorimetric method (continuous flow analysis, CFA, method). The salinity of calibration solutions were adjusted to the salinity of this CRM ± 0.5.

Metrological Traceability

Each certified value of nitrate, nitrite, and phosphate of KANSO CRMs were calibrated versus one of Japan Calibration Service System (JCSS) standard solutions for each nitrate ions, nitrite ions, and phosphate ions. JCSS standard solutions are calibrated versus the secondary solution of JCSS for each of these ions. The secondary solution of JCSS is calibrated versus the specified primary solution produced by Chemicals Evaluation and Research Institute (CERI), Japan. CERI specified primary solutionsare calibrated versus the National Metrology Institute of Japan (NMIJ) primary standards solution of nitrate ions, nitrite ions and phosphate ions, respectively.

For a certified value of silicate of KANSO CRM was determined by one of Merck KGaA silicon standard solution 1000 mg L^{-1} Si traceable to National Institute of Standards and Technology (NIST) SRM of silicon standard solution (SRM 3150).

The certified values of nitrate, nitrite, and phosphate of KASNO CRM are thus traceable to the International System of Units (SI) through an unbroken chain of calibrations, JCSS, CERI and NMIJ solutions as stated above, each having stated uncertainties. The certified values of silicate of KANSO CRM are traceable to the International System of Units (SI) through an unbroken chain of calibrations, Merck KGaA and NIST SRM 3150 solutions, each having stated uncertainties.

As stated in the certificate of NMIJ CRMs each certified value of dissolved silica, nitrate ions, and nitrite ions was determined by more than one method using one of NIST (National Institute of Standards and Technology) SRM of silicon standard solution and NMIJ primary standards solution of nitrate ions and nitrite ions. The concentration of phosphate ions as stated information value in the certificate was determined NMIJ primary standards solution of phosphate ions. Those values in the certificate of NMIJ CRMs are traceable to the International System of Units (SI).

One of analytical methods used for certification of NMIJ CRM for nitrate ions, nitrite ions, phosphate ions and dissolved silica was colorimetric method (continuous mode and batch one). The colorimetric method is same as the analytical method (continuous mode only) used for certification of

KANSO CRM. For certification of dissolved silica, exclusion chromatography/isotope dilution-inductively coupled plasma mass spectrometry and Ion exclusion chromatography with post-column detection were used. For certification of nitrate ions, Ion chromatography by direct analysis and Ion chromatography after halogen-ion separation were used. For certification of nitrite ions, Ion chromatography by direct analysis was used.

NMIJ CRMs were analysed at the time of certification process for CRM and the results were confirmed within expanded uncertainty stated in the certificate of NMIJ CRMs.

(5.1) CRM for this cruise

These CRM assignments were completely done based on random number. The CRM bottles were stored at a room in the ship, BIOCHEMICAL LAB., where the temperature was maintained around 20.6 degree Celsius – 24.4 degree Celsius.

(5.2) CRM concentration

We used nutrients concentrations for CRM lots CK, CD, CJ, CB and BZ as shown in Table 2.7.2.

Table 2.7.2 Certified concentration and uncertainty (k=2) of CRMs.

unit: μmol kg^{-1}

Lot	Nitrate	Nitrite	Silicate	Phosphate	Ammonia*
CK	0.02 ± 0.03	0.01 ± 0.01	0.73 ± 0.08	0.048 ± 0.012	0.84
CD	5.50 ± 0.05	0.02 ± 0.00	13.93 ± 0.10	0.446 ± 0.008	1.11
CJ	16.20 ± 0.20	0.03 ± 0.01	38.50 ± 0.40	1.190 ± 0.020	0.77
CB	35.79 ± 0.27	0.12 ± 0.01	109.20 ± 0.62	2.520 ± 0.022	0.77
BZ	43.35 ± 0.33	0.22 ± 0.01	161.00 ± 0.93	3.056 ± 0.033	0.49

*For ammonia values are references

(6) Nutrients standards

(6.1) Volumetric laboratory ware of in-house standards

All volumetric glass ware and polymethylpentene (PMP) ware used were gravimetrically calibrated. Plastic volumetric flasks were gravimetrically calibrated at the temperature of use within 4 K.

(6.1.1) Volumetric flasks

Volumetric flasks of Class quality (Class A) are used because their nominal tolerances are 0.05 % or less over the size ranges likely to be used in this work. Class A flasks are made of borosilicate glass, and the standard solutions were transferred to plastic bottles as quickly as possible after they are made up to volume and well mixed in order to prevent excessive dissolution of silicate from the glass. PMP volumetric flasks were gravimetrically calibrated and used only within 4 K of the calibration temperature.

The computation of volume contained by glass flasks at various temperatures other than the calibration temperatures were done by using the coefficient of linear expansion of borosilicate crown

glass.

Because of their larger temperature coefficients of cubical expansion and lack of tables constructed for these materials, the plastic volumetric flasks were gravimetrically calibrated over the temperature range of intended use and used at the temperature of calibration within 4 K. The weights obtained in the calibration weightings were corrected for the density of water and air buoyancy.

(6.1.2) Pipettes

All pipettes have nominal calibration tolerances of 0.1 % or better. These were gravimetrically calibrated in order to verify and improve upon this nominal tolerance.

(6.2) Reagents, general considerations

(6.2.1) Specifications

For nitrate standard, "potassium nitrate 99.995 suprapur®" provided by Merck, Lot. B1452165836, CAS No. 7757-79-1, was used.

For nitrite standard solution, we used "nitrite ion standard solution (NO_2^- 1000) provided by Wako, Lot APJ6212, Code. No. 140-06451." This standard solution was certified by Wako using Ion chromatograph method. Calibration result is 1003 mg L^{-1} at 20 degree Celsius. Expanded uncertainty of calibration (k=2) is 0.7 % for the calibration result.

For the silicate standard, we use "Silicon standard solution SiO_2 in NaOH 0.5 M CertiPUR®" provided by Merck, Code. No. 170236, of which lot number is HC73014836 are used. The silicate concentration is certified by NIST-SRM3150 with the uncertainty of 0.7 %. HC73014836 is certified as 1000 mg L^{-1}.

For phosphate standard, "potassium dihydrogen phosphate anhydrous 99.995 suprapur®" provided by Merck, Lot. B1642608851, CAS No.: 7778-77-0, was used.

For ammonia standard, "Ammonium Chloride" provided by NMIJ, CAS No. 12125-02-9. We used NMIJ CRM 3011-a. The purity of this standard was greater than 99.9 %. Expanded uncertainty of calibration (k=2) is 0.065 %.

(6.2.2) Ultra-pure water

Ultra-pure water (Milli-Q water) freshly drawn was used for preparation of reagent, standard solutions and for measurement of reagent and system blanks.

(6.2.3) Low nutrients seawater (LNSW)

Surface water having low nutrient concentration was taken and filtered using 0.20 μm pore capsule cartridge filter at MR18-04 cruise on August, 2018. This water is stored in 20 L cubitainer with cardboard box.

LNSW concentrations were assigned to March, 2019 in JAMSTEC.

(6.2.4) Concentrations of nutrients for A, D, B and C standards

Concentrations of nutrients for A, D, B and C standards are set as shown in Table 2.7.3. The C standard is prepared according recipes as shown in Table 2.7.4. All volumetric laboratory tools were calibrated prior the cruise as stated in chapter (6.1) Then the actual concentration of nutrients in each fresh standard was calculated based on the ambient, solution temperature and determined factors of volumetric laboratory wares.

The calibration curves for each run were obtained using 5 levels, C-1, C-2, C-3, C-4 and C-5.

Table 2.7.3 Nominal concentrations of nutrients for A, D, B and C standards.

	A	D	B	C-1	C-2	C-3	C-4	C-5
NO_3 (μM)	45000	1800	900	LNSW	9	18	35	54
NO_2 (μM)	21800	870	26	LNSW	0.26	0.52	1.04	1.56
SiO_2 (μM)	34800		2845	LNSW	29	58	114	172
PO_4 (μM)	6000		60	LNSW	0.7	1.3	2.5	3.7
NH_4 (μM)	4000		160	LNSW	1.6	3.2	6.4	9.6

Table 2.7.4 Working calibration standard recipes.

C Std.	B Std.
C-2	5 mL
C-3	10ml
C-4	20ml
C-5	30ml

(7.2.5) Renewal of in-house standard solutions

In-house standard solutions as stated in paragraph (6.2) were renewed as shown in Table 2.7.5 to 2.7.7.

Table 2.7.5 Timing of renewal of in-house standards.

NO_3, NO_2, SiO_2, PO_4, NH_4	Renewal
A-1 Std. (NO_3)	maximum a month
A-2 Std. (NO_2)	commercial prepared solution
A-3 Std. (SiO_2)	commercial prepared solution
A-4 Std. (PO_4)	maximum a month
A-5 Std. (NH_4)	maximum a month
D-1 Std.	maximum 8 days
D-2 Std.	maximum 8 days
B Std. (mixture of A-1, D-2, A-3, A-4 and A-5 std.)	maximum 8 days

Table 2.7.6 Timing of renewal of working calibration standards.

Working standards	Renewal
C Std. (dilute B Std.)	every 24 hours

Table 2.7.7 Timing of renewal of in-house standards for reduction estimation.

Reduction estimation	Renewal
36 μM NO_3 (dilute D-1 Std.)	when C Std. renewed
35 μM NO_2 (dilute D-2 Std.)	when C Std. renewed

(8) Quality control

(8.1) Precision of nutrients analyses during the cruise

Precision of nutrients analyses during this cruise was evaluated based on the 5 to 13 measurements, which are measured every 7 to 14 samples, during a run at the concentration of C-5 std. Summary of precisions are shown in Table 2.7.8. The precisions for each parameter are generally good considering the analytical precisions during the R/V Mirai cruses conducted in 2009 - 2017. During in this cruise, analytical precisions were 0.13 % for nitrate, 0.13 % for nitrite, 0.12 % for silicate, 0.10 % for phosphate and 0.17 % for ammonia in terms of median of precision, respectively. Then we can conclude that the analytical precisions for nitrate, nitrite, silicate, phosphate and ammonia were maintained throughout this cruise.

Table 2.7.8 Summary of precision based on the replicate analyses.

	Nitrate CV %	Nitrite CV %	Silicate CV %	Phosphate CV %	Ammonia CV %
Median	0.12	0.15	0.14	0.15	0.25
Mean	0.13	0.15	0.14	0.16	0.26
Maximum	0.19	0.24	0.21	0.30	0.43
Minimum	0.06	0.12	0.05	0.07	0.10
N	11	11	11	11	11

(8.2) CRM lot. BZ measurement during this cruise

CRM lot. BZ was measured every run to keep the comparability. The results of lot. BZ during this cruise are shown as 2.7.9.

Table 2.7.9 Summary of CRM-BZ in this cruise.

	Nitrate	Nitrite	Silicate	Phosphate	Ammonia
Median (μmol kg^{-1})	43.40	0.23	161.63	3.064	0.82
Mean (μmol kg^{-1})	43.40	0.23	161.66	3.060	0.78
S.D. (μmol kg^{-1})	0.05	0.01	0.10	0.008	0.12
C.V. (%)	0.10	3.20	0.06	0.27	14.94
N	11	11	11	11	11

(8.3) Carry over

We can also summarize the magnitudes of carry over throughout the cruise. These are small enough within acceptable levels as shown in Table 2.7.10.

Table 2.7.10 Summary of carry over throughout this cruise.

	Nitrate %	Nitrite %	Silicate %	Phosphate %	Ammonia %
Median	0.34	0.11	0.19	0.19	0.60
Mean	0.34	0.13	0.19	0.20	0.64
Maximum	0.41	0.29	0.22	0.33	0.91
Minimum	0.28	0.00	0.17	0.14	0.41
N	11	11	11	11	11

(9) Problems / improvements occurred and solutions.

Nothing happened during this cruise.

(10) List of reagent

List of reagent is shown in Table2.7.11.

Table 2.7.11 List of reagent in this cruise.

IUPAC name	CAS Number	Formula	Compound Name	Manufacture	Grade
4-Aminobenzenesulfonamide	63-74-1	$C_6H_8N_2O_2S$	Sulfanilamide	Wako Pure Chemical Industries, Ltd.	JIS Special Grade
Ammonium Chloride	12125-02-9	NH_4Cl	Ammonium Chloride	National Institute of Advanced Industrial Science and Technology	Certified Reference Material
Antimony potassium tartrate trihydrate	28300-74-5	$K_2(SbC_4H_2O_6)_2 \cdot 3H_2O$	Bis[(+)-tartrato]diantimonate(III) Dipotassium Trihydrate	Wako Pure Chemical Industries, Ltd.	JIS Special Grade
Boric acid	10043-35-3	H_3BO_3	Boric Acid	Wako Pure Chemical Industries, Ltd.	JIS Special Grade
Hydrogen chloride	7647-01-0	HCl	Hydrochloric Acid	Wako Pure Chemical Industries, Ltd.	JIS Special Grade
Imidazole	288-32-4	$C_3H_4N_2$	Imidazole	Wako Pure Chemical Industries, Ltd.	JIS Special Grade
L-Ascorbic acid	50-81-7	$C_6H_8O_6$	L-Ascorbic Acid	Wako Pure Chemical Industries, Ltd.	JIS Special Grade
N-(1-Naphthalenyl)-1,2-ethanediamine, dihydrochloride	1465-25-4	$C_{12}H_{16}Cl_2N_2$	N-1-Naphthylethylenediamine Dihydrochloride	Wako Pure Chemical Industries, Ltd.	for Nitrogen Oxides Analysis
Oxalic acid	144-62-7	$C_2H_2O_4$	Oxalic Acid	Wako Pure Chemical Industries, Ltd.	Wako Special Grade
Phenol	108-95-2	C_6H_6O	Phenol	Wako Pure Chemical Industries, Ltd.	JIS Special Grade
Potassium nitrate	7757-79-1	KNO_3	Potassium Nitrate	Merck KGaA	Suprapur®
Potassium dihydrogen phosphate	7778-77-0	KH_2PO_4	Potassium dihydrogen phosphate anhydrous	Merck KGaA	Suprapur®
Sodium citrate dihydrate	6132-04-3	$Na_3C_6H_5O_7 \cdot 2H_2O$	Trisodium Citrate Dihydrate	Wako Pure Chemical Industries, Ltd.	JIS Special Grade
Sodium dodecyl sulfate	151-21-3	$C_{12}H_{25}NaO_4S$	Sodium Dodecyl Sulfate	Wako Pure Chemical Industries, Ltd.	for Biochemistry
Sodium hydroxide	1310-73-2	NaOH	Sodium Hydroxide for Nitrogen Compounds Analysis	Wako Pure Chemical Industries, Ltd.	for Nitrogen Analysis
Sodium hypochlorite	7681-52-9	NaClO	Sodium Hypochlorite Solution	Kanto Chemical co., Inc.	Extra pure
Sodium molybdate dihydrate	10102-40-6	$Na_2MoO_4 \cdot 2H_2O$	Disodium Molybdate(VI) Dihydrate	Wako Pure Chemical Industries, Ltd.	JIS Special Grade
Sodium nitroferricyanide dihydrate	13755-38-9	$Na_2[Fe(CN)_5NO] \cdot 2H_2O$	Sodium Pentacyanonitrosylferrate(III) Dihydrate	Wako Pure Chemical Industries, Ltd.	JIS Special Grade
Sulfuric acid	7664-93-9	H_2SO_4	Sulfuric Acid	Wako Pure Chemical Industries, Ltd.	JIS Special Grade
tetrasodium;2-[2-[bis(carboxylatomethyl)amino]ethyl-(carboxylatomethyl)amino]acetate;tetrahydrate	13235-36-4	$C_{10}H_{12}N_2Na_4O_8 \cdot 4H_2O$	Ethylenediamine-N,N,N',N'-tetraacetic Acid Tetrasodium Salt Tetrahydrate (4NA)	Dojindo Molecular Technologies, Inc.	-
Synonyms: t-Octylphenoxypolyethoxyethanol 4-(1,1,3,3-Tetramethylbutyl)phenyl-polyethylene glycol Polyethylene glycol tert-octylphenyl ether	9002-93-1	$(C_2H_4O)_nC_{14}H_{22}O$	Triton™ X-100	Sigma-Aldrich Japan G.K.	-

(11) Data archives

These data obtained in this cruise will be submitted to the Data Management Group of JAMSTEC, and will be opened to the public via “Data Research System for Whole Cruise Information in JAMSTEC (DARWIN)” in JAMSTEC web site.

<http://www.godac.jamstec.go.jp/darwin/e>

(12) References

Grasshoff, K. 1976. Automated chemical analysis (Chapter 13) in Methods of Seawater Analysis. With contribution by Almgreen T., Dawson R., Ehrhardt M., Fonselius S. H., Josefsson B., Koroleff F., Kremling K. Weinheim, New York: Verlag Chemie.

Grasshoff, K., Kremling K., Ehrhardt, M. et al. 1999. Methods of Seawater Analysis. Third, Completely Revised and Extended Edition. WILEY-VCH Verlag GmbH, D-69469 Weinheim (Federal Republic of Germany).

Hydes, D.J., Aoyama, M., Aminot, A., Bakker, K., Becker, S., Coverly, S., Daniel, A., Dickson, A.G., Grosso, O., Kerouel, R., Ooijen, J. van, Sato, K., Tanhua, T., Woodward, E.M.S., Zhang, J.Z., 2010. Determination of Dissolved Nutrients (N, P, Si) in Seawater with High Precision and Inter-Comparability Using Gas-Segmented Continuous Flow Analysers, In: GO-SHIP Repeat Hydrography Manual: A Collection of Expert Reports and Guidelines. IOCCP Report No. 14, ICPO Publication Series No 134.

Kimura, 2000. Determination of ammonia in seawater using a vaporization membrane permeability method. 7th auto analyzer Study Group, 39-41.

Murphy, J., and Riley, J.P. 1962. Analytica chimica Acta 27, 31-36.

2.8 Trace metals

Koji SUGIE (JAMSTEC RIGC)

(1) Objectives

Some trace metals such as iron, manganese and zinc are essential for phytoplankton growth because they are co-factors of many essential enzymes. However, trace metal distribution at monitoring station K2 was rarely investigated before. In the western subarctic Pacific, trace metal, especially iron regulates phytoplankton productivity during summer. However, the data of trace metal other than iron is scarce and data availability is mostly limited during summer (August and September). In this cruise, we collected seawater samples for multiple trace metals for the first time using R/V Mirai at St. K2.

(2) Instruments and methods

Samples were collected at 1, 20, 30, 40, 50, 75, 100, 125, 151, 200, 300, and 500 m depth using acid-washed Teflon coated Niskin-X sampling bottles attached to a CTD-CMS system.

(3) Parameters

Macronutrients (NO_3, NO_2, NH_4, PO_4, $Si(OH)_4$) and Al, Mn, Fe, Co, Ni, Cu, Zn, and Cd.

(4) Observation log

St. A7: June 6 (UTC), 2019 at 46°59'N, 160°01'W

(5) Data archives

All data obtained during MR19-02 cruise will be submitted to Data Management Group (DMG) of JAMSTEC after the sample analysis and validation. The data will be opened to the public via "Data Research System for Whole Cruise Information (DARWIN)" in JAMSTEC web site or elsewhere.

(6) Preliminary data

Vertical profiles of macronutrients are shown in Figure 2.8.

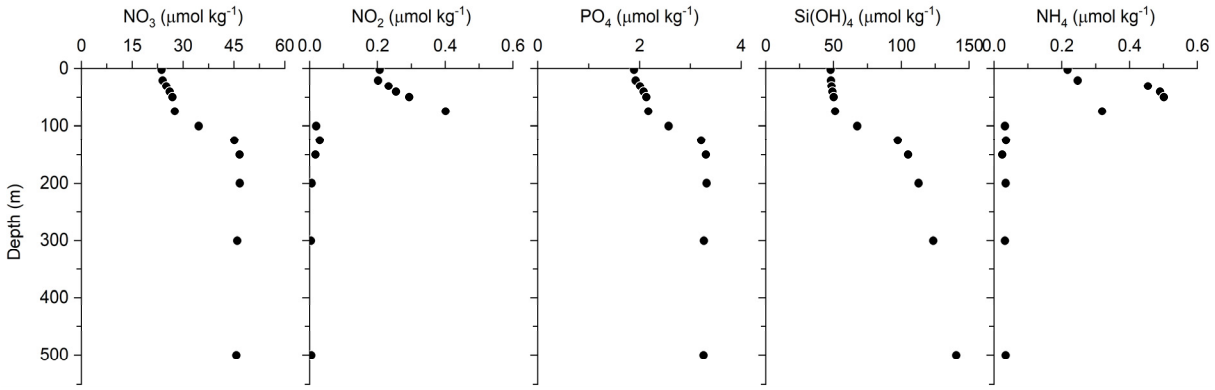

Fig. 2.8. Vertical profile of Nitrate, nitrite, phosphate, silicic acid and ammonia (from left to right).

2.9 Total alkalinity

Masahide WAKITA (JAMSTEC MIO)
Masahiro ORUI (MWJ)
Yasuhiro ARII (MWJ)

(1) Objective

Onboard total alkalinity measurement of seawater corrected in sampling bottles

(2) Methods, Apparatus and Performance

(2)-1 Seawater sampling

Seawater samples were collected by 12 L water sampling bottles mounted on the CTD/Carousel Water Sampling System and a bucket at 9 stations. The seawater from the water sampling bottle was filled into the 100 mL borosilicate glass bottles (SHOTT DURAN) using a sampling silicone rubber tube with PFA tip. The water was filled into the bottle from the bottom smoothly, without rinsing, and overflowed for 2 times bottle volume (10 seconds). These bottles were pre-washed in advance by soaking in 5 % alkaline detergent (decon90, Decon Laboratories Limited) for more than 3 hours, and then rinsed 5 times with tap water and 3 times with Milli-Q deionized water. The samples were stored in a refrigerator at approximately 5 °C before the analysis, and were put in the water bath with its temperature of about 25 °C for one hour just before analysis.

(2)-2 Seawater analyses

The total alkalinity was measured using a spectrophotometric system (Nihon ANS, Inc.) using a scheme of Yao and Byrne (1998). The calibrated volume of sample seawater (ca. 42 mL) was transferred from a sample bottle into the titration cell with its light path length of 4 cm long via dispensing unit. The TA is calculated by measuring two sets of absorbance at three wavelengths (730, 616, and 444) nm applied by the spectrometer (TM-UV/VIS C10082CAH, Hamamatsu Photonics). One is the absorbance of seawater sample before injecting an acid with indicator solution (bromocresol green sodium salt) and another the one after the injection. For mixing the acid with indicator solution and the seawater sufficiently, they are circulated through the line by a peristaltic pump equipped with periodically renewed TYGON tube 5 minutes before the measurement. Nitrogen bubble were introduced into the titration cell for degassing CO_2 from the mixed solution sufficiently.

The TA is calculated based on the following equation:

$$\begin{aligned} pH_T = {} & 4.2699 + 0.002578 \times (35 - S) \\ & + \log ((R(25) - 0.00131) / (2.3148 - 0.1299 \times R(25))) \\ & - \log (1 - 0.001005 \times S), \end{aligned} \quad (1)$$

$$\begin{aligned} A_T = {} & (N_A \times V_A - 10^{pHT} \times DensSW(T, S) \times (V_S + V_A)) \\ & \times (DensSW(T, S) \times V_S)^{-1}, \end{aligned} \quad (2)$$

where R(25) represents the difference of absorbance at 616 nm and 444 nm between before and after the injection. The absorbance of wavelength at 730 nm is used to subtract the variation of absorbance caused by the system. DensSW (T, S) is the density of seawater at temperature (T) and salinity (S), N_A the concentration of the added acid, V_A and V_S the volume of added acid and seawater, respectively.

(3) Preliminary result

A few replicate samples were taken at most of stations and the difference between each pair of analyses was plotted on a range control chart (see fig. 2.9-1). The average of the difference was provisionally 2.57 μmol kg^{-1} (n = 26) with its standard deviation of 2.17 μmol kg^{-1} (excluding the data exceeding 3σ).

(4) Data archive

These data obtained in this cruise will be submitted to the Data Management Group (DMG) of JAMSTEC, and will opened to the public via "Data Research System for Whole Cruise Information in JAMSTEC (DARWIN)" in JAMSTEC web site.
<http://www.godac.jamstec.go.jp/darwin/e>

(5) References

Dickson, A. G., Sabine, C. L. & Christian, J. R. (Eds.). (2007). *Guide to best practices for ocean CO2 measurements, PICES Special Publication 3*: North Pacific Marine Science Organization.

Yao, W. and Byrne, R. H. (1998). Simplified seawater alkalinity analysis: Use of linear array spectrometers. *Deep-Sea Research I*, 45, 1383-1392.

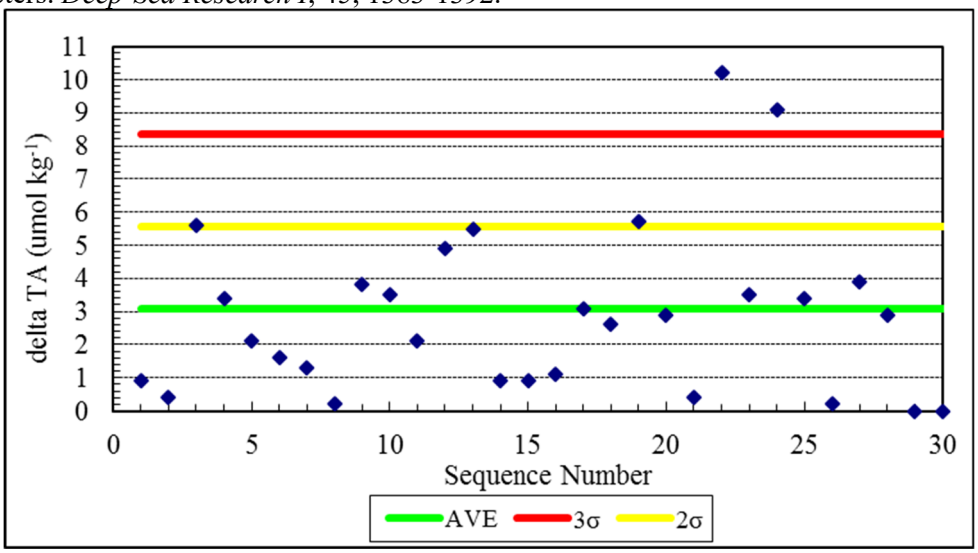

Figure 2.9-1 Range control chart of the absolute differences of replicate measurements of TA carried out during this cruise. AVE represents the average of absolute difference, 3σ the upper control limit (standard deviation of AVE × 3), and 2σ upper warning limit (standard deviation of AVE × 2).

2.10 Dissolved inorganic carbon

Masahide WAKITA (JAMSTEC MIO)
Yasuhiro ARII (MWJ)
Masahiro ORUI (MWJ)

(1) Objective

Onboard total dissolved inorganic carbon (DIC) concentration measurement of seawater collected in sampling bottles

(2) Methods, Apparatus and Performance

(2)-1 Seawater sampling

Seawater samples were collected by 12 liter water sampling bottles mounted on the CTD/Carousel Water Sampling System and a bucket at 9 stations. Seawater was sampled in a 250 mL glass bottle (SHOTT DURAN) that was previously soaked in 5 % alkaline detergent solution (decon 90, Decon Laboratories Limited) at least 3 hours and was cleaned by fresh water for 5 times and Milli-Q deionized water for 3 times. A sampling silicone rubber tube with PFA tip was connected to the water sampling bottle when sampling was carried out. The glass bottles were filled from its bottom gently, without rinsing, and were overflowed for 20 seconds. They were sealed using the polyethylene inner lids with its diameter of 29 mm with care not to leave any bubbles in the bottle. Within about one hour after collecting the samples on the deck, the glass bottles were carried to the laboratory to be poisoned. Small volume (3 mL) of the sample (1 % of the bottle volume) was removed from the bottle and 100 μL of over saturated solution of mercury (II) chloride was added. Then the samples were sealed by the polyethylene inner lids with its diameter of 31.9 mm and stored in a refrigerator at approximately 5 °C. About one hour before the analysis, the samples were taken from refrigerator and put in the water bath kept about 20 °C.

(2)-2 Seawater analysis

Measurements of DIC were made with total CO_2 measuring system (Nihon ANS Inc.). The system comprise of seawater dispensing unit, a CO_2 extraction unit, and a coulometer (Model 3000, Nihon ANS Inc.)

The seawater dispensing unit has an auto-sampler (6 ports), which dispenses the seawater from a glass bottle to a pipette of nominal 15 mL volume. The pipette was kept at 22.00 °C ± 0.05 °C by a water jacket, in which water circulated through a thermostatic water bath (NESLAB RTE10, Thermo Fisher Scientific).

The CO_2 dissolved in a seawater sample is extracted in a stripping chamber of the CO_2 extraction unit by adding 10 % phosphoric acid solution. The stripping chamber is made approx. 25 cm long and has a fine frit at the bottom. First, a constant volume of acid is added to the stripping chamber from its bottom by pressurizing an acid bottle with nitrogen gas (99.9999 %). Second, a seawater sample kept in a pipette is introduced to the stripping chamber by the same method. The seawater and phosphoric acid are stirred by the nitrogen bubbles through a fine frit at the bottom of the stripping chamber. The stripped CO_2 is carried to the coulometer through two electric dehumidifiers (kept at 2 °C) and a chemical desiccant (magnesium perchlorate) by the nitrogen gas (flow rate of 140 mL min^{-1}).

Measurements of system blank (phosphoric acid blank), 1.5 % CO_2 standard gas in a nitrogen base, and seawater samples (6 samples) were programmed to repeat. The variation of our own made JAMSTEC DIC reference material was used to correct the signal drift results from chemical alternation of coulometer solutions.

(3) Preliminary result

A few replicate samples were taken at most of the stations and difference between each pair of analyses was plotted on a range control chart (fig. 2.10-1). The average of the differences was 1.19 μmol kg^{-1}, with its standard deviation of 1.07 μmol kg^{-1} (n = 29), which indicate the analysis was sufficiently accurate (< 1.5 μmol kg^{-1}) according to Dickson et al. (2007).

(4) Data archive

These data obtained in this cruise will be submitted to the Data Management Group (DMG) of JAMSTEC, and will opened to the public via "Data Research System for Whole Cruise Information in JAMSTEC (DARWIN)" in JAMSTEC web site.
<http://www.godac.jamstec.go.jp/darwin/e>

(5) Reference

Dickson, A. G., Sabine, C. L. & Christian, J. R. (Eds.). (2007). *Guide to best practices for ocean CO2 measurements, PICES Special Publication 3*: North Pacific Marine Science Organization.

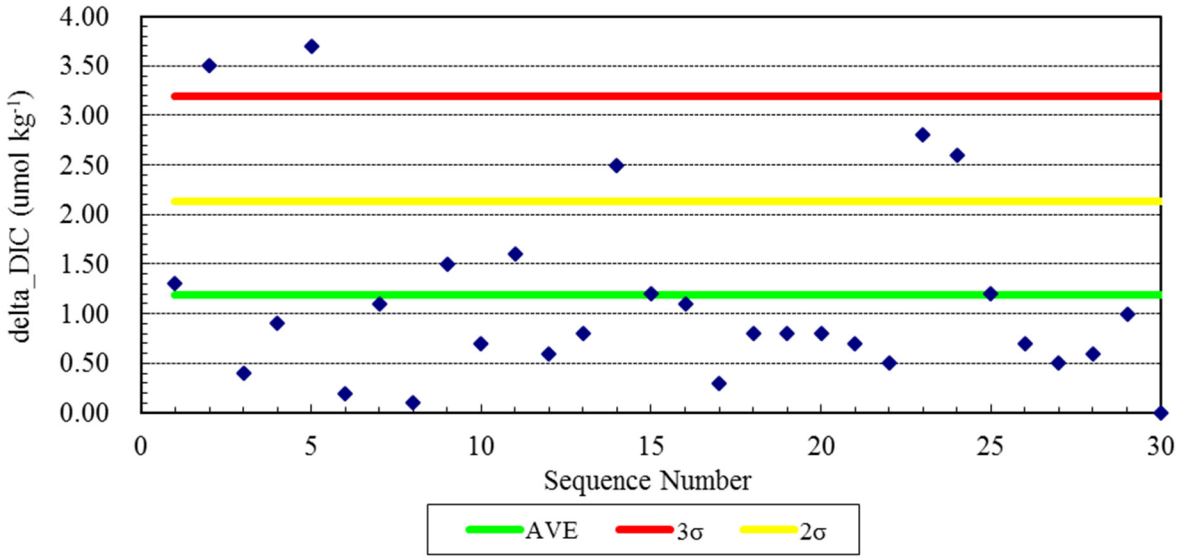

Figure 2.10-1 Range control chart of the absolute differences of replicate measurements of DIC carried out during this cruise. AVE represents the average of absolute difference, 3σ the upper control limit (standard deviation of AVE × 3), and 2σ upper warning limit (standard deviation of AVE × 2).

2.11 Dissolved organic carbon and total dissolved nitrogen

Masahide WAKITA (JAMSTEC MIO)

(1) Objectives

Variabilities in the concentration of dissolved organic carbon (DOC) in seawater have a potentially great impact on the carbon cycle in the marine system, because DOC is a major global carbon reservoir. A change by < 10% in the size of the oceanic DOC pool, estimated to be ~ 700 GtC (IPCC, 2013), would be comparable to the annual primary productivity in the whole ocean. In fact, it was generally concluded that the bulk DOC in oceanic water, especially in the deep ocean, is quite inert based upon ^{14}C-age measurements. Nevertheless, it is widely observed that in the ocean DOC accumulates in surface waters at levels above the more constant concentration in deep water, suggesting the presence of DOC associated with biological production in the surface ocean. This study presents the distribution of DOC in the western subarctic North Pacific.

(2) Sampling

Seawater samples of DOC and TDN were collected by 10 liter Niskin bottles mounted on the CTD/Carousel Water Sampling System and a bucket and brought the total to ~220. Seawater from each Niskin bottle was transferred into 60 ml High Density Polyethylene bottle (HDPE) rinsed with same water three times. Water taken from the surface to bottom is filtered using precombusted (450°C) GF/F inline filters as they are being collected from the Niskin bottle. After collection, samples are frozen upright and preserved at ~ -20 °C cold until analysis in our land laboratory. Before use, all glassware was muffled at 550 °C for 5 hrs.

(3) Analysis

Prior to analysis, samples are returned to room temperature and acidified to pH < 2 with concentrated hydrochloric acid. DOC/TDN analysis was basically made with a high-temperature catalytic oxidation (HTCO) system improved a commercial unit, the Shimadzu TOC-L with a TNM-L units (Shimadzu Co.). In this system, the non-dispersive infrared was used for carbon dioxide produced from DOC during the HTCO process (temperature: 720 °C, catalyst: 0.5% Pt-Al_2O_3). Non-purgeable dissolved nitrogen compounds are combusted and converted to NO which, when mixed with ozone, chemiluminesces for detection by a photomultiplier. The consensus reference material for DOC and TDN (Hansell 2005) was analyzed during the sample measurements.

(3) Preliminary result

The distributions of DOC and TDN will be determined as soon as possible after this cruise.

(4) Data archive

These obtained data will be submitted to JAMSTEC Data Management Group (DMG).

2.12 Particle organic matters

Yoshihisa MINO (Nagoya University)
Makio HONDA (JAMSTEC RIGC)

(1) Objective

Carbon and nitrogen stable isotope ratios ($\delta^{13}C$ and $\delta^{15}N$) of particulate organic matters in the ocean can provide insights into biogeochemical processes, formation and microbial transformation of particles since a mass-dependent isotopic fractionation occurs in each pathway. In this study we examine the vertical distribution of $\delta^{13}C$ and $\delta^{15}N$ of suspended particles to elucidate particle dynamics in subarctic station A7 (K2) in the western North Pacific. A detailed profile of the upper layer particulate organic carbon (POC) concentrations is also determined in several stations, in order to calibrate data from optical backscattering sensor attached to the CTD rosette against POC measurements.

(2) Sampling

For $\delta^{13}C$ and $\delta^{15}N$ analyses, about 10 to 60 liters of seawater were collected by CTD-RMS at the depths from surface to 3,000 m depths in station A7, and filtered through pre-combusted 47 -mm Whatman GF/F filters and the filters were kept frozen until analysis on shore. In a same manner, 2 liters of sample water at 0–300 m in stations A1, A3, A5, A7, and A9 was filtered through 25-mm GF/F filters for POC analysis.

(3) Analysis

The filter samples are exposed to HCl fumes overnight to remove carbonates, dried in vacuum, and then pelletized with a tin disk. Particulate $\delta^{13}C$ and $\delta^{15}N$ in the pellets are measured with an elemental analyzer (EA) combined with a continuous flow isotope-ratio mass spectrometer (IRMS, Thermo Fisher Scientific) at Nagoya University. POC analysis is performed by using EA (PerkinElmer) at JAMSTEC.

(4) Data archive

Data will be submitted to JAMSTEC Data Data Management Group (DMG) within 2 years.

2.13 Sea surface water monitoring

Hiroshi UCHIDA (JAMSTEC RIGC)
Katsunori SAGISHIMA (MWJ)

(1) Objective

Our purpose is to obtain temperature, salinity, dissolved oxygen, fluorescence, and total dissolved gas pressure data continuously in near-sea surface water.

(2) Parameters

Temperature
Salinity
Dissolved oxygen
Fluorescence
Turbidity
Total dissolved gas pressure

(3) Instruments and Methods

The Continuous Sea Surface Water Monitoring System (Marine Works Japan Co. Ltd.) has four sensors and automatically measures temperature, salinity, dissolved oxygen, fluorescence, and turbidity in near-sea surface water every one minute. This system is located in the "sea surface monitoring laboratory" and connected to shipboard LAN-system. Measured data, time, and location of the ship were stored in a data management PC. Sea water was continuously pumped up to the laboratory from an intake placed at the approximately 4.5 m below the sea surface and flowed into the system through a vinyl-chloride pipe. The flow rate of the surface seawater was adjusted to 1.0 L min^{-1}.

a. Instruments

Software

Seamoni-kun Ver.1.2.0

Sensors

Specifications of the each sensor in this system are listed below.

Temperature and Conductivity sensor

Model:	SBE-45, SEA-BIRD ELECTRONICS, INC.
Serial number:	4552788-0264
Measurement range:	Temperature -5 ºC - +35 ºC
	Conductivity 0 S m^{-1} - 7 S m^{-1}
Initial accuracy:	Temperature 0.002 ºC
	Conductivity 0.0003 S m^{-1}
Typical stability (per month):	Temperature 0.0002 ºC
	Conductivity 0.0003 S m^{-1}
Resolution:	Temperature 0.0001 ºC
	Conductivity 0.00001 S m^{-1}

Bottom of ship thermometer

Model:	SBE 38, SEA-BIRD ELECTRONICS, INC.
Serial number:	3852788-0457
Measurement range:	-5 ºC - +35 ºC
Initial accuracy:	±0.001 ºC
Typical stability (per 6 month):	0.001 ºC
Resolution:	0.00025 ºC

Dissolved oxygen sensor

Model:	RINKO II, JFE ADVANTECH CO. LTD.
Serial number:	0035 (From 2019/05/24 To 2019/06/06) 0013 (From 2019/06/07 To 2019/06/12)
Measuring range:	0 mg L^{-1} - 20 mg L^{-1}
Resolution:	0.001 mg L^{-1} - 0.004 mg L^{-1} (25 ºC)
Accuracy:	Saturation ± 2 % F.S. (non-linear) (1 atm, 25 ºC)

Fluorescence & Turbidity sensor

Model:	C3, TURNER DESIGNS
Serial number:	2300384
Measuring range:	Chlorophyll in vivo 0 µg L^{-1} – 500 µg L^{-1}
Minimum Detection Limit:	Chlorophyll in vivo 0.03 µg L^{-1}
Measuring range:	Turbidity 0 NTU - 1500 NTU
Minimum Detection Limit:	Turbidity 0.05 NTU

Total dissolved gas pressure sensor

Model:	HGTD-Pro, PRO OCEANUS
Serial number:	37-394-10
Temperature range:	-2 °C - 50 °C
Resolution:	0.0001 %
Accuracy:	0.01 % (Temperature Compensated)
Sensor Drift:	0.02 % per year max (0.001 % typical)

(4) Observation log

Periods of measurement, maintenance, and problems during this cruise are listed in Table 2.13-1.

Table 2.13-1 Events list of the Sea surface water monitoring during MR19-02

System Date [UTC]	System Time [UTC]	Events	Remarks
2019/05/24	07:00	All the measurements started and data was available.	Start
2019/06/02	02:30	Water flow stopped.	Maintenance
2019/06/02	03:20	Water flow started.	
2019/06/03	08:17	Total dissolved gas pressure sensor removed.	Maintenance

2019/06/03	13:44	Total dissolved gas pressure sensor attached.	
2019/06/06	21:00	Water flow stopped. Dissolved oxygen sensor (S/N:0035) removed	Maintenance
2019/06/07	00:24	Dissolved oxygen sensor (S/N:0013) attached. Water flow started.	
2019/06/12	04:00	All the measurements stopped.	End

We took the surface water samples from this system once a day to compare sensor data with bottle data of salinity, dissolved oxygen, and chlorophyll a. The results are shown in fig. 2.13-2. All the salinity samples were analyzed by the Model 8400B "AUTOSAL" manufactured by Guildline Instruments Ltd. (see 2.5), and dissolve oxygen samples were analyzed by Winkler method (see 2.6), chlorophyll a were analyzed by 10-AU manufactured by Turner Designs. (see 2.16 (a)).

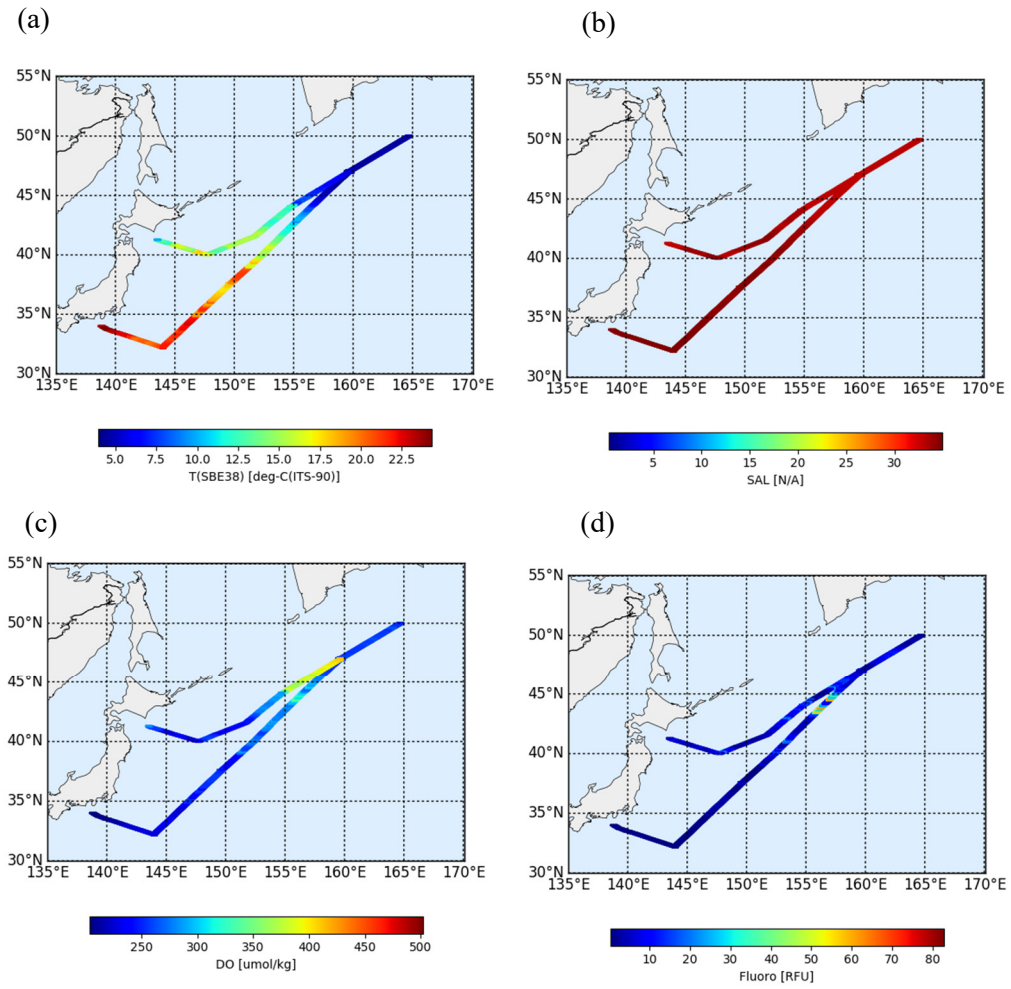

Figure 2.13-1 Spatial and temporal distribution of (a) temperature, (b) salinity, (c) dissolved oxygen, and (d) fluorescence in MR19-02 cruise.

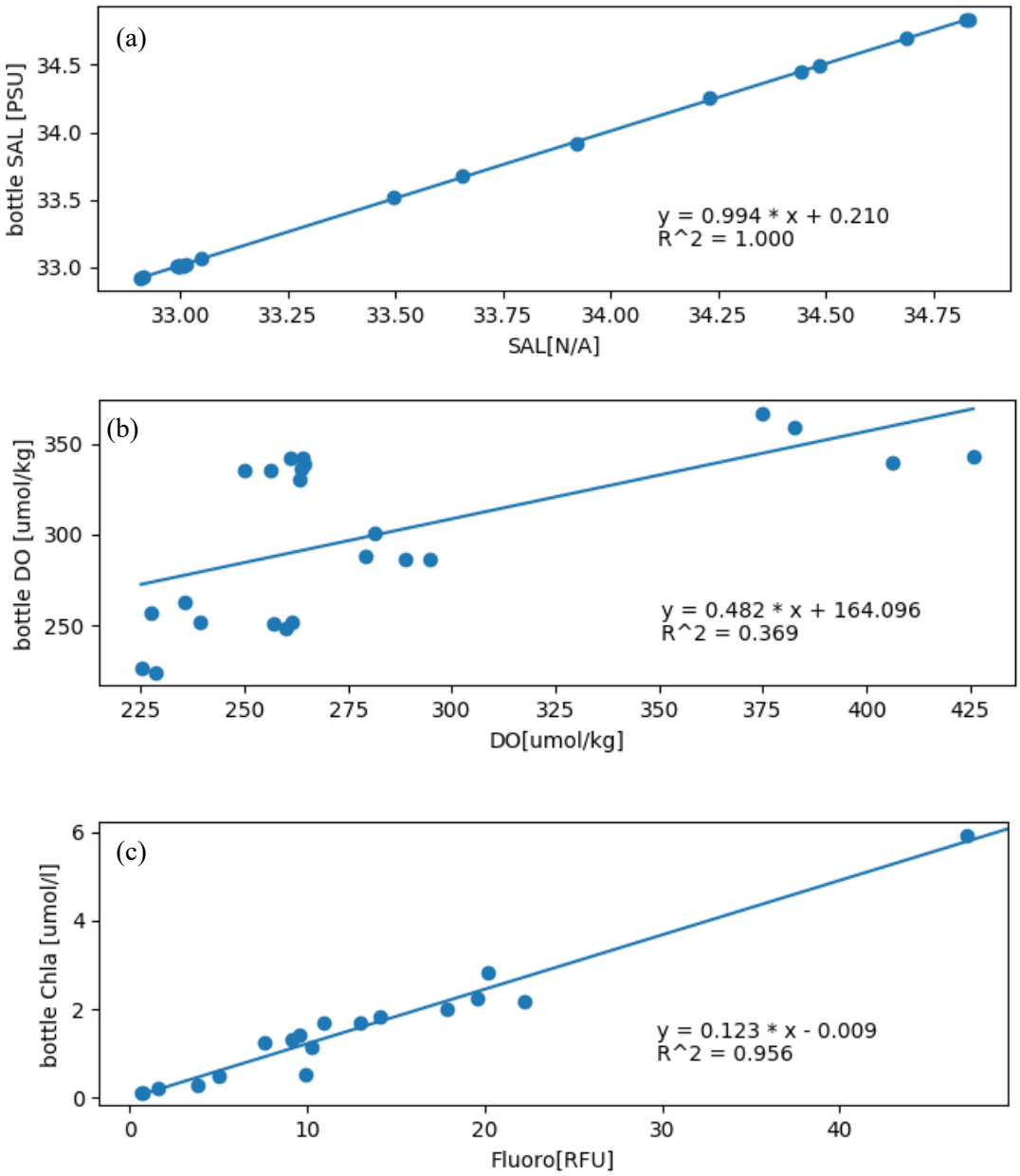

Figure 2.13-2 Correlation of (a) salinity between sensor data and bottle data, (b) dissolved oxygen between sensor data and bottle data and (c) fluorescence between sensor data and bottle data.

(6) Data archives

These data obtained in this cruise will be submitted to the Data Management Group (DMG) of JAMSTEC, and will opened to the public via “Data Research System for Whole Cruise Information in JAMSTEC (DARWIN)” in JAMSTEC web site.

<http://www.godac.jamstec.go.jp/darwin/e>

2.14 In situ filtration system

Yoshihisa MINO (Nagoya University)
Makio HONDA (JAMSTEC RIGC)
Katsunori KIMOTO (JAMSTEC RIGC)
Tetsuichi FUJIKI (JAMSTEC RIGC)

(1) Objective

Suspended particulate matter (SPM) in the ocean plays a vital role in the cycling of trace elements and isotopes. Even microanalyses of SPM, however, require filtering hundreds liters of seawater to collect samples. In this cruise, we deployed in situ large volume filtration system at stations A1 and A7 to measure pigment, DNA, organic and inorganic carbon, isotopic compositions as well as foraminifera shells in the suspended particles.

(2) Sampling

In situ pump filtering was conducted three times by using McLane WTS-LV samplers, one of which was installed with a customized pump by Offshore-technologies, at multi-layers as shown in Table 1.

Table 1. Setting for in situ filtration. *Pump didn't work properly.

Date & station	Depth (m)	Filtration rate (L)	Filters	Measurements	PIC
2019/05/26 A1 (KEO)	63	0*	GF/F, 300 μm mesh	Pigments, DNA, $\delta^{13}C$, $\delta^{15}N$, POC, PIC	Fujiki, Mino Honda
	100	757	GF/F, 300 μm mesh		
	200	676	GF/F, 300 μm mesh		
	400	718	GF/F, 300 μm mesh		
	1000	707	GF/F, 300 μm mesh		
	2000	696	GF/F, 300 μm mesh		
	2000	0*	GF/F, 300 μm mesh		
	3000	674	GF/F, 300 μm mesh		
2019/06/02 A7 (K2)	100	673	GF/F, 55 μm mesh	Carbonate particle,	Kimoto,
	250	570	GF/F, 55 μm mesh		
	350	604	GF/F, 55 μm mesh		
	500	605	GF/F, 55 μm mesh		
	550	609	GF/F, 55 μm mesh		
	600	0*	GF/F, 55 μm mesh		
	650	614	GF/F, 55 μm mesh		
	700	590	GF/F, 55 μm mesh		

2019/06/07 A7 (K2)	50 100 200 500 1000 2000 3000	670 784 687 749 763 777 741	GF/F, 300 μm mesh GF/F, 300 μm mesh GF/F, 300 μm mesh GF/F, 300 μm mesh GF/F, 300 μm mesh GF/F, 300 μm mesh GF/F, 300 μm mesh	Pigments, DNA, $\delta^{13}C$, $\delta^{15}N$, POC, PIC	Fujiki, Mino Honda

(3) Analysis

Particles larger than 55 μm were rinsed by fresh water and fixed by the ethanol (99.5 %). Carbonate shelled foraminifera was picked up by the brush under the stereomicroscope and dried on the assemblage slide at room temperature. Their shell density will be measured by Micro-focus X-ray CT (MXCT, ScanXmate-DF160TS105, Comscan Tecno, Co.Ltd) installed in JAMSTEC HQ.

Phytoplankton pigments in the SPM on GF/F were extracted with *N,N*-dimethylformamide for at least 24 h at –20 °C in the dark and then analyzed with an HPLC modular system (Agilent Technologies) on the sea.

For DNA analysis, filter SPM samples were put in the vial including 1 ml of DNA-degradation inhibitor (0.25 M EDTA, 20 % DMSO, and saturated NaCl liquid). The samples will be analyzed at Tsukuba University.

$\delta^{13}C$ and $\delta^{15}N$ of particulate organic matters will be measured by using EA-IRMS at Nagoya University.

Total carbon (TC) and organic carbon (OC) of the particles will be measured by using EA at JAMSTEC. Inorganic carbon is determined from the difference between the TC and OC.

(4) Data archive

Data will be submitted to JAMSTEC Data Data Management Group (DMG) within 2 years.

2.15 POC optical observation

Makio HONDA (JAMSTEC RIGC)
Yoshihisa MINO (Nagoya University)
Kazuhiko MATSUMOTO (JAMSTEC RIGC)

(1) Objectives

Settling particle in the ocean, sometimes called “marine snow”, plays a crucial role in the “biological carbon pump”, which transports atmospheric carbon dioxide to the ocean interior. Traditionally the study of settling particle has been conducted by using sediment trap. However, much attention has been paid to optical observation of settling particles recently. Optical sensor such as backscatter meter is installed on drifting buoy and spatio-temporal variability of marine particle has been observed all over the world ocean and, consequently, biogeochemistry has been discussed. In order to study settling particles, mainly particulate organic carbon (POC), optically, backscatter meters were deployed during this cruise. Main purpose was that data obtained by backscatter meter (pressure, temperature, chlorophyll and backscatter) are compared with data obtained by well-calibrated CTD and onboard-measured chlorophyll and POC data and to propose empirical equation. After basic data was obtained, some backscatter meters were installed on K2 “hybrid” mooring system and deployed for time-series optical observation of settling particles.

(2) Instruments and methods

1) Backscatter meter

Principal specification of backscatter meters (BS) used during this cruise are as follows:

Maker	model	S/N	Max depth (m)	Depth sensor	Temp	Fluorometer	Backscatter bbp470	Backscatter bbp700
Wetlab	Eco Triplet	891	600	O	O	O	O	O
Wetlab	Eco Triplet	905	600	O	O	O	O	O
Seabird Sci.	FLBBSB	5167	300	-	-	O	-	O
Seabird Sci.	FLBBSB	5168	300	-	-	O	-	O
Seabird Sci.	FLBBSB	5172	300	-	-	O	-	O
Seabird Sci.	FLBBSB	5175	300	-	-	O	-	O
Seabird Sci.	BBSB	1742	300	-	-	-	-	O

These BSs were installed on carousel water sampling system with CTD (Photo 1) and in situ filtration system (McLane WTS-LV. Detail is described in section “in situ filtration”) (Photo 2). Concentration of

chlorophyll (Chl-a) and backscatter intensity observed by BS were compared with Chl-a measured onboard by ordinally method (Welschmeyer "Non-acidification method" with Turner designed fluorometer. Detail is described in section "phytoplankton") and turbidity observed by turbidity meter (detail is described in section "CTD cast and water sampling"), respectively. Backscatter intensity and also observed with POC measured onboard and will be also compared with particulate organic carbon (POC) measured on land laboratory.

2) Underwater video camera
Underwater video camera (UVC) consists of Raspberry Pi camera module / computer circuit system and transparent pressure hull (maximum depth: 200 m). This UVC and underwater light were developed by Dr. Kazumasa Oguri from JAMSTEC. This UVC camera was installed on in situ filtration system (McLane LVP) and deployed at around 200 m at stations A1 (KEO) and A7 (K2).

(3) Preliminary result
1) BS on CTD
a) Pressure and Temperature
Data of pressure and temperature observed by BS (Triplet S/N 891 and S/N 905) were compared with these observed by CTD. Temperature observed by BS correlated well with that observed by CTD (Fig.1 a). Although pressure observed by one BBS (Triplet S/N 891) had large intercept, pressure observed by BS also correlated well with CTD-based pressure (Fig. 1b).

b) Chl-a
BS-based Chl-a was compared with CTD-based Chl-a. Although slope coefficient and intercept for respective BS were different, BS-based Chl-a positively correlated well with CTD-based Chl-a (Fig. 2).

c) Backscatter intensity
Backscatter intensity observed by BS were compared with turbidity observed by CTD.
Backscatter intensity for 700 nm light (reddish light) (bbp700) observed by four of seven BSs (Triplet S/N 905, FLBBSB S/N 5172, 5175, BBSB S/N 1742) showed good correlation with CTD-based turbidity (Fig. 3 a, b, c, d). On the other hand, although backscatter observed by three BSs (Triplet S/N 891, FLBBSB S/N 5167, 5168) correlated positively with turbidity, its absolute value drifted largely for respective deployment (Fig. 3 e, f, g). Although there is possibility that CTD frame on which BS was installed affected BS data, this reason is still open question.

d) Comparison of BS data with bottle data
i) Chl-a
Chl-a data observed by BS (Chl-a(BS)) were compared with Chl-a concentration in collected seawater and measured onboard (Chl-a(bottle)). As shown in Fig.4, Chl-a(BS) correlated well with Chl-a(bottle).

ii) POC
BS backscatter data observed by BS (bbp(700)) were compared with POC concentration in collected seawater and measured onboard (POC(bottle)). As shown in Fig.5, bbp(700) tended to correlate with POC(bottle).

2) BS on LVP

At station A7 (K2), three BSs were installed on three LVPs (100 m, 200 m, 500 m) and, during in situ filtration period (240 minutes), BS data was obtained with sampling interval of 30 minutes and sampling time of three minutes. Temporal variability of BS chl-a data and bbp(700) at three depth were shown in Fig. 6. Chl-a data at 100 m and 200 m were comparable with Chl-a data observed by BS on CTD at night (Fig. 6a). bbp(700) data at 100 m and 200 m were comparable with or slightly larger than Chl-a data observed by BS on CTD at night (Fig. 6b).

2) UVC

Still photo and three minutes-long video were successfully taken per 30 minutes during in situ pumping observation (220 minutes at station A1: KEO and 240 minutes at station A7: K2). After cruise, image analysis about particles will be conducted and these data will be compared with backscatter meter's data and

(4) Data archive

These obtained data will be submitted to JAMSTEC Data Management Group (DMG) or will be opened on original data base.

Funding

This observation is financially supported by MEXT KAKENHI: grant-in-aid for scientific research "Mathematization of POC vertical attenuation by using optical method: Proposition of Martin curve in the Western Pacific ocean".

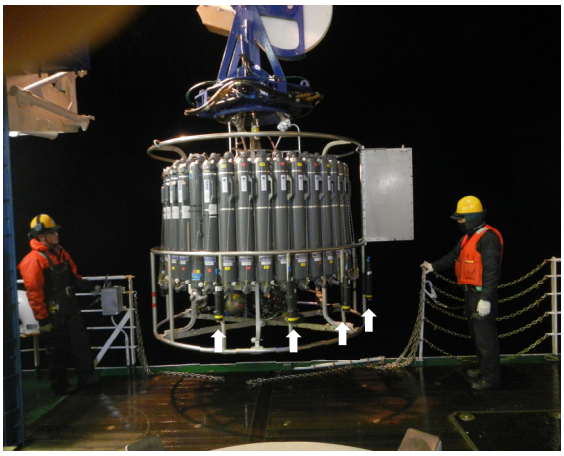

Photo 1 BS (white arrow) on Carousel multiple Water Sampling System

Photo 2 BS (white arrow) and UVC (yellow arrow) on LVP

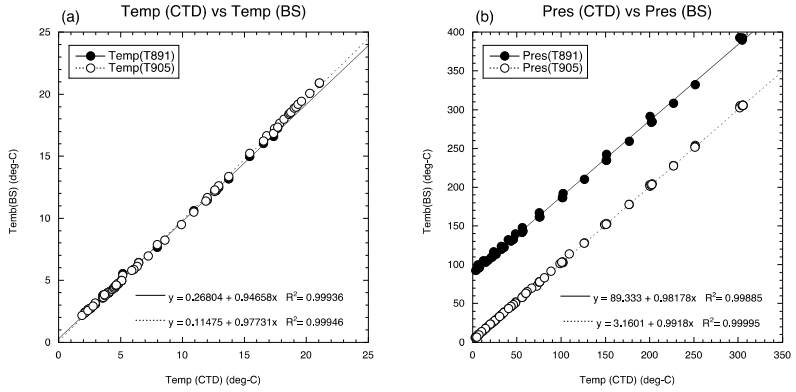

Fig. 1 (a) Temperature observed by CTD (Temp(CTD) vs Temperature observed by backscatter meter (Temp(BS)) (b) Pressure observed by CTD (Pres (CTD) vs Pressure observed by backscatter meter (Pres (BS))

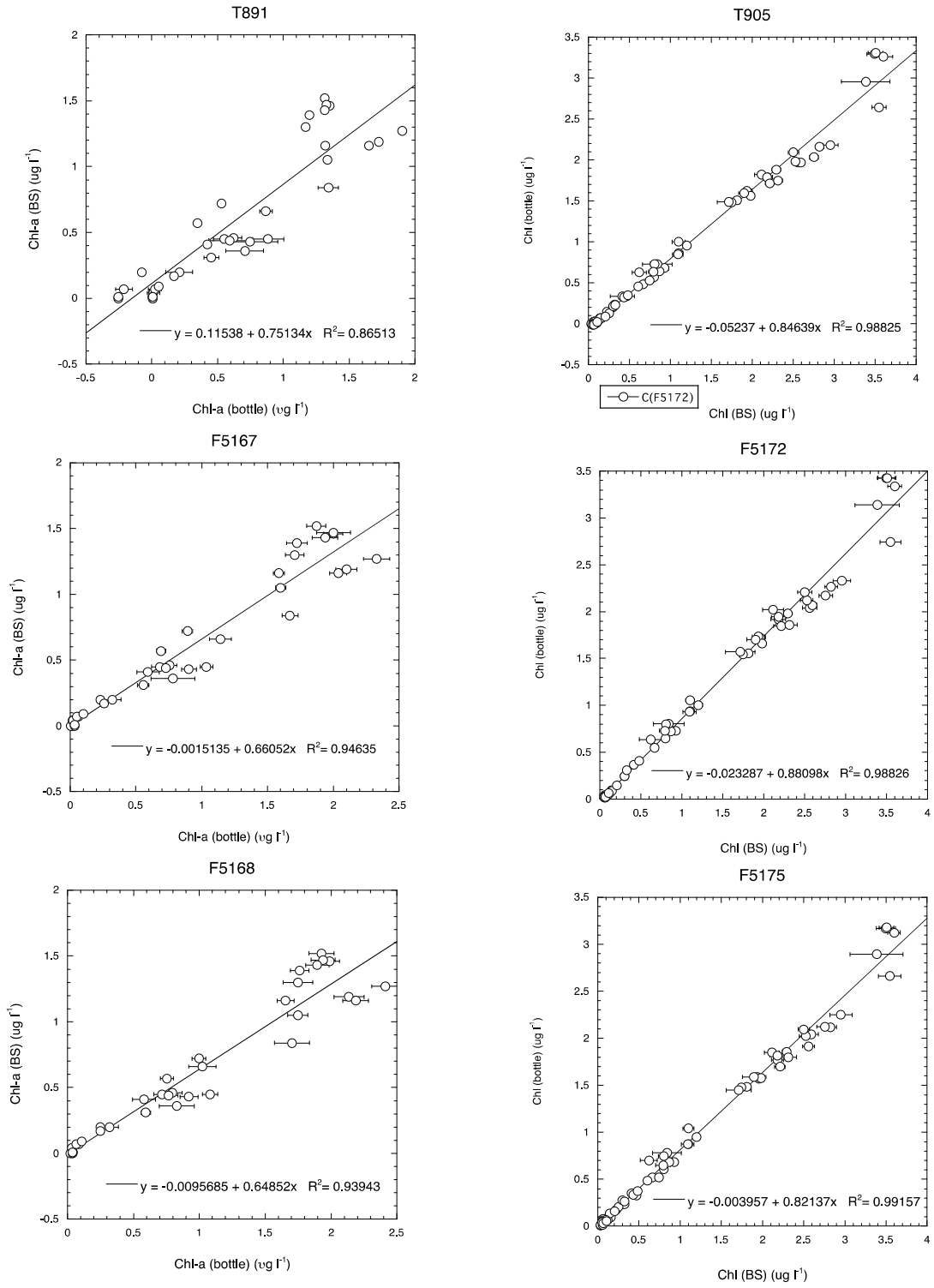

Fig.2 Chl-a (BS) vs Chl-a (CTD)

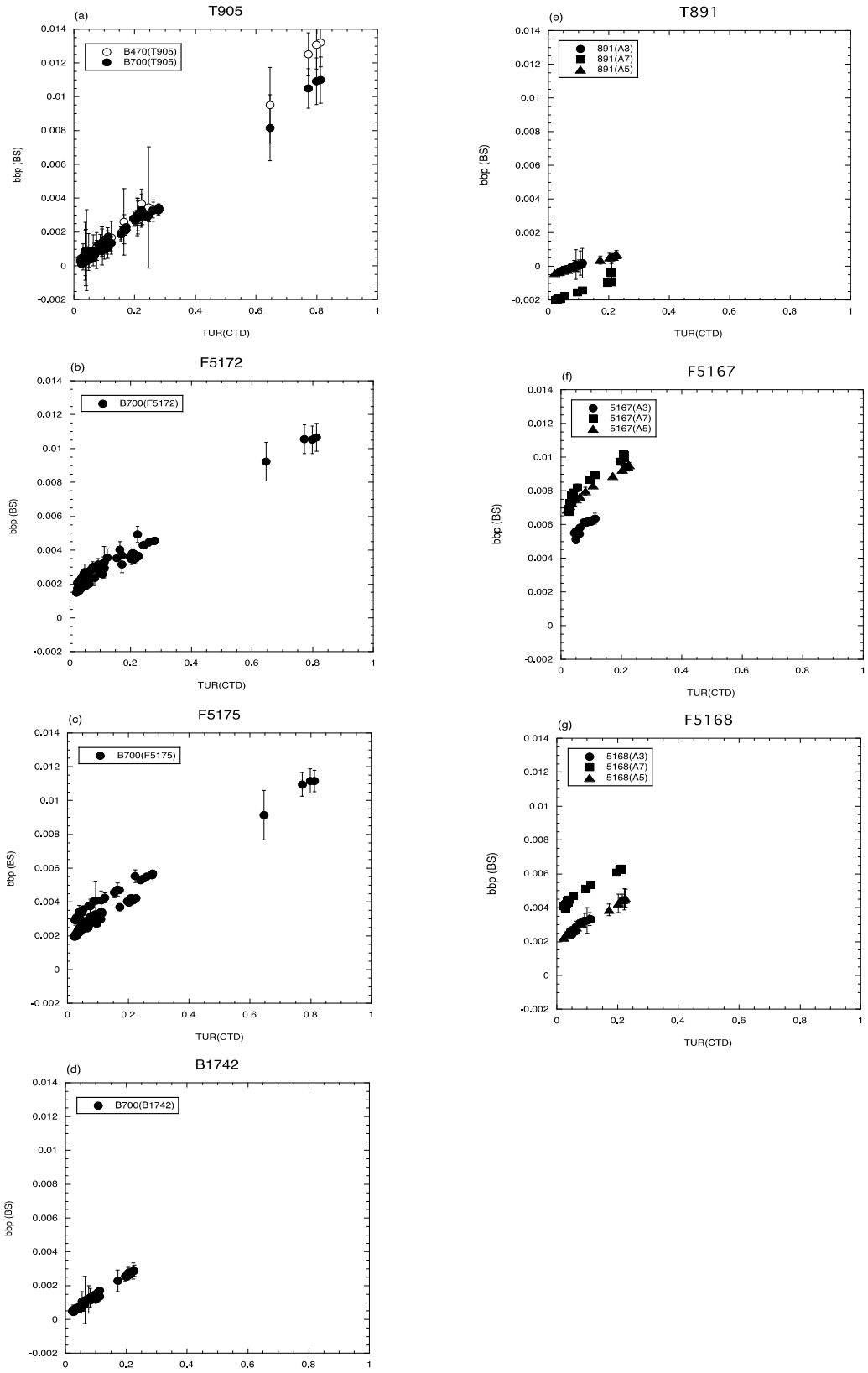

Fig. 3 Turbidity observed by CTD (Turb(CTD)) vs backscatter (700) observed by BS (bbp(BS)), Different symbols in Fig. 3 (e) (f) (g) show bbp data from different deployment.

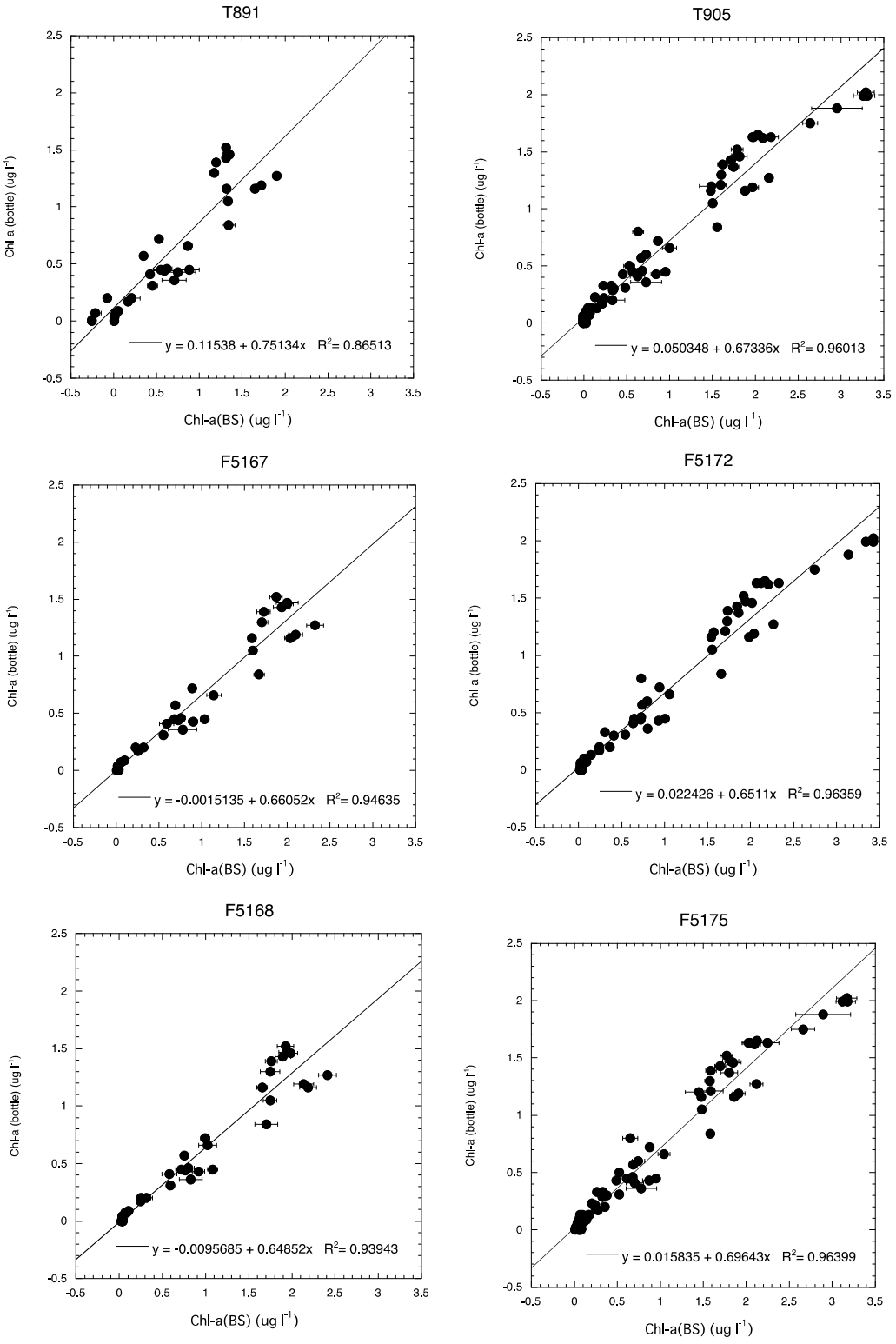

Fig.4 Chl-a(BS) vs Chl-a(bottle)

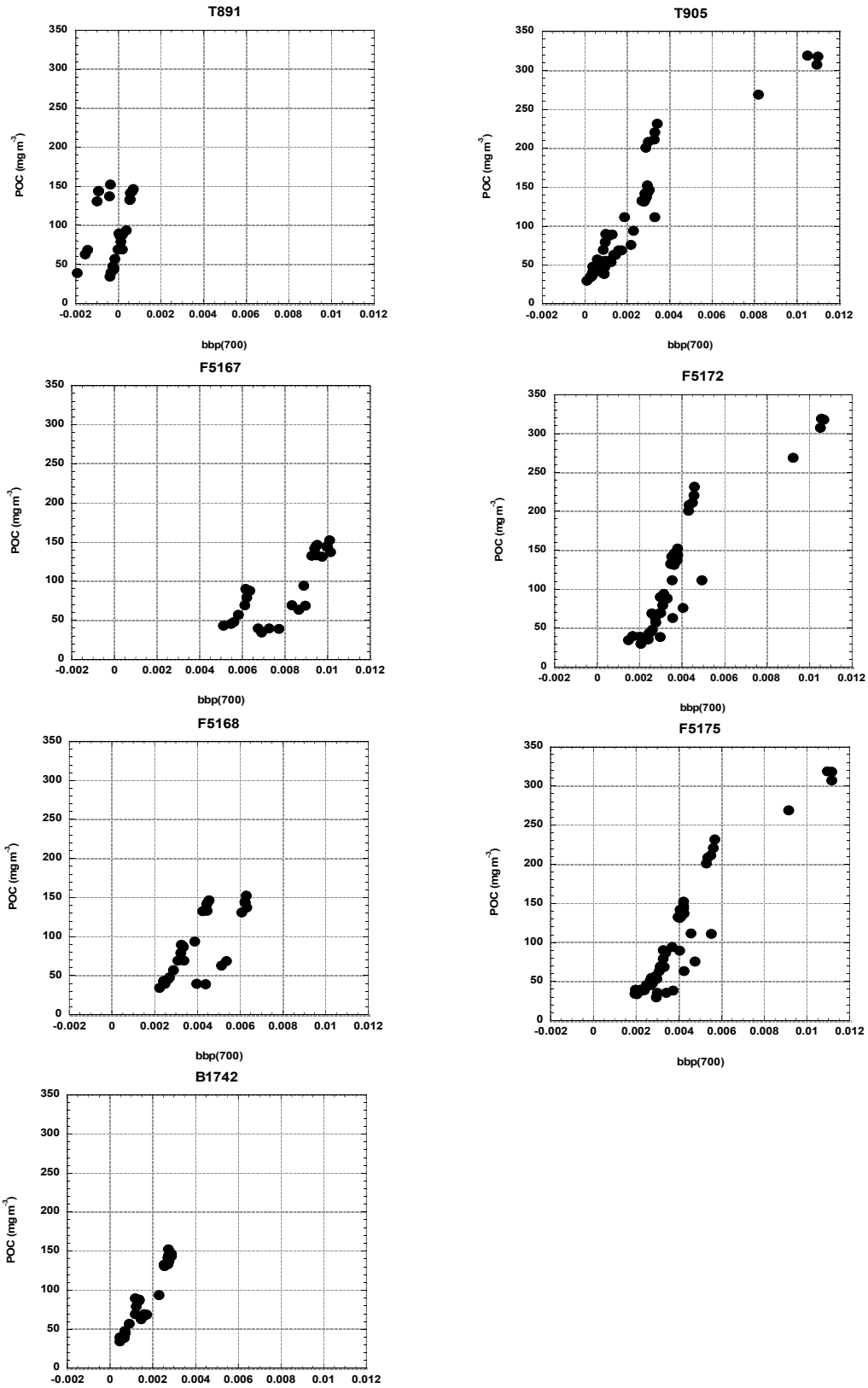

Fig.5 bbp(700) vs POC(bottle)

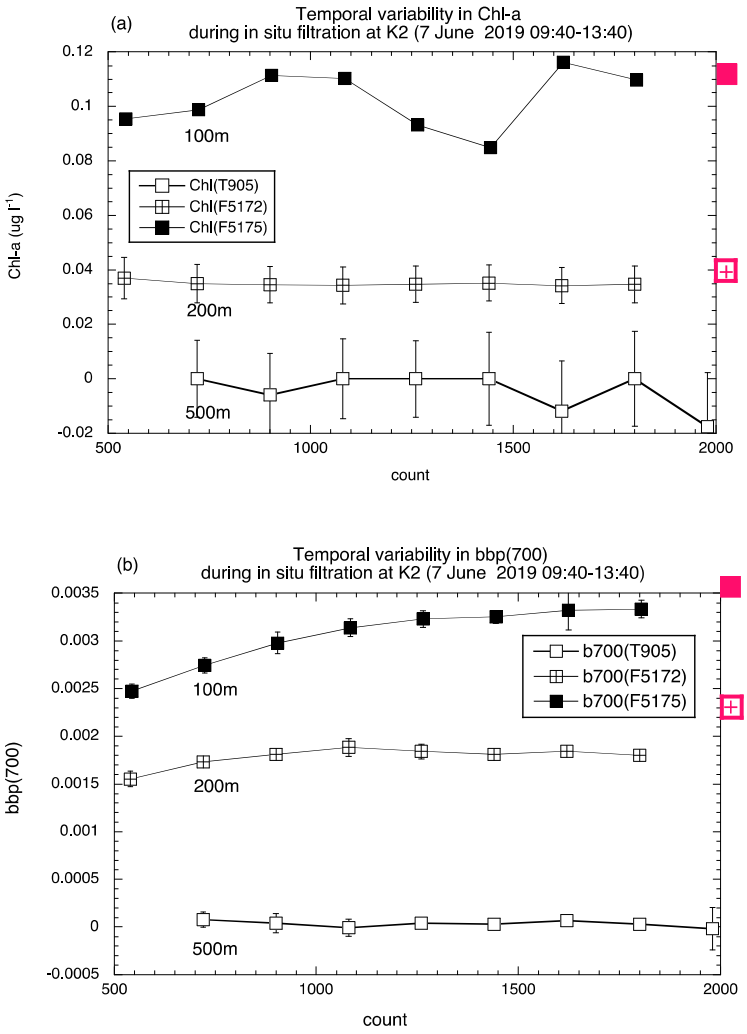

Fig.6 Temporal variability in (a) Chl-a(BS) and (b) backscatter intensity during LVP observation at station K2

2.16 Phytoplankton

2.16 (a) Chlorophyll *a* measurements by fluorometric determination

Tetsuichi FUJIKI (JAMSTEC RIGC)
Hideki YAMAMOTO (MWJ)
Hiroshi HOSHINO (MWJ)
Takayuki SUNAGAWA (MWJ)

(1) Objective

Phytoplankton biomass can estimate as the concentration of chlorophyll *a*, because all oxygenic photosynthetic plankton contain chlorophyll *a*. Phytoplankton exist various species in the ocean, but the species are roughly characterized by their cell size. The objective of this study is to investigate the vertical distribution of phytoplankton and their size fractionations as chlorophyll *a* by using the fluorometric determination.

(2) Parameters

Total chlorophyll *a*
Size-fractionated chlorophyll *a*

(3) Instruments and Methods

We collected samples for total chlorophyll a from 3 to 18 depths and size-fractionated chlorophyll *a* from 8 to 9 depths between the surface and 300 m depth including a chlorophyll *a* maximum layer. The chlorophyll *a* maximum layer was determined by a Chlorophyll Fluorometer (Seapoint Sensors, Inc.) attached to the CTD system.

Seawater samples for total chlorophyll *a* were vacuum-filtrated (< 0.02 MPa) through glass microfiber filter (Whatman GF/F, 25mm-in diameter). Seawater samples for size-fractionated chlorophyll *a* were passed through 10 µm, 3 µm and 1 µm polycarbonate filters (Nuclepore filter, 47-mm in diameter) and glass microfiber filter (Whatman GF/F, 25mm-in diameter) under gentle vacuum (< 0.02 MPa). Phytoplankton pigments retained on the filters were immediately extracted in a polypropylene tube with 7 ml of N,N-dimethylformamide (FUJIFILM Wako Pure Chemical Corporation Ltd.) (Suzuki and Ishimaru, 1990). The tubes were stored at -20 °C under the dark condition to extract chlorophyll *a* at least for 24 hours.

Chlorophyll *a* concentrations were measured by the fluorometer (10-AU, TURNER DESIGNS), which was previously calibrated against a pure chlorophyll *a* (Sigma-Aldrich Co., LLC). To estimate the chlorophyll *a* concentrations, we applied to the fluorometric “Non-acidification method” (Welschmeyer, 1994).

(4) Station list

The number of samples, stations and the sampling positions were shown in table 2.16(a).2 and fig. 2.16(a).1.

(5) Preliminary Results

The results of total chlorophyll *a* at station were shown in fig. 2.16(a).2 to fig. 2.16(a).5. The results of size fractionated chlorophyll *a* at station were shown in fig. 2.16(a).6 to fig. 2.16(a).15. At each station, water samples were taken in replicate for water of chlorophyll *a* maximum layer. Results of replicate samples were shown in table 2.16(a).1.

(6) Data archives

These data obtained in this cruise will be submitted to the Data Management Group of JAMSTEC, and will be opened to the public via "Data Research System for Whole Cruise Information in JAMSTEC (DARWIN)" in JAMSTEC web site.

http://www.godac.jamstec.go.jp/darwin/e

(7) Reference

Suzuki, R., and T. Ishimaru (1990), An improved method for the determination of phytoplankton chlorophyll using N, N-dimethylformamide, *J. Oceanogr. Soc. Japan*, 46, 190-194.

Welschmeyer, N. A. (1994), Fluorometric analysis of chlrophyll *a* in the presence of chlorophyll *b* and pheopigments. *Limnol. Oceanogr.* 39, 1985-1992.

Table 2.16(a).1. Results of the replicate sample measurements.

	All samples
Number of replicate sample pairs	17
Standard deviation (μg L^{-1})	0.02

Table 2.16(a).2. Number of samples and casts.

	Number of samples	Number of casts
Total chlorophyll *a*	194	18
size-fractionated chlorophyll *a*	83	10

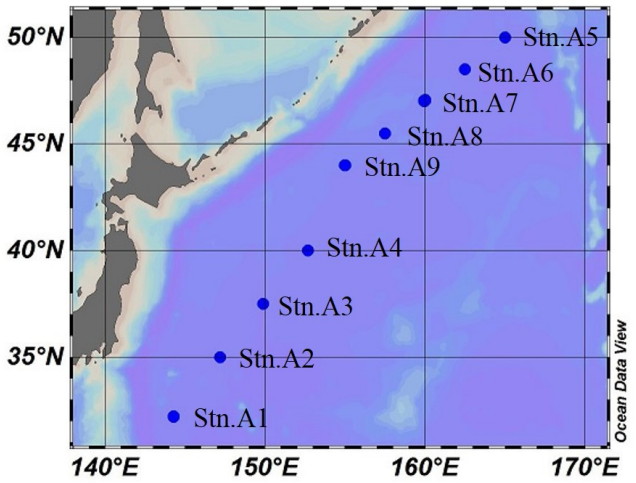

Figure 2.16(a).1. Sampling position of chlorophyll *a* samples in MR19-02.

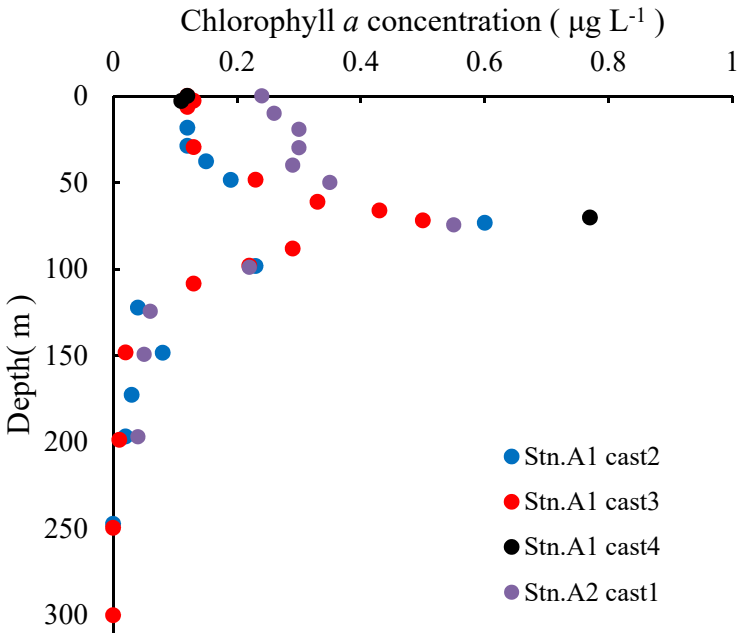

Figure 2.16(a).2. Vertical distribution of chlorophyll *a* at Stn.A1 cast 2 to 4 and Stn.A2.

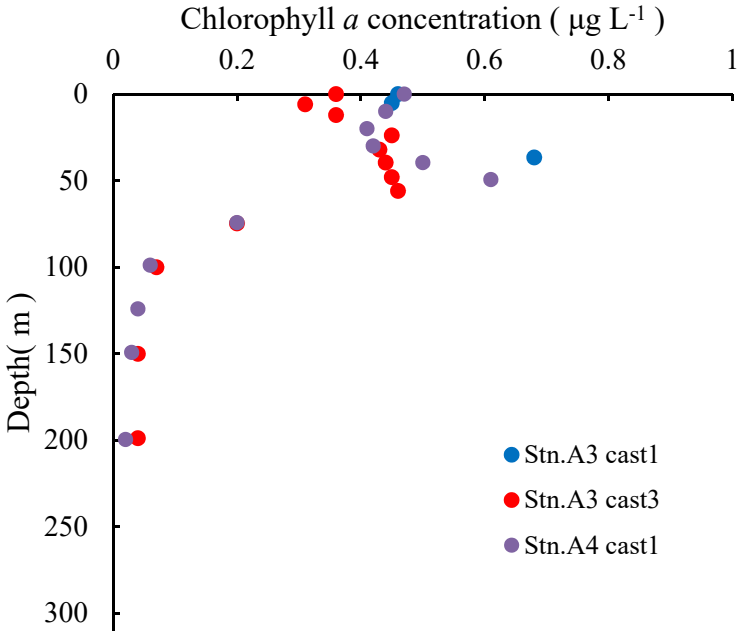

Figure 2.16(a).3. Vertical distribution of chlorophyll *a* at Stn.A3 cast 1, cast 3 and Stn.A4.

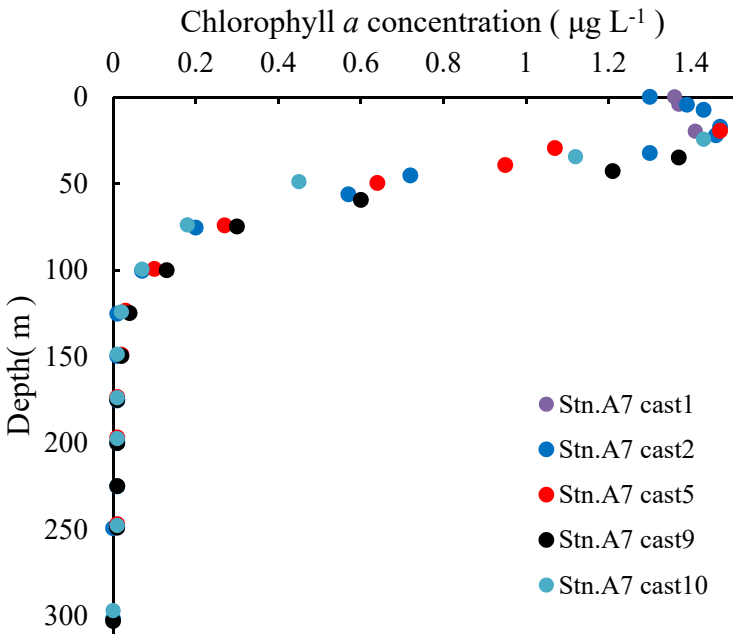

Figure 2.16(a).4. Vertical distribution of chlorophyll *a* at Stn.A7.

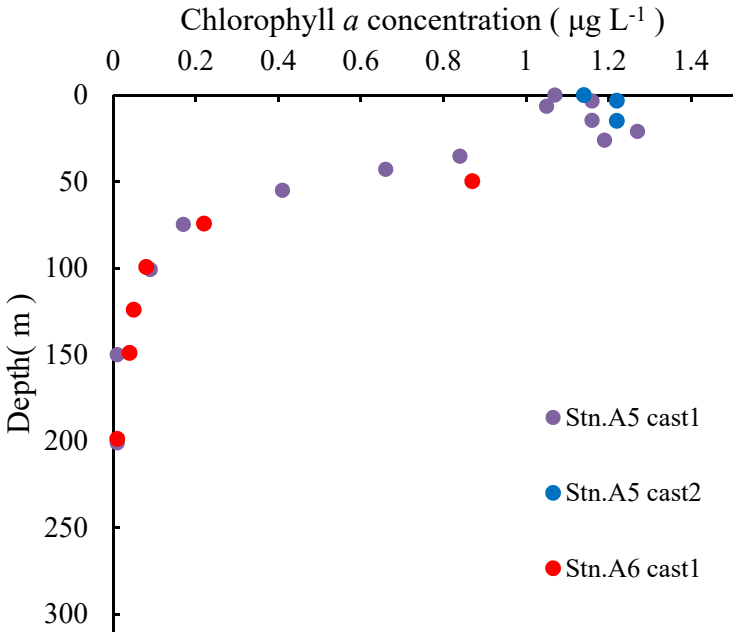

Figure 2.16(a).5. Vertical distribution of chlorophyll *a* at Stn.A5 cast1, 2 and Stn.A6.

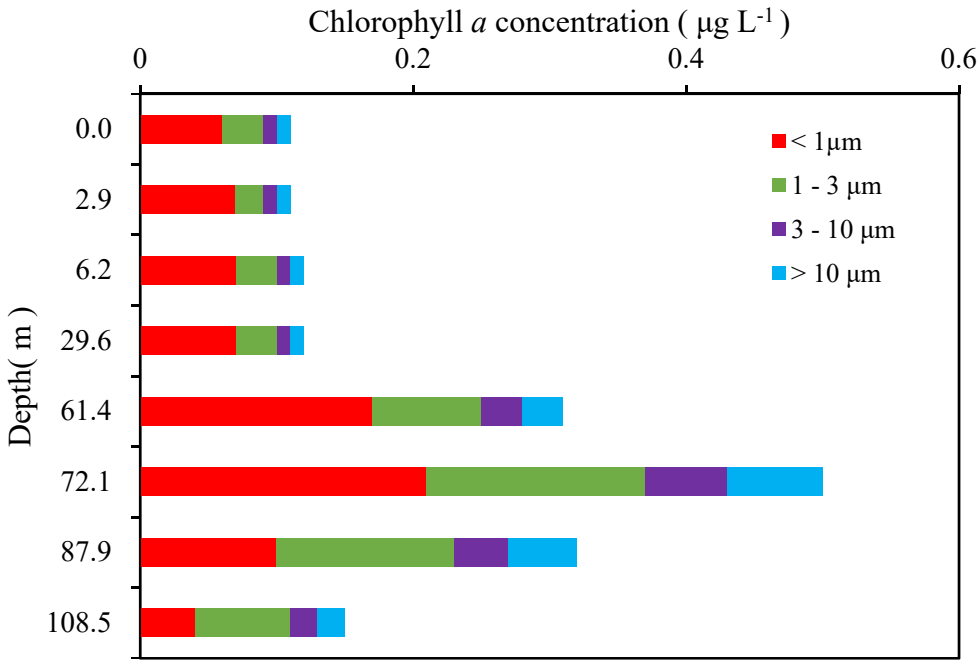

Figure 2.16(a).6. Vertical distribution of size-fractionated chlorophyll *a* at Stn.A1 cast3.

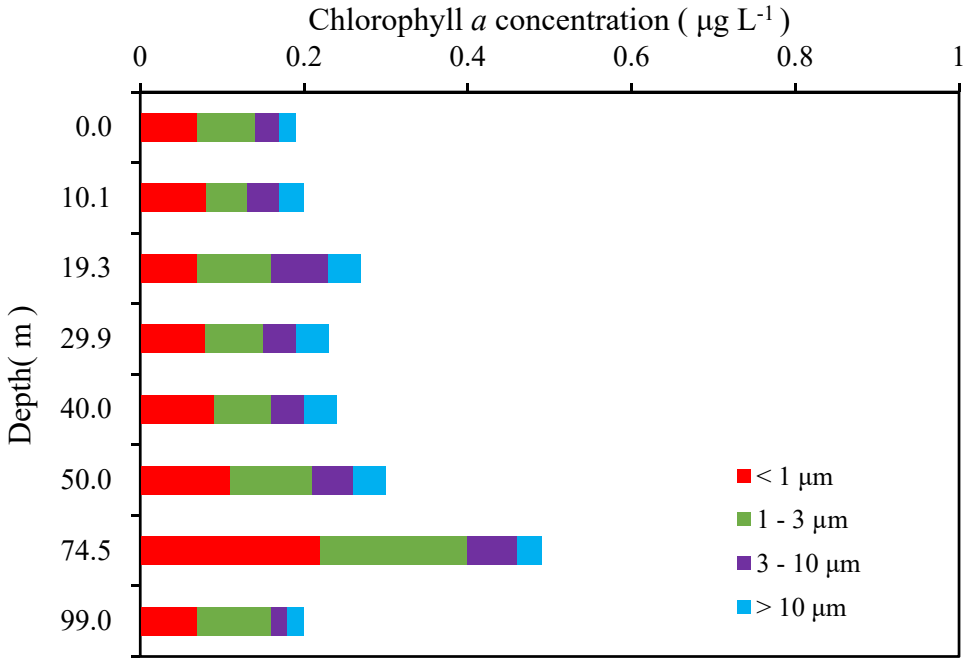

Figure 2.16(a).7. Vertical distribution of size-fractionated chlorophyll *a* at Stn.A2 cast1.

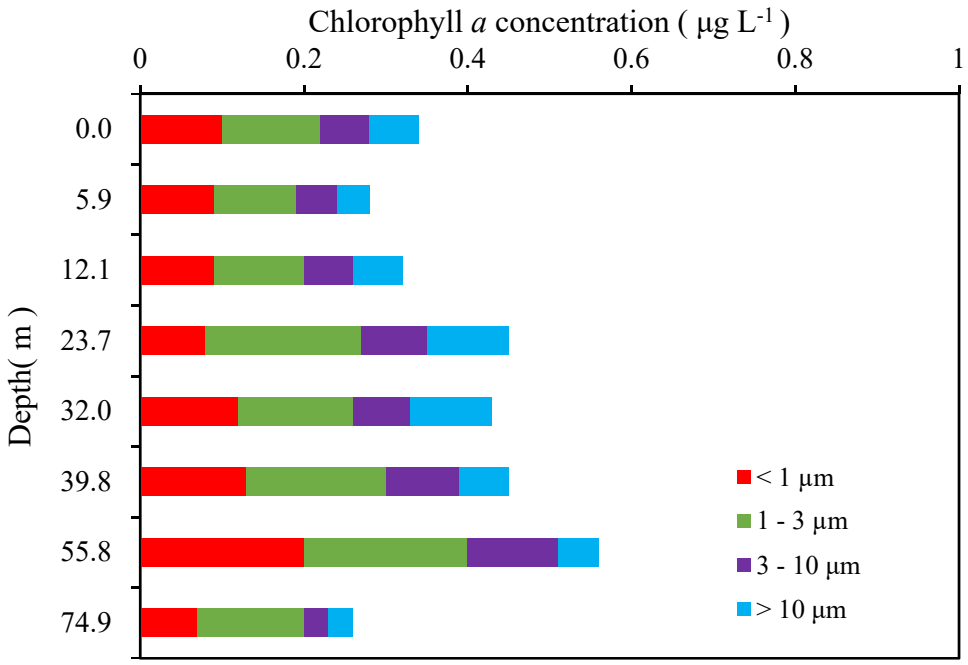

Figure 2.16(a).8. Vertical distribution of size-fractionated chlorophyll *a* at Stn.A3 cast3.

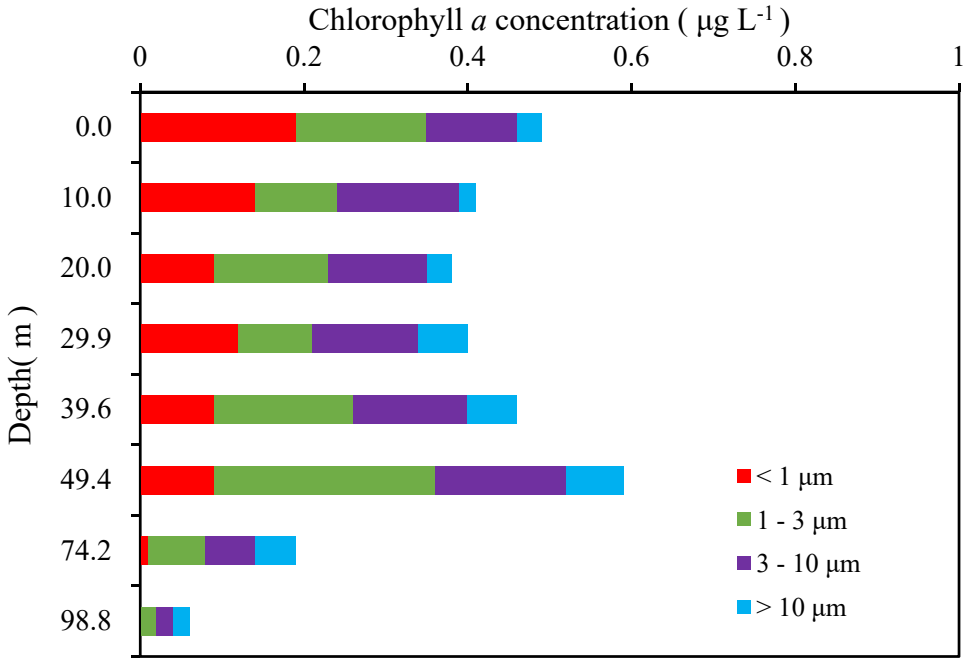

Figure 2.16(a).9. Vertical distribution of size-fractionated chlorophyll *a* at Stn.A4 cast1.

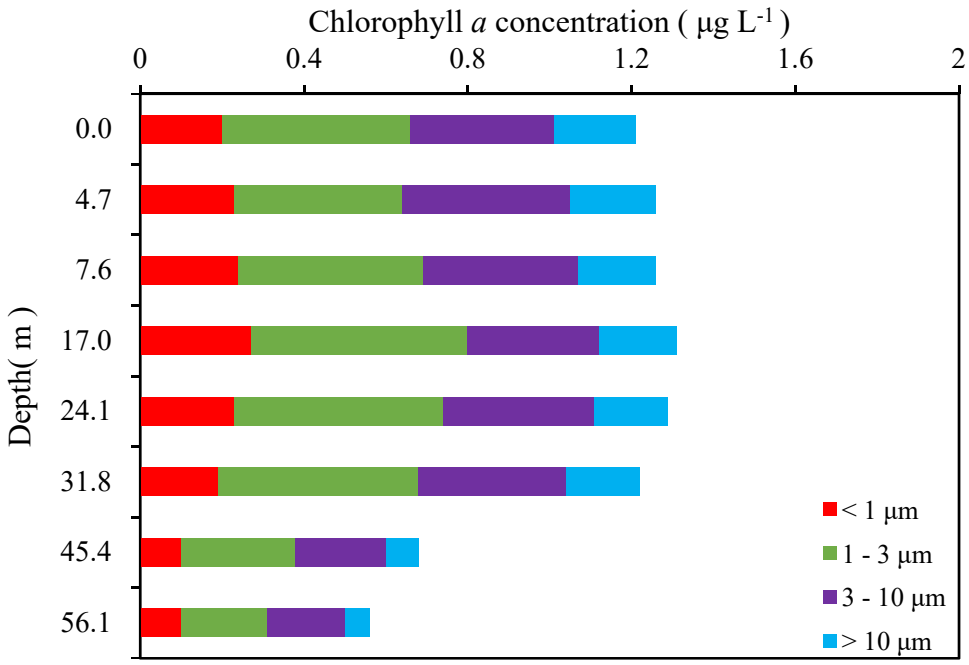

Figure 2.16(a).10. Vertical distribution of size-fractionated chlorophyll *a* at Stn.A7 cast2.

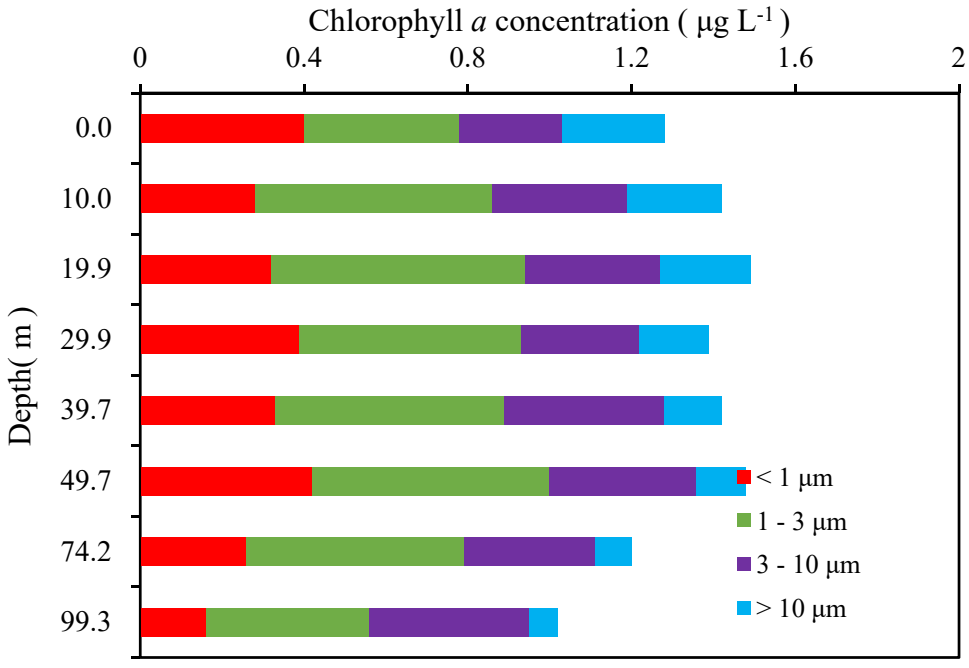

Figure 2.16(a).11. Vertical distribution of size-fractionated chlorophyll *a* at Stn.A7 cast9.

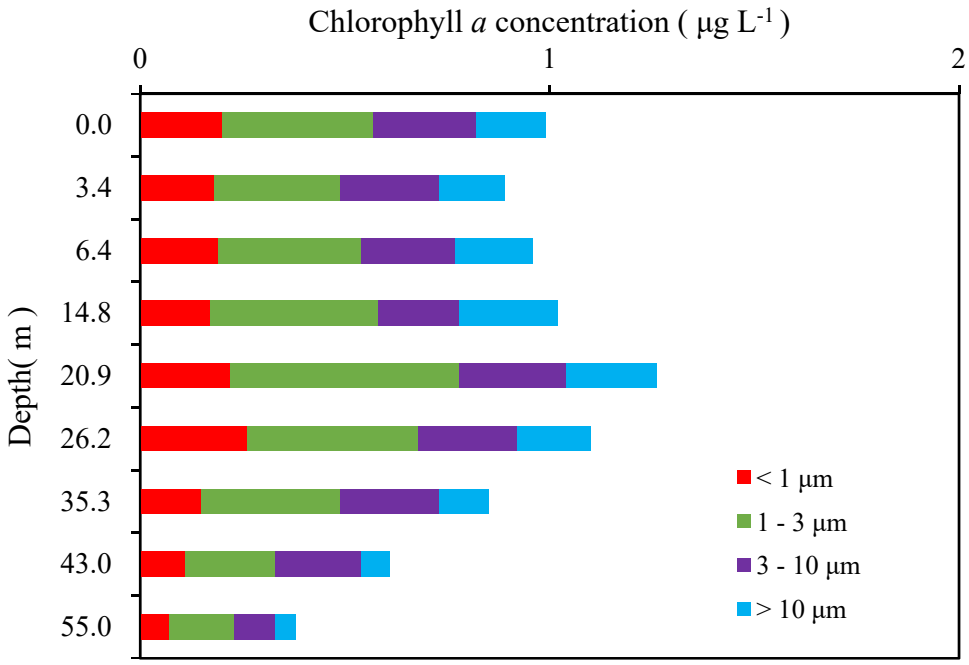

Figure 2.16(a).12. Vertical distribution of size-fractionated chlorophyll *a* at Stn.A5 cast1.

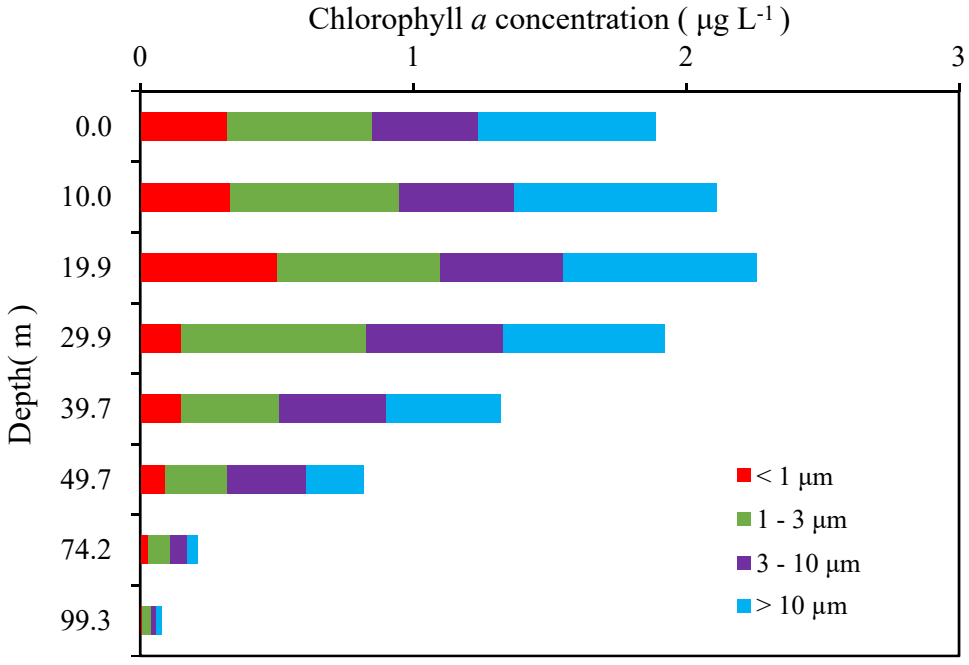

Figure 2.16(a).13. Vertical distribution of size-fractionated chlorophyll *a* at Stn.A6 cast1.

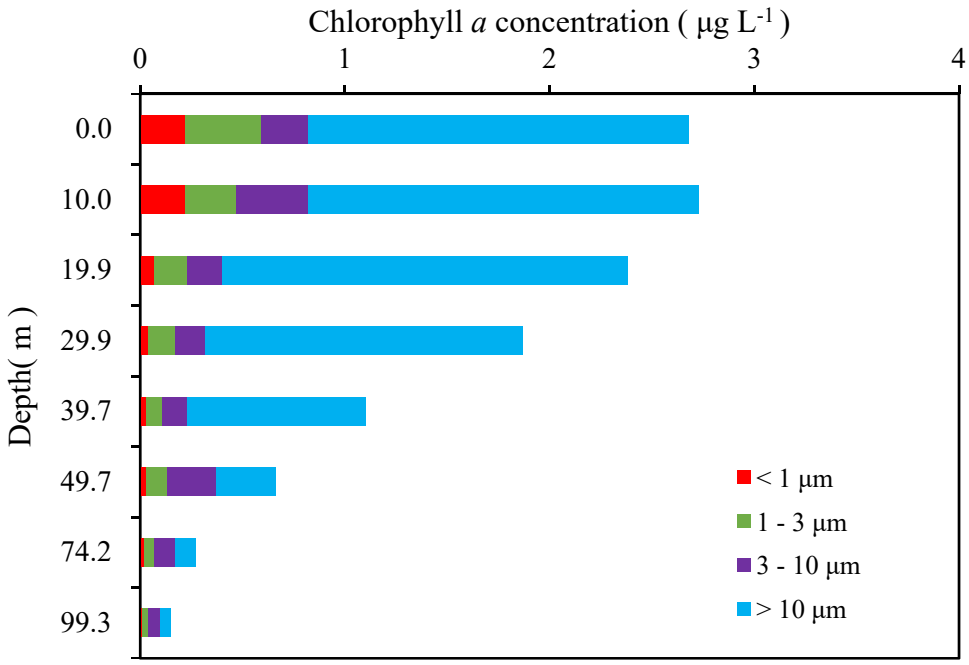

Figure 2.16(a).14. Vertical distribution of size-fractionated chlorophyll *a* at Stn.A8 cast1.

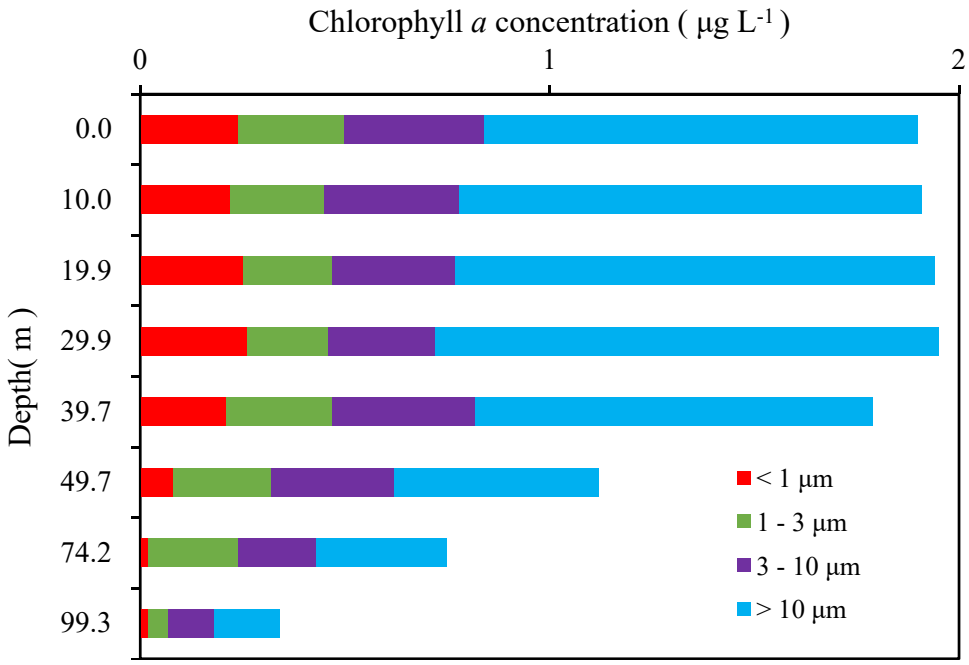

Figure 2.16(a).15. Vertical distribution of size-fractionated chlorophyll *a* at Stn.A9 cast1.

2.16 (b) HPLC measurements of marine phytoplankton pigments

Tetsuichi FUJIKI (JAMSTEC RIGC)
Hiroshi HOSHINO (MWJ)

(1) Objectives

The chemotaxonomic assessment of phytoplankton populations present in natural seawater requires taxon-specific algal pigments as good biochemical markers. A high-performance liquid chromatography (HPLC) measurement is an optimum method for separating and quantifying phytoplankton pigments in natural seawater. In this cruise, we measured the marine phytoplankton pigments by HPLC to investigate the marine phytoplankton community structure in the western Pacific.

(2) Instruments and Methods

i) Sample collection and treatment

Seawater samples were collected from 8 depths between the surface and 110 m. Seawater samples were collected using Niskin bottles, except for the surface water, which was taken by a bucket. 1 or 2 L of seawater samples were filtered through the 47 mm diameter Whatman GF/F filter under the vacuum condition (approx. -0.02 MPa(G)). To remove retaining seawater in the sample filters, GF/F filters were vacuum-dried in a freezer (0 °C) within 3.5 hours. Subsequently, phytoplankton pigments retained on a filter were extracted in a glass vial with 4 ml of N,N-dimethylformamide (HPLC-grade) for at least 24 hours in a freezer (-20 °C), and analyzed by HPLC system within a few days.

Residua cells and filter debris were removed through PTFE syringe filter (pore size: 0.2 μm) before the analysis. 125 μl of pigment extract was mixed with 125 μl of 28 mmol L^{-1} tetrabutylazanium;acetate (tetrabutylammonium acetate) buffer (pH 6.5), and then injected into HPLC system. These process were conducted by the autosampler. Phytoplankton pigments were quantified based on C_8 column method (Heukelem & Thomas, 2001).

ii) HPLC System

HPLC System was composed by Agilent 1200 modular system, G1311A quaternary pump (low-pressure mixing system), G1329A autosampler and G7115A photodiode array detector.

iii) Stationary phase

Analytical separation was performed using a ZORBAX Eclipse XDB-C_8 column (150×4.6 mm). The column was maintained at 60 °C in the column heater box.

iv) Mobile phases

The eluant A was the 7:3 (v:v) mixture of methanol and 28 mmol L^{-1} tetrabutyl ammonium acetate buffer (pH 6.5). The eluant B was a methanol. Methanol was the HPLC-grade.

v) Calibrations

HPLC was calibrated using the standard pigments (Table 2.16(b).1.).

vi) Internal standard

Internal standard was not added into the both standard samples and pigment extracts.

vii) Working standard

502 μg L^{-1} of chlolophyll *a* standard solution was measured with both standard samples and sea water samples as the working standard. The mean and coefficient of variation (CV) of chromatogram area shown below (Figure 2.16(b).1.):

231.8 ± 1.4 (n = 40), CV=0.6 %

viii) Pigment detection and identification

Chlorophylls and carotenoids were detected by photodiode array spectroscopy (350 nm - 750 nm). Pigment concentrations were calculated from the chromatogram area at the different two channels (Table 2.16(b).1). First channel was allocated at 450 nm of wavelength for the carotenoids and chlorophyll *b*. Second channel was allocated at 667 nm for the chlorophyll *a* and its metabolites.

(3) Preliminary result

Vertical profiles of major pigments at station A01M003, A07M002 and A07M009 were shown in Figure 2.16(b).2. to 2.16(b).4.

(4) Data archive

The processed data file of pigments will be submitted to the JAMSTEC Data Management Group (DMG) within a restricted period. Please ask PI for the latest information.

(5) References

Heukelem, L. V. & Thomas, C. S. (2001). Computer-assisted high-performance liquid chromatography method development with applications to the isolation and analysis of phytoplankton pigments. *J. Chromatogr. A* 910, 31-49

Jeffrey S. W., Mantoura R. F. C. & Wright S. W. (Eds.). (1997) *Phytoplankton pigments in oceanography: guidelines to modern methods*, 7 place de Fontenoy, Paris, United Nations Educational, Scientific and Cultural Organization.

Table 2.16(b).1. Retention time and wavelength of identification for pigment standards.

ID	Pigment[1]	Productions	Retention Time (minute)	Wavelength of identification (nm)
1	Chlorophyll *c*3	DHI Laboratory Products	3.895	450
3	Mg-2,4-divinyl pheoporphyrin *a*5	DHI Laboratory	6.134	450

	monomethyl ester	Products		
4	Chlorophyll *c*2	DHI Laboratory Products	6.021	450
5	Peridinin	DHI Laboratory Products	10.184	450
6	Pheophorbide *a*	DHI Laboratory Products	8.387	667
7	19'-Butanoyloxyfucoxanthin	DHI Laboratory Products	13.276	450
8	Fucoxanthin	DHI Laboratory Products	13.568	450
9	9'-*cis*-Neoxanthin	DHI Laboratory Products	14.125	450
10	Prasinoxanthin	DHI Laboratory Products	14.684	450
11	19'-Hexanoyloxyfucoxanthin	DHI Laboratory Products	15.121	450
12	Violaxanthin	DHI Laboratory Products	14.961	450
13	Diadinoxanthin	DHI Laboratory Products	16.240	450
16	Alloxanthin	DHI Laboratory Products	17.466	450
17	Diatoxanthin	DHI Laboratory Products	18.099	450
18	Zeaxanthin	DHI Laboratory Products	18.876	450
19	Lutein	DHI Laboratory Products	18.707	450
22	Chlorophyll *b*	DHI Laboratory Products	23.893	450
23	Divinyl Chlorophyll *a*	DHI Laboratory Products	24.559	667
24	Chlorophyll *a* from *Anacystis nidulans* algae	Sigma-Aldrich Co., LCC	24.738	667
25	Pheophytin *a*	DHI Laboratory Products	26.269	667
26	Alpha-carotene	DHI Laboratory Products	27.656	450
27	Beta-carotene	DHI Laboratory Products	27.738	450

[1]IUPAC names of the pigments; see Jeffrey et al., 1997.

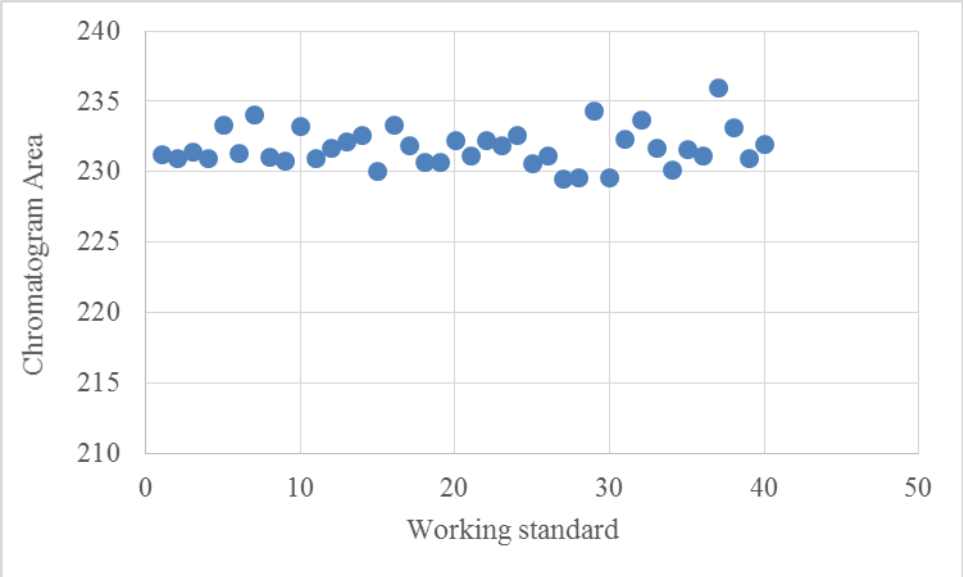

Figure 2.16(b).1. Variability of chromatogram area for working standard.

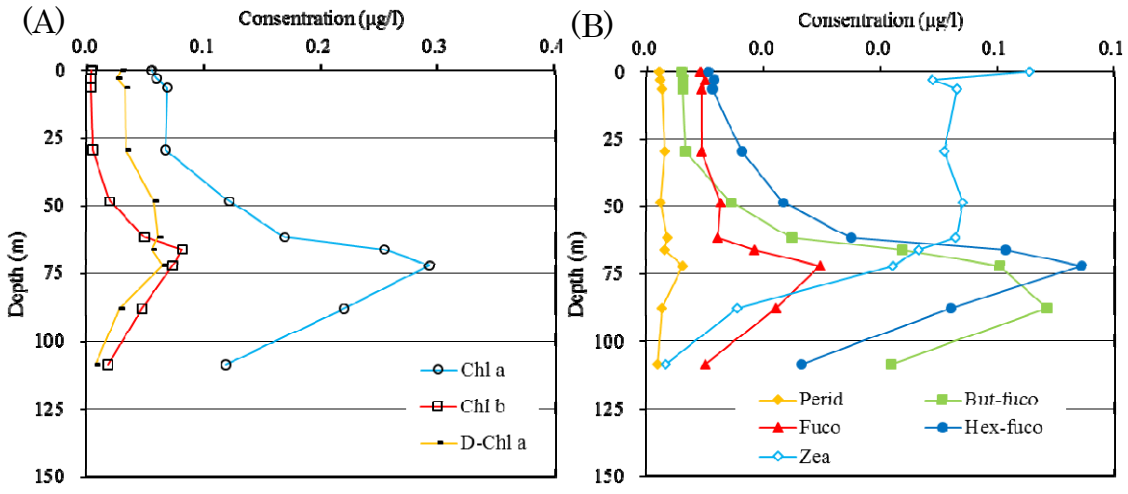

Figure 2.16(b).2.-(A). Vertical distributions of major phytoplankton pigments (chlorophyll *a*, chlorophyll *b*, and Divinyl Chlorophyll *a*) at Stn. A01M003.
Figure 2.16(b).2.-(B). Vertical distributions of major phytoplankton pigments (peridinin, 19'-butanoyloxyfucoxanthin, fucoxanthin, 19'-hexanoyloxyfucoxanthin, and zeaxanthin) at Stn. A01M003.

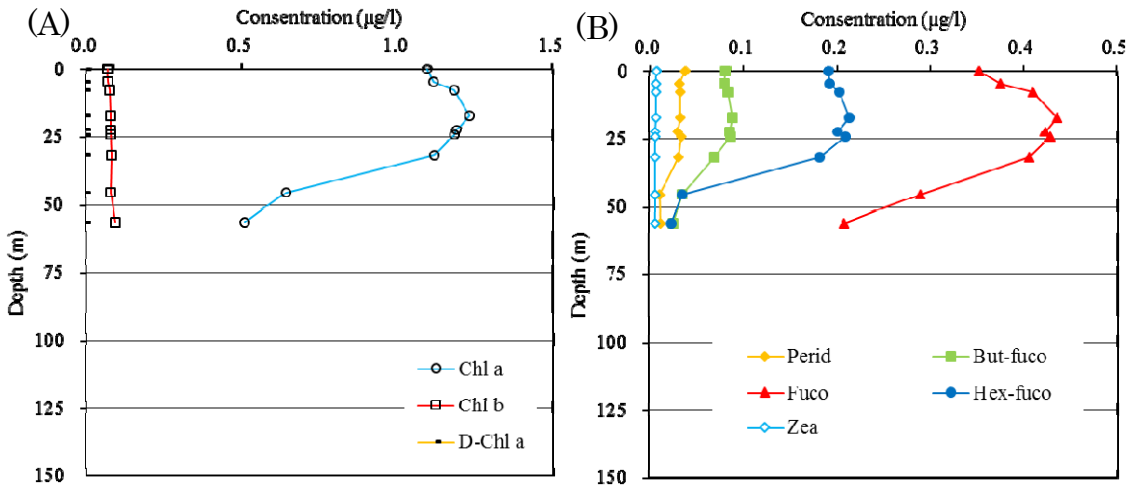

Figure 2.16(b).3.-(A). Vertical distributions of major phytoplankton pigments (chlorophyll *a*, chlorophyll *b*, and Divinyl Chlorophyll *a*) at Stn. A07M002.
Figure 2.16(b).3.-(B). Vertical distributions of major phytoplankton pigments (peridinin, 19'-butanoyloxyfucoxanthin, fucoxanthin, 19'-hexanoyloxyfucoxanthin, and zeaxanthin) at Stn. A07M002.

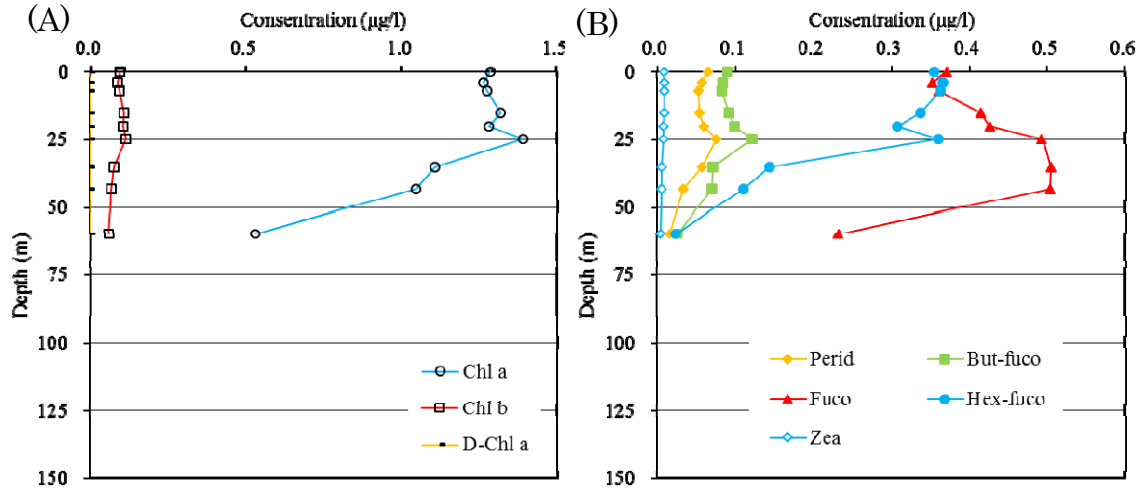

Figure 2.16(b).4.-(A). Vertical distributions of major phytoplankton pigments (chlorophyll *a*, chlorophyll *b* and Divinyl Chlorophyll *a*) at Stn. A07M009.
Figure 2.16(b).4.-(B). Vertical distributions of major phytoplankton pigments (peridinin, 19'-butanoyloxyfucoxanthin, fucoxanthin, 19'-hexanoyloxyfucoxanthin, and zeaxanthin) at Stn. A07M009.

2.16 (c) Primary Production (carbon fixation)

Kazuhiko MATSUMOTO (JAMSTEC RIGC)
Keitaro MATSUMOTO (MWJ)
Atsushi ONO (MWJ)

(1) Objectives

Primary production can be divided into particulate primary production and dissolved primary production. To understand the processes of biogeochemical cycles, oceanic total primary production was estimated at the stations of A01(KEO), A03, A05, A07(K2) and A09.

(2) Methods and Instruments

i. Sampling

Sampling was conducted immediately before the incubation experiment. Seawater samples were collected using Niskin bottles installed acid-cleaned O-ring, except for the surface water, which was taken by a bucket. For the on-deck incubation, samplings were conducted at seven depths in the euphotic layer according to the light levels of the incubation containers adjusted with the blue acrylic plate. The light levels of the incubation containers were shown in Table 2.16.C-1. For the P vs. E curve experiment, samplings were conducted at three depths.

ii. Incubation

(a) On-deck incubation

Seawater samples were transferred into acid-cleaned, transparent polycarbonate bottles. Just before the incubation, $NaH^{13}CO_3$ was added to each bottle at a final concentration of 0.2 mM, sufficient to enrich the bicarbonate concentration by about 10%. The time-zero sample was filtered immediately after the addition of ^{13}C solution. The incubation bottles within the light-controlled containers were placed in the water bath cooled by running surface seawater or by immersion cooler on deck. Incubations were conducted from dawn for 24 h. Another experiments to estimate the incorporation rate of nitrate were conducted during noon and before dawn for 2 h with adding $K^{15}NO_3$, respectively.

(b) P vs. E curve experiment

To investigate the relationship between phytoplankton photosynthetic rate (P) and scalar irradiance (E), incubations for the P vs. E curve experiment were conducted in the laboratory. Just before the incubation, $NaH^{13}CO_3$ was added to each bottle. Three incubators were filled with water, and water temperature was controlled appropriately by circulating water coolers, respectively. Each incubator was illuminated at one end by a 500W halogen lamp, and bottles were arranged linearly against the lamp and controlled light intensity by shielding with a neutral density filter on lamp side. Incubations for the P vs. E curve experiment were conducted around noon for 3 h.

iii. Measurement

(a) Particulate fraction

After the incubation, water samples were immediately filtered through a pre-combusted GF/F filter, then the filters were dehydrated in a dry oven (45 ºC), and the remained inorganic carbon in the

filter was removed by fuming HCl. The incorporation of inorganic ^{13}C and ^{15}N content of the particulate fraction will be measured with a stable isotope analyzer (EcovisION, Elementar Analysensysteme GmbH) based on the method of Hama et al. (1983). The analytical function and parameter values used to describe the relationship between the photosynthetic rate (P) and scalar irradiance (E) are best determined using a least-squares procedure from the following equation (Platt et al., 1980).

$$P = P_{max}(1-e^{-\alpha E/Pmax})e^{-b\alpha E/Pmax}$$

where, P_{max} is the light-saturated maximum photosynthetic rate, α is the initial slope of the P vs. E curve, b is a dimensionless photoinhibition parameter.

(b) Dissolved fraction

The filtrate of the on-deck 24 h incubation samples were desalinated using an electro dialyzer equipped with AC-220-550 cartridge (Micro Acilyzer S3, ASTOM Corp.). The frozen desalinated seawater samples, which are brought back to land, are concentrated to 5 mL with a rotary evaporator at 45 ºC, and the dissolved inorganic carbon is removed by adding HCl and subsequent degassing. The samples are further concentrated to about 500 μL and absorbed onto pre-combusted GF/F filter in a tin capsule, and dehydrated in a dry oven (45 ºC). The ^{13}C content of the dissolved fraction (extracellular release of phytoplankton) will be measured as described above.

(3) Data archive

The data obtained during this cruise will be submitted to the JAMSTEC Data Management Group (DMG).

(4) References

Hama T, Miyazaki T, Ogawa Y, Iwakuma T, Takahashi M, Otsuki A, Ichimura S (1983) Measurement of photosynthetic production of a marine phytoplankton population using a stable 13C isotope. Marine Biology 73: 31-36.

Platt T, Gallegos CL, Harrison WG (1980) Photoinhibition of photosynthesis in natural assemblages of marine phytoplankton. Journal of Marine Research 38: 687-701.

Table 2.16.C-1. Light levels of the incubation containers

Number	Light level
#1	100%
#2	55%
#3	34%
#4	11%
#5	5.5%
#6	2.6%
#7	0.9%

2.16 (d) Primary production (oxygen evolution)

Osamu ABE (Nagoya University)
Tetsuichi FUJIKI (JAMSTEC RIGC)

(1) Objectives

An understanding of the variability in phytoplankton productivity provides a basic knowledge of how aquatic ecosystems are structured and functioning. Primary productivity in the world ocean has been measured mostly with the methods of carbon tracer or oxygen evolution. In incubations of 24 hours, the former method provides the values closest to net primary productivity (NPP), while the latter comes closest to gross primary productivity (GPP). The GPP is defined as total amount of oxygen released by phytoplankton photosynthesis. The NPP/GPP ratio provides fundamental information on the metabolic balance and carbon cycle in the ocean. In the MR19-02, the GPP were measured using the light bottle incubation for dissolved O_2 spiked with $H_2{}^{18}O$ and fast repetition rate (FRR) fluorometry.

(2) Methods

Light bottle incubation of dissolved O_2 spiked with $H_2{}^{18}O$

Seawater samples were collected at stations A1, A3, A5, A7 (K2), and A9 (KNOT), from 7 depth layers corresponding to 100, 55, 34, 11, 5.5, 2.6, and 0.9 % of surface light intensity. At Station A7, we conducted incubation experiments twice on 1st and 8th June. Four samples were collected basically at each depth, namely for *Oinitial*, *^{18}Oinitial*, *Ofinal* (light bottle for O_2 concentration at time 24) and *^{18}Ofinal* (light bottle for spiked $^{18}O/^{16}O$ ratio). In addition to them, another sample were collected at light levels of 55 and 34 % for the duplicate of *^{18}Ofinal*. All samples were collected using 12-L Niskin-X sampler attached to CTD rosette system, except for the light level of 100 % which was taken by the bucket. O_2 concentrations in *Oinital* bottles were determined immediately after collection by Winkler titration method, described in Section 2.6. The *^{18}Ofinal* bottles were spiked with ^{18}O-labeled water (approximated $H_2{}^{18}O$ of 10 %) of 1.5 mL to be the $H_2{}^{18}O$ concentration of 0.15 %, then put into light- and temperature-controlled water baths on deck, with 7 light levels described above, along with *Ofinal* bottles.

After 24-hour incubation, O_2 concentrations in *Ofinal* bottles were determined by Winkler titration method. Water of ~80 mL in *^{18}Ofinal* bottles were collected into pre-evacuated vacuum flasks for the determination of $\delta^{18}O$ of dissolved O_2. Aliquots of 3 mL were then collected for the determination of isotopic composition of incubating water ($\delta^{18}O_{water}$).

GPP will be calculated according to the following mass balance equation (Bender et al. 2000).

$$GPP = [(\delta^{18}O_f - \delta^{18}O_{avg})O_{2f} - (\delta^{18}O_i - \delta^{18}O_{avg})O_{2i}] / [\delta^{18}O_{water} - (\delta^{18}O_{avg} + \varepsilon_R)]$$

where the subscripts i, f, avg are initial, final and average of them, respectively, and ε_R denotes isotope fractionation factor during oxygen consumption.

FRR fluorometry

The FRR fluorometer (Diving Flash-14, Kimoto Electric) together with a scalar irradiance sensor and a pressure gauge were deployed several times a day using a ship winch. These instrument packages lowered gently from surface to 100-150m depth and up again at a rate of 0.2 m s^{-1} and measured vertical profiles of GPP.

(3) Data archives

These obtained data will be submitted to JAMSTEC Data Management Group (DMG).

(4) References

Bender, M. L., M. L. Dickson and J. Orchardo. 2000. Net and gross production in the Ross Sea as determined by incubation experiments and dissolved O_2 studies. *Deep-Sea Res. II* **47**: 3141–3158.

2.16 (e) Incubation experiments

Koji SUGIE (RIGC, JAMSTEC)

(1) Objectives

Ongoing climate change such as increasing temperature and CO_2 concentration would affect biogeochemical processes in the ocean. To understand the impact of climate change on the dynamics of plankton communities, (a) short term (24 h) dulution experiments were performed to test the effects of temperature and CO_2 levels on phytoplankton dynamics and microzooplankton grazing pressure at four stations. In addition, in the western subarctic Pacific, iron availability is one of the major factors driving biogeochemical cycling of nutrients because iron-limitation suppress phytoplankton activity. Although, it is well documented that iron-limitation regulates phytoplankton productivity in the subarctic Pacific, the role of iron on phytoplankton dynamics are poorly investigated. Iron sources to the open subarctic Pacific is estimated coming from aeolian dust via westerly jets and/or subsurface iron-rich water mass via eddy diffusion. However, the bioavailability of iron in those sources did not investigated before. In this study, we conducted (b) bioassay experiment to understand the iron availability of in situ and subsurface water masses and aeolian dust for phytoplankton in the surface. This work can contribute to better understand the role of iron on ecosystem function in the western subarctic Pacific.

(2) Instruments and methods

In this study, four treatment was established in the (a) short-term dilution experiment as follows:

LT: Unamended controls

LTHC: High CO_2 condition, which was achieved by adding CO_2 saturated (at 1 atm) filtered seawaters to the controls to make the seawater pCO_2 ca. 700–1000 µatm.

HT: Plus 4–5°C relative to the LT treatment

HTHC: Plus 4–5°C relative to the LTHC treatment

For short-term dilution experiment, seawater was collected from 10 m depth using Niskin X sampling bottles using CTD-CMS system. First, each of 200 µm sieved with Teflon® mesh and 0.2 µm filtered with capsule filter (Pall Corp.) seawater were collected in acid-washed 9-L polycarbonate (PC) tanks and added nitrate (5 µmol L^{-1} in final concentration) phosphate (0.5 µmol L^{-1} in final concentration) and ammonia (5 µmol L^{-1} in final concentration) into both tanks. Seawater samples were dispensed into four 2-L PC bottles for 200 µm sieved seawater (four bottles) and into four bottles for 0.2 µm filtered seawater. To achieve high CO_2 conditions for HC treatment (see below), small amount of CO_2 saturated seawater was added into four 2-L PC bottles; two 2-L PC bottles of both 200 µm sieved and 0.2 µm filtered seawater. Untreated and CO_2 added treatments of both 200 µm sieved and 0.2 µm filtered seawater (i.e., four 2-L PC bottles) were incubated in in situ temperature and another set of four 2-L PC bottles were incubated in 4–5°C higher temperature compared to in situ conditions for 24 h to acclimate incubation conditions and to avoid growth lag phase after the seawater collection. After the 24 h acclimation, dilution experiment was conducted by mixing 11% and 89% of 200 µm sieved and 0.2 µm filtered seawater, respectively, in three 600 mL acid washed PC bottles per treatment. In addition, two 600 mL PC bottles were filled with 200 µm sieved seawater without dilution by 0.2 µm filtered seawater per treatment; i.e., bottles were prepared in triplicate for diluted and duplicate for non-diluted treatments. Totally, 20 bottles were incubated in onboard water tanks. Temperature of two water tanks was controlled by thermostatic circulators. Incubation experiments lasted for 24 hours.

Seawater samples for (b) Fe bioavailability experiment were collected using Teflon-coated, acid-washed Niskin-X sampling bottles with CTD-CMS system at 10 m for plankton community (~9 L in PC bottles) and filtered seawater (ca. 42 L using two 12 L PC and 20 L polypropylene carboys) and at 100 m for filtered seawater (ca. 4 L). In Fe bioavailability experiment (b), we established six treatments; unamended controls in in situ and 4°C higher temperature (hereafter, Control and HT), lower and higher amount of dust-added treatments (dust-L and dust-H), and lower and higher amount of subsurface (100 m depth) seawater-added treatments (SS_{SW}-L and SS_{SW}-H). To achieve both clarifying phytoplankton dynamics and decreasing microzooplankton grazing, 200 μm sieved seawater was diluted with 0.2 μm filtered seawater collected at 10 m and/or 100 m at five-fold; i.e., 20% of in situ plankton density in incubation bottles. Because phytoplankton growth in a five-fold diluted water is statistically indistinguishable to no grazing condition (Chen, 2014), we applied this mixing ratio. The dust we used in this experiment was collected in Hokkaido prefecture in Japan during massive dust fall event during spring. A 1.5 mg of dust was suspended in 15 mL 0.2 μm filtered seawater just before the experiment and added to make final concentration of 0.3 μg L^{-1} and 10 μg L^{-1} for dust-L and dust-H treatments, respectively. Those concentrations were determined based on the reported values during summer (back ground level) and dust event during spring in the western subarctic Pacific (Uematsu et al. 2003; Iwamoto et al. 2011), which were suspended in 30 m-thick surface mixed layer. For subsurface water addition treatment, added subsurface water to the SS_{SW}-L treatment was set at 4% relative to the volume of 600 mL PC bottles; 24 mL of filtered subsurface water was replaced with filtered surface seawater. The mixing ratio was estimated from the situation of deepening of surface mixed layer during summer to early winter that nearly 30 m deepening during 120 days at the sampling station (Fujiki et al. 2014). The subsurface water mixing ratio in the SS_{SW}-H was 80% to estimate iron bioavailability in the subsurface water. Prior to experiment, phytoplankton community (200 μm sieved seawater) was poured into 4-L acid washed PC bottle, double bagged in polyethylene bag, and incubated in temperature-controlled water tanks at in situ and in situ (ca. 4.5°C) plus 4°C for two days to reduce intracellularly stored iron (Sugie et al. 2011). Seawater mixing was conducted in temperature-controlled room at ca. 5°C under a laminar flow clean bench, and bottles were incubated for three days. Totally, 36 bottles were prepared for 6 treatments with triplicate bottles and 2 samplings at days 1 and 3.

(3) Parameters

In short-term dilution experiment, samples for size fractionated chlorophyll-*a* (>10 μm and ~0.7–10 μm), nutrients (NO_3, NO_2, NH_4, PO_4, $Si(OH)_4$), and pico- and nano-sized phytoplankton with flowcytmetry were collected at the beginning and the end of the experiment. Samples for larger plankton such as microzooplankton and diatoms with microscopy and dissolved inorganic carbon and total alkalinity for the estimation of carbonate chemistry were collected at the beginning of the experiment. Temperature, photosynthetic active radiation, were recorded during the course of both experiments.

In Fe bioavailability experiments, size fractionated chlorophyll-*a*, nutrients, and pico- and nano-sized phytoplankton samples were collected at the beginning, days 1 and 3. Samples for light microscopy were collected at the beginning and day 3. Filtered seawater for trace metal analysis were dispensed from 20 L polypropylene carboy for 10 m depth water and 4 L PC bottles for 100 m depth water at the beginning of the experiment. To estimate trace metal dissolution from the aeolian dust, one mL of dust stock solution (1.5 mg dust per 15 mL filtered seawater) was filtered and diluted using 99 mL of 0.22 μm filtered seawater collected at 10 m depth.

(4) Observation log
Sampling locations are shown in Fig. 2.16e.1.
Short-term dilution experiments
St. A1: May 26 (UTC), 2019 at 32°11’N, 144°18’E
St. A4 :May 29 (UTC), 2019 at 40°00’N, 152°41’E
St. A7: June 2 (UTC), 2019 at 47°04’N, 160°00’E
St. A9: June 10 (UTC), 2019 at 44°00’N, 155°00’W

Fe bioavailability experiment
St. A7: June 5 (UTC), 2019 at 47°00’N, 159°58’W

(5) Data archives
All data obtained during MR19-02 cruise will be submitted to Data Management Group (DMG) of JAMSTEC after the sample analysis and validation. The data will be opened to the public via “Data Research System for Whole Cruise Information (DARWIN)” in JAMSTEC web site or elsewhere.

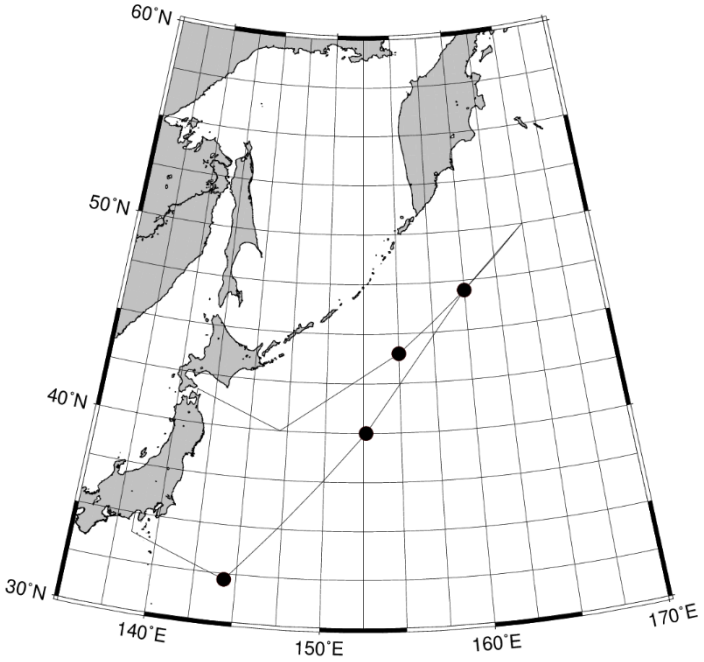

Figure 2.16e.1. Sampling location (black circle) and cruise track (thin line).

2.17 Zooplankton

2.17 (a) Planktic foraminifers and Thecosomatous pteropods

Katsunori KIMOTO (JAMSTEC RIGC)
Arisa TAKASHIMA (Tohoku University)
Minoru KITAMURA (JAMSTEC RIGC)
Keisuke SHIMIZU (Exetor University, UK)

(1) Objectives

The ocean has already absorbed about 30% of the total anthropogenic CO_2 (approximately 155 GtC) since the industrial revolution (IPCC AR5, 2013). This reduces ocean pH (Ocean acidification, OA) and causes wholescale shift in seawater carbonate chemistry. OA also give several impacts to the biological processes; one well-known effect is the lowering of calcium carbonate saturation state, which give negative impact to shell-forming marine organisms such as pteropods and planktic foraminifers etc. OA also affect zooplankton other than the shell-forming organisms, and characteristics of the zooplankton community will be changed. So, we are observing long-term change of zooplankton biomass at K2 and adjacent areas in the North Pacific by using the plankton collecting apparatus and performing some biological/geochemical analysis to evaluate the biological impact to OA.

In this cruise, for better understanding of biological responses to carbonate saturation status, we aimed for following themes,

a) understanding vertical distributions of pteropods and planktonic foraminifer communities, and change of their shell densities with water depths,
b) clarifying genetic diversities of planktic foraminifers with water depth in the North Pacific,
c) understanding phenotypic and genetic variabilities in the mixed layer for pteropods, and their population structure.

(2) Methods

All plankton samplings were conducted at KEO (Sta. A1), K2 (Sta. A7) and adjacent stations (See Table 2.17.1). For the purpose (a), we collected specimens by using the Vertical Multi-depth Plankton Sampler (VMPS-3K, Tsurumi Seiki co., Ltd, Fig. 2.17.1). VMPS-3K equipped 3 or 4 plankton nets (63 μm mesh, NXX25), magnetic flow-meter, fluorometer (Wet Lab) and CTD sensors (Sea-bird Electrics), and was hauled vertically at a speed of 0.5 m/sec. Opening/closing of each net is electrically controlled from the lab on the ship, we can collect vertically stratified sample sets together with the environmental sensing data. Collected samples were immediately fixed by the ethanol (99.5 %) and stored at the room temperature (~23 °C). For the purpose of (b), planktic foraminifers were picked under the stereomicroscope and transported to the microslides with ethanol (99.5 %) and stored in the refrigerator (~ 4 °C).

For the purposes of (c), a twin-NORPAC net (63 μm mesh, NXX25) with a large cod end (2,000 ml polypropylene bottles) was vertically hauled. Living pteropods were immediately sorted under the stereomicroscope and fixed by 99.5 % EtOH, and then stored in the refrigerator at the 4 °C temperature.

During this cruise, we performed cultivation experiment for thecosomatous pteropod *Limacina helicina*. In order to observe shell growing during cultivation, we used the natural seawater (collected from 10m, 100m, and 300m water depth at Sta. A7) with calcein (fluorescent regent, 100uM)

for each 10 individuals. All *L. helicina* was incubated in the culture vessels (500 ml plastic bottles) in 24 hours at 4 degree C, and then, they were fixed and stocked in the deep freezer (-80 degree C).

(3) Onshore study in the future

We will perform the experiment of observation of *L. helicina* by using the fluorescence microscope at the onshore laboratory to evaluate shell growing during cultivation in the seawater that recovered from different water depth.

Pteropod and planktonic foraminiferal shells will be analyzed by the Micro-focus X-ray CT (MXCT) equipped in JAMSTEC HQ in order to elucidate relationships between oceanic carbonate chemistry and individual shell density. The preserved samples of planktic foraminifers will be extracted all DNA and then perform SSU rDNA analysis for genetic diversity analysis. For the population analysis of pteropods, DNA extraction from the preserved specimens and amplifying of gene sequences for the COI region of mtDNA will be performed. After the sequence alignments, population genetic analysis will be performed.

(4) Data Archive

All data will be submitted to JAMSTEC Data Management group (DMG).

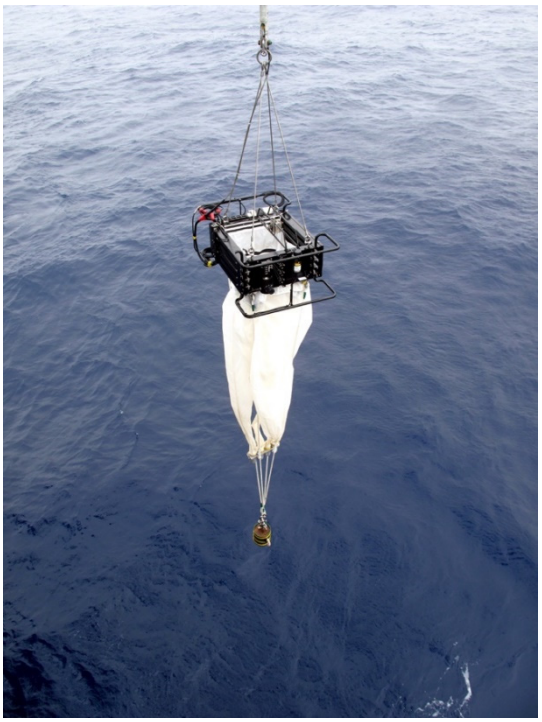

Fig. 2.17.1 The overview of VMPS (Vertical Multi-layer Plankton Sampler).

Table 2.17.1. Sampled locations and its detail during the MR19-02.

No.	Sample ID#	Fixiation	Station	Latitude			Longitude			water depth	Date yy/mm/dd			Time	
1	A1_VMPS-1	99% Ethernol	Sta. A1	32	12	N	144	18	E	300-500	2019	May	26	14:10	JST
2	A1_VMPS-2	99% Ethernol	Sta. A1	32	12	N	144	18	E	200-300	2019	May	26	14:20	JST
3	A1_VMPS-3	99% Ethernol	Sta. A1	32	12	N	144	18	E	150-200	2019	May	26	14:30	JST
4	A1_VMPS-4	99% Ethernol	Sta. A1	32	12	N	144	18	E	100-150	2019	May	26	14:40	JST
5	A1_VMPS-5	99% Ethernol	Sta. A1	32	12	N	144	18	E	50-100	2019	May	26	14:50	JST
6	A1_VMPS-6	99% Ethernol	Sta. A1	32	12	N	144	18	E	0-50	2019	May	26	15:00	JST
7	A1_NORPAC-1	99% Ethernol	Sta. A1	32	12	N	144	18	E	0-200	2019	May	26	17:20	JST
8	A1_NORPAC-2	99% Ethernol	Sta. A1	32	12	N	144	18	E	0-200	2019	May	26	17:40	JST
9	A1_NORPAC-3	99% Ethernol	Sta. A1	32	12	N	144	18	E	0-200	2019	May	26	18:00	JST
10	A2_VMPS-1	99% Ethernol	Sta. A2	35	00	N	147	13	E	300-500	2019	May	27	17:40	JST
11	A2_VMPS-2	99% Ethernol	Sta. A2	35	00	N	147	13	E	200-300	2019	May	27	17:50	JST
12	A2_VMPS-3	99% Ethernol	Sta. A2	35	00	N	147	13	E	150-200	2019	May	27	18:00	JST
13	A2_VMPS-4	99% Ethernol	Sta. A2	35	00	N	147	13	E	100-150	2019	May	27	18:10	JST
14	A2_VMPS-5	99% Ethernol	Sta. A2	35	00	N	147	13	E	50-100	2019	May	27	18:20	JST
15	A2_VMPS-6	99% Ethernol	Sta. A2	35	00	N	147	13	E	0-50	2019	May	27	18:30	JST
16	A2_NORPAC-1	99% Ethernol	Sta. A2	35	00	N	147	13	E	0-200	2019	May	27	19:10	JST
17	A2_NORPAC-2	99% Ethernol	Sta. A2	35	00	N	147	13	E	0-200	2019	May	27	19:30	JST
18	A2_NORPAC-3	99% Ethernol	Sta. A2	35	00	N	147	13	E	0-200	2019	May	27	19:50	JST
19	A3_VMPS-1	99% Ethernol	Sta. A3	37	30	N	149	54	E	300-500	2019	May	28	13:40	JST
20	A3_VMPS-2	99% Ethernol	Sta. A3	37	30	N	149	54	E	200-300	2019	May	28	13:50	JST
21	A3_VMPS-3	99% Ethernol	Sta. A3	37	30	N	149	54	E	150-200	2019	May	28	14:00	JST
22	A3_VMPS-4	99% Ethernol	Sta. A3	37	30	N	149	54	E	100-150	2019	May	28	14:10	JST
23	A3_VMPS-5	99% Ethernol	Sta. A3	37	30	N	149	54	E	50-100	2019	May	28	14:20	JST
24	A3_VMPS-6	99% Ethernol	Sta. A3	37	30	N	149	54	E	0-50	2019	May	28	14:30	JST
25	A3_NORPAC-1	99% Ethernol	Sta. A3	37	30	N	149	54	E	0-200	2019	May	28	19:20	JST
26	A3_NORPAC-2	99% Ethernol	Sta. A3	37	30	N	149	54	E	0-200	2019	May	28	19:40	JST
27	A3_NORPAC-3	99% Ethernol	Sta. A3	37	30	N	149	54	E	0-200	2019	May	28	20:00	JST
28	A4_VMPS-1	99% Ethernol	Sta. A4	40	00	N	152	41	E	300-500	2019	May	30	0:10	JST
29	A4_VMPS-2	99% Ethernol	Sta. A4	40	00	N	152	41	E	200-300	2019	May	30	0:20	JST
30	A4_VMPS-3	99% Ethernol	Sta. A4	40	00	N	152	41	E	150-200	2019	May	30	0:30	JST
31	A4_VMPS-4	99% Ethernol	Sta. A4	40	00	N	152	41	E	100-150	2019	May	30	0:40	JST
32	A4_VMPS-5	99% Ethernol	Sta. A4	40	00	N	152	41	E	50-100	2019	May	30	0:50	JST
33	A4_VMPS-6	99% Ethernol	Sta. A4	40	00	N	152	41	E	0-50	2019	May	30	1:00	JST
34	A4_NORPAC-1	99% Ethernol	Sta. A4	40	00	N	152	41	E	0-200	2019	May	30	1:40	JST
35	A4_NORPAC-2	99% Ethernol	Sta. A4	40	00	N	152	41	E	0-200	2019	May	30	2:00	JST
36	A4_NORPAC-3	99% Ethernol	Sta. A4	40	00	N	152	41	E	0-200	2019	May	30	2:20	JST
37	A7_VMPS-1	99% Ethernol	Sta. A7	47	00	N	160	00	E	300-500	2019	June	1	8:10	JST
38	A7_VMPS-2	99% Ethernol	Sta. A7	47	00	N	160	00	E	200-300	2019	June	1	8:20	JST
39	A7_VMPS-3	99% Ethernol	Sta. A7	47	00	N	160	00	E	150-200	2019	June	1	8:30	JST
40	A7_VMPS-4	99% Ethernol	Sta. A7	47	00	N	160	00	E	100-150	2019	June	1	8:40	JST
41	A7_VMPS-5	99% Ethernol	Sta. A7	47	00	N	160	00	E	50-100	2019	June	1	8:50	JST
42	A7_VMPS-6	99% Ethernol	Sta. A7	47	00	N	160	00	E	0-50	2019	June	1	9:00	JST
43	A7_NORPAC-1	99% Ethernol	Sta. A7	47	00	N	160	00	E	0-150	2019	June	1	9:30	JST
44	A7_NORPAC-2	99% Ethernol	Sta. A7	47	00	N	160	00	E	0-150	2019	June	1	9:50	JST
45	A7_NORPAC-3	99% Ethernol	Sta. A7	47	00	N	160	00	E	0-150	2019	June	1	10:10	JST
46	A5_NORPAC-1	99% Ethernol	Sta. A5	50	00	N	165	00	E	0-150	2019	June	4	3:20	JST
47	A5_NORPAC-2	99% Ethernol	Sta. A5	50	00	N	165	00	E	0-150	2019	June	4	3:40	JST
48	A5_NORPAC-3	99% Ethernol	Sta. A5	50	00	N	165	00	E	0-150	2019	June	4	4:00	JST
49	A5_VMPS-1	99% Ethernol	Sta. A5	50	00	N	165	00	E	300-500	2019	June	4	8:10	JST
50	A5_VMPS-2	99% Ethernol	Sta. A5	50	00	N	165	00	E	200-300	2019	June	4	8:20	JST
51	A5_VMPS-3	99% Ethernol	Sta. A5	50	00	N	165	00	E	150-200	2019	June	4	8:30	JST
52	A5_VMPS-4	99% Ethernol	Sta. A5	50	00	N	165	00	E	100-150	2019	June	4	8:40	JST
53	A5_VMPS-5	99% Ethernol	Sta. A5	50	00	N	165	00	E	50-100	2019	June	4	8:50	JST
54	A5_VMPS-6	99% Ethernol	Sta. A5	50	00	N	165	00	E	0-50	2019	June	4	9:00	JST
55	A6_VMPS-1	99% Ethernol	Sta. A6	48	30	N	162	30	E	300-500	2019	June	5	0:10	JST
56	A6_VMPS-2	99% Ethernol	Sta. A6	48	30	N	162	30	E	200-300	2019	June	5	0:20	JST
57	A6_VMPS-3	99% Ethernol	Sta. A6	48	30	N	162	30	E	0-200	2019	June	5	0:30	JST
58	A6_VMPS-4	99% Ethernol	Sta. A6	48	30	N	162	30	E	100-150	2019	June	5	0:40	JST
59	A6_VMPS-5	99% Ethernol	Sta. A6	48	30	N	162	30	E	50-100	2019	June	5	0:50	JST
60	A6_VMPS-6	99% Ethernol	Sta. A6	48	30	N	162	30	E	0-50	2019	June	5	1:00	JST
61	A6_NORPAC-1	99% Ethernol	Sta. A6	48	30	N	162	30	E	0-150	2019	June	5	1:30	JST
62	A6_NORPAC-2	99% Ethernol	Sta. A6	48	30	N	162	30	E	0-150	2019	June	5	1:50	JST
63	A6_NORPAC-3	99% Ethernol	Sta. A6	48	30	N	162	30	E	0-150	2019	June	5	2:10	JST

Table 2.17.1 (continued) Sampled locations and its detail during the MR19-02.

No.	Sample ID#	Fixiation	Station	Latitude	Longitude	water depth	Date yy/mm/dd	Time
64	A7-2_VMPS-1	99% Ethernol	Sta. A7	47 00 N	160 00 E	300-500	2019 June 7	5:40 JST
65	A7-2_VMPS-2	99% Ethernol	Sta. A7	47 00 N	160 00 E	200-300	2019 June 7	5:50 JST
66	A7-2_VMPS-3	99% Ethernol	Sta. A7	47 00 N	160 00 E	150-200	2019 June 7	6:00 JST
67	A7-2_VMPS-4	99% Ethernol	Sta. A7	47 00 N	160 00 E	100-150	2019 June 7	6:10 JST
68	A7-2_VMPS-5	99% Ethernol	Sta. A7	47 00 N	160 00 E	50-100	2019 June 7	6:20 JST
69	A7-2_VMPS-6	99% Ethernol	Sta. A7	47 00 N	160 00 E	0-50	2019 June 7	6:30 JST
70	A7-2_NORPAC-1	99% Ethernol	Sta. A7	47 00 N	160 00 E	0-150	2019 June 8	3:30 JST
71	A7-2_NORPAC-2	99% Ethernol	Sta. A7	47 00 N	160 00 E	0-150	2019 June 8	3:50 JST
72	A7-2_NORPAC-3	99% Ethernol	Sta. A7	47 00 N	160 00 E	0-150	2019 June 8	4:10 JST
73	A8_VMPS-1	99% Ethernol	Sta. A8	45 30 N	157 30 E	300-500	2019 June 9	5:10 JST
74	A8_VMPS-2	99% Ethernol	Sta. A8	45 30 N	157 30 E	200-300	2019 June 9	5:20 JST
75	A8_VMPS-3	99% Ethernol	Sta. A8	45 30 N	157 30 E	150-200	2019 June 9	5:30 JST
76	A8_VMPS-4	99% Ethernol	Sta. A8	45 30 N	157 30 E	100-150	2019 June 9	5:40 JST
77	A8_VMPS-5	99% Ethernol	Sta. A8	45 30 N	157 30 E	50-100	2019 June 9	5:50 JST
78	A8_VMPS-6	99% Ethernol	Sta. A8	45 30 N	157 30 E	0-50	2019 June 9	6:00 JST
79	A8_NORPAC-1	99% Ethernol	Sta. A8	45 30 N	157 30 E	0-150	2019 June 9	6:40 JST
80	A8_NORPAC-2	99% Ethernol	Sta. A8	45 30 N	157 30 E	0-150	2019 June 9	7:10 JST
81	A9_VMPS-1	99% Ethernol	Sta. A9	44 00 N	155 00 E	300-500	2019 June 10	3:40 JST
82	A9_VMPS-2	99% Ethernol	Sta. A9	44 00 N	155 00 E	200-300	2019 June 10	3:50 JST
83	A9_VMPS-3	99% Ethernol	Sta. A9	44 00 N	155 00 E	0-200	2019 June 10	4:00 JST
84	A9_VMPS-4	99% Ethernol	Sta. A9	44 00 N	155 00 E	100-150	2019 June 10	4:10 JST
85	A9_VMPS-5	99% Ethernol	Sta. A9	44 00 N	155 00 E	50-100	2019 June 10	4:20 JST
86	A9_VMPS-6	99% Ethernol	Sta. A9	44 00 N	155 00 E	0-50	2019 June 10	4:30 JST
87	A9_NORPAC-1	99% Ethernol	Sta. A9	44 00 N	155 00 E	0-150	2019 June 10	11:20 JST
88	A9_NORPAC-2	99% Ethernol	Sta. A9	44 00 N	155 00 E	0-150	2019 June 10	11:40 JST
89	A9_NORPAC-3	99% Ethernol	Sta. A9	44 00 N	155 00 E	0-150	2019 June 10	12:00 JST

2.17 (b) Mesozooplankton

Minoru KITAMURA (JAMSTEC RIGC)

(1) Objective

Generally, current studies on the zooplankton ecology are heavily dependent on analysis of collected specimens. Thus, temporal and spatial resolutions of many ecological data sets for zooplankton are rough. Acoustical technics may solve such a problem, but applying of them to the zooplankton study are still scarce. In this study, to understand vertical distribution of zooplankton in high resolution (about 1 m), acoustical observation was conducted.

(2) Methods

To understand vertical distribution of zooplankton in high resolution, a horizontally looking multi-frequency echo sounder (AZFP; Acoustic Zooplankton Fish Profiler, S/N; 55050) was hauled from 150 m to sea surface at a speed of 0.1 m/sec. AZFP sampled acoustic data at 125, 200, 455, and 769 kHz in this study, but I was not able to use the collected data from 455 and 769 kHz due to mechanical problem with the transducer. The settings of the AZFP for acoustic data samplings are summarized in the following table. These parameter settings are same as those in the cruises of OS026 (T/S *Oshoro Maru*, June-July 2016) and MR17-04 (July, 2017). Because AZFP has no depth sensor, depths of the acoustic sampling are recorded by using a depth sensor (DEFI2-D50, JFE-Advantec Co. Ltd; S/N 0AZ6003) attached to the AZFP frame. Interval of data sampling of the DEFI2-D50 was one second. To identify main acoustic scatterer, a zooplankton sampling between 150 and 0 m by vertical haul of a twin NORPAC net (45 cm in mouth diameter, 0.33 mm in mesh size) was conducted just after every AZFP cast. One of the two net samples was fixed and preserved in 5% formalin seawater for taxonomic analysis, and another one was preserved in –20 °C for measurement of bulk biomass.

Table 2.17(b)-1. AZFP settings

AZFP parameters and setting files	
Burst interval (s)	0.02
Ping period (s)	1
Pulse length	300
Digitization rate (kS s^{-1})	20
Number of pings per burst (pings)	1
Average burst pings	No
Bin averaging (m)	1
Lockout (m)	0
Deployment file	150901_KARE19.mfawcpl
Configuration file	55050_151209.cfg

(3) Acoustic data analysis after the cruise

Total 17 AZFP casts and net samplings were conducted at K2 as the following tables. After back to the land laboratory, volume backscattering strength will be calculated from the observed acoustic data set.

Table 2.17(b)-2. Summary of AZFP.

MR19-02 List of AZFP casts

Stn.	Cast ID	Date (yyyy/mm/dd) and Time				Position		Max. depth	NORPAC cast	Remarks
		LST		UTC		Lat. (N)	Long. (E)	(m)		
KEO	KEO-1	2019/5/25	22:34	2019/5/25	13:34	32° 15.23'	144° 17.60'	175	KEO-1	
	KEO-2	2019/5/26	13:03	2019/5/26	4:04	32° 11.88'	144° 18.07'	151	KEO-2	
	KEO-3	2019/5/26	15:08	2019/5/26	6:08	32° 13.55'	144° 18.71'	151	KEO-3	
A2	A2	2019/5/27	16:15	2019/5/27	7:15	34° 58.84'	147° 11.96'	149	A2	tidal front
A3	A3	2019/5/28	21:21	2019/5/28	12:21	37° 32.05'	149° 49.41'	152	A3	many fish
K2	K2-1	2019/6/2	4:59	2019/6/1	17:59	47° 00.60'	159° 58.56'	152	K2-1	many *N. cristatus*
	K2-2	2019/6/2	12:13	2019/6/2	1:13	47° 03.74'	159° 59.23'	150	K2-2	
	K2-3	2019/6/2	21:59	2019/6/2	10:59	47° 00.45'	159° 50.37'	152	K2-3	
	K2-4	2019/6/7	7:10	2019/6/6	20:10	46° 58.84'	160° 00.10'	? >142	K2-4	*1
	K2-5	2019/6/7	14:57	2019/6/7	3:57	47° 01.94'	160° 00.39'	159	K2-5	
KNOT	KNOT-1	2019/6/10	10:06	2019/6/9	23:06	44° 00.26'	155° 00.47'	150	KNOT-1	
	KNOT-2	2019/6/10	14:09	2019/6/10	3:09	43° 59.75'	155° 00.02'	150	KNOT-2	

LST at KEO, A2, and A3: UTC+9h
at K2 and KNOT: UTC+11h

*1: depth data between 20:09-20:14 was unrecorded

Table 2.17(b)-3. Summary of NORPAC net samplings.

List of NORPAC net samplings_MR19-02

Rewind speed: 1.0 m/sec

Stn.	Cast ID	Date (yyyy/mm/dd) and Time				Position		Wire out	Wire angle	Flow-meter revolution		Filtering vol. (m^3)		Remarks
		LST		UTC		Lat. (N)	Long. (E)	(m)	(°)	No. 2373	No.3120	No. 2373	No.3120	
KEO	KEO-1	2019/5/25	22:16	2019/5/25	13:16	32° 15.23'	144° 17.60'	150	0	1500	1541	21.0	20.0	
	KEO-2	2019/5/26	13:29	2019/5/26	4:29	32° 12.26'	144° 18.28'	150	0	1522	1518	21.3	19.7	
	KEO-3	2019/5/26	15:39	2019/5/26	6:39	32° 13.55'	144° 18.71'	150	0	1592	1498	22.3	19.5	
A2	A2	2019/5/27	16:43	2019/5/27	7:43	34° 58.12'	147° 11.44'	150	0	1478	1511	20.7	19.6	many sapla in sample
A3	A3	2019/5/28	22:02	2019/5/28	13:02	37° 32.29'	149° 48.84'	150	0	1525	1749	21.4	22.7	many sapla in sample
K2	K2-1	2019/6/2	5:03	2019/6/1	20:03	47° 00.03'	159° 58.90'	150	0	1508	1535	21.1	20.0	
	K2-2	2019/6/2	12:43	2019/6/2	3:43	47° 03.97'	159° 59.53'	150	0	1570	1571	22.0	20.4	
	K2-3	2019/6/2	22:03	2019/6/2	13:03	47° 00.44'	159° 58.15'	150	0	1480	1503	20.7	19.5	
	K2-4	2019/6/7	7:37	2019/6/6	22:37	46° 58.66'	160° 00.17'	150	0	1534	1478	21.5	19.2	
	K2-5	2019/6/7	15:28	2019/6/7	6:28	47° 01.76'	160° 00.26'	150	0	1540	1576	21.6	20.5	
KNOT	KNOT-1	2019/6/10	10:34	2019/6/9	1:34	44° 00.24'	155° 00.51'	150	0	1508	1603	21.1	20.8	
	KNOT-2	2019/6/10	13:54	2019/6/10	4:54	43° 59.82'	155° 00.01'	150	0	1738	1970	24.3	25.6	

LST at KEO, A2, and A3: UTC+9h
at K2 and KNOT: UTC+11h

(4) Data archive

Volume backscattering data of all AZFP casts will be submitted to the Data Management group, JAMSTEC.

2.17 (c) Respiration experiments of pelagic copepods

Noriaki NATORI (SOKA University)
Gu QIANYI (SOKA University)

(1) Objectives

Copepods (Crustacea: Copepoda) are the most abundant group on earth and the major link between primary production and higher trophic levels in aquatic food webs (Mauchline 1998). These free-living calanoid copepods present all marine regions and usually make up 70% more of all net collected plankton (Lalli and Parsons 1993). The aim of this study is to determine the oxygen consumption of pelagic calanoid copepods by using a recently developed fiberoptic oxygen meter with their high sensitivity, their ability to measure low oxygen concentrations with a high precision, their driftless signals and their application to microscales (Köster *et al.* 2008). Direct measurements of oxygen consumption of copepods in a controlled system provide a robust estimate of the organisms' metabolic demand and energy expenditure (Brown *et al.* 2004; Ikeda 1985).

(2) Instruments and methods

i) Oxygen measurements using an oxygen-dependent luminescence

Respiration rates of copepods were estimated from reduction rates of dissolved oxygen (DO) concentration measured with a 4-channel fiberoptic oxygen meter (FireSting O_2, PyroScience GmbH, Aachen, Germany). Three 5-mL DO glass vials were used to rear copepods, and another DO glass vial was used for control. Planar oxygen sensor spots (5 mm diameter, PyroScience GmbH) were pasted onto the inner walls of the DO glass vials with double sticky tape. The sensor spots are coated with the REDFLASH indicators which use red light excitation and lifetime detection in the near infrared, with PET foil as carrier material. The measuring principle of the optical oxygen meter is based on the quenching of the REDFLASH indicator luminescence caused by collision between oxygen molecules and the REDFLASH indicator. The REDFLASH indicators are excitable with red light and show an oxygen-dependent luminescence. The sensor signal was read out using a fiber spot sensor connecting via the channel of the FireSting O_2 to PC.

ii) Rearing of copepods

Copepods were collected with a plankton net (60 cm diameter, 180-μm mesh size, with a plastic bottle at the bottom) from four stations located on the western Pacific; KEO, K2, S1 and S4. The copepods were immediately transferred into seawater collected at the site and kept in a cold room at temperature about 4 °C. The sample was inspected with a dissecting microscope (WILD M10, Leica) to sort target species. As representative species occurring the western Pacific, we selected 11 species on board; *Candacia* sp., *Euchaeta* sp., *Gaetanus simplex*, *Gaidius* sp., *Metridia pacifica*, *Neocalanus cristatus*, *Neocalanus gracilis*, *Phaenna* sp., *Pleuromamma xyphais*, *Pleuromamma* sp.1 and *Pleuromamma* sp.2. Copepods collected were transferred to DO glass vials and reared in an incubator. DO concentration of each DO glass vial was continuously measured by 4-channel fiberoptic oxygen meter. Respiration rate (R, nmol O_2 ind^{-1} h^{-1}) was estimated from the slope of the linear regression line of oxygen concentration in both experimental and control DO glass vials against incubation time using the following equation:

$$R = (\Delta O_{exp} - \Delta O_c)V/N$$

where ΔO_{exp} and ΔO_c are the coefficients of oxygen consumption (μmol O_2 L^{-1} h^{-1}) estimated as the slope of the regression lines in the three experimental vials and slope in the control vials, respectively, using the least-square method, and V and N are volume of the DO glass vial and number of copepods in the control vial (Liu and Ban 2016).

(3) Preliminary result

Estimated respiration rates of copepod collected were shown in Table 2.1.1. The oxygen measurements were carried out at several temperatures or densities on each species. The conditions of measurements were shown in Table 2.1.1.

Table 2.1.1. Individual respiration rates of copepods collected by a plankton net (nmol O_2 ind^{-1} h^{-1})

Species	Vial 1	Vial 2	Vial 3	Mean	SD
A1_sp.1_17°C	16.0	3.66	8.82	9.49	6.19
A1_sp.1_20°C	20.0	21.0	21.7	20.9	0.81
A1_sp.1_23°C	52.1	33.3	26.8	37.4	13.2
A1_sp.2_16°C	13.3	15.9	11.6	13.6	2.17
A1_sp.2_19°C	2.57	3.92	3.96	3.48	0.76
A1_sp.2_22°C	4.96	16.2	6.05	9.06	6.18
A3_sp.1_17°C	11.9	8.22	12.7	10.9	2.36
A3_sp.1_20°C	8.15	7.85	14.5	10.2	3.76
A3_sp.1_23°C	8.10	6.87	22.1	12.3	8.49
A3_sp.2_17°C	14.3	10.8	14.2	13.1	2.00
A3_sp.2_20°C	7.06	5.41	8.89	7.12	1.74
A3_sp.2_23°C	55.1	35.1	89.8	60.0	27.7
K2_sp.1_4°C	15.8	22.0	19.3	19.0	3.14
K2_sp.1_6°C	18.5	24.8	26.4	23.3	4.18
K2_sp.1_8°C	21.0	30.0	33.1	28.0	6.28
K2_sp.2_3°C	8.26	33.0	15.6	18.9	12.7
K2_sp.2_5°C	-	24.6	18.6	14.3	-
K2_sp.2_7°C	19.1	20.6	20.3	20.0	0.78
K2_sp.3_4°C	19.4	18.1	11.0	16.1	4.55
K2_sp.3_6°C	4.35	5.22	0.403	3.32	2.56
K2_sp.3_8°C	6.69	8.47	1.90	5.69	3.40
K2_sp.4_3°C	11.5	13.6	16.3	13.8	2.38
K2_sp.4_5°C	27.0	25.3	11.2	21.2	8.64
K2_sp.4_7°C	23.2	27.3	17.6	22.7	4.90
A9_sp.1_7°C	2.24	4.55	1.52	2.77	1.58
A9_sp.1_10°C	3.86	6.01	3.33	4.40	1.42
A9_sp.1_13°C	7.09	8.48	4.51	6.69	2.01

(4) Data archive

These obtained data will be submitted to JAMSTEC Data Management Group (DMG).

(5) References

Brown, J. H., J. F. Gillooly, A. P. Allen, V. M. Savage and G. B. West (2004) Toward a metabolic theory of ecology. *Ecology*, 85, 1771–1789.

Ikeda, T. (1985) Metabolic rates of epipelagic marine zooplankton as a function of body mass and temperature. *Mar. Biol.*, 85, 1–11.

Köster, M., C. Karause and G. A. Paffenhöfer (2008) Time-series measurements of oxygen consumption of copepod nauplii. *Mar. Ecol. Prog. Ser.*, 353, 157–164.

Lalli, C. M. and T. R. Parsons (1993) Biological oceanography: An introduction. Butterworth Heinemann Ltd, Oxford.

Liu, X. and S. Ban (2016) Effects of acclimatization on metabolic plasticity of *Eodiaptomus japonicus* (Copepoda: Calanoida) determined using an optical oxygen meter. *J. Plankton Res.*, 39, 111–121.

Mauchline, J. (1998) The biology of calanoid copepods. *Adv. Mar. Biol.*, 33, 1–710.

2.18 Fluorescent dissolved organic matter (FDOM)

Masahito SHIGEMITSU (JAMSTEC RIGC)
Masahide WAKITA (JAMSTEC MIO)

(1) Objectives

Marine dissolved organic matter (DOM) is known to be one of the largest reservoirs of reduced carbon on Earth, and most of the carbon exists as refractory DOM (RDOM) (Hansell et al., 2009). RDOM is thought to be generated by microbial mineralization of organic matter produced in the sunlit surface ocean, and play an important role in carbon sequestration (Jiao et al., 2010). Some components of the RDOM can be detected as fluorescent DOM (FDOM).

In this cruise, we try to gain insights into the spatial and temporal variations in RDOM in the western North Pacific.

(2) Methods

Seawater samples were obtained from Niskin bottles on a CTD-rosette system at 3 stations (stations A1 [KEO], A7 [K2], and A9 [KNOT]). Each sample was filtered using a pre-combusted (450 °C for 4 hours) 47-mm Whatman GF/F filter. The filtration was carried out by connecting a spigot of the Niskin bottle through silicone tube to an inline plastic filter holder. Filtrates were collected in pre-combusted borosilicate glass vials, and were immediately stored frozen until analysis.

The frozen samples will be thawed at room temperature, and excitation-emission matrix (EEM) fluorescence will be measured using a fluorometer (Aqualog, Horiba). Fluorescence intensities will be normalized to Raman area. In order to separate discrete fluorescent fractions from the measured EEMs, we will apply parallel factor analysis (PARAFAC) to the data obtained, by using the DOMFluor toolbox (Stedmon and Bro, 2008). The EEMs of the excitation wavelengths from 240 nm to 450 nm and emission wavelengths from 300 nm to 560 nm will be used for the PARAFAC modeling, and several components model will be used.

(3) References

Hansell, D. A., C. A. Carlson, D. J., Repeta, and R. Schlitzer, Dissolved organic matter in the ocean: A controversy stimulates new insights, Oceanogr. 22, 202-211, 2009

Jiao, N. et al., Microbial production of recalcitrant dissolved organic matter: long-term carbon storage in the global ocean, Nat. Rev. Microbiol. 8, 593-599, 2010.

Stedmon, C. A. and R. Bro, Characterizing dissolved organic matter fluorescence with parallel factor analysis: a tutorial, Limnol. Oceanogr. Methods 6, 572-579, 2008.

2.19 Seawater density and sound velocity

Hiroshi UCHIDA (JAMSTEC RIGC)

(1) Objectives

The objective of this study is to collect Absolute Salinity (also called "density salinity") data and to evaluate the algorithm to estimate Absolute Salinity provided along with TEOS-10 (the International Thermodynamic Equation of Seawater 2010) (IOC et al., 2010).

(2) Instruments and methods

i) Density salinity measurement by an oscillation-type density meter

Seawater densities for water samples were measured with an oscillation-type density meter (DMA 5000M [serial no. 80570578], Anton-Paar GmbH, Graz, Austria) with a sample changer (Xsample 122 [serial no. 80548492], Anton-Paar GmbH). The sample changer is used to load samples automatically from up to ninety-six 12-mL glass vials.

The water samples were collected in 100-mL aluminum bottles (Mini Bottle Can, Daiwa Can Company, Japan) at deep casts of stations from A1 to A9. The bottles were stored at room temperature (~23 ºC) upside down. Densities of the samples were measured at 20 ºC by the density meter two times for each bottle and averaged to estimate the density. When the difference between the two measurements was greater than 0.002 kg/m^3, additional measurements were conducted until two samples satisfying the above criterial were obtained.

Time drift of the density meter was monitored by periodically measuring the density of ultra-pure water. The ultra-pure water was prepared from Yokosuka (Japan) tap water in June 2017 by using an ultra purification water system (model UL-Pure KE0196, Komatsu Electronics Co., Ltd., Komatsu, Ishikawa, Japan). The true density at 20 ºC of the ultra-pure water was estimated to be 998.2041 kg m^{-3} from the isotopic composition (δD = –8.86 ‰, δ^{18}O = –59.9 ‰) and International Association for the Properties of Water and Steam (IAPWS)-95 standard. An offset correction was applied to the measured density by using the ultra-pure water measurements ($\rho_{pure\text{-}water}$) with a slight modification of the density dependency (Uchida et al., 2011). The offset (ρ_{offset}) of the measured density (ρ) was reevaluated for the serial no. 80570578 in November 2014 as follows:

$$\rho_{offset} = (\rho_{pure\text{-}water} - 998.2041) - (\rho - 998.2041) \times 0.000411 \text{ [kg m}^{-3}\text{]}.$$

The offset correction was verified by periodically measuring Reference Material for Density in Seawater (prototype PRE19) developed with Kanso Technos Co., Ltd., Osaka, Japan, usually every 20 measurements (Table 2.19.1).

Density salinity was back calculated from measured density and temperature (20 ºC) with TEOS-10.

Results of density measurements of the Reference Material for Density in Seawater were shown in Table 2.19.2. A total of 20 pairs of replicate samples were measured, and the root-mean square of the absolute difference of replicate samples was 0.0008 g/kg. The measured density salinity anomalies (δS_A) are shown in Fig. 2.19.1.

Table 2.19.1. Properties of the Reference Material for Density in Seawater (prototype PRE19).

Property	Value	Note
Practical Salinity correction	34.2744	with batch offset
Reference composition salinity (S_R)	34.4360 g/kg	TEOS-10
Nitrate	27.213 µmol/kg	
Silicate	61.484 µmol/kg	
Dissolved inorganic carbon	2140.54 µmol/kg	
Total alkalinity	2303.16 µmol/kg	
Absolute Salinity anomaly (δS_A) equation	0.0075 g/kg	Pawlowicz et al. (2011)
Absolute Salinity	34.4435 g/kg	$S_R + \delta S_A$
Estimated density	1024.2186 kg/m^3	TEOS-10

Table 2.19.2. Results of density measurements of the Reference Material for Density in Seawater (prototype PRE19). Number in parentheses shows number of measurements.

Date	Stations	Serial no. of PRE19	Mean density of PRE19 (kg/m3)
2019/05/27-28	A01_2, A02_1	049	1024.2185 ± 0.0004 (8)
2019/05/30	A03_2, A04_1	056	1024.2190 ± 0.0011 (8)
2019/06/04-05	A07_5, A06_1, A05_2	050	1024.2173 ± 0.0004 (12)
2019/06/08-09	A07_10, A08_1	048	1024.2181 ± 0.0007 (12)
2019/06/10-11	A09_2	047	1024.2178 ± 0.0005 (8)
		Average	1024.2181 ± 0.0007

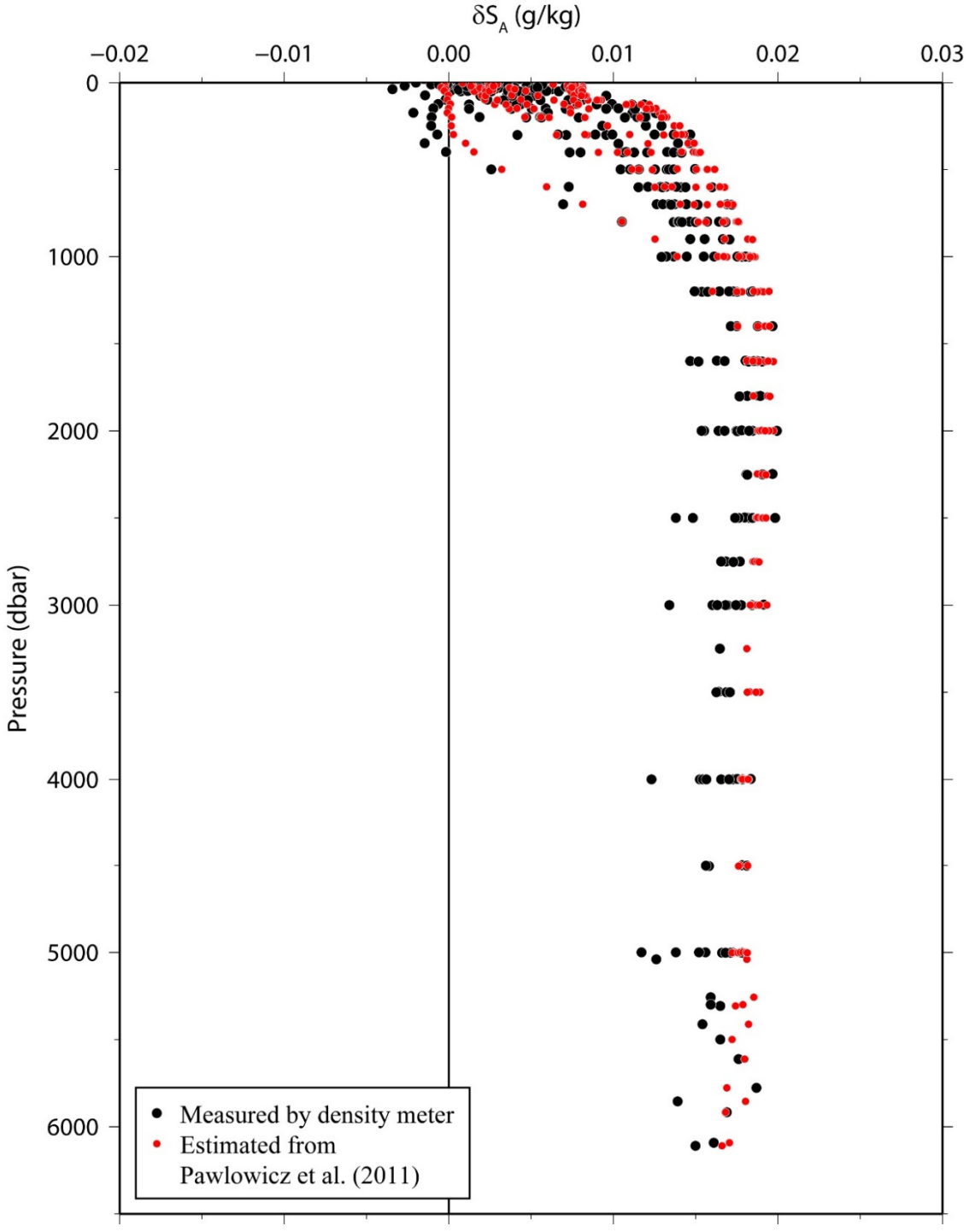

Figure 2.19.1. Vertical distribution of density salinity anomalies measured by the density meter. Absolute Salinity anomalies estimated from nutrients and carbonate system parameters (Pawlowicz et al., 2011) are also shown for comparison.

ii) Density salinity measurement by a developing refractive index density sensor

Seawater densities were continuously measured at all CTD casts with a refractive index density sensor. The density sensor was developed by combining a density measuring cell and a commercially available thickness meter (SI-F80, Keyence Co., Osaka, Japan), providing a measurement at depths up to 10,500 m. The density sensor was attached to the CTD frame and level of the measuring cell was almost same as that of the CTD temperature sensor. Sensor output (the thickness data and the returned laser beam intensity) were obtained through serial uplink port of the CTD at a sampling rate of about 46 Hz. The thickness data will be combined with the CTD temperature and pressure data measured at a sampling rate of 24 Hz to estimate seawater density. To correct temperature dependency of the thickness meter, temperature in the pressure-tight housing of the density sensor was monitored by a temperature logger (Duet T.D. deep [serial no. 95974], RBR Ltd., Ottawa, Canada) at a sampling rate of 1 Hz. The seawater density data will be calibrated in situ referred to the Absolute Salinity measured by the density meter for water samples.

iii) Density salinity measurement by a velocimeter

Sound velocity profiles were measured at the deep CTD casts by using a velocimeter (MiniSVP [serial no. 49618], Valeport Ltd., Devon, United Kingdom). The sound velocity sensing elements are a ceramic transducer (signal sound pulse of 2.5 MHz frequency), a signal reflector, and spacer rods to control the sound path length (10 cm), providing a measurement at depths up to 6000 m. The velocimeters were attached to the CTD frame and level of the sound path of the velocimeter was same as that of the CTD temperature sensors. Sound velocity data were stored in the velocimeter at a sampling rate of 8 Hz. Although temperature and pressure data were also measured by the MiniSVP, only sound velocity data will be combined with the CTD temperature and pressure data measured at a sampling rate of 24 Hz to estimate Absolute Salinity. Absolute Salinity can be back calculated from measured sound velocity, temperature and pressure and will be calibrated in situ referred to the Absolute Salinity measured by the density meter for water samples.

(3) Data archive

These obtained data will be submitted to JAMSTEC Data Management Group (DMG).

(4) References

IOC, SCOR and IAPSO (2010): The international thermodynamic equation of seawater – 2010: Calculation and use of thermodynamic properties. Intergovernmental Oceanographic Commission, Manuals and Guides No. 56, United Nations Educational, Scientific and Cultural Organization (English), 196 pp.

Pawlowicz, R., D. G. Wright and F. J. Millero (2011): The effects of biogeochemical processes on ocean conductivity/salinity/density relationships and the characterization of real seawater. *Ocean Science*, 7, 363–387.

Uchida, H., T. Kawano, M. Aoyama and A. Murata (2011): Absolute salinity measurements of standard seawaters for conductivity and nutrients. *La mer*, 49, 119−126.

2.20 Turbidity and oxygen sensor testing

Hiroshi UCHIDA (JAMSTEC RCGC)

(1) Objectives

The objective of this measurement is to evaluate the turbidity sensor by comparing with the Sea-Bird CTD, and to examine time-dependent pressure-induced effect on the oxygen sensors.

(2) Instruments and methods

To measure low turbidity in the open ocean, the high sensitivity optical backscatter logger (model ATU6-CMP, JFE Advantech Co., Ltd, Nishinomiya, Hyogo, Japan) was attached to the CTD frame at 4 CTD casts (Table 2.20.1), and turbidity was measured at a sampling rage of 1 Hz. The ATU6-CMP was calibrated by using the formazine standard solution (400 FTU, Kishida Chemical Co., Ltd, Osaka, Japan) before the cruise (March 19, 2019). The calibration coefficients are as follows:

$$\text{Turbidity\_cor [FTU]} = -0.041975 + 0.963713\ \text{Turbidity\_raw}$$

The ATU6-CMP data was compared with the CTD turbidity data (Seapoint Sensors, Inc., Exeter, New Hampshire, USA), and also the CTD turbidity data was compared with the beam attenuation coefficient measured by the transmissometer (C-Star Transmissometer, WET Labs, Inc., Philomath, Oregon, USA) (Fig. 2.20.1).

To examine time-dependent pressure-induced effect on oxygen sensors, RINKO-I oxygen sensors (AROD-USB, JFE Advantech Co., Ltd.) were attached to the CTD frame or the in-situ filteration device (Table 2.20.1). An optode oxygen sensor (Compact-Optode, Alec Electronics Co., Ltd., Kobe, Japan [Compact-Optode uses Oxygen Optode 3830, Aanderaa Data Instruments AS, Bergen, Norway, with a datalogger and an internal battery and memory in titanium housing designed for mooring observation.]) was also used for comparison. At station A07_10, the CTD package was stopped for 1 hour at 200 dbar of down-cast and for 2 hours at 5260 dbar of up-cast. At the in-situ filteration observation at station A07 (K02), the RINKO and Optode data were obtained at about 3000 dbar for more than 4 hours. Depth of the sensors was measured by using a CTD (SBE-37 SM, Sea-Bird Electronics, Inc., Bellevue, Washington, USA).

Table 2.20.1. List of serial number of the sensors used in this testing.

Sensor	Station no.	Sensing foil	Station_cast no. tested
Turbidity meter	0009	none	A10_1, A05_1, A05_2, A06_1
RINKO-I	0004	182822_pressure-aging (no. 4)	A07_4, A07_5
RINKO-I	0005	182822_pressure-aging (no. 5)	A07_4, A07_5
			A07_9, A07_10, In-situ filteration
RINKO-I	0006	182822_pressure-aging (no. 10)	A07_4, A07_5
RINKO-I	0007	182822_without_pressure-aging	A07_4, A07_5

Optode filteration	0003	A07_9, A07_10, In-situ

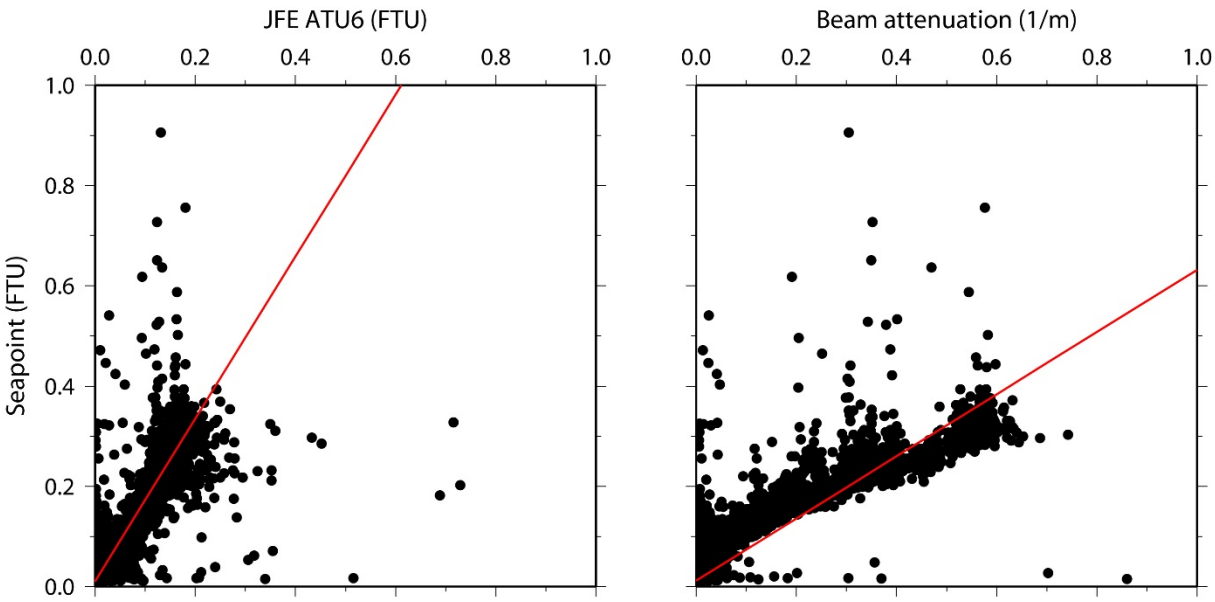

Figure 2.20.1. Comparison of turbidity data between the Seapoint and ATU6-CMP (left panel), and the Seapoint and beam attenuation coefficient measured by the transmissometer (right panel).

(3) Data archive

These obtained data will be submitted to JAMSTEC Data Management Group (DMG).

3. Ocean observation platforms

3.1 Hybrid profiling buoy system

3.1 (a) Recovery and deployment

Tetsuichi FUJIKI (JAMSTEC RIGC)
Minoru KITAMURA (JAMSTEC RIGC)
Masahide WAKITA (JAMSTEC MIO)
Hiroshi UCHIDA (JAMSTEC RIGC)
Yoshiyuki NAKANO (JAMSTEC MARE^3)
Makio HONDA (JAMSTEC RIGC)
Hiroki USHIROMURA (MWJ)

Hybrid profiling buoy is combined two moorings, BGC mooring (biogeochemistry) and POPPS mooring (ocean productivity profiling system). We recovered Hybrid profiling buoy system at Station K-2 which were deployed at MR18-04Leg1 and deployed Hybrid profiling buoy system at Station K-2. Deployment operation took approximately 5 hours. After sinker was dropped, we positioned the mooring systems by measuring the slant ranges between research vessel and the acoustic releaser. The position of the mooring is finally determined as follow:

Table 3.1(a).1. Mooring positions of respective mooring systems.

	Recovery	Deployment
Mooring Number	K2H180729	K2H190606
Working Date	Jul. 29 2018	Jun. 06 2019
Latitude	47 ° 00.46 N	47 ° 00.26 N
Longitude	159 ° 58.40 E	159 ° 58.48 E
Sea Beam Depth	5,220 m	5,213 m

The deployment Hybrid profiling buoy consists of a top buoy with 24lbs (11kg) buoyancy, underwater winch, instruments, wire and ropes, recovery buoy with 496lbs (225kg) buoyancy, glass floats (Benthos 17” glass ball), dual releasers (Edgetech) and 4,911lbs (2,228kg) sinker. An ARGOS compact mooring locator was mounted on underwater winch, and a submersible re covery strobe was mounted on the top buoy. This mooring system was planned to keep the following time-series observational instruments are mounted approximately 130 m below sea surface. On the Hybrid profiling buoy, three Sediment Traps are installed on the 500 m, 1,000 m and 4,800 m. two Auto Sampling Systems (RAS) are installed on the 200 m and 300m. four Backscatter Meter are mounted on the SUS frame (175 m), Sediment Trap, RAS, one Underwater Video Camera are mounted on the SUS frame (175 m), CTD (SBE-37) and Do Sensor (RINKO and Optode) are mounted on the dual acoustic releaser and inline SUS frame (175 m, 250 m and 780 m), Sediment Trap, RAS, underwater winch, top buoy. Details for each instrument are described below (section 3.1(c), 3.1(d), 3.1(e), 3.1(f), 3.1(g), 3.1(h), 3.1(i)). Serial number of instruments are as follows:

Table 3.1(a).2. Serial numbers of instruments.

Recover			Deployment	
Station and type Mooring Number	K2 K2H180729		Station and type Mooring Number	K2 K2H190606
Top Buoy(130m) Iridium Transmiter Storobo FRRF PAR RINKO CTD (SBE19plusV2) AFP07	- - G02-009 780263011 20554 0264 7681 187,189		Top Buoy (CT608B ABS BUOY)	-
Winch(150m) Argos Transmitter SBE37 OPTODE	- C01-081 1893 03		Recovery buoy Argos Transmitter Storobo	- F01-038 E10-024
(175m) SBE37 OPTODE	Wire 1892 6		(175m) SBE37 OPTODE Backscatter Meter Underwater Video Camera	SUS frame 1892 6 5167 2
RAS (200m) SBE37 OPTODE HpHS(HPS-14) SUNA V2 SUNA Battery	ML11241-09 2239 50 60100265002 NTR-1004 BAT-1049		RAS (200m) SBE37 OPTODE HpHS(HPS-14) Backscatter Meter Depth Sensor	ML11241-09 2239 50 60100265001 5168 0AGG026
(250m) SBE37 RINKO	SUS frame 2756 0004		(250m) SBE37 RINKO	SUS frame 2756 0092
RAS (300m) SBE37 RINKO	ML11241-10 2289 051		RAS (300m) SBE37 RINKO Backscatter Meter	ML11241-07 2289 051 1742
ADCP(370m) SBE37 OPTODE	1533 2288 9		ADCP(370m) SBE37 OPTODE	1434 2288 9
(475m) SBE37 OPTODE	Wire 10737 10		Sediment Trap(500m) SBE37 OPTODE Backscatter Meter	STC98025 2748 10 891

-	-		(780m) SBE37 OPTODE	SUS frame 2738 5
Sediment Trap(1000m) SBE37 RINKO	ML10236-02 2285 0007		Sediment Trap(1000m) SBE37 OPTODE	ML12401-02 2285 7
(2000m) SBE37 RINKO	SUS frame 2748 0006		-	-
RAS(3000m) SBE37 RINKO	ML11241-11 2738 0005		-	-
Sediment Trap(4800m)	ML10558-01		Sediment Trap(4800m)	ML11241-22
Releaser Releaser SBE-37	28533 27868 2731		Releaser Releaser SBE-37 RINKO	27815 34040 2731 0004

Table 3.1(a).3. Recovery Hybrid profiling buoy system record.

Mooring Number K2H180729

Project	Time-Series		Depth	5,220.0	m
Area	North Pacific		Planned Depth	5,218.0	m
Station	K2		Length	5,088.9	m
Target Position	**47°00.35**	**N**	Depth of Buoy	130	m
	159°58.32	**E**	Period	1	year
ACOUCTIC RELEASERS					
Type	Edgetech		Edgetech		
Serial Number	28533		27868		
Receive F.	11.0	kHz	11.0	kHz	
Transmit F.	14.0	kHz	14.0	kHz	
RELEASE C.	**223307**		**335534**		
Enable C.	201054		322710		
Disable C.	201077		322756		
Battery	2 years		2 years		
Release Test	OK		OK		
RECOVERY					
Recorder	Hiroki Ushiromura		Work Distance	3.1	Nmile
Ship	R/V MIRAI		Send Enable C.	0:24	
Cruise No.	MR19-02		Slant Renge	-	msec
Date	2019/6/1		Send Release C.	0:32	
Weather	f		Discovery Buoy	0:34	
Wave Hight	2.1	m	Pos. of Top Buoy	47°00.76	N
Seabeam Depth	-	m		159°58.37	E
Ship Heading	170	deg	Pos. of Start	47°00.66	N
Ship Ave.Speed	-	knot		159°58.40	E
Wind	< 198 deg > 4.7	m/s	Pos. of Finish	46°57.19	N
Current	< 041 deg > 0.1	cm/s		159°55.40	E

Table 3.1(a).4. Deployment Hybrid profiling buoy system record.

Mooring Number K2H190606

Project	Time-Series		Depth	5,213.0	m
Area	North Pacific		Planned Depth	5,220.0	m
Station	K2		Length	5,090.0	m
Target Position	**47°00.35**	**N**	Depth of Buoy	-	m
	159°58.32	**E**	Period	1	year
ACOUCTIC RELEASERS					
Type	Edgetech		Edgetech		
Serial Number	27815		34040		
Receive F.	11.0	kHz	11.0	kHz	
Transmit F.	14.0	kHz	14.0	kHz	
RELEASE C.	**344657**		**233770**		
Enable C.	361035		221130		
Disable C.	361073		221155		
Battery	2 years		2 years		
Release Test	OK		OK		
DEPLOYMENT					
Recorder	Hiroki Ushiromura		Start	4.9	Nmile
Ship	R/V MIRAI		Overrun	500	m
Cruise No.	MR19-02		Let go Top Buoy	20:58	
Date	2019/6/5~6/6		Let go Anchor	0:28	
Weather	O		Sink Top Buoy	1:08	
Wave Hight	2.0	m	Pos. of Start	47°01.90	N
PDR Depth	5,212	m		160°04.64	E
Ship Heading	250	deg	Pos. of Drop. Anc.	47°00.11	N
Ship Ave.Speed	-	knot		159°57.96	E
Wind	< 254 deg > 10.8	m/s	Pos. of Mooring	47°00.2551	N
Current	< 172 deg > 0.5	cm/s		159°58.4788	E

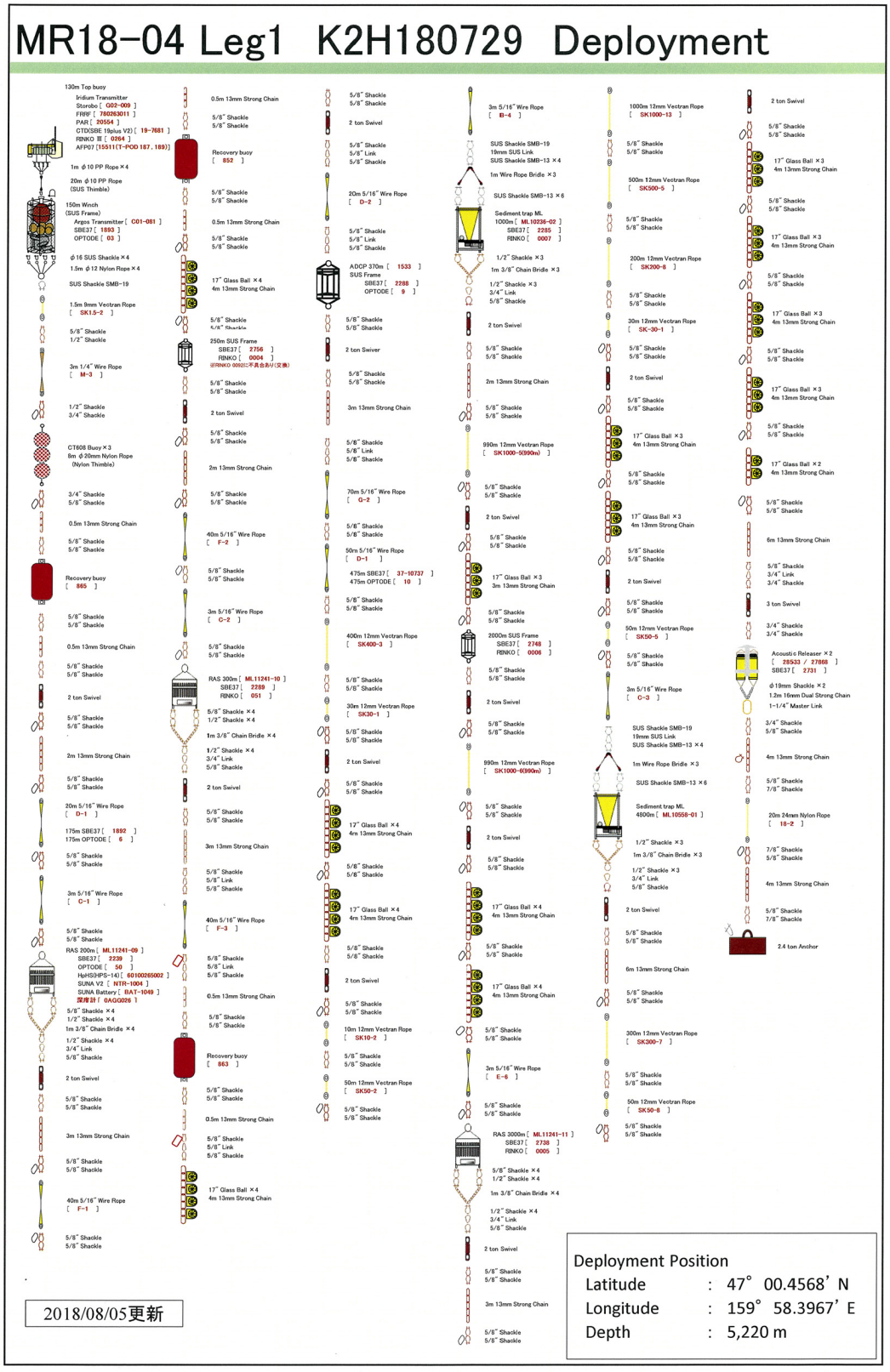

Figure 3.1(a).1. Hybrid profiling buoy system recovered.

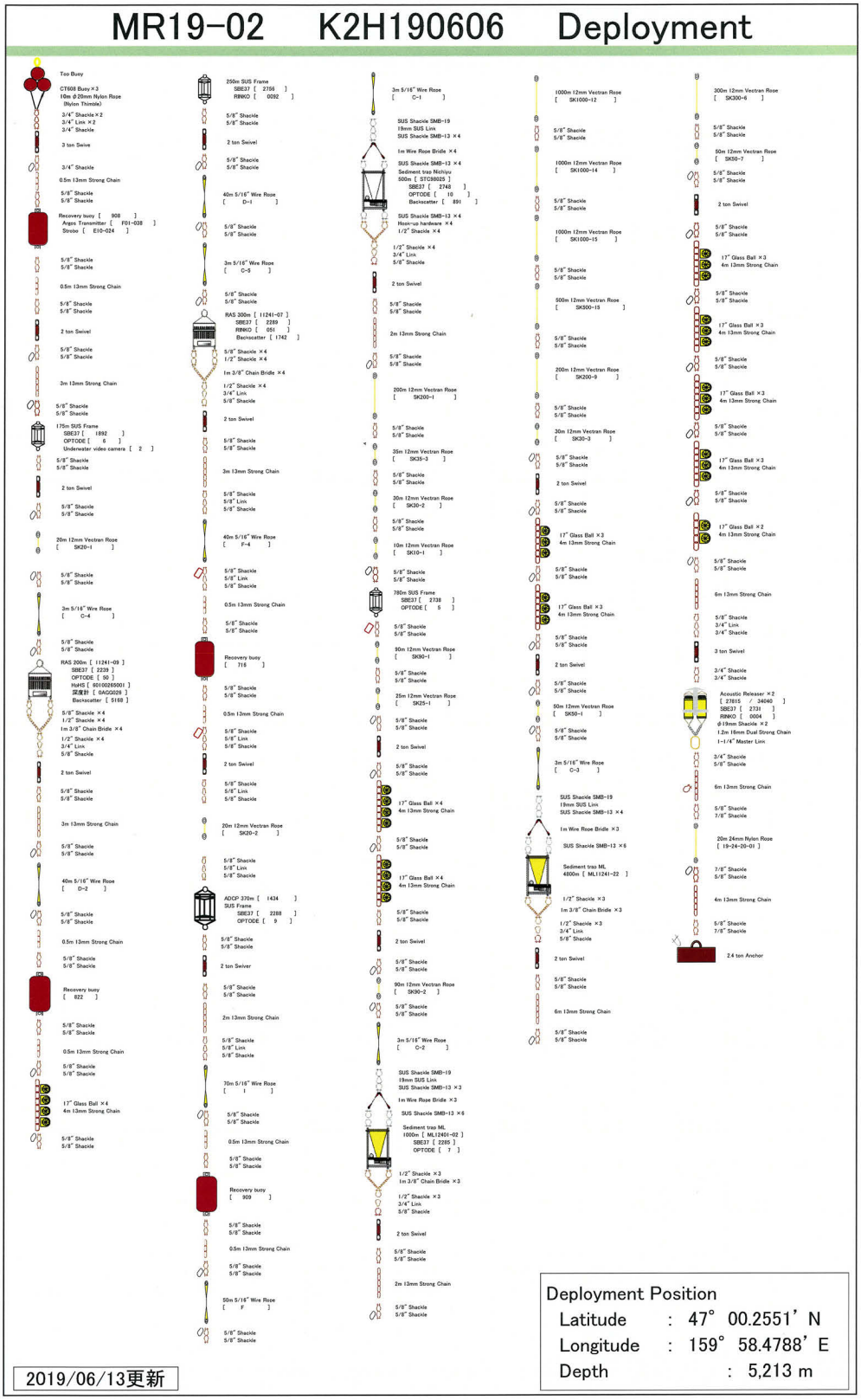

Figure 3.2(a).2. Hybrid profiling buoy system deployed.

3.1 (b) Instruments

Tetsuichi FUJIKI (JAMSTEC RIGC)
Minoru KITAMURA (JAMSTEC RIGC)
Masahide WAKITA (JAMSTEC MIO)
Hiroshi UCHIDA (JAMSTEC RIGC)
Yoshiyuki NAKANO (JAMSTEC MARE^3)
Makio HONDA (JAMSTEC RIGC)
Hiroki USHIROMURA (MWJ)

On mooring systems, instruments for details are as follows:

*Top buoy and underwater winch, RAS, Hybrid pH sensor, ADCP, Sediment trap, CTD, DO Backscatter meter and Underwater video camera are described below (section 3.1(c), 3.1(d), 3.1(e),3.1(f),3.1(g), 3.1(h) , 3.1(i)).

(1) ARGOS Beacon

The NOVATECH MMA-7500 ARGOS Beacon contains an ARGOS satellite transmitter designed as a ruggedized incident alerting system for oceanographic applications deployed anywhere in the world. It may be submerged for long periods in ocean depths to 7,500 m (24,000feet).

The device can be turned ON or OFF by triggering the internal reed switch with a magnet. The activation of the MMA-7500 is completely automatic and water sensor controlled. The water sensor is located in the antenna base – when submerged, the beacon goes into low-power hibernation mode.

The water sensor hysteresis is approx. 90 seconds. The beacon will continue to transmit for up to 90 seconds when submerged and will begin transmitting within 90 seconds of surfacing. At the surface the beacon transmits an ARGOS position data massage for 90 days.

(Specifications)

Transmitter Output:	1 watt
Harmonics:	-40 db minimum
Batteries:	8 CR123A Lithium cells
Battery Life:	90days at the surface
Operating Temp:	-40 °C to +60°C
Transmit Freq:	401.6300 MHz - 401.6800 MHz
Antenna:	Field replaceable 1/4 wave whip
Max Depth:	7,500 m
Weight:	In air 1.25lbs (0.56kg), In water 0.75lbs (0.34kg)
Dimensions:	16.5"long (420mm),1.0"diameter (250mm)

(2) Submersible Recovery Strobe

The NOVATECH MMF-7500 Mini-Flasher is intended to aid in the marking or recovery of oceanographic instruments, manned vehicles, remotely operated vehicles, buoys or structures. Due to the occulting (firing closely spaced bursts of light) nature of this design, it is much more visible than conventional marker strobes, particularly in poor sea conditions.

(Specifications)

Flash Rate:	Double burst 4 second delay.
Visible Range:	Up to 5 Nm
Battery Type:	7×CR123A Lithinm
Life:	Approximately 6 days, standard configuration (Double burst every 4s @ 170 lm)
Max. Depth:	7,500m
Switch:	Water conductivity
Weight:	air 1.44lbs(0.66kg) water 0.96lbs(0.44kg)
Dimensions:	Length 15.00” (381mm) Diameter 1.44” (29mm)

3.1 (c)1 Remote Automatic Sampler (RAS)

Masahide WAKITA (JAMSTEC MIO)
Hiroshi Uchida (JAMSTEC RIGC)
Yoshihisa Mino (Nagoya University)

In order to investigate the seasonal variation of pH in the intermediate layer, and the vertical gradients of biogeochemical properties which affects vertical diffusion flux across the boundary with the thermocline, RAS on 200m and 300m (Figure 1) will work following schedule (Table 1) and collect samples of dissolved inorganic carbon (DIC), total alkalinity (TA), nutrients (Phosphate, Nitrate + Nitrite, Silicate), $^{15}NO_3$ and salinity. We will compare these properties from 10 liter Niskin bottles mounted on the CTD/Carousel Water Sampling System for calibration on RAS samples at K2.

Salinity of RAS seawater samples were measured by salinometer (Model 8400B "AUTOSAL" Guildline Instruments). Salinity of RAS samples should be lower than ambient seawater, because RAS samples were diluted with 20% saturated $HgCl_2$ solution. Salinity measured by salinometer will be slightly lower than that observed by SBE-37 sensor (CTD). RAS samples (~500ml) were diluted with 2.5 ml of 20% saturated $HgCl_2$ solution for preservative. For chemical properties, the dilutions of RAS samples by $HgCl_2$ must be corrected by a ratio of salinity by SBE-37 to that by salinometer. We will correct measurements of DIC, TA and nutrients. We used coulometric and potentiometric techniques to measure DIC and TA, respectively. Nutrient (silicate, phosphate, and nitrate) concentrations were measured with a continuous flow analyzer. $^{15}NO_3$ will be measured by Tokai University.

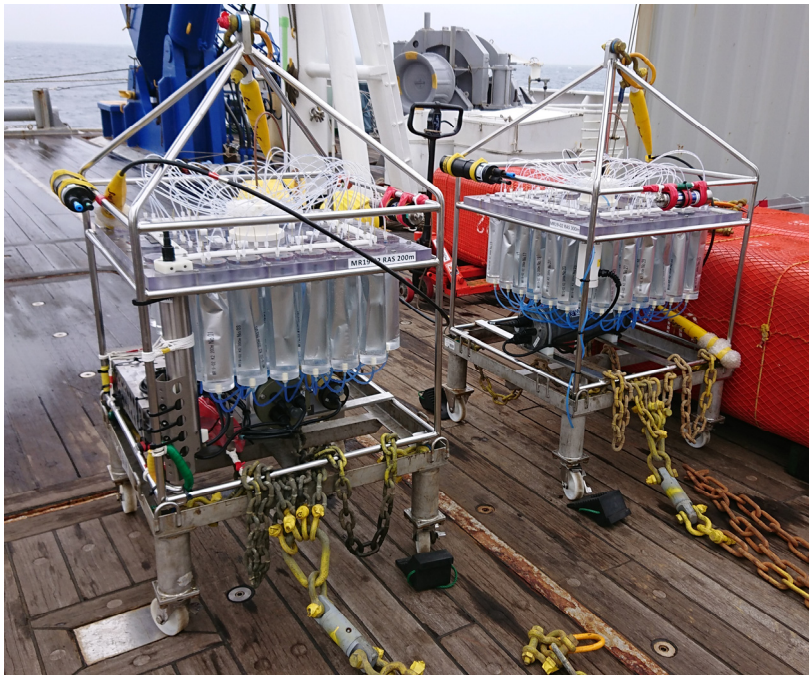

Figure 1 Remote Automatic Samplers deployed on 200m (left) and 300m (right).

Table 1 Sampling schedule of RAS in 200m and 300m on Hybrid mooring at station K2.

	RAS 200m		**RAS 300m**			
RAS No.	ML11241-09 Interval 10days		ML11241-07 Interval 10days		Memo	
#	mm/dd/yyyy	Time(UTC)	mm/dd/yyyy	Time(UTC)		
1	06/08/2019	1:00:00	06/08/2019	1:00:00	20% Saturated $HgCl_2$ 0.5ml	Interval 1 hour for duplicate sampling
2	06/08/2019	2:00:00	06/08/2019	2:00:00	20% Saturated $HgCl_2$ 0.5ml	
3	06/18/2019	1:00:00	06/18/2019	1:00:00	20% Saturated $HgCl_2$ 0.5ml	
4	06/28/2019	1:00:00	06/28/2019	1:00:00	20% Saturated $HgCl_2$ 0.5ml	
5	07/08/2019	1:00:00	07/08/2019	1:00:00	20% Saturated $HgCl_2$ 0.5ml	
6	07/18/2019	1:00:00	07/18/2019	1:00:00	20% Saturated $HgCl_2$ 0.5ml	
7	07/28/2019	1:00:00	07/28/2019	1:00:00	20% Saturated $HgCl_2$ 0.5ml	
8	08/07/2019	1:00:00	08/07/2019	1:00:00	20% Saturated $HgCl_2$ 0.5ml	
9	08/17/2019	1:00:00	08/17/2019	1:00:00	20% Saturated $HgCl_2$ 0.5ml	
10	08/27/2019	1:00:00	08/27/2019	1:00:00	20% Saturated $HgCl_2$ 0.5ml	
11	09/06/2019	1:00:00	09/06/2019	1:00:00	20% Saturated $HgCl_2$ 0.5ml	Interval 1 hour for duplicate sampling
12	09/06/2019	2:00:00	09/06/2019	2:00:00	20% Saturated $HgCl_2$ 0.5ml	
13	09/16/2019	1:00:00	09/16/2019	1:00:00	20% Saturated $HgCl_2$ 0.5ml	
14	09/26/2019	1:00:00	09/26/2019	1:00:00	20% Saturated $HgCl_2$ 0.5ml	
15	10/06/2019	1:00:00	10/06/2019	1:00:00	20% Saturated $HgCl_2$ 0.5ml	
16	10/16/2019	1:00:00	10/16/2019	1:00:00	20% Saturated $HgCl_2$ 0.5ml	
17	10/26/2019	1:00:00	10/26/2019	1:00:00	20% Saturated $HgCl_2$ 0.5ml	
18	11/05/2019	1:00:00	11/05/2019	1:00:00	20% Saturated $HgCl_2$ 0.5ml	
19	11/15/2019	1:00:00	11/15/2019	1:00:00	20% Saturated $HgCl_2$ 0.5ml	
20	11/25/2019	1:00:00	11/25/2019	1:00:00	20% Saturated $HgCl_2$ 0.5ml	
21	12/05/2019	1:00:00	12/05/2019	1:00:00	20% Saturated $HgCl_2$ 0.5ml	
22	12/15/2019	1:00:00	12/15/2019	1:00:00	20% Saturated $HgCl_2$ 0.5ml	
23	12/25/2019	1:00:00	12/25/2019	1:00:00	20% Saturated $HgCl_2$ 0.5ml	Interval 1 hour for duplicate sampling
24	12/25/2019	2:00:00	12/25/2019	2:00:00	20% Saturated $HgCl_2$ 0.5ml	
25	01/04/2020	1:00:00	01/04/2020	1:00:00	20% Saturated $HgCl_2$ 0.5ml	
26	01/14/2020	1:00:00	01/14/2020	1:00:00	20% Saturated $HgCl_2$ 0.5ml	
27	01/24/2020	1:00:00	01/24/2020	1:00:00	20% Saturated $HgCl_2$ 0.5ml	
28	02/03/2020	1:00:00	02/03/2020	1:00:00	20% Saturated $HgCl_2$ 0.5ml	
29	02/13/2020	1:00:00	02/13/2020	1:00:00	20% Saturated $HgCl_2$ 0.5ml	
30	02/23/2020	1:00:00	02/23/2020	1:00:00	20% Saturated $HgCl_2$ 0.5ml	
31	03/04/2020	1:00:00	03/04/2020	1:00:00	20% Saturated $HgCl_2$ 0.5ml	
32	03/14/2020	1:00:00	03/14/2020	1:00:00	20% Saturated $HgCl_2$ 0.5ml	
33	03/24/2020	1:00:00	03/24/2020	1:00:00	20% Saturated $HgCl_2$ 0.5ml	
34	04/03/2020	1:00:00	04/03/2020	1:00:00	20% Saturated $HgCl_2$ 0.5ml	
35	04/13/2020	1:00:00	04/13/2020	1:00:00	20% Saturated $HgCl_2$ 0.5ml	Interval 1 hour for duplicate sampling
36	04/13/2020	2:00:00	04/13/2020	2:00:00	20% Saturated $HgCl_2$ 0.5ml	
37	04/23/2020	1:00:00	04/23/2020	1:00:00	20% Saturated $HgCl_2$ 0.5ml	Interval 5 days
38	04/28/2020	1:00:00	04/28/2020	1:00:00	20% Saturated $HgCl_2$ 0.5ml	
39	05/03/2020	1:00:00	05/03/2020	1:00:00	20% Saturated $HgCl_2$ 0.5ml	
40	05/08/2020	1:00:00	05/08/2020	1:00:00	20% Saturated $HgCl_2$ 0.5ml	
41	05/13/2020	1:00:00	05/13/2020	1:00:00	20% Saturated $HgCl_2$ 0.5ml	
42	05/18/2020	1:00:00	05/18/2020	1:00:00	20% Saturated $HgCl_2$ 0.5ml	
43	05/23/2020	1:00:00	05/23/2020	1:00:00	20% Saturated $HgCl_2$ 0.5ml	
44	05/28/2020	1:00:00	05/28/2020	1:00:00	20% Saturated $HgCl_2$ 0.5ml	
45	06/02/2020	1:00:00	06/02/2020	1:00:00	20% Saturated $HgCl_2$ 0.5ml	
46	06/07/2020	1:00:00	06/07/2020	1:00:00	20% Saturated $HgCl_2$ 0.5ml	
47	06/12/2020	1:00:00	06/12/2020	1:00:00	20% Saturated $HgCl_2$ 0.5ml	
48	06/17/2020	1:00:00	06/17/2020	1:00:00	20% Saturated $HgCl_2$ 0.5ml	

3.1 (d) Hybrid pH sensor

Yoshiyuki NAKANO (JAMSTEC MARE[3])

(1) Objective

We have been developing newly stable and accurate *in situ* system for pH measurement using hybrid technique (potentiometric and spectrophotometric). In this cruise, we aim at testing the new Hybrid pH sensor (HpHS) in the open sea. We recovered HpHS at K2 which was deployed at MR18-04 with Hybrid profiling buoy system (200m). The HpHS was deployed mooring with Hybrid profiling buoy system (200m) in this cruise for about one year.

(2) Method

The HpHS is constituted two types of pH sensors (i.e. potentiometric pH sensor and spectrophotometric pH sensor). The spectrophotometric pH sensor can measure pH correctly and stably, however it needs large power consumption and a lot of reagents in a long period of observation. On the other hand, although the potentiometric pH sensor is low power consumption and high-speed response (within 20 seconds), drifts in the pH of the potentiometric measurements may possibly occur for a long period of observation. The HpHS can measure in situ pH correctly and stably combining advantage of both pH sensors. The HpHS is correcting the value of the potentiometric pH sensor (measuring frequently) by the value of the spectrophotometric pH sensor (measuring less frequently). It is possible to calibrate in situ with standard solution (Tris buffer) on the spectrophotometric pH sensor. Therefore, the drifts in the value of potentiometric pH measurements can be compensated using the pH value obtained from the spectrophotometric pH measurements. Thereby, the sensor can measure accurately the value of pH over a long period of time with low power consumption.

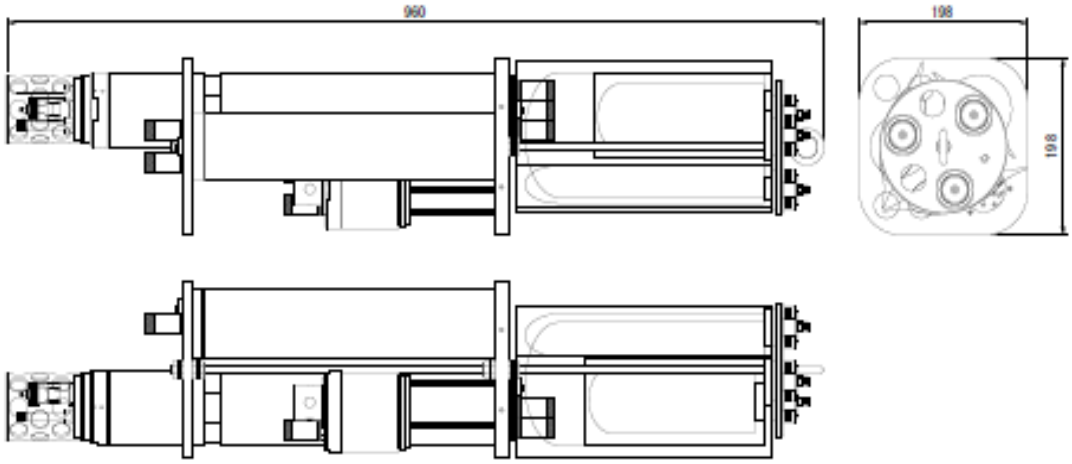

Fig. 3.1(d)-1. Side view of HpHS.

Table 3.1(d)-1. Specification of HpHS

	Potentiometry	Spectrophotometry

Range	6.0～8.3 pH	7.2～8.2 pH
Initial Accuracy	0.01 pH	0.002 pH
Analytical Method	Glass Electrode	m-cresol purple
Response speed	20 sec (90%, 25 deg C)	3 min (90%)
Resolution	0.001 pH	
Sample rate	1 sec	
Temperature range	0～40 deg C (Resolution: 0.01 deg C)	
Dimension	198×198×960 mm	
Weight	10 kg（in air）	
Depth rating	3,000 m	

(3) Preliminary results

We succeeded in recovering the HpHS with RAS in Hybrid profiling buoy system and obtaining long term (about one year) pH data every four hours.

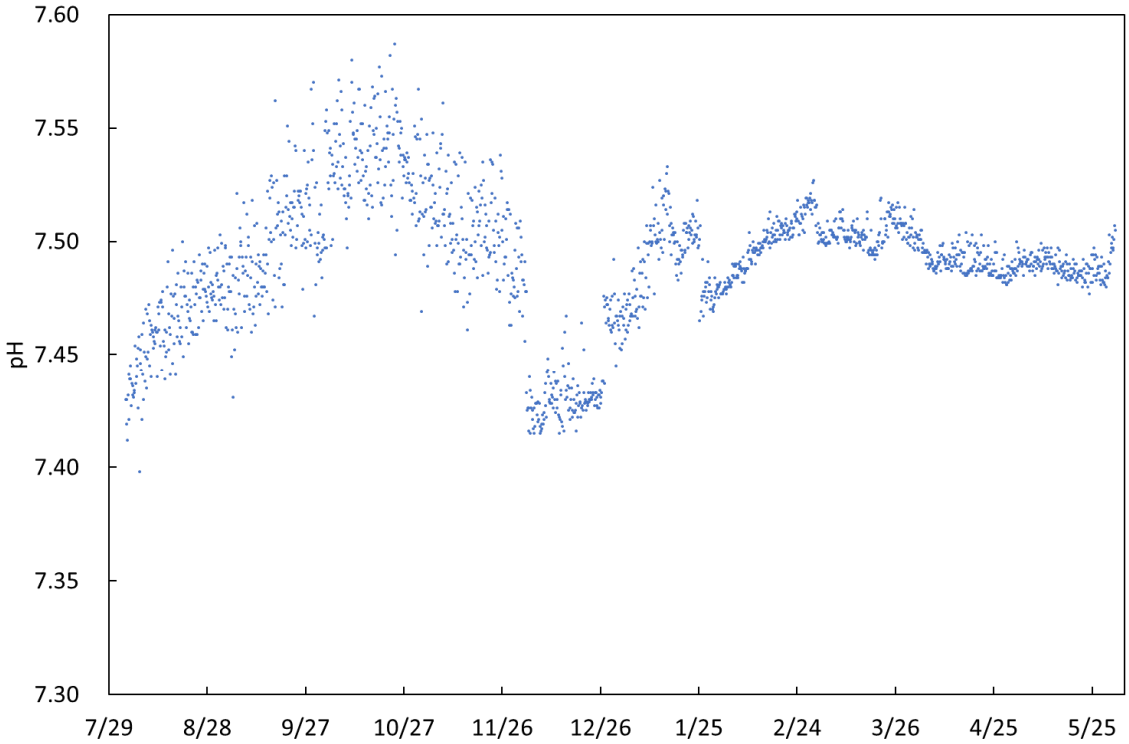

Fig. 3.1(d)-2. Diurnal and seasonal changes of pH for a year at 200m depth from 3 August 2018 to 1 June 2019 in the station K2. Variation of potentiometric pH (after preliminary correction ●).

(4) Data Archive

All data will be submitted to JAMSTEC Data Management Office (DMO) and is currently

under its control.

Reference

DICKSON, A.G., SABINE, C.L. and CHRISTIAN, J.R. (Eds.) (2007) Guide to best practices for ocean CO_2 measurements. PICES Special Publication 3, 191 pp.

LIU, X., PATSAVAS, M.C. and BYRNE, R.H. (2011) Purification and characterization of meta-cresol purple for spectrophoto-metric seawater pH measurements. Environ. Sci. Technol., 45, pp. 4862-4868.

PATSAVAS, M.C., BYRNE, R.H. and LIU, X. (2013) Purification of meta-cresol purple and cresol red by flash chromatography: Procedures for ensuring accurate spectrophotometric seawater pH measurements. Mer. Chem., 150, pp. 19-24.

3.1 (e) ADCP

Minoru KITAMURA (JAMSTEC RIGC)

An Acoustic Doppler Current Profiler (ADCP) was installed at a depth of 370 m on the K2 mooring. Purposes of data samplings (and investigators) are as follows;

(1) to observe seasonal current structure fluctuation (A. Nagano and M. Wakita, JAMSTEC),

(2) to understand zooplankton dynamics (M. Kitamura, JAMSTEC)

Using the former data, we will be able to understand mixing/stratifying processes in the surface layer and nutrient supply to the surface layer due to vertical diffusion. On the other hand, ADCP have been used not only physical oceanography but also biological researches. That is, zooplankton biomass can be estimated using acoustic backscattering intensities collected from ADCP. So, we will also analyze zooplankton dynamics at K2.

Specifications

Model: Workhorse LongRanger (Teledyne RD Instruments, Poway, CA, USA)
S/N: 1533 (recovered ADCP), 1434 (deployed ADCP)
Frequency: 75 kHz
Max. depth: 1500m
Dimensions: 1014 mm in length, 550 mm in width
Weights: ADCP; 86 kg in air and 55 kg in water
Frame; 46 kg in water (recovered), 54 kg in air and 47 kg in water (deployed)
Beam angle/width: 20°/4°
DC input: 20-60VDC, four internal alkaline battery packs
Voltage: 42V DC (new), 28V DC (depleted)
Velocity resolution: 1mm/s

Setting parameters for data sampling

Depth cell size: 8 m
Number of depth cells: 60
Ping per ensemble: 30
Intervals: 60 min.
Mode: Broadband mode

3.1 (f) Sediment trap

Minoru KITAMURA (JAMSTEC RIGC)

(1) Objective

To observe long-term trend of the sinking carbon flux at K2, the sediment trap experiment is conducted. Two sediment traps which moored at 1000 m and 4810 m were recovered from the K2H180729 mooring on 29 July, 2018. And three traps were newly installed at 500, 1000 m and 4810 m in the K2H190606 mooring which deployed on 6 June, 2019.

(2) Description of instruments

Two kinds of sediment trap were used in this experiment, MARK78H-21 (McLane Research Laboratories, INC., MA, USA) and SMD26S-6000 (NiGK Corporation, Tokyo, Japan). The former trap which had 21 sampling cups was installed at 1000 and 4810 m of the recovered mooring, 1000 and 4810 m of the deployed mooring. Sampling interval of the McLane trap was every 20 days for the recovered mooring and 18 days for the deployed one. The latter model of trap with 26 sampling cups was attached at 500 m of the deployed mooring. Shorter interval of sampling (9 days) will be scheduled during the season of high primary productivity while samplings will be conducted every 18 days in other seasons. Specifications and serial numbers of the two traps are summarized in the following tables:

Table 3.1(f)-1. Specifications of two sediment traps

	SMD26S-6000 (NiGK Corporation)	MARK78H-21 (McLane Research Lab.)
Max. depth (m)	6000	7000
Dimensions (diameter × height, cm)	104 × 160	91 ×164
Mouth area (m^2)	0.5	0.5
Weights (kg)	86 in air, 46 in water	72 in air, 39 in water
No. of sampling bottles	26	21
Volume of sampling bottles (ml)	270	250
Battery	Alkaline/Lithium pack	14 Alkaline batteries or a Battery pack
Communication cables	RMG4-USB	RMG3-Serial port-USB
Software	N-SMD	Crosscut
OS	Win 7	Win 7

Table 3.1(f)-2. Serial numbers and battery types

	Model	S/N	Battery
Recovery from			
1000 m	McLane, MARK78H-21	ML10236-02	Battery pack
4810 m	McLane, MARK78H-21	ML10558-01	14 Alkaline batteries
Deployed at			
500 m	NiGK, SMD26S-6000	STC98025	Alkaline/Lithium pack
1000 m	McLane, MARK78H-21	No record*	14 Alkaline batteries
4810 m	McLane, MARK78H-21	ML11241-22	14 Alkaline batteries

*ML12401-02 or ML10558-01

(3) Sampling schedules

Sampling schedules of the recovered and deployed sediment traps were summarized in the following tables. Internal clock of each sediment trap was set in UTC. The deployed mooring systems will be recovered during *Mirai* cruise held in 2020.

Table 3.1(f)-3. Sampling schedules and volume flux of the recovered trap.

McLane Sediment Trap 1000 m

Bottle No.	Sampling (UTC, yyyy/mm/dd)				Height	Flux
	Start	End	Interval (days)		(cm)	($cm^3/m^2/day$)
No.1	2018/07/30 13:00	2018/08/19 13:00	20		4.3	7.84
No.2	2018/08/19 13:00	2018/09/08 13:00	20		5.3	9.65
No.3	2018/09/08 13:00	2018/09/28 13:00	20		4.3	7.78
No.4	2018/09/28 13:00	2018/10/18 13:00	20		5.7	10.38
No.5	2018/10/18 13:00	2018/11/07 13:00	20		2.7	4.95
No.6	2018/11/07 13:00	2018/11/27 13:00	20		2.1	3.86
No.7	2018/11/27 13:00	2018/12/17 13:00	20		1.2	2.11
No.8	2018/12/17 13:00	2019/01/06 13:00	20		0.8	1.51
No.9	2019/01/06 13:00	2019/01/26 13:00	20		0.8	1.39
No.10	2019/01/26 13:00	2019/02/15 13:00	20		0.5	0.97
No.11	2019/02/15 13:00	2019/03/07 13:00	20		0.7	1.27
No.12	2019/03/07 13:00	2019/03/27 13:00	20		2.6	4.65
No.13	2019/03/27 13:00	2019/04/16 13:00	20		2.5	4.59
No.14	2019/04/16 13:00	2019/05/06 13:00	20		1.5	2.65
No.15	2019/05/06 13:00	2019/05/26 13:00	20		2.4	4.28
No.16	2019/05/26 13:00	2019/06/15 13:00	20			
No.17	2019/06/15 13:00	2019/07/05 13:00	20			
No.18	2019/07/05 13:00	2019/07/25 13:00	20			
No.19	2019/07/25 13:00	2019/08/14 13:00	20			
No.20	2019/08/14 13:00	2019/09/03 13:00	20			
No.21	2019/09/03 13:00	2019/09/23 13:00	20			

McLane Sediment Trap 4800 m

Bottle No.	Sampling (UTC)				Height	Flux
	Start	End	Interval (days)		(cm)	($cm^3/m^2/day$)
No.1	2018/07/30 13:00	2018/08/19 13:00	20		2.0	3.68
No.2	2018/08/19 13:00	2018/09/08 13:00	20		2.3	4.22
No.3	2018/09/08 13:00	2018/09/28 13:00	20		2.9	5.25
No.4	2018/09/28 13:00	2018/10/18 13:00	20		5.0	9.11
No.5	2018/10/18 13:00	2018/11/07 13:00	20		3.8	6.82
No.6	2018/11/07 13:00	2018/11/27 13:00	20		2.7	4.89
No.7	2018/11/27 13:00	2018/12/17 13:00	20		2.0	3.56
No.8	2018/12/17 13:00	2019/01/06 13:00	20		1.1	2.05
No.9	2019/01/06 13:00	2019/01/26 13:00	20		1.0	1.81
No.10	2019/01/26 13:00	2019/02/15 13:00	20		0.8	1.45
No.11	2019/02/15 13:00	2019/03/07 13:00	20		1.0	1.87
No.12	2019/03/07 13:00	2019/03/27 13:00	20		0.7	1.21
No.13	2019/03/27 13:00	2019/04/16 13:00	20		1.7	3.02
No.14	2019/04/16 13:00	2019/05/06 13:00	20		2.0	3.68
No.15	2019/05/06 13:00	2019/05/26 13:00	20		0.1	0.12
No.16	2019/05/26 13:00	2019/06/15 13:00	20			
No.17	2019/06/15 13:00	2019/07/05 13:00	20			
No.18	2019/07/05 13:00	2019/07/25 13:00	20			
No.19	2019/07/25 13:00	2019/08/14 13:00	20			
No.20	2019/08/14 13:00	2019/09/03 13:00	20			
No.21	2019/09/03 13:00	2019/09/23 13:00	20			

Table 3.1(f)-4. Sampling schedules of the deployed traps.

NGK Sediment trap_500 m

Bottle No.	Sampling (UTC, yyyy/mm/dd) Start	End	Interval (days)
No.1	2019/06/09 0:00	2019/06/18 0:00	9
No.2	2019/06/18 0:00	2019/06/27 0:00	9
No.3	2019/06/27 0:00	2019/07/15 0:00	18
No.4	2019/07/15 0:00	2019/08/02 0:00	18
No.5	2019/08/02 0:00	2019/08/20 0:00	18
No.6	2019/08/20 0:00	2019/09/07 0:00	18
No.7	2019/09/07 0:00	2019/09/25 0:00	18
No.8	2019/09/25 0:00	2019/10/13 0:00	18
No.9	2019/10/13 0:00	2019/10/31 0:00	18
No.10	2019/10/31 0:00	2019/11/18 0:00	18
No.11	2019/11/18 0:00	2019/12/06 0:00	18
No.12	2019/12/06 0:00	2019/12/24 0:00	18
No.13	2019/12/24 0:00	2020/01/11 0:00	18
No.14	2020/01/11 0:00	2020/01/29 0:00	18
No.15	2020/01/29 0:00	2020/02/16 0:00	18
No.16	2020/02/16 0:00	2020/03/05 0:00	18
No.17	2020/03/05 0:00	2020/03/23 0:00	18
No.18	2020/03/23 0:00	2020/04/10 0:00	18
No.19	2020/04/10 0:00	2020/04/19 0:00	9
No.20	2020/04/19 0:00	2020/04/28 0:00	9
No.21	2020/04/28 0:00	2020/05/07 0:00	9
No.22	2020/05/07 0:00	2020/05/16 0:00	9
No.23	2020/05/16 0:00	2020/05/25 0:00	9
No.24	2020/05/25 0:00	2020/06/03 0:00	9
No.25	2020/06/03 0:00	2020/06/12 0:00	9
No.26	2020/06/12 0:00	2020/06/21 0:00	9

McLane Sediment trap_1000 & 4800 m

Bottle No.	Sampling (UTC, yyyy/mm/dd) Start	End	Interval (days)
No.1	2019/06/09 0:00	2019/06/27 0:00	18
No.2	2019/06/27 0:00	2019/07/15 0:00	18
No.3	2019/07/15 0:00	2019/08/02 0:00	18
No.4	2019/08/02 0:00	2019/08/20 0:00	18
No.5	2019/08/20 0:00	2019/09/07 0:00	18
No.6	2019/09/07 0:00	2019/09/25 0:00	18
No.7	2019/09/25 0:00	2019/10/13 0:00	18
No.8	2019/10/13 0:00	2019/10/31 0:00	18
No.9	2019/10/31 0:00	2019/11/18 0:00	18
No.10	2019/11/18 0:00	2019/12/06 0:00	18
No.11	2019/12/06 0:00	2019/12/24 0:00	18
No.12	2019/12/24 0:00	2020/01/11 0:00	18
No.13	2020/01/11 0:00	2020/01/29 0:00	18
No.14	2020/01/29 0:00	2020/02/16 0:00	18
No.15	2020/02/16 0:00	2020/03/05 0:00	18
No.16	2020/03/05 0:00	2020/03/23 0:00	18
No.17	2020/03/23 0:00	2020/04/10 0:00	18
No.18	2020/04/10 0:00	2020/04/28 0:00	18
No.19	2020/04/28 0:00	2020/05/16 0:00	18
No.20	2020/05/16 0:00	2020/06/03 0:00	18
No.21	2020/06/03 0:00	2020/06/21 0:00	18

(4) Preliminary result

Sequential samples of the sinking particles were collected both from the 1000 m and 4810 m recovery traps. Onboard, heights of the particle samples in the collecting cups were measured with scale in order to know general view of their seasonal change. Using base area of collecting cup (18.1 cm^2), we estimated volume flux for each collecting period (20 days). The volume fluxes ($cm^3/m^2/day$) were summarized in the table 3.1(f)-3. And seasonal change of the volume fluxes at the two depths were shown in the following figure.

Figure 3.1(f)-1. Seasonal changes of volume fluxes at 500 and 4810 m of the station K2.

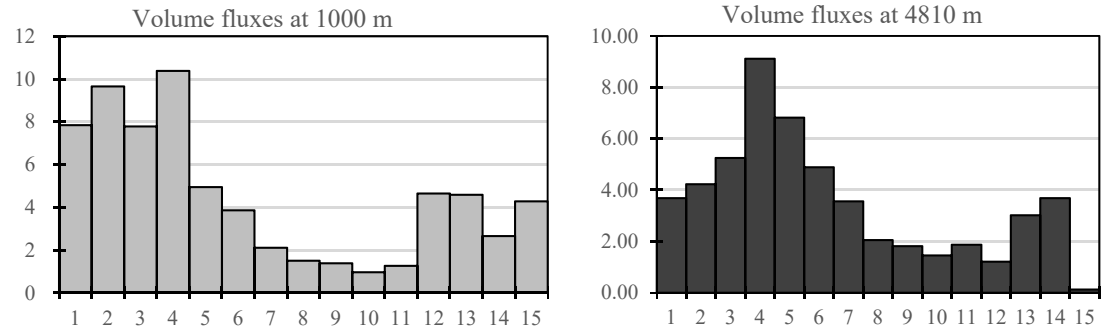

(5) Sample archives

All samples are stored in JAMSTEC/Yokosuka. Each sample will be divided into ten aliquots and these subsamples will be distributed to co-researchers for further analysis by cruise PI.

3.1 (g) CTD and DO sensors

Hiroshi UCHIDA (JAMSTEC RIGC)
Masahide WAKITA (JAMSTEC MIO)

(1) Objectives

The objective of this study is to grasp variability of temperature, salinity and oxygen at the K2 mooring site.

(2) Instruments and methods

Pressure, temperature and salinity were measured by CTDs (SBE37SM or SBE37SMP, Sea-Bird Scientific, Bellevue, Washington, USA). Dissolved oxygen was measured by optical oxygen sensors (Oxygen Optode model 3830, Aanderaa Data Instruments AS, Bergen, Norway, and RINKO-I [ARO-USB] or RINKO-I DSP [AROD-USB], JFE Advantech Co. Ltd., Hyogo, Japan). The Oxygen Optode sensor was attached to a datalogger with an internal battery and memory in a titanium housing (Compact-OPTODE, Alec Electronics Co., Ltd., Kobe, Japan). A sampling interval was set to 1 hour for the CTD and oxygen sensors.

Sensors used in the K2 mooring observation are summarized in Table 3.1 (g).1, and obtained potential temperature, salinity and oxygen data are plotted in Figs. 3.1 (g).1 and 3.1 (g).2. The data obtained in the previous mooring period (July 2017 – July 2018) were also shown.

(3) Data archive

These obtained data will be submitted to JAMSTEC Data Management Group (DMG).

Table 3.1 (g).1 Serial number of the CTD and oxygen sensors recovered from the K2 mooring.

Planned depth	CTD	Oxygen	Note
150 m	1893 (SBE37SM)	0003 (CompactOPTODE)	Winch
175 m	1892 (SBE37SM)	0006 (CompactOPTODE)	Wire
200 m	2239 (SBE37SM)	0050 (CompactOPTODE)	RAS
250 m	2756 (SBE37SM)	0004 (RINKO-I DSP)	SUS frame
300 m	2289 (SBE37SM)	0051 (RINKO-I)	RAS
370 m	2288 (SBE37SM)	0009 (CompactOPTODE)	ADCP
475 m	10737 (SBE37SMP)	0010 (CompactOPTODE)	Wire
1000 m	2285 (SBE37SM)	0007 (RINKO-I DSP)	Trap
2000 m	2748 (SBE37SM)	0006 (RINKO-I DSP)	SUS frame
3000 m	2738 (SBE37SM)	0005 (RINKO-I DSP)	RAS
Bottom	2731 (SBE37SM)	none	Releasers

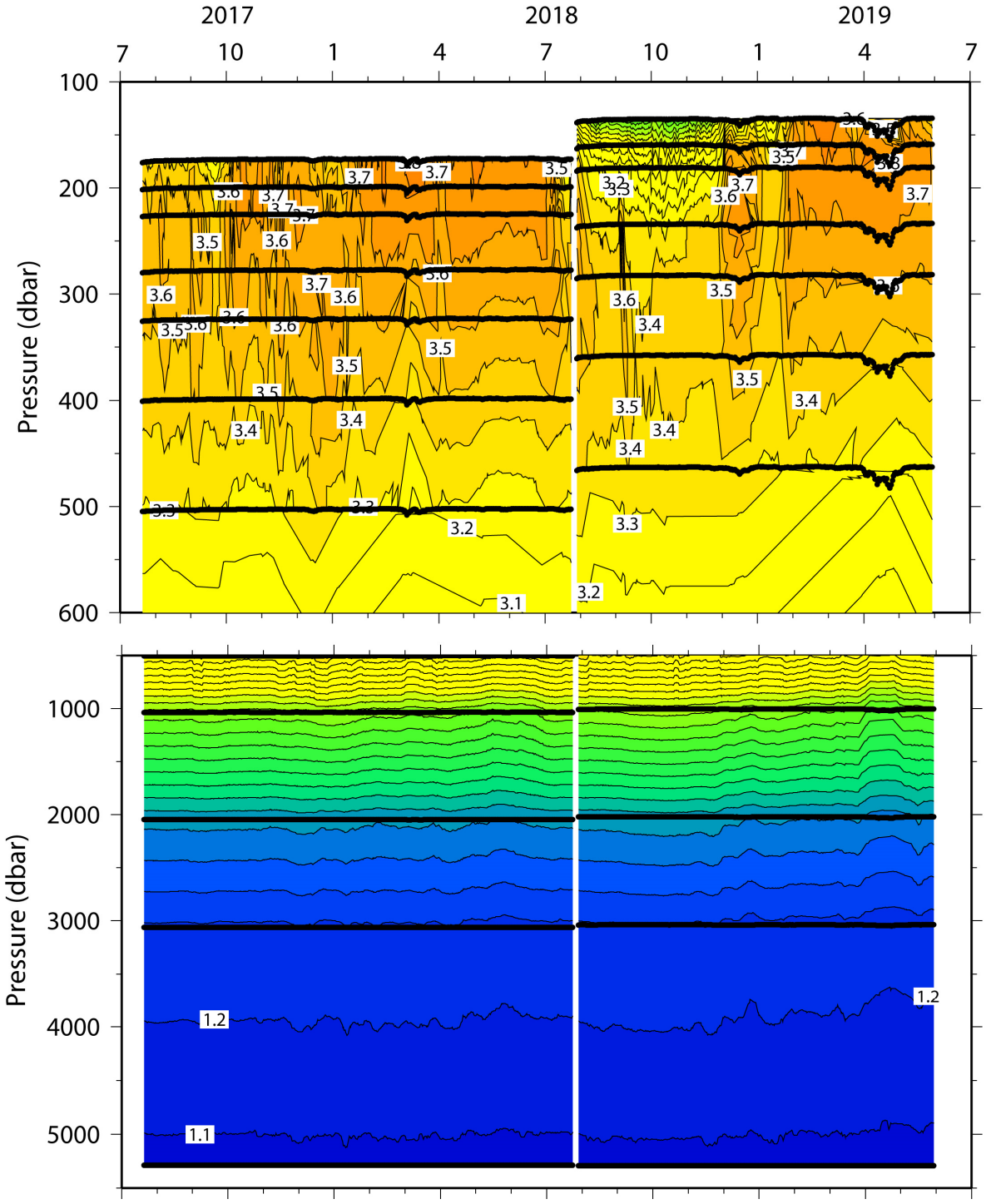

Fig. 3.1 (g). 1 Time series of potential temperature (in ^{o}C).

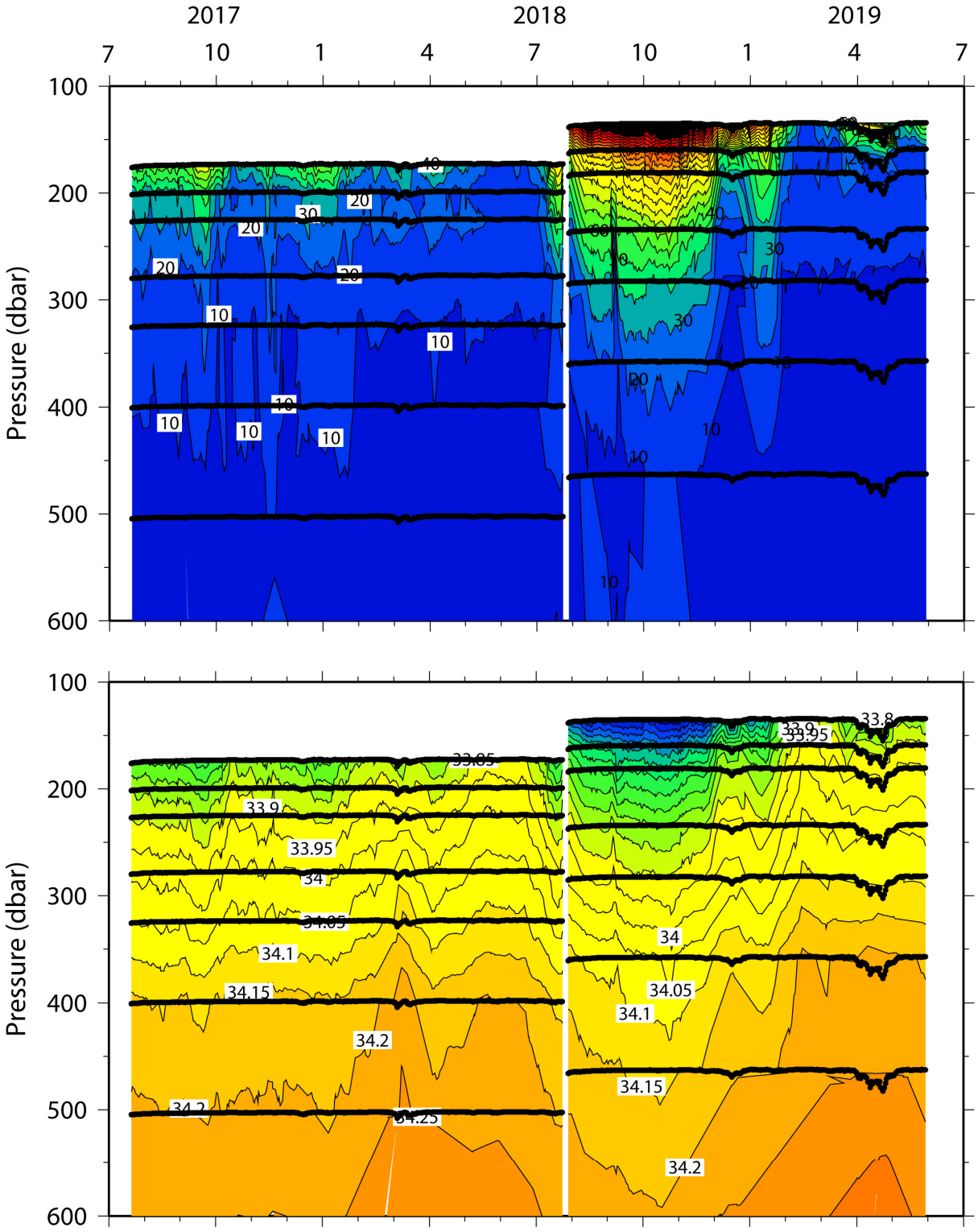

Fig. 3.2 (g). 2 Time series of oxygen (in µmol/kg, upper panel) and practical salinity (lower panel).

3.1 (h) Backscatter meter and Underwater video camera

Makio HONDA (JAMSTEC RIGC)

Yoishihisa MINO (Nagoya University)

Kazuhiko MATSUMOTO (JAMSTEC RIGC)

In order to observe settling particles optically, following backscatter meters (BS) and under water video camera (UVC) were installed on K2 “hybrid” mooring system and deployed during this cruise. Details of BS and UVC are described elsewhere (2-14-2 POC optical observation).

Nominal depth	Instrument	Sampling interval	Sampling time	Start (LST: JST+2 hr.)
175 m (on CTD)	BS FLBBSB #5167	6 hours	30 seconds	6 June 2019 06:00:00
	UVC #2	9 days	3 minutes	10 June 2019 00:00:00
200 m (on RAS)	BS FLBBSB #5168	6 hours	30 seconds	6 June 2019 06:00:00
300 m (on RAS)	BS BBSB #1742	6 hours	30 seconds	6 June 2019 06:00:00
500m (on ST)	BS Triplet #891	6 hours	30 seconds	6 June 2019 06:00:00

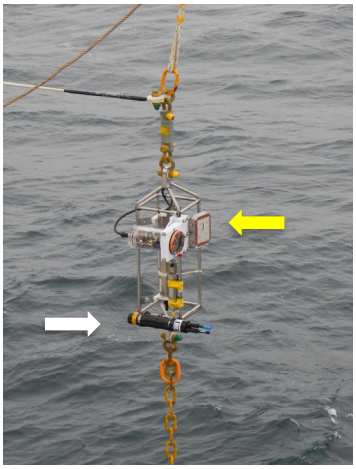

Photo 1 BS (white arrow) and UVC (yellow arrow) on 175 m CTD

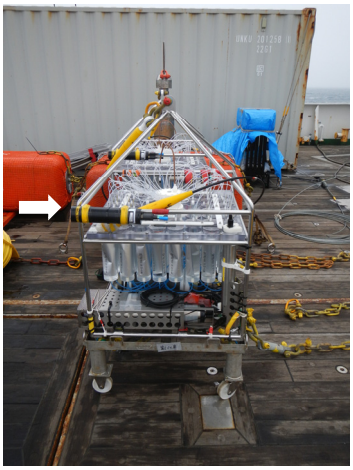

Photo 2 BS (white arrow) on RAS

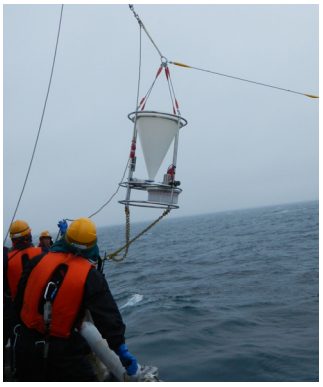

Photo 3 BS (white arrow) on 500 m Sediment Trap (ST)

3.2 Biogeochemical ARGO floats

Tetsuichi FUJIKI (JAMSTEC RIGC)
Shuhei MASUDA (JAMSTEC RIGC)
Shigeki HOSODA (JAMSTEC RIGC)
Kanako SATO (JAMSTEC RIGC)
Mizue HIRANO (JAMSTEC RIGC)
Shinsuke TOYODA (MWJ)
Yasushi HASHIMOTO (MWJ)

(1) Objectives

The objective of this study is to clarify the mechanisms of ocean ecosystem and biogeochemical cycle changes by monitoring in the global ocean. To achieve the objective, automatically long-term measurements of biogeochemical parameters are carried out with deployment of biogeochemical (BGC) Argo floats at the time-series stations K2 (47°N, 160°E) and KEO (32°N, 144°E) in the western North Pacific Ocean.

Three BGC Argo floats (BGC Navis, the two at K2 and one at KEO) have been deployed, which measures biogeochemical parameters, temperature and salinity down to a depth of 2000dbar. The purpose of the observation is to clarify changes of phytoplankton community related to environmental parameters. In collaboration with shipboard and mooring observations at K2 and KEO, long-term and spatial variability of biogeochemical process will be captured in the western North Pacific. The deployed float will also contribute to the international project of BGC Argo to construct the global array.

The BGC Argo float data will also apply to the ESTOC, which is 4D-VAR data assimilation system to estimate state of global ocean for climate changes, to investigate whole mechanism of long-term changes in the ocean.

(2) Parameters

・Water temperature, salinity, pressure, dissolved oxygen, backscattering, CDOM[FDOM], chlorophyll, nitrate and pH

(3) Methods

We launched BGC Navis floats manufactured by the Sea-Bird Scientific. The two floats equipped SBE41 CTD sensor, SBE63 optical DO sensor and Deep SUNA nitrate sensor manufactured by the Sea-Bird Scientific and FLBBCD backscattering, CDOM and chlorophyll sensors manufactured by WET Labs. The other float equipped SBE41 CTD sensor, SBE63 optical DO sensor and SeaFET pH sensor manufactured by the Sea-Bird Scientific and FLBBCD backscattering, CDOM and chlorophyll sensors manufactured by WET Labs.

The float drifts at a depth of 1000 dbar (called the parking depth) until next vertical measurements, then goes upward from a depth of 2000 dbar to the sea surface every 5 days. During the ascent, physical and biogeochemical values are measured every 2 dbar or at depths following depth table. During surfacing for a few ten minutes, the float sends all measured data to the land via

the Iridium satellite telecommunication system with Rudics protocol. Those float observations will be sustained for about a few years depending on internal battery lifetime. The status of float and its launching information is shown in Table 3.2.1.

Table 3.2.1 Status of floats and their launches

BGC Navis Floats (2000dbar) (WMO ID: 2903394, 2903395)

Float Type	BGC Navis float manufactured by Sea-Bird Scientific
CTD sensor	SBE41 manufactured by Sea-Bird Scientific
Oxygen sensor	SBE63 optical DO sensor by Sea-Bird Scientific
Backscatter CDOM Chlorophyll sensors	FLBBCD manufactured by WET Labs Backscattering: wavelength: 700nm CDOM[FDOM]: ex/em→ 370/460nm Chlorophyll: ex/em→ 470/695nm
Nitrate sensor	Deep SUNA manufactured by Sea-Bird Scientific
Cycle	Every 5 days
Iridium transmit type	Router-Based Unrestricted Digital Internetworking Connectivity Solutions (RUDICS)
Target Parking Pressure	1000 dbar
Sampling layers	2dbar or given depth interval from 2000 dbar to surface

BGC Navis Float (2000dbar) (WMO ID: 2903396)

Float Type	BGC Navis float manufactured by Sea-Bird Scientific
CTD sensor	SBE41 manufactured by Sea-Bird Scientific
Oxygen sensor	SBE63 optical DO sensor by Sea-Bird Scientific
Backscatter CDOM Chlorophyll sensors	FLBBCD manufactured by WET Labs Backscattering: wavelength: 700nm CDOM[FDOM]: ex/em→ 370/460nm Chlorophyll: ex/em→ 470/695nm
pH sensor	Deep SUNA manufactured by Sea-Bird Scientific
Cycle	Every 5 days
Iridium transmit type	Router-Based Unrestricted Digital Internetworking Connectivity Solutions (RUDICS)
Target Parking Pressure	1000 dbar
Sampling layers	2dbar or given depth interval from 2000 dbar to surface

Launches

Float S/N	WMOID	Date and Time of Launch (UTC)	Location of Launch	Station
F0951	2903394	2019/05/25 05:18	32-12 [N] 144-17 [E]	KEO
F0955	2903395	2019/06/02 04:24	47-04 [N] 160-00 [E]	K2
F0952	2903396	2019/06/02 04:26	47-04 [N] 160-00 [E]	K2

(4) Data archive

The Argo float data with real-time quality control are provided to meteorological organizations, research institutes, and universities via Global Data Assembly Center (GDAC: http://www.usgodae.org/argo/argo.html, http://www.coriolis.eu.org/) and Global Telecommunication System (GTS) within 24 hours following the procedure decided by Argo data management team. Delayed mode quality control is conducted for the float data within 6 months ~ 1 year, to satisfy their data accuracy for the use of research. Those quality controls of data are freely available via internet and utilized for not only research use but also weather forecasts and any other variable uses. Below figures show vertical profiles of BGC Navis (WMO ID: 2903394) launched at KEO and BGC Navis (WMO ID: 2903395) launched at K2 as samples.

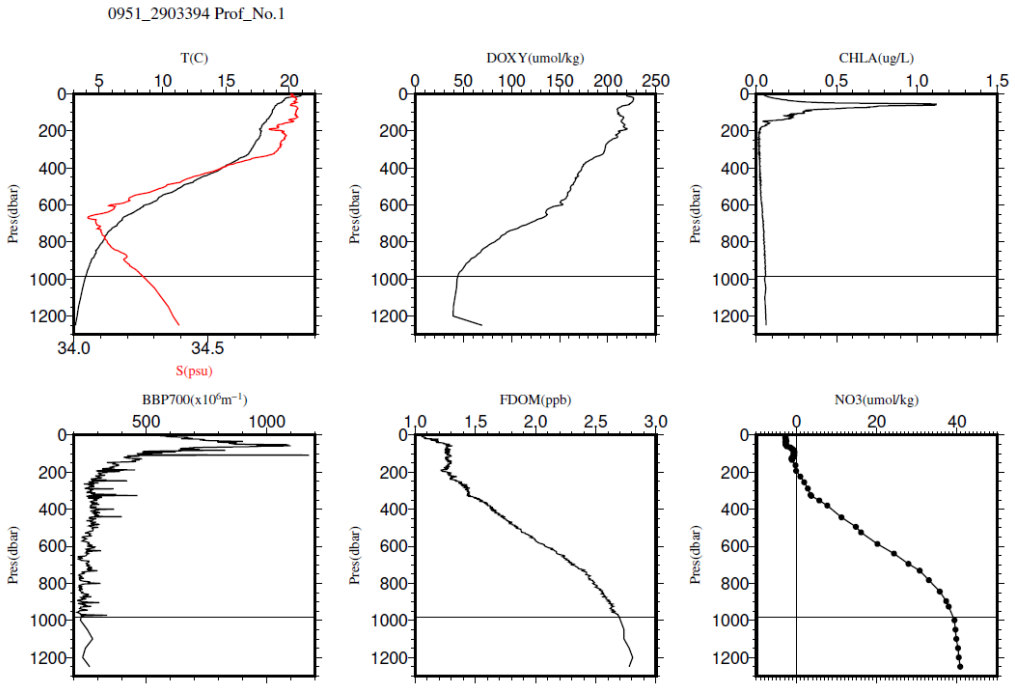

WMO ID: 2903394
DATE: 2019/05/26 02:27
POSITION: 32.338N, 144.231E

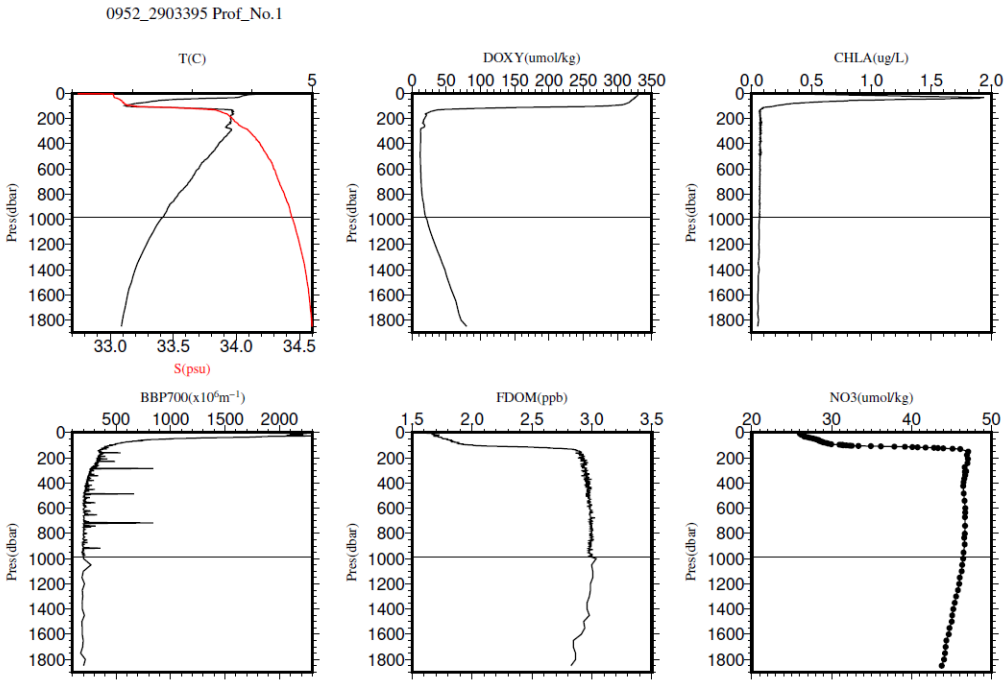

WMO ID: 2903395
DATE: 2019/06/03 1:39
POSITION: 47.032N, 159.972E

Fig. 3.2.1. Vertical profiles of first measurements (temperature [T], salinity [S], dissolved oxygen [DOXY], chlorophyll a [CHLA], backscattering [BBP700], fluorescent dissolved organic matter [FDOM] and nitrate [NO3]) on deployed BGC Argo floats at KEO (upper panel) and K2 (lower panel).

3.3 Satellite image acquisition (MCSST from NOAA/HPRT)

Tetsuichi FUJIKI (JAMSTEC RIGC)
Wataru TOKUNAGA (NME)
Satomi OGAWA (NME)
Yoichi INOUE (MIRAI crew)

(1) Objectives

The objectives are to collect cloud data in a high spatial resolution mode from the Advance Very High Resolution Radiometer (AVHRR) on the NOAA and MetOp polar orbiting satellites.

(2) Methods

We received the down link High Resolution Picture Transmission (HRPT) signal from satellites, which passed over the area around the R/V MIRAI. We processed the HRPT signal with the in-flight calibration and computed the brightness temperature (MCSST). A cloud image map around the R/V MIRAI was made from the data for each pass of satellites.

We received and processed polar orbiting satellites data throughout this cruise.

(3) Preliminary results

Fig.3.3.1 show the MCSST image during this cruise.

(4) Data archives

The raw data obtained during this cruise will be submitted to the Data Management Group (DMG) in JAMSTEC.

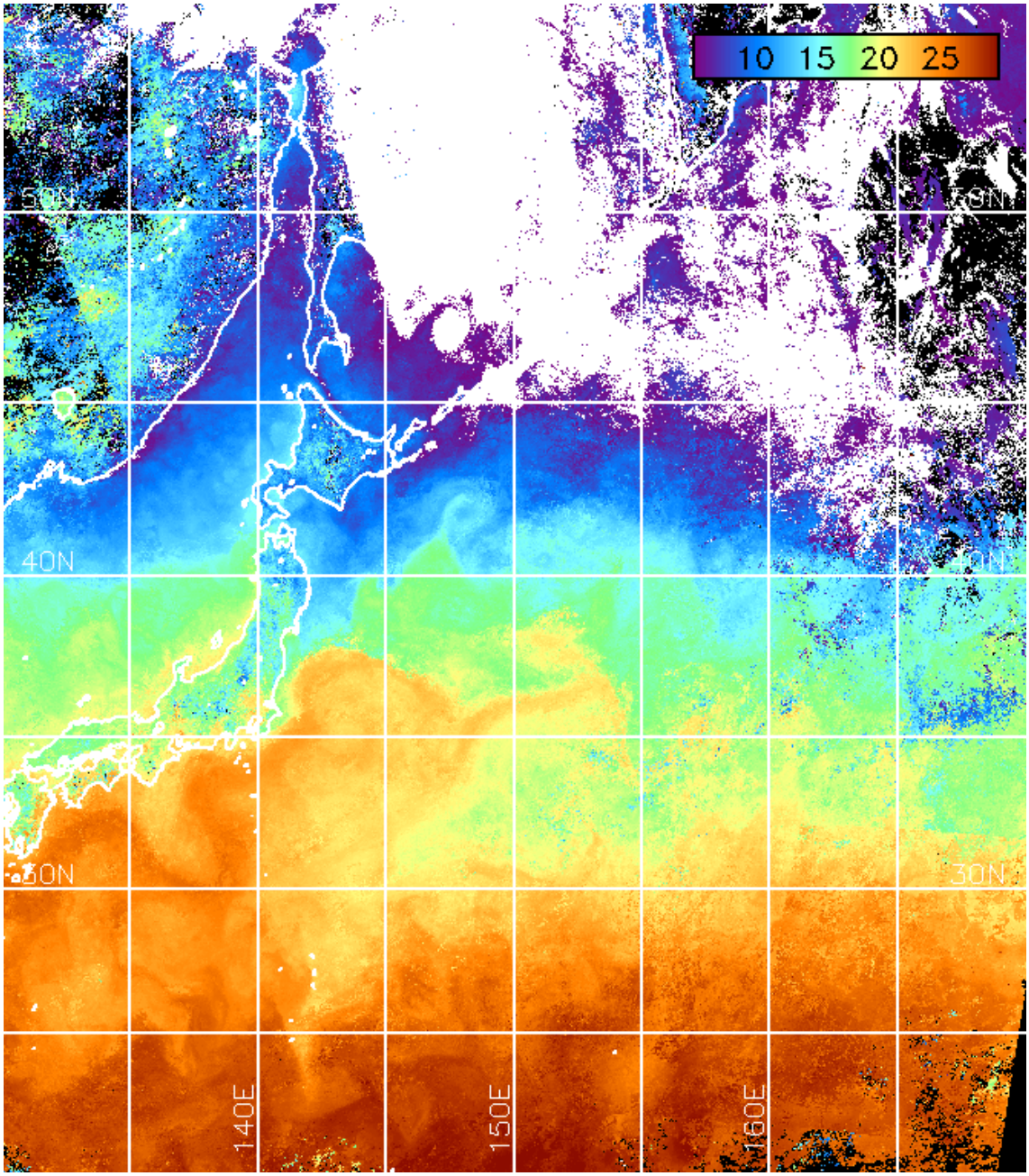

Fig.3.3.1 MCSST image during this cruise (24th May to 13th June)